

**Design and Optimization of Gas Cooler for Performance
Enhancement of Trans-critical CO₂ Refrigeration
System in Indian Context**

THESIS

Submitted in partial fulfilment of the requirements for the degree of

DOCTOR OF PHILOSOPHY

by

DILEEP KUMAR GUPTA

(2008PHXF426P)

Under the Supervision of

Prof. M. S. DASGUPTA



BITS Pilani
Pilani | Dubai | Goa | Hyderabad

**BIRLA INSTITUTE OF TECHNOLOGY & SCIENCE
PILANI – 333 031 (RAJASTHAN) INDIA**

2014



**BIRLA INSTITUTE OF TECHNOLOGY & SCIENCE
PILANI - 333 031 (RAJASTHAN) INDIA**

CERTIFICATE

This is to certify that the thesis entitled “**Design and Optimization of Gas Cooler for Performance Enhancement of Trans-critical CO₂ Refrigeration System in Indian Context**” submitted by **Dileep Kumar Gupta**, ID.No. 2008PHXF426P for award of Ph.D. Degree of the institute, embodies original work done by him under my supervision.

Signature: 

Prof. M. S. DASGUPTA

Professor , Mechanical Engineering Department
BITS-Pilani, Pilani Campus

Date: 26/4/2014

Dedicated

to

my loving parents

(who had a dream for me and made the dream come true)

&

my little champ "***Khush***"

ACKNOWLEDGEMENTS

First and foremost, I praise God, the almighty for providing me this opportunity and granting me the capability to proceed successfully and with his blessings, only I have accomplished this huge task.

I am grateful to my honorable supervisor Prof. M.S. Dasgupta, for his constant guidance and active interest towards the completion of my thesis. He has always supported me with his patience and persistence. He helped me focus on my quest, always gave the right critique, and kept our meetings lighthearted and fun.

I thank our Vice Chancellor, Directors, Deputy Directors and Deans for providing me the opportunity to teach in the Department of Mechanical Engineering of BITS-Pilani, Pilani Campus and allowing me to pursue my doctoral thesis by providing necessary facilities and support. I express my gratitude to Prof. S.K. Verma, Dean, Academic Research Division (Ph.D. Programme), BITS-Pilani, Pilani Campus for his constant official support and encouragement.

I thank Prof. K.S. Sangwan, (Head of Department) and entire faculty and staff of Department of Mechanical Engineering, BITS-Pilani, Pilani Campus for their kind moral support and assistance.

I thank members of Doctoral Research Committee (DRC), Prof. N.N. Sharma, Prof. K.S. Sangwan, Prof. B.K. Rout and Doctoral Advisory Committee (DAC) members, Dr. M.S. Soni and Prof. P. Srinivasan, who spared their precious time to provide valuable suggestions that immensely helped me in improving the quality of my Ph.D. thesis.

I would also like to thank all my colleagues in BITS Pilani and in particular, Dr. M. Palla, Dr. Amit K. Singh, Dr. Gunjan Soni, Dr. Sharad Srivastava, Mr. Jitendra S. Rathore, Mr. K. Vinayak, Mr. Sachin U. Belgamwar and all others, who kept me motivated while I was engulfed into the thesis work.

Special thanks to Mr. Maheshwar Dwivedy, Mr. Satish K. Dubey, and Mr. Arshad Javed, for always being there with me during the rough times. We always had lots of fruitful discussion that helped me face all the difficult situations during my entire work.

I express my sincere thanks to Mr. Santosh Kumar Saini (ARC Division) for his help in word-processing of the thesis.

Finally and most importantly so, special thanks must go to my lovable family.. My sincere thanks to my parents and in laws for their blessing and support. I am heartily thankful to my elder brother Mr. Basant Gupta and my sister Priya for their unconditional sacrifices with their career to make all my dreams come true. I am also thankful to my younger brother Mukesh Gupta, whom I always found with me during all ups and down right from the starting of my career. Their love, support, motivation and all physical help have been immeasurable. My special loving thanks to my wife Shipra for all the sacrifices she has gone through all these years towards the successful completion of my thesis. Last but not the least, I thank God to having given me my little champ Khush, whose smile made me forget all the pain and trouble that I would have faced in my journey.

Dileep Kumar Gupta

ABSTRACT

Environmental concerns and enactments of Montreal and Kyoto Protocol for sustainable growth enforce research for ecologically safe and natural refrigerants and cost effective designs of refrigeration systems. Carbon dioxide (CO₂) is one such natural refrigerant that, although was abandoned earlier due to the invention and vigorous promotion of synthetic refrigerants, has acquired tremendous attention as a potential candidate for replacement of synthetic refrigerant due to its environmental and personal safety features. The commercial success of CO₂ as a refrigerant, however, demands, cost effective and widely accepted technology operable at various environmental conditions. This has led to the subsequent development of trans-critical carbon dioxide cycles where the condenser in the conventional vapour compressor system gets replaced by a gas cooler. Introduction of gas cooler, with heat rejection taking place over an unusually large temperature glide, offers several unique possibilities such as heating, cooling, simultaneous cooling and heating, heat pump drying, etc. applications.

Due to lower critical temperature of CO₂ (i.e. 31.1°C), the gas cooler needs to be operated above the critical point and in this zone the properties of CO₂ changes rapidly. Hence the design of gas cooler is the most complex and crucial factor which affects the system performance. The focus of this work is on the design of gas cooler and optimization of the same for various operating and design conditions for Indian climate (or any tropical climate condition) to achieve the best possible performance of the system.

In this work, the performance of a finned tube air cooler gas cooler for trans-critical CO₂ refrigeration system has been analyzed extensively. The conservation equations have been discretized using the finite difference scheme and code is developed in MATLAB[®] to solve these equations. Consequently simulated results are validated using published experimental data. The validated model is used to analyze the performance of possible alternative designs of the gas cooler with an aim to enhance heat transfer or reduce approach temperature for typical Indian climatic conditions considering three temperature zones.

Further, the model is extended for analyzing the performance of the overall system using respective alternate and optimized design of the gas cooler at various operating conditions. An attempt is also made to optimize the gas cooler design and operating conditions to achieve the best possible COP of the system, including the fan power consumption, which is a novel approach. The effect of evaporator temperature and compressor isentropic efficiency are also analyzed in the study. Consequently, in order to improve the performance of the system, the analysis is extended for trans-critical CO₂ system with work recovery turbine as expansion device.

It is found during the study that each temperature zone has a different optimum design of the gas cooler and operating condition. In other words the trans-critical CO₂ refrigeration systems that need to be tuned to local environment condition for performance enhancement. Therefore, ^TThis work can help in formulating design guidelines for the components and its operating conditions for trans-critical CO₂ refrigeration system to achieve the best possible COP.

Keywords: CO₂ refrigeration systems, heat transfer simulation, trans-critical refrigeration system, eco-friendly refrigerant, modeling and simulation, gas cooler, finned tube gas cooler, heat exchanger.

<i>Acknowledgements</i>	i-ii
<i>Abstract</i>	iii-iv
<i>Table of Contents</i>	v-viii
<i>List of Tables</i>	ix
<i>List of Figures</i>	x-xiii
<i>List of Abbreviations/Symbols</i>	xiv-xvi
Chapter 1 Introduction	1-16
1.1 Natural Refrigerants	3
1.2 Carbon Dioxide - As Natural Refrigerant	5
1.2.1 Background	5
1.2.2 Properties of CO ₂	8
1.2.3 Application areas	12
1.2.4 Commercial aspects	13
1.3 Motivation and Objective	14
1.3.1 Objectives of the research	15
1.4 Preview of the Thesis	15
Chapter 2 Literature Review	17-62
2.1 CO ₂ Trans-Critical Cycle	18
2.1.1 Optimum high pressure	19
2.1.2 Applications of trans-critical CO ₂ Systems	20
2.2 Components of Trans-Critical CO ₂ Refrigeration System	25
2.2.1 Compressor	25
2.2.2 Gas cooler	28
<i>2.2.2.1 Supercritical CO₂ heat transfer and pressure drop</i>	28

2.2.2.2 <i>Heat transfer correlations for supercritical CO₂ cooling</i>	30
2.2.2.3 <i>Gas cooler design</i>	41
2.2.3 Evaporator	45
2.2.4 Expansion device - throttling process	47
2.3 Cycle Modification on Trans-Critical CO ₂ Refrigeration System	49
2.3.1 System with internal heat exchanger	49
2.3.2 Multi stage system	51
2.3.3 Ejector-expansion	53
2.3.4 Expansion turbine	56
2.4 Summary of the Literature Review	60
2.5 Gap Area in Existing Research	61
Chapter 3 Problem Identification and Description	63-75
3.1 CO ₂ Refrigeration System in Indian Conditions	63
3.2 Effect of Gas Cooler Outlet Temperature and Operating Pressure	66
3.3 Temperature Zones in Indian Conditions	69
3.4 Ideal Cycle Based Performance Analysis at Different Temperature Zones	70
3.5 Ideal Cycle Based Guideline for Operating Conditions	73
Chapter 4 Modeling and Simulation	76-90
4.1 Gas Cooler Geometry	76
4.2 Mathematical Modeling	77
4.2.1 Discretization	77
4.2.1.1 <i>Refrigerant side modeling</i>	79
4.2.1.2 <i>Air side modeling</i>	80
4.2.2 Numerical implementation through MATLAB code	81
4.3 Model Validation	82

Chapter 5	Analysis of Gas Cooler and CO₂ Trans-Critical Refrigeration System	91-109
5.1	Modified Design of Gas Cooler and Operating Conditions	91
5.2	Model Application	95
5.3	Results and Discussion	96
5.3.1	Performance of gas cooler	96
5.3.1.1	<i>Temperature zone I</i>	96
5.3.1.2	<i>Temperature zone II</i>	99
5.3.1.3	<i>Temperature zone III</i>	101
5.3.2	Performance of trans-critical CO ₂ refrigeration system	103
5.3.2.1	<i>Temperature zone I</i>	103
5.3.2.2	<i>Temperature zone II</i>	105
5.3.2.3	<i>Temperature zone III</i>	109
6	Optimization of Gas Cooler	110-135
6.1	Selection of Input Combinations of Geometric and Operating parameters.	110
6.2	Model Application	114
6.3	Results and Discussion	115
6.3.1	Performance of gas cooler and overall system	115
6.3.1.1	<i>Temperature zone I</i>	115
6.3.1.2	<i>Temperature zone II</i>	121
6.3.1.3	<i>Temperature zone III</i>	125
6.3.2	Effect of compressor isentropic efficiency and evaporator temperature	130
6.3.2.1	<i>Two pass gas cooler</i>	130
6.3.2.2	<i>Three pass gas cooler</i>	132
6.3.2.3	<i>Four pass gas cooler</i>	133

Chapter 7	Performance of CO₂ Trans-Critical Refrigeration System with work recovery Turbine	136-160
7.1	Selection of Input Combinations of Geometric and Operating parameters	137
7.2	Model Application	139
7.3	Results and Discussion	140
7.3.1	Performance of trans-critical CO ₂ refrigeration system	140
7.3.1.1	<i>Temperature zone I</i>	141
7.3.1.2	<i>Temperature zone II</i>	143
7.3.1.3	<i>Temperature zone III</i>	145
7.3.2	Effect of isentropic efficiency and evaporator temperature	147
7.3.2.1	<i>Temperature zone I</i>	147
7.3.2.2	<i>Temperature zone II</i>	151
7.3.2.3	<i>Temperature zone III</i>	156
Chapter 8	Conclusion and Future Scope of Work	161-166
8.1	Conclusions	161
8.2	Suggestions for Future Work	165
References		
Appendix A		
Appendix B		
List of Publications		
Brief Biography of the candidate		
Brief Biography of the Supervisor		

LIST OF TABLES

Table No.	Title	Page No.
1.1	Most commonly known refrigerants and their ODP and GWP	1
1.2	Overview of selected natural refrigerants	3
1.3	Thermo-physical properties of most common refrigerants	9
1.4	CO ₂ properties at pseudo-critical temperature	10
2.1	Value of n, B, and s in the Krasnoshchekov equation	31
2.2	Value of 'm' and 'n' in the Baskov et al. equation for $T_{bt}/T_{pc} > 1$	32
2.3	Summary of heat transfer correlations of supercritical CO ₂ cooling	38
2.4	Prediction performances of the available correlations for supercritical CO ₂ cooling	39
3.1	Outside design conditions of major cities in India	64
3.2	Temperature zones and its range of temperature	69
3.3	Operating pressure and maximum COP at different approach temperature	74
4.1	Specification of tested gas cooler	77
4.2	Tested input operating conditions	85
5.1	Combination of simulation conditions	92
6.1	Modified operating conditions and simulation parameters for optimization	114
7.1	Modified operating conditions and simulation parameters for modified system	139

LIST OF FIGURES

Fig. No.	Title of the Figure	Page No.
1.1	Historical introduction of refrigerants	07
1.2	Phase diagram of CO ₂	09
1.3	Specific heat versus temperature supercritical	10
1.4	Density versus temperature supercritical	11
1.5	Conductivity versus temperature supercritical	11
1.6	Viscosity versus temperature supercritical	11
2.1	P-h diagram of trans-critical CO ₂ cycle	18
2.2	Summary of literature based on applications	60
2.3	Summary of literature based on component design	60
2.4	Summary of literature with system modification	61
3.1	Trans-critical cycle for CO ₂	66
3.2	Variation of compression work with compressor discharge pressure	67
3.3	Variation of refrigeration capacity with gas cooler outlet temperature at different operating pressure	67
3.4	Variation of COP with gas cooler outlet temperature at different operating pressure	68
3.5	Number of cities in India and its design temperatures	69
3.6	Percentage of cities in India at selected temperatures zones	70
3.7	Variation of compressor work with the compressor discharge pressure	70
3.8	Variation of refrigeration capacity with gas cooler outlet temperature at different AT	71
3.9	Variation of COP with gas cooler outlet temperature at different AT	72

Fig. No.	Title of the Figure	Page No.
3.10	Pressure at which the maximum COP achievable at different AT	73
3.11	Variation of maximum possible COP with AT with different zones	74
4.1	Three dimensional geometry of gas cooler	76
4.2	Co-ordinates of the elements in the discretized geometry of the gas cooler	78
4.3	Control volume element with flow directions	79
4.4	Temperatures at grid points in an element	82
4.5	Detail flow chart of MATLAB [®] code, its computer implementation	83
4.6	Temperature profile of refrigerant with operating pressure 9MPa	87
4.7	Temperature profile of refrigerant with operating pressure 11MPa	88
4.8	Temperature profile of refrigerant with operating pressure 10MPa	89
4.9	Comparison of experimental and simulated result of the gas cooler outlet temperature	90
5.1	Modified circuit arrangement of gas cooler	93
5.2	Modified geometry with different circuit arrangement of gas cooler	94
5.3	Performance of gas cooler at temperature zone I	97
5.4	Performance of gas cooler at temperature zone II	100
5.5	Performance of gas cooler at temperature zone III	102
5.6	Performance of overall system at temperature zone I	104
5.7	Performance of overall system at temperature zone II	107
5.8	Performance of overall system at temperature zone III	108
6.1	Modified geometry with different circuit arrangement of <i>(two pass)</i> gas cooler	111
6.2	Modified geometry with different circuit arrangement of <i>(three pass)</i> gas cooler	112

Fig. No.	Title of the Figure	Page No.
6.3	Modified geometry with different circuit arrangement of (<i>four pass</i>) gas cooler	113
6.4	Performance of (<i>two pass</i>) gas cooler and overall system at zone I	117
6.5	Performance of (<i>three pass</i>) gas cooler and overall system at zone I	118
6.6	Performance of (<i>four pass</i>) gas cooler and overall system at zone I	120
6.7	Performance of (<i>two pass</i>) gas cooler and overall system at zone II	122
6.8	Performance of (<i>three pass</i>) gas cooler and overall system at zone II	123
6.9	Performance of (<i>four pass</i>) gas cooler and overall system at zone II	125
6.10	Performance of (<i>two pass</i>) gas cooler and overall system at zone III	126
6.11	Performance of (<i>three pass</i>) gas cooler and overall system at zone III	128
6.12	Performance of (<i>four pass</i>) gas cooler and overall system at zone III	129
6.13	Comparison of performance of overall system with (<i>two pass</i>) gas cooler	131
6.14	Comparison of performance of overall system with (<i>three pass</i>) gas cooler	132
6.15	Comparison of performance of overall system with (<i>four pass</i>) gas cooler	133
7.1	Improvement in COP with modification	137
7.2	Reduction in optimum operating pressure with modification	137
7.3	Modified geometry with different circuit arrangement of gas cooler	138
7.4	Performance of gas cooler and overall system with expander expansion at zone I	142
7.5	Performance of gas cooler and overall system with expander expansion at zone II	144
7.6	Performance of gas cooler and overall system with expander expansion at zone III	146
7.7	Performance of overall system at zone I (evaporator temperature 268K)	148
7.8	Performance of overall system at zone I (evaporator temperature 273K)	149

Fig. No.	Title of the Figure	Page No.
7.9	Performance of overall system at zone I (evaporator temperature 278K)	150
7.10	Performance of overall system at zone II (evaporator temperature 268K)	153
7.11	Performance of overall system at zone II (evaporator temperature 273K)	154
7.12	Performance of overall system at zone II (evaporator temperature 278K)	155
7.13	Performance of overall system at zone III (evaporator temperature 268K)	157
7.14	Performance of overall system at zone III (evaporator temperature 273K)	158
7.15	Performance of overall system at Zone III (evaporator temperature 278K)	159

LIST OF ABRVATIONS

ACC	Automotive Air Conditioning
AT	Approach Temperature
CO ₂	Carbon dioxide
CFC	Chlorofluorocarbon
COP	Coefficient of Performance
EEV	Electronic expansion valves
GWP	Global Warming Potential
HCFC	Hydro-chlorofluorocarbon
HFC	Hydro-fluorocarbon
IHX	Internal heat exchanger
IPCC	Intergovernmental Panel on Climate Change
LMTD	Logarithmic Mean Temperature Difference
MARD	Mean absolute relative deviation
MRD	Mean relative deviation
NH ₃	Ammonia
ODP	Ozone Depletion Potential
SLHX	Suction line heat exchanger
SHSC	Semi hermetic sealed compressor

NOMENCLATURE

A	Surface area
C	Total heat capacity
C_p	Specific heat capacity
\bar{C}_p	Average specific heat capacity
CR	Total heat capacity ratio
d	Tube diameter
d_e	Equivalent Diameter
G	Mass Flux (kg m ⁻²)
h	Heat transfer coefficient (W m ⁻² K ⁻¹)
H	Enthalpy (kJ kg ⁻¹)
K	Thermal conductivity (W m ⁻¹ K ⁻¹)
\dot{M}	Mass flow rate (kg s ⁻¹)
Nu	Nusselt number
p	Perimeter (m)
P	Pressure (Pa)
ΔP	Pressure Drop
Pr	Prandtl number
\dot{q}	Heat flux (W m ⁻²)
Qt	Total heat (kJ)
Re	Reynolds's number Reynolds's number
RE	Refrigerating effect
T	Temperature
u	Velocity (m s ⁻¹)
U_o	Overall heat transfer coefficient
W	Work (kW)
ϕ	Friction coefficient

OK not!

η_o	Over all surface efficiency
σ	Wall shear stress
ρ	Density (kg m^{-3})
η_{isen}	Isentropic efficiency
η_{fin}	Fin efficiency
η_{fan}	Gas cooler fan efficiency

omit one gap.
(It seems there are two gaps?)

Subscript

a	air
i	inner
in	inside wall
o	outer
r	refrigerant
ci	compressor inlet
co	compressor outlet
ei	evaporator inlet
eo	evaporator outlet
gci	gas cooler inlet
gco	gas cooler outlet
fr	friction
ta	total air side
wt	wall ^t temperature

include the following

γ_{ei}
 γ_{ci}

max
min

γ } ref eq. 4.13
 U }

Introduction

The quest of comfort leads us to built environment which promises healthy and pollution free living condition. Refrigeration and air conditioning are thus becoming essential and vital for the modern life style. This on the other hand, has given rise to serious concern on energy and environmental front. Therefore, the field of refrigeration and air conditioning has become associated with new and emerging technologies, that are more environmentally sustainable and energy efficient. The harmful environmental effects of commonly used refrigerants have generated worldwide concern which have resulted in to their phase-out in recent years. The ozone depletion effect of refrigerants containing chemicals such as bromine and chlorine and their contribution to global warming factors have led to international accords, Montreal Protocol and Kyoto Protocol, to stop production of refrigerants having harmful effects. Policymakers and environmentalists inked the Montreal Protocol (1987) and subsequently the London and Copenhagen amendments (1990, 1992) to abandon the production of CFC (chlorofluorocarbon) by the end of 1995 and HCFC (hydro-8chlorofluorocarbon) by 2030 due to higher ozone depletion potential (ODP). The HFC (hydro-fluorocarbon) refrigerants, once considered the most promising long term substitute of CFCs and HCFCs, have also proven to be harmful owing to their high; global warming potential (GWP). Table 1.1 shows the ODP and GWP of some commonly used refrigerants.

This is not listed in the document

Table 1.1: Most commonly known refrigerants and their ODP and GWP (Zhao, 2001)

Refrigerant			Formula	ODP ¹	GWP ²	Phase-out
Type	Name or Composition	No.				
CFCs	Trichlorofluoromethane	R-11	CCl3F	1.0	4000	1996
	Dichlorodifluoromethane	R-12	CCl2F2	1.0	8500	
	Chloropentafluoroethane	R-115	CClF2CF3	0.6	9300	
	Trichlorotrifluoroethane	R-113	CCl2FCClF2	0.1	4800- 6000	
HCFCs	Chlorodifluoromethane	R-22	CHClF2	0.055	1700	2030
	Dichlorofluoroethane	R-141b	CCl2FCH3	0.11	630	

↑ do necessary correction to subscript e.g. CCl₃F

Refrigerant			Formula	ODP ¹	GWP ²	Phase-out
Type	Name or Composition	No.				
	Chlorodifluoroethane	R-142b	CH ₃ CClF ₂	0.065	2000	
	R-22/115 (48.8/51.2)	R-502	--	0.333	5575	
HFCs	Pentafluoroethane	R-125	CHF ₂ CF ₃	0	3200	Undetermined
	Tetrafluoroethane	R-134a	CH ₂ FCF ₃	0	1300	
	Trifluoroethane	R-143a	CH ₃ CF ₃	0	4400	
	Difluoroethane	R-152a	CH ₃ CHF ₃	0	140	
	R-125/143a/134a (44/52/4)	R-404A	-	0	3750	
	R-32/125/134a (23/25/52)	R-407C	-	0	1600	
	R-32/125 (50/50)	R-410A	-	0	2200	
Natural Refrigerants	Air	-	-	0	0	Not Likely
	Ammonia	R-717	NH ₃	0	0	
	Carbon Dioxide	R-744	CO ₂	0	1	
	Isobutene	R-600a	CH(CH ₃) ₃	0	3	
	Propane	R-290	C ₃ H ₈	0	3	

1. The values of ODP are based on R-12 = 1.0

2. The values of GWP are based on CO₂ = 1.0 for time horizon of 100 years.

Attention is now focused toward issues related to GWP with a view of reducing greenhouse gas emissions. CO₂ is taken as one in GWP scale and HFCs have GWP of 1000-3000 times in the same scale as reported by Neksa (2002). This is the reason, that despite being chlorine free, HFCs, are included in the Kyoto agreement as materials which are to be regulated. Further, the recent release of the assessment report of 2007 of the Intergovernmental Panel on Climate Change (IPCC) has led environmental groups calling on governments around the world to accelerate the phase-out of HCFCs in the wake of findings that action under the ozone layer treaty could do more to combat global warming than the Kyoto Protocol. A renewed interest has already been observed towards environmentally benign natural refrigerants, and such findings are expected to emphasize a switch to these refrigerants. Due to the inherent non-eco-friendly nature of synthetic refrigerants, the demand for natural refrigerants based technology is rising. Natural refrigerants such as air, water, noble gases, hydrocarbons, ammonia, nitrogen and carbon dioxide are ecologically safe since they are part of the environment and are already

available in bulk quantity in the biosphere. Among these natural refrigerants, carbon dioxide is the preferred choice owing to its non-toxicity, non-flammability character along with its eco-friendly nature. It is also abundant and cheap. Hence, carbon dioxide has the potential to offer itself as a long term substitute with respect to environmental and personal safety.

1.1 Natural Refrigerants

Although the ODP of some of the HFCs is zero, GWP of these refrigerants makes them unfit as a long term substitute. Naturally occurring substances can be a viable alternative. Apart from air and water, natural refrigerants are derived as from hydrocarbons, ammonia and carbon dioxide. Hydrocarbons are in use for low charge systems in residential and commercial applications and low capacity air conditioners for automotive and space cooling. Commonly used hydrocarbon refrigerants are propane, propylene, butane, isobutene and their blends. These refrigerants are highly flammable which narrows down their application range in terms of safety. Ammonia is an age old natural refrigerant, widely used in medium and large refrigeration systems. Its thermodynamic and transport properties are found better than these of the hydrocarbons. As a byproduct of the nitrogen cycle, ammonia is an inexpensive refrigerant as well. However, its toxicity restricts it to industrial and commercial applications with special safety precautions. An overview of selected natural refrigerants is summarized in Table 1.2

Table 1.2: Overview of selected natural refrigerants (Zhao, 2001)

↑ This is not
 ← Protected circle
 "References"

Refrigerant	General Characteristics	Major Advantages	Major Disadvantages
Ammonia (NH₃)	Ammonia is a well-known refrigerant in large scale industrial refrigeration plants. It has been used as a refrigerant for more than 120 years, but until now it has not been widely used in small plants.	<ul style="list-style-type: none"> - More than 120 years of practical use - Excellent thermodynamic and thermophysical properties - Higher energy efficiency in most temperature ranges - Well known oil tolerance - Great tolerance to water contamination - Simple and immediate leak detection - No ODP or GWP - Lower cost - Smaller pipe dimensions leading to lower plant investments 	<ul style="list-style-type: none"> - Toxic at low concentrations in air (above 500ppm) - No tolerance to some materials, e.g. copper - No miscibility with most known oils - High discharge temperatures - Flammable at 15-30% Vol.

Refrigerant	General Characteristics	Major Advantages	Major Disadvantages
Water (H₂O)	Environmentally attractive, water has potential as a longterm acceptable refrigerant. Water offers high plant energy efficiency.	<ul style="list-style-type: none"> - Higher Carnot COP due to the use of direct heat exchanger - High mechanical efficiency of compressor - Production of vacuum ice - Low energy consumption - No ODP or GWP 	<ul style="list-style-type: none"> - Process under vacuum - Good only for cooling/refrigeration above 0°C
Carbon Dioxide (CO₂)	In recent years, after the Montreal Protocol, much development activity has been devoted to CO ₂ as a refrigerant. This development is based on new material technology which allows high pressures in the thermodynamic cycle. CO ₂ is quite harmless; it is environmentally attractive, and is neither toxic, flammable nor explosive.	<ul style="list-style-type: none"> - Low weight and small dimensions of plant - Large refrigeration capacity - Tolerance with well known oils - Low compression ratio - Low environmental impact - Low price, ample supply 	<ul style="list-style-type: none"> - High pressure - Low critical temperature (31°C)
Hydrocarbons	The measures taken to find suitable "natural" refrigerants as substitutes for CFC and HCFC have called attention to two hydrocarbons (propane and isobutene) that have properties similar to the most widely used CFCs and HCFCs.	<ul style="list-style-type: none"> - Compatible with materials normally used in refrigeration plants, such as copper and mineral oil - Similar physical properties to CFC-12 (isobutane) and HCFC-22 (propane) - Small amount of refrigerant needed - Lower prices than HFCs - Low environmental impact 	<ul style="list-style-type: none"> - Flammable at concentration of 1-10% v/v (requires additional safety measures) - Smaller volumetric cooling capacity

Hence, due to the flammable and toxic nature of hydrocarbons and ammonia, respectively, carbon dioxide is the most promising refrigerant and is viewed as a long term substitute. Along with its eco-friendly and safe characteristics, CO₂ based vapour compression systems offer many additional advantages over conventional systems such as a lower compression ratio, high volumetric cooling capacity, excellent heat transfer properties and compatibility with construction material. It is also an inexpensive and easily available natural refrigerant. However, due to its low critical temperature (31.1°C), these systems need to operate above critical pressure. It has been observed that CO₂ systems are more suitable for heat pump applications. Using CO₂ in cooling application has its own challenges. A detailed discussion is presented in the subsequent sections.

1.2 Carbon Dioxide - A Natural Refrigerant

1.2.1 Background

The term refrigerant got standardized in the year 1830 when Perkins first used sulphuric acid as a refrigerant in his invention; vapour compression machine. CO₂ also known as carbonic acid gas and carbonic anhydride is an old refrigerant. In the early part of the 20th century, CO₂ was one of the prominent refrigerants in marine systems and comfort air conditioning. Though Alexander Twining had first proposed CO₂ as a refrigerant in the year 1850, but it was Thaddeus S.C. Lowe, who first built a CO₂ system for ice production in 1867 and received a British patent as reported by William et al. (1999). In subsequent developments, Carl Linde built the first CO₂ machine in 1881. Three years later, W. Raydt built the first CO₂ based compression ice-making system. At this point of time, development in the field of CO₂ refrigerant was rather slow until Franz Windhausen of Germany designed a carbon dioxide compressor in the year 1886. The first continuous production of carbon dioxide refrigeration equipment started in USA in 1897 and in the late 19th century, application areas of CO₂ were widening rapidly and efforts were taking place to improve the basic cycle. J&E Company demonstrated the first two stage CO₂ compressor in 1889 (Thevenot ^{delete} R 1979). On the basis of Windhausen design, the Great Britain company J&E started manufacturing compressors in about 1890 until the middle of the 20th century, CO₂ based refrigeration systems were in the forefront and CO₂ was the leading refrigerant in marine applications.

The advent of refrigeration and air conditioning in the late 1800s had an enormous impact on thousands of industries. In Europe, where CO₂ refrigeration machines were the only choice at that time due to a ban on other toxic and flammable refrigerants such as NH₃ and SO₂. Refrigeration and air conditioning were changing the industrial world and creating its impact on society. Due to the limited choice of refrigerants at that time, United States was also using CO₂ during the 1890s. Ammonia and sulphur dioxide, being toxic and flammable, carbon dioxide was the preferred choice in refrigeration systems such as small cold storage systems, display counters, food markets, and kitchen and restaurant systems. Even in comfort air conditioning systems including passenger ships, hospitals, theatres and restaurants, carbon dioxide based systems were in use. In most of these systems, calcium chloride solution was used as a secondary refrigerant. Conclusively, being a safe refrigerant, all the public places and in food industries, CO₂ was the preferred refrigerant. However, then CO₂ systems were

technically inferior, e.g. compressors were slow running single or double acting cross head machines with crankcases at atmospheric pressure, expansion valves were manually controlled and condensers were often water cooled double pipe units (William et al. 1999). Though the technology they used was ancient by current standards, CO₂ machinery functioned satisfactorily.

It was reported that CO₂ caused loss of capacity and also offered low COP at high heat rejection temperature especially in warm climates. Moreover, with the available sealing technology at that time, it was difficult to build high pressure containment. To overcome some of these limitations, a modification was proposed through variations of two stage arrangements. However, these demerits led to carbon dioxide being marked as a low profile refrigerant and prompted people to search for new refrigerants, which are safe in operation and can offer better performance even at higher temperature and also can operate at low pressure. The outcome of all these efforts was the invention of fluorocarbons in the 1930s.

1930s was the revolutionary era in the field of refrigeration with the invention of a clan of fluorinated refrigerants by Thomas Modgley, Jr. The invention of these refrigerants changed the entire scenario of refrigeration and air conditioning industry. These non-flammable and nontoxic refrigerants eventually replaced the old refrigerants such as ammonia and sulphur dioxide in most of the applications owing to its better overall performance. Factors such as efficiency and capacity loss at high temperature, high pressure containment problems, no improvement in the system design to follow modern trends and the aggressive marketing of CFC products were some of the probable reasons for decline and demise of CO₂ refrigeration system. By 1950, CO₂ was completely out of business and not in use in any of the refrigeration applications. However, NH₃ was still the preferred refrigerant in large industrial applications but CFCs and HCFCs, were steadily making inroads in the range of refrigerant industry. Ironically, in both fronts, it turned out to be wrong with the fact that these refrigerants are rather harmful to the environment and are the main culprits behind damage of ultraviolet protecting stratospheric ozone layer. The understanding cambered the environmentalists to demand banning most of the CFCs and HCFCs in all the applications leading to the Montreal Protocol (1987). This compelled researchers to hunt for suitable and viable alternative refrigerants which are safe, environment friendly and should perform at least at efficiencies comparable to the CFCs. Efforts bore fruit resulting in the introduction of

alternative HFCs, having zero ODP and offering similar or better performance than the CFCs and the system could be retrofitted equally well.

Presently, in many refrigeration systems HFC, R134a, is in use on a large scale. But HFCs have substantial global warming potential which is thousand times more than that of carbon dioxide. Eventually HFCs are started to be treated as transitional refrigerants. It is worth mentioning that hydrocarbon based refrigerants are also on the same platform due to their flammability problem. Hence the refrigeration community was again in search for viable alternatives.

Today, extensive research are in progress to design newer but environmentally safer synthetic refrigerants as well as revival of interest towards natural refrigerants such as CO₂. The technological shortcoming that lead to failure of CO₂ technology are related to high pressure and temperature resistance material, high pressure compressor design, suitable material for heat exchanger etc. and these are partially solved already. Fig. 1 shows the historical graph of the progress and history of major refrigerants.

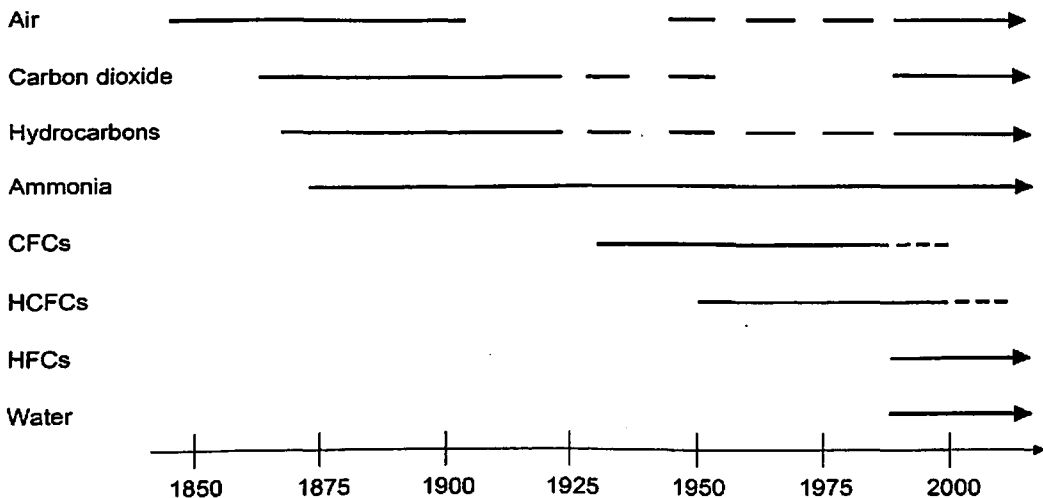


Figure 1.1: Historical introduction of refrigerants (Lorentzen & Pettersen, 1993)

In general, it is always better to select a refrigerant which is in harmony with the nature and already exist in abundance in the biosphere. Further, the cost of these compounds is expected to be much lower compared to synthetically produced compounds. In terms of environmental sustainability, technical acceptability, cost and safety, CO₂ can be one of the best choices for both heating and cooling applications of the system designed appropriately. Norwegian Professor Gustav Lorentzen was the first to reassure that the old refrigerant CO₂ is fit for its use in refrigeration, air conditioning and heat pump systems. In

the early 1990s, Lorentzen et.al,(1993), Lorentzen (1994, 1995) proposed an all new CO₂ cycle for car air conditioning, which operates in a trans-critical mode due to a low critical temperature at high ambient temperatures and high side pressure is regulated by throttle valve. Being a trans-critical cycle, heat rejection takes place in the supercritical region; hence condenser gets replaced by a gas cooler. Suitability of the CO₂ cycle for automobile air conditioning, a sector that dominates the global CFC emission, depends largely on its high working pressure. With today's advancement in technology, high design pressure of CO₂ systems is no longer a critical issue. On the contrary, high pressure systems may give considerable practical and economical advantages, due to reduction in dimensions and weight. In 1993, Lorentzen and Pettersen conducted experiments on a prototype CO₂ system for automobile air conditioning and concluded that considering all the practical factors, performance of the CO₂ system was at par with R12 system with equal heat exchanger dimension and design capacity (Lorentzen et al. 1994). These results had a significant impact on the research community that renewed interest on CO₂ systems almost dramatically. Subsequently, refrigeration industry and various research groups initiated several projects to make improvements in the basic trans-critical system and proposed many new concepts to overcome some of the inherent difficulties of a CO₂ system.

1.2.2 Properties of CO₂

Refrigerant properties are important and critical for the refrigeration system design and performance. The properties of CO₂ are quite unique in a certain range and the distinctness need to be considered from conventional refrigerants. CO₂ properties are compared with the most commonly used refrigerants in Table 1.3 The most distinguishing features of CO₂ are its low critical temperature (31.2°C) with relatively higher critical pressure (73.8 bar). Owing to its low critical temperature, CO₂ systems operate at high pressure trans-critical region, significantly higher than that of conventional refrigerants, as it is not possible to transfer heat to the ambient above this critical temperature by condensation. In a trans-critical cycle, high side pressure and temperature can be independently controlled in supercritical region to get the optimum operating condition. High pressure is advantageous since it attains very high volumetric cooling capacity leading to a compact design. Application areas where gliding temperature of heat discharge is favorable, such as in a heat pump, can easily adapt the trans-critical process of the CO₂ cycle which has a temperature glide in the gas cooler. The phase diagram of CO₂ is shown in Fig. 1.2 on P-T plane.

For 1994 there is only
single author

So it should be "Lorentzen et al."

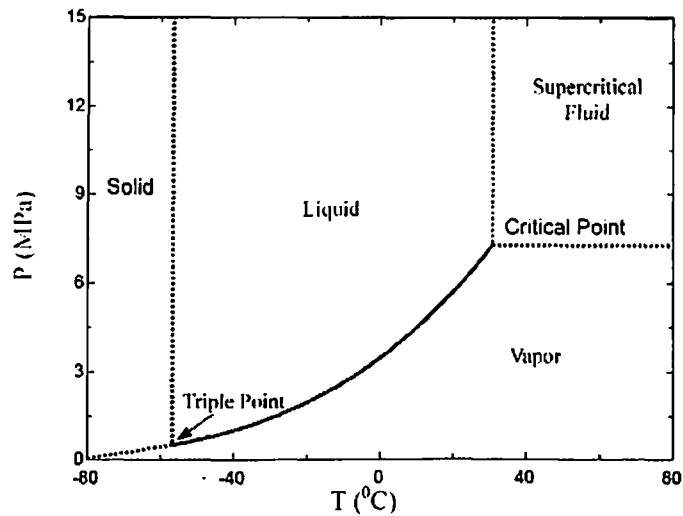


Figure 1.2: Phase diagram of CO₂ (Kim et al., 2004)

Table 1.3: Thermo-physical properties of most common refrigerants
(Lorentzen & Pettersen 1993, Riffat et al. 1997, Kim et al. 2004)

Refrigerant	R12	R22	R134a	R600a	R717	R744
ODP	0.82	0.055	0.0	0.0	0.0	0.0
GWP IPCC value (100 yrs)	8100	1700	1300	0.0	0.0	1
Flammable	No	No	No	Yes	Yes	No
Toxic	No	No	No	No	Yes	No
Molecular weight	120.9	86.5	102.03	58.0	17.03	44.01
Normal boiling point (°C)	-29.8	-40.8	-26.2	-11.6	-33.3	-78.4
Critical pressure (bar)	41.1	49.7	40.7	36.4	114.27	73.8
Critical temperature (°C)	112.0	96.0	101.1	134.7	133.0	31.2
Saturation pressure at (0°C)	3.09	4.98	2.93	1.56	4.29	34.8
Volumetric refrigeration capacity at 0°C (kJ/m ³)	2740	4344	2860	1509	4360	22545

The temperature and pressure for the triple point are -56.6°C and 0.52 MPa , respectively and the normal boiling point is -78.4°C . On low pressure side, the CO₂ system operates near to the critical point due to low critical temperature and high reduced pressure. The vapour pressure of CO₂ is much higher compared to other refrigerants. Owing to system operation near the critical point, vapour density of CO₂ that is encountered is much higher and the corresponding density ratio is much smaller resulting in a more homogeneous flow in the two-phase region compared to other refrigerants. Being a supercritical fluid, CO₂ properties change rapidly near the critical point with temperature in an isobaric process. This is an important characteristic of CO₂ which significantly influences the system design and analysis. CO₂ also offers excellent heat transfer properties.

In the supercritical region, the pseudo-critical temperature is defined as the temperature at which the corresponding specific isobaric heat capacity has the maximum value. The pseudo-critical region is very important since the thermo-physical properties of a supercritical fluid change drastically in this region. In Fig. 1.3, there are humps of specific heat near the pseudo-critical temperatures. The humps shift towards larger temperature values and become smoother as the absolute pressure increases. Some thermo-physical properties of carbon dioxide at pseudo-critical temperature are listed in Table 1.4.

Table 1.4: CO₂ properties at pseudo-critical temperature

	8MPa	9MPa	10MPa
T_{pc} (°C)	34.7	40	45
C_p (kJ kg ⁻¹ K ⁻¹)	35.2	12.8	8.08
ρ (kg m ⁻³)	456	486	498
K (W m ⁻¹ K ⁻¹)	0.08874	0.07081	0.06485
μ (kg m ⁻¹ s ⁻¹)	32.2	34.6	35.8

insert dot
provide reference from which these values are taken

This particular temperature point plays a very important role in heat transfer behavior because the specific heat capacity is directly related to the heat transfer coefficient. Usually, a higher specific heat will induce a higher heat transfer coefficient. But, near the pseudo-critical temperature, not only the specific heat, but also density, conductivity, and viscosity have uneven values as shown in Fig. 1.3 - Fig. 1.6. Those uneven properties make the heat transfer characteristics much different from that of the normal, single-phase fluid.

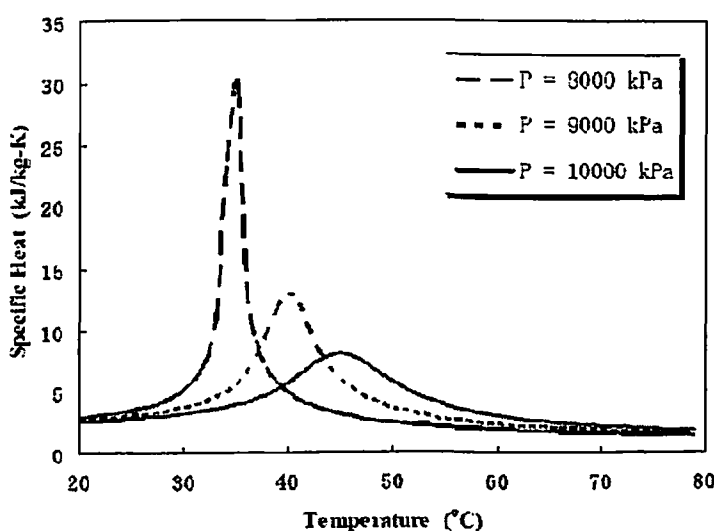


Figure 1.3: Specific heat versus temperature in supercritical range
(Robinson and Groll 1998)

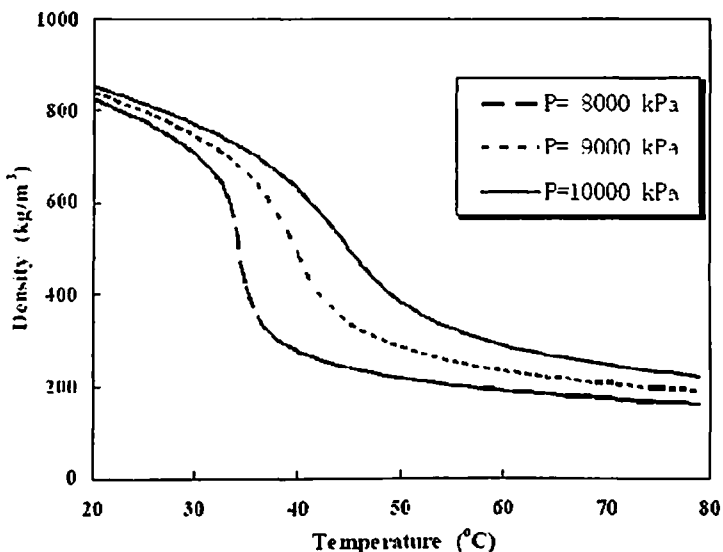


Figure 1.4: Density versus temperature in supercritical range (Robinson and Groll 1998)

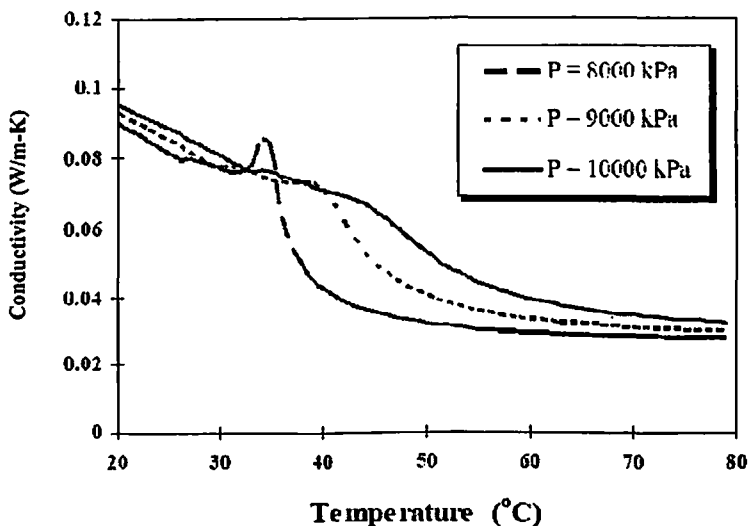


Figure 1.5: Conductivity versus temperature in supercritical range (Robinson and Groll 1998)

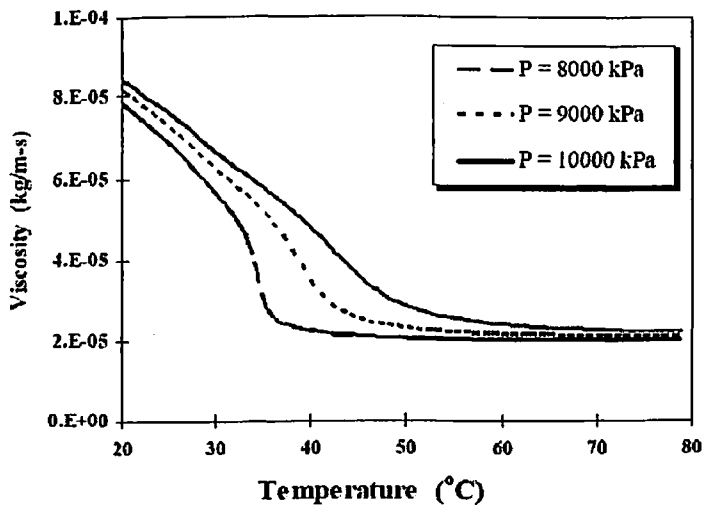


Figure 1.6: Viscosity versus temperature in supercritical range (Robinson and Groll 1998)

In brief, the thermo-physical, thermodynamic and transport properties of carbon dioxide are at least comparable to other refrigerants. Further, CO₂ has a number of advantages as a refrigerant which are presented below:

1. It has a successful past as a refrigerant.
2. It has good compatibility with normal lubricants and commonly employed machine materials.
3. Being a naturally occurring substance, it is an environment friendly refrigerant characterized by zero ODP and GWP of 1.
4. It is non-flammable and non-toxic refrigerant.
5. Easily sourced from biosphere and no recycling is required.
6. Pressure and temperature can be independently controlled in the supercritical region.
7. CO₂ systems are quite compact due to high volumetric efficiency at high working pressure.
8. Its properties are well established and modeled.
9. Pressure ratio is much lower compared to conventional refrigerants.
10. Large temperature glides occur in the gas cooler during heat transfer and wider applicable temperature range is possible with such systems.

1.2.3 Application areas

Current research on trans-critical CO₂ systems have investigated a variety of possible applications. As described earlier, thermo-physical properties of CO₂ especially in supercritical region are quite different and unique which can be exploited favorably in various applications as reported by Kim et al. (2004). The first application of CO₂ systems was as a heat pump in water heater due to large refrigerant temperature glide. A CO₂ heat pump water heater may produce hot water with a temperature of up to 90 °C with marginal loss in efficiency. Mobile air conditioning systems have been and still are a dominating source of refrigerant emission to the atmosphere. Due to its high volumetric cooling capacity, mobile air conditioning is probably the most promising application area of CO₂ trans-critical cycle. It is possible to make an ultra compact gas cooler, which increases energy efficiency indirectly by enabling more

aerodynamically streamlined vehicle design. Several car manufacturers have already adapted the CO₂ technology. Carbon dioxide heat pump systems can be used for heating of the passenger compartment during winter. These systems can also be employed as a heat pump dryer. It is reported that due to better temperature adaptation, CO₂ vapour compression dryer are energy efficient. One other application where a CO₂ system can be used efficiently is situations where simultaneous heating and cooling is required, e.g. in food processing and dairy industry, process heating or domestic applications with various heating and cooling combinations.

1.2.4 Commercial aspects

Use of CO₂ is not only restricted to trans-critical cycle; investigations are in progress to use CO₂ as a secondary fluid or as a bottoming (sub-critical) cycle refrigerant in cascade systems with other natural refrigerants. Being natural refrigerants, NH₃-CO₂ pair is well sought after in the industrial sector. In industrial refrigeration, 500 kW plants are now using CO₂ as a refrigerant in the low-temperature stage to manufacture ice-cream. Stellar Group of USA commissioned the world's largest NH₃-CO₂ plant in the year 2002. In 2003, Gresco B.V. from the Netherlands introduced NH₃-CO₂ based cascade system for freezing applications. In a joint venture, Kansai Electric Power Co. and Mayekawa Mfg. Co. have successfully tested an 80 kW NH₃-CO₂ ultra low temperature cascade system using CO₂ as a bottoming cycle refrigerant. Several other fluid combinations are already in operation in the Nordic countries employing CO₂ as a volatile secondary refrigerant.

Several Japanese companies brought CO₂ heat pump water heaters in market in the recent past. Denso of Japan is the pioneer of CO₂ heat pump water heater. By using the patented Shecco technology, they developed CO₂ heat pump hot water supply unit named EcoCute. Using waste heat from an industrial NH₃ refrigeration system, a 25 kW pilot plant was installed in a food-processing factory in Larvik, Norway. The *Refrigerants, "Naturally!"* initiative was launched in 2004 by Coca Cola, Unilever and McDonald's, and subsequently Carlsberg, IKEA and PepsiCo joined the network in 2006. It is an alliance for the food and drink, food service and retail sectors that require point-of-sale cooling technology. Over the last few years these companies, together with their suppliers, have developed and tested innovative, commercially viable HFC-free refrigeration technologies primarily based on CO₂. In 2005, this initiative was the recipient of the U.S. Environmental Protection Agency's Climate Protection Award in recognition for its leadership in developing innovative ways to

aerodynamically streamlined vehicle design. Several car manufacturers have already adapted the CO₂ technology. Carbon dioxide heat pump systems can be used for heating of the passenger compartment during winter. These systems can also be employed as a heat pump dryer. It is reported that due to better temperature adaptation, CO₂ vapour compression dryer are energy efficient. One other application where a CO₂ system can be used efficiently is situations where simultaneous heating and cooling is required, e.g. in food processing and dairy industry, process heating or domestic applications with various heating and cooling combinations.

1.2.4 Commercial aspects

Use of CO₂ is not only restricted to trans-critical cycle; investigations are in progress to use CO₂ as a secondary fluid or as a bottoming (sub-critical) cycle refrigerant in cascade systems with other natural refrigerants. Being natural refrigerants, NH₃-CO₂ pair is well sought after in the industrial sector. In industrial refrigeration, 500 kW plants are now using CO₂ as a refrigerant in the low-temperature stage to manufacture ice-cream. Stellar Group of USA commissioned the world's largest NH₃-CO₂ plant in the year 2002. In 2003, Gresco B.V. from the Netherlands introduced NH₃-CO₂ based cascade system for freezing applications. In a joint venture, Kansai Electric Power Co. and Mayekawa Mfg. Co. have successfully tested an 80 kW NH₃-CO₂ ultra low temperature cascade system using CO₂ as a bottoming cycle refrigerant. Several other fluid combinations are already in operation in the Nordic countries employing CO₂ as a volatile secondary refrigerant.

Several Japanese companies brought CO₂ heat pump water heaters in market in the recent past. Denso of Japan is the pioneer of CO₂ heat pump water heater. By using the patented Shecco technology, they developed CO₂ heat pump hot water supply unit named EcoCute. Using waste heat from an industrial NH₃ refrigeration system, a 25 kW pilot plant was installed in a food-processing factory in Larvik, Norway. The *Refrigerants, "Naturally!"* initiative was launched in 2004 by Coca Cola, Unilever and McDonald's, and subsequently Carlsberg, IKEA and PepsiCo joined the network in 2006. It is an alliance for the food and drink, food service and retail sectors that require point-of-sale cooling technology. Over the last few years these companies, together with their suppliers, have developed and tested innovative, commercially viable HFC-free refrigeration technologies primarily based on CO₂. In 2005, this initiative was the recipient of the U.S. Environmental Protection Agency's Climate Protection Award in recognition for its leadership in developing innovative ways to

combat global warming by promoting the development of environmentally friendly refrigeration technology. Several car manufacturers have had test vehicles on the road since late nineties. After years of research and development, CO₂ technology for mobile air conditioning has reached a very advanced level. Nissan is planning to launch the fuel cell vehicle installed with a CO₂ air conditioning system. Car manufacturers (BMW, Daimler-Benz, Rover, Volvo, Volkswagen), system suppliers (Behr, Valeo), and a compressor manufacturer (Danfoss) are working together to develop a vehicle carbon dioxide air conditioning system. Dorin of Italy has been manufacturing semi-hermetic CO₂ compressor (Pettersen et al. 1994) while Sanyo, Tecumseh and Danfoss are the new brands for CO₂ hermetic compressors.

CHK it: It should be Pettersen and Skarzen
OR
Pettersen et al. 1998
OR
2000 c1994

1.3 Motivation and Objective

CO₂ trans-critical system offers several application possibilities in all walks of life such as mobile air conditioning, heat pump based water heating and simultaneous heating and cooling. One of the major advantages of trans-critical CO₂ heat pump systems is the high temperature lift compared to others. However, system performance deteriorates at high heat rejection temperature. The majority of the work reported are for heating application, which are suitable for colder climatic conditions. However in Indian condition, the application will be mainly for cooling. Using the system for cooling purposes has its own challenges, especially when it is used in warmer climatic conditions. The environmental temperature and the design conditions in India vary drastically from place to place. The optimum operating conditions for CO₂ system in trans-critical cycle will also vary with the environmental temperature. Hence it is required to analyze and optimize the performance of the system at different clusters of the temperature zones. For each temperature zones it is required to have a specific design of components with optimum operating conditions to achieve best possible performance of the system. The high heat rejection temperature is major challenge for CO₂ trans-critical cycle (Especially in warmer climatic conditions), hence the gas cooler is one of the most sensitive component of the overall system and its design is very much crucial. The trans-critical refrigeration cycle has two independent parameters in pressure and temperature, while conventional sub-critical cycles have only one in temperature. Consequently, unlike the sub-critical cycle, pressure can be independently controlled in a trans-critical cycle to optimize the

system performance. Design of the components and selection of the operating conditions must look to optimize the performance of a trans-critical refrigeration system. Based on the above discussion, the present work focuses on the design and optimization of gas cooler for trans-critical CO₂ refrigeration system in Indian context.

1.3.1 Objectives of the research

This research work in doctoral thesis is aimed to optimize the gas cooler through simulation study for trans-critical CO₂ refrigeration system in Indian conditions. The following object have been laid down for this research work:

1. Modeling and simulation of heat transfer in gas cooler for trans-critical CO₂ based refrigeration system.
2. Model validation and parameter optimization for enhanced heat transfer to explore the usefulness in high ambience temperature application (typical Indian atmosphere).
3. Formulation of design guidelines for optimized performance of gas coolers in CO₂ based trans-critical refrigeration systems.

1.4 Overview of the Thesis

This report presents, design and optimization of gas cooler for trans-critical carbon dioxide refrigeration system. The work reported in this thesis has been organized into eight chapters. The content of each chapter is briefly described below:

Chapter 1 gives an introduction to the thesis. An introduction accompanied by a brief history of CO₂ as a refrigerant, its revival, thermodynamic and transport properties and comparison with other refrigerants is presented in this chapter. Application areas and recent information on the commercial aspects of CO₂ based systems and aim of the present work is also elucidated.

Chapter 2 deals with a comprehensive review of relevant literature. It includes a survey of the research efforts made on the various aspects of the trans-critical cycle including component design and system design issues, cycle modifications such as multi pressure cycle, work recovery turbine, etc. and application oriented progress followed by detailed reviews on the various design aspects of gas cooler and cycle modification to improve the performance of the trans-critical CO₂ refrigeration system.

Chapter 3 covers the various issues and challenges associated with trans-critical CO₂ refrigeration systems in Indian conditions. It also discusses the ideal cycle based theoretical analysis of the system and gas cooler design issues at different clusters of the temperature zones in Indian conditions. Finally guideline for operating conditions for an ideal cycle are explored.

Chapter 4 discusses the detailed mathematical modeling of gas cooler followed by the overall system. Numerical implementation of the model, discretization, boundary conditions and MATLAB code are discussed. Further the validation of model using published experimental results are provided.

Chapter 5 presents the simulation results for modified dimensions and operating conditions of the gas cooler using the model proposed in chapter 4. The performance analysis of the gas cooler and their alternative modified design followed by overall systems are separately discussed for each temperature zones.

Chapter 6 presents the simulation results for optimization of the gas cooler using the above model. The chapter investigates the performance optimization of the gas cooler and their alternative modified design followed by overall systems performance are discussed for each temperature zones separately. The investigation consider power consumed by the gas cooler fan for simulating the overall performance of the system.

Chapter 7 presents the simulation results for optimization of the gas cooler using the above model along with the modified cycle. The performance optimization of the gas cooler together with alternative modified design was investigated and overall system with work recovery turbine are discussed for each temperature zones separately. In this case, the power consumed by the gas cooler fan have also been consider for the overall performance.

concludes the thesis
Chapter 8 ~~The thesis work concludes~~ with important findings based on this study. The major conclusions and recommendations for future work are also presented.

This can be used as the reference ↓

Lorentzen G, Pettersen J. (1992) New possibilities for non-CFC refrigeration. in: Pettersen J. editor, IIR International Symposium on Refrigeration, Energy and Environment. Trondheim, Norway, 147-163 ←

Literature Review

This chapter presents a comprehensive survey of reported studies related to trans-critical CO₂ systems and applications. Studies focusing on the components and modifications on the cycles such as work recovery turbines, ejector expansion, multi stage cycles and internal heat exchanger to improve the system performance are discussed.

The literature review attempts to summarize, more than two hundred research papers published during 1993 and 2013, in various reputed journals such as International Journals of Refrigeration, Applied Thermal Engineering, ASHRAE Transactions, HVAC&R Research, and conference proceedings namely IIR, ASHRAE, and IRAC.

CO₂ (R-744) was introduced as a refrigerant in 1870s, but due to lack of adequate technology, the COP was low. Development of synthetic refrigerants with high COP like CFCs in the 1930's and HCFCs in 1940's led to almost disappearance of CO₂ based systems. Some research activities were noticed in the 1900s related to cycle modification and compressor design to improve the CO₂ system performance, but such technologies are obsolete now.

include a reference for proving this statement

← In 1992, when Lorentzen brought forward the theory of CO₂ trans-critical refrigeration cycle and built a CO₂ based Automotive Air Conditioning (AAC) prototype leading to renewed interest worldwide towards efficient CO₂ system as reported in Lorentzen et. al. (1993), and Lorentzen (1994, 1995).

and Pettersen

After the revival of CO₂ as a refrigerant in trans-critical cycle, many changes have taken place towards development of CO₂ trans-critical system. Now researchers are trying to bring new and more efficient breed of trans-critical CO₂ systems by blending old concepts with state of the art technology. Overall, this chapter reflects detailed research developments on various aspects of CO₂ trans-critical systems.

2.1 CO₂ Trans-Critical Cycle

The working of CO₂ cycle is different from other conventional refrigerant based subcritical cycles owing to its unique properties; low critical temperature (31.2°C) with relatively higher critical pressure (73.8 bar). CO₂ systems with normal refrigeration, heat pump and air conditioning temperature range operate at high pressure, typically 5-10 times higher than that with conventional refrigerants, in the trans-critical region as it is not possible to transfer heat to the ambient at temperature below this. Hence the modified vapour compression cycle for CO₂ is named as trans-critical cycle where evaporation takes place at sub-critical pressure similar to conventional refrigerants while heat rejection takes place at supercritical pressure.

^{and Pettersen} Lorentzen ~~et. al.~~ (1993), Lorentzen (1994, 1995) have shown in their seminal studies that difficulties concerning low critical temperature of CO₂ can be successfully overcome by operating the system in the trans-critical mode, where single-phase heat rejection occurs above the critical temperature in the gas cooler instead of condenser as in conventional systems, and where pressure and temperature can be controlled independently to obtain optimum performance.

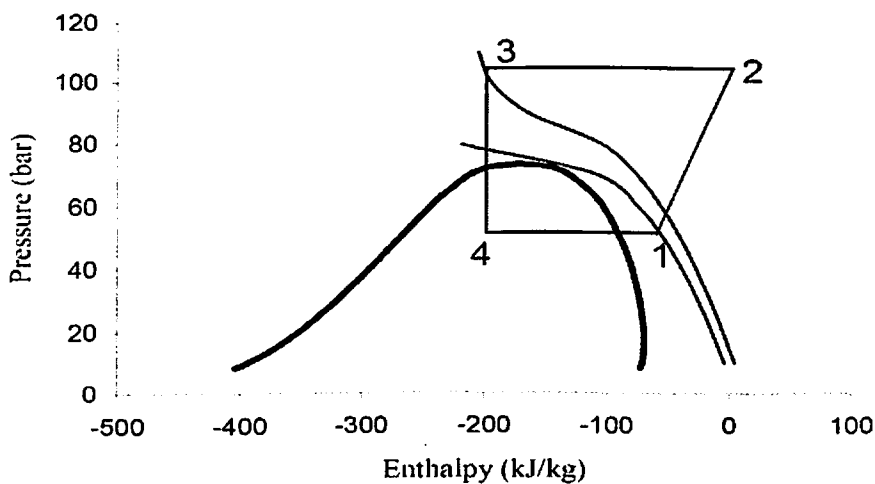


Figure 2.1: P-h diagram of trans-critical CO₂ cycle

^{and Skarhagen} Pettersen ~~et al.~~ (1994), reported that the gas cooler pressure is an influential parameter where increase in gas cooler pressure does not always lower the COP in a trans-critical cycle unlike in conventional subcritical systems. This can be attributed to the unique behavioral pattern of CO₂ properties around the critical point and beyond, where the slope of the isotherms is quite modest for a specific pressure range; at pressure above and below this range, the isotherms become much steeper as shown in Fig. 2.1

Increasing the high side pressure increases the COP initially and then starts decreasing because beyond a certain pressure, increase in compressor work overtakes the gain in refrigeration capacity due to steep isotherms. To obtain the optimum pressure which yields a maximum COP, correlations have been suggested by various authors discussed in subsequent sections.

2.1.1 Optimum high pressure

Several authors like Inokuty (1928), Kauf (1999), Liao (2000), Sarkar (2004), and Chen (2005) etc. especially focused on the optimization problem of a trans-critical system high pressure. By means of different simplifying assumption, the same authors theoretically worked out expressions to define the optimal cycle high pressure as a function of the refrigerating cycle variables, which are mainly the gas cooler refrigerant outlet temperature and the evaporating temperature. Inokuty (1928), has suggested a graphical method for finding the compression pressure of CO₂ refrigerant machine for maximizing COP. Considering component performance data, Kauf (1999), optimized the high side pressure in terms of ambient temperature based on a steady state simulation model. Liao et al. (2000), have developed correlations for the optimum heat rejection pressure in terms of appropriate parameters for specific conditions and verified that the optimum heat rejection pressure is mainly a function of gas cooler outlet temperature, evaporator temperature and compressor performance.

Sarkar et al. (2004) developed the correlations based on their steady state analysis for optimum COP and gas cooler pressure in terms of gas cooler exit and evaporator temperatures for simultaneous cooling and heating applications. Later, based on cycle simulation, Chen et al. (2005) obtained a correlation for optimum compressor discharge pressure in term of system parameters, emphasizing internal heat exchanger effectiveness and derived a practical effectiveness expression for internal heat exchanger. Sarkar et al. (2007), again discuss the optimum COP and gas cooler pressure in terms of gas cooler exit and evaporator temperatures for high temperature heating applications. Cabello et al. (2008), compared optimal gas cooler pressures of an experimental plant with the proposed relations, finding significant deviations between the experimental and calculated values. More recently, Luca et al. (2010) analyzed the different approximated solutions of the optimization problem and proposed a better approximation through finned coiled gas cooler simulation for trans-critical cycle.

this reference is not available at the end list of references

Zhang et al. (2011) reported correlation-free on-line optimal control method for CO₂ trans-critical refrigeration systems. It uses the on-line correction formula to track the optimal pressure set point. The results showed that the proposed method can well track the optimal pressures and is robust enough to resist the sampling noise.

Most recently, Qi et al. (2013) investigated experimentally, the optimal heat rejection pressure for a trans-critical CO₂ heat pump water heater. Variation of COP on the optimal heat rejection pressure with gas cooler outlet refrigeration temperature range from 25 to 45°C at different ambient temperatures was reported.

2.1.2 Applications of trans-critical CO₂ systems

Several researcher have reported numerous simulation and experimental based analysis of trans-critical CO₂ systems for specific applications. Summarizing all the major application of CO₂ system are in mobile air-conditioning, heat pumps, water heaters, drier and simultaneous heating and cooling.

Pettersen (1997), showed experimentally that the effect of evaporator temperature on the heating capacity and COP of heat pump, it was found weaker compared to other refrigerants which makes it possible to maintain a high heating capacity even at low ambient temperature with the CO₂ systems. The heating capacity increases rapidly initially with rise in discharge pressure followed by a flatter trend above the optimum discharge pressure. However, other factors such as maximum allowable pressure, maximum motor load and compressor temperature limit the discharge pressure. In comparison with condenser exit temperature of conventional refrigerants, cooling COP of CO₂ system is more sensitive to gas cooler exit temperature due to large throttling losses. The lower temperature approach of a CO₂ gas cooler yields a significant improvement in actual COP.

Schmidt et al. (1998), has compared the thermodynamic behavior of two dehumidification drying heat pump cycles using the subcritical R134a process and the trans-critical CO₂ process. Neksa et al. (1998, 1999), presented experimental results for a prototype CO₂ heat pump and showed that CO₂ is very well suited as a working fluid for tap water heating. Hwang et al. (1999), developed a laboratory prototype CO₂ refrigeration system to experimentally investigate the performance potential of the system in comparison with R-22 for water chilling applications and showed that the actual CO₂ cycle performance was similar to the R-22 cycle.

Wang and Radermacher (1999)

OR
Hwang et al. (2005)

which is correct

This is not listed under
reference
Add it separately.

Klockner et al. (2001)

Andrey et al. (2001), reported a theoretical analysis of a trans-critical CO₂ air conditioning system. Performance of the system was analyzed with semi hermetical compressor and the effects of compressor efficiency on the system were discussed. Later, KloE. cker et al. (2001) had experimentally investigated the trans-critical CO₂ heat pump for laundry dryers. Brown et al. (2002), has evaluated the performance of CO₂ with suction line heat exchanger (SLHX) and R134a automotive air conditioning systems using semi-theoretical cycle model. White et al. (2002), developed a prototype for trans-critical CO₂ heat pump for water heating to temperatures greater than 65°C while providing refrigeration at less than 2°C. Richter et al. (2003), experimentally compared the performance of a commercially available R410A heat pump and a prototype CO₂ system in heating mode using aluminum micro channel heat exchangers and semi-hermetic compressor. The measured heating COP was reported to be slightly lower but capacity was higher with the CO₂ system.

Simultaneous air conditioning and water heating using CO₂ as the refrigerant was demonstrated to be promising as an energy recovery system by Adriansyah (2004). Results showed that the combined system is more effective compared to an air conditioning system without heat recovery. Sergio et al. (2004) have tested the trans-critical CO₂ system used for supermarket operations in the North of Italy since January 2003. The seasonal COP was calculated, based on prior laboratory measurements, and a comparison made with a conventional direct expansion system using R404A. Bullard et al. (2004), presented a thermodynamic cycle analysis that accounted for the presence of realistic heat exchanger sizes in a residential air to air heat pump system. The analyses explored a variety of options for integrating domestic water heating into the heating and cooling cycles. Fartaj et al. (2004), presented a second law analysis of the trans-critical CO₂ refrigeration cycle considering individual component separately and indicated that the compressor and the gas cooler exhibit the largest irreversibility. Later on, a comparative study on exergy analysis was presented by Yang et al. (2005), for trans-critical CO₂ refrigeration cycles employing a throttle valve and an expander. The results showed that the COP and exergy efficiency improve significantly when an expander is used instead of a throttle valve. Rigola et al. (2005), reported a numerical study of a trans-critical carbon dioxide refrigerating cycle. The heat exchangers in particular, and the whole cycle in general, are simulated under a carbon dioxide refrigerating system. An experimental unit, specially designed to be used with carbon dioxide as refrigerant fluid, was used to validate the numerical results.

Cecchinato et al. (2005) investigated, the design of air/water heat pumps for tap water using CO₂ in trans-critical cycle and compared the performance with conventional system. Neksa (2005), has experimentally tested the CO₂ heat pump systems for combine space and water/air heating applications. Cho et al. (2005) experimentally tested the performance of a CO₂ heat pump by varying the refrigerant charge amount at standard cooling condition. A comparison of the performance & sensitivity of the CO₂ system as a function of refrigerant charge for the R22, R410A, and R407C systems is made. The cooling COP of the CO₂ system was reported to be more sensitive to refrigerant charge. Liu et al. (2005) experimentally tested a CO₂ automotive air conditioner prototype with swash plate compressor, finned tubes gas cooler and evaporator, manual expansion valve and an internal heat exchanger. The effect of lubricant, CO₂ charge, evaporator outlet pressure, compressor speed, air inlet temperature, flow rate of the gas cooler, and the air flow rate of the evaporator was discussed. Adeyefa et al. (2006) experimentally investigated a direct evaporating CO₂ cooling device designed for the verification of a centralized aircraft on-board cooling system, where optimal pressures calculated from process states are passed to an integrated pressure control. *uok*

Sarkar et al. (2006) presented a steady state simulated model including heat transfer and fluid flow effects for a CO₂ trans-critical system, suitable for dairy application where there is a demand for simultaneous cooling (4°C) and heating (73°C). Based on the simulation results, correlations for optimum system COP and optimum discharge pressure were developed. A monogram was developed to obtain an optimal design in terms of area ratio and discharge pressure to attain the maximum cooling COP. Dubey et al. (2008) have discussed the pros and cons of CO₂ as a refrigerant and presented the recent developments and state of art technology for adopting CO₂ in various refrigeration, air conditioning and heat pump applications. Sarkar et al. (2008) carried out a comprehensive exergy analysis of the trans-critical CO₂ heat pump systems for simultaneous heating and cooling applications including heat transfer and fluid flow effects. Results shown that almost 11% exergy loss in the throttle valve occurs which is in contrast to conventional systems. Cabello et al. (2008) experimentally evaluated the energy efficiency and optimal gas cooler pressures of a single-stage refrigerating plant working with carbon dioxide as refrigerant in trans-critical conditions. The performance of the plant was tested at three different evaporating temperatures (-0.9, -10.1 and -18.1°C), for three gas cooler refrigerant

chk
the
year
otherw
it u
not
resto
unde
refe
Co

outlet temperatures (31.2, 33.6 and 40°C) at each evaporating temperature and in a wide range of gas cooler pressures (74.4-104.7 bar).

Zha et al. (2008), reported a modified construction of reciprocating compressor with economizer port, a Voorhees compressor was introduced and the heat pump cycle with Voorhees economizer was compared with the traditional screw or scroll economizer cycles. Eisenhower et al. (2009) discuss the multiplicity of stable solutions in a trans-critical hot water heat pump used in their prototype units that two steady states exist. Reduced order dynamic modeling highlight the state-dependent heat transfer coefficient in the evaporator dynamics as a contributing cause to this bistable phenomena. Specifically, the bilinear nature of the controlled gas cooler and its coupling to the dynamic nonlinearity in the evaporator induces a system wide bifurcation in the equilibrium conditions with regard to system efficiency. Byrne et al. (2009) simulated the heat pump for simultaneous heating and cooling (HPS) designed for hotels, luxury dwellings and smaller office buildings. The main advantage of the HPS was to carry out simultaneously space heating and space cooling in a dual mode. The ambient air was used as a balancing source to run in heating or cooling mode.

Kim et al. (2009) experimentally investigated the effects of the operating parameters on the cooling performance of a trans-critical CO₂ automotive air conditioning system. Effect of Gas cooler and evaporator air inlet temperature, evaporator air flow rate, compressor speed, and optimum high pressure were investigated. Gas cooler air inlet temperature was taken as 25°C and 35°C during idling condition, and the effect of gas cooler air inlet temperature of 35°C and 45°C during driving condition, and micro channel type with Al tube gas cooler was selected for the studied. Fernandez et al. (2010) tested the performance of a CO₂ heat pump water heater and investigated the effect of ambient temperature and hot water temperature on the overall coefficient of performance (COP) during full tank heating in three scenarios typical of residential water heating. Two stage compression with internal heat exchanger and single stage with suction line heat exchanger were used for the analysis.

Sarkar et al. (2010) presented the experimental results of a trans-critical CO₂ heat pump prototype for simultaneous water cooling and heating applications. System behavior and performances such as cooling capacity, heating capacity, and system COP

have been studied experimentally for various operating parameters. Water cooler type gas cooler and evaporator used in the experiment.

Yang et al. (2010), has developed a mathematical model for steady-state simulation of trans-critical CO₂ water-to-water heat pump system with an expander. Simulation result is presented for discharge pressure range from 7.5MPa to 11.5MPa.

Goodman et al. (2011a) developed a trans-critical CO₂ heat pump water heating system model incorporating analytical heat exchanger models and an empirical compressor model. The effects of a SLHX and different water heating schemes were investigated. Same is experimentally tested in Goodman et al. (2011a). Chen et al. (2010) analyzed the dynamic performance of a solar driven carbon dioxide trans-critical power system by simulations for typical Swedish climatic conditions. Ge (2011a) described the modeling procedure employed in the supermarket simulation model 'SuperSim' for the simulation of the performance of centralized vapour compression refrigeration systems and their interaction with the building envelope and HVAC systems. Their model was validated against data from a supermarket for comparing R404A and CO₂ refrigeration systems and the optimization of the performance of trans-critical CO₂ systems. These results are presented in Ge (2011b) as Part II of the paper.

Cecchinato et al. (2011) developed a CO₂ commercial single door bottle cooler that was not only cost competitive but also matches the performance of typical cost optimized R404A and R134a systems. Compressors with different displacement and efficiency values were evaluated for refrigerating systems with fin and tube and steel wire-on-tube gas coolers. Capillary tubes were also tested. Minetto (2011), described the development of a CO₂ air/water heat pump for the production of tap hot water in a residential building. System performance was analyzed with a single-stage piston compressor, a coaxial type gas cooler, an electronic expansion valve, a finned tube evaporator and a low pressure receiver. A new control method for the upper cycle pressure was proposed to maximize the COP of the heat pump, while the water mass flow was adjusted to maintain the set water temperature at the gas cooler exit.

Ferdinando et al. (2011) tested the similar system for a CO₂ household heat pump dryer. Chesi et al. (2012) have investigated refrigerating cycles and equipment performance which operates with CO₂ refrigerant in trans-critical cycle at different evaporator and gas cooler pressure and 20 - 40°C of gas cooler outlet temperature. The study also includes experimental data obtained while testing a reciprocating

compressor and a single-stage cycle layout both with and without using an internal heat exchanger.

Wang et al. (2013),^{insert "dot"} experimentally investigated the air-source transcritical CO₂^{delete} heat pump water heater system at a fixed water inlet temperature of 12°C. A prototype was tested in a range of ambient temperatures (-15°C to 35°C) and water outlet temperatures (55°C to 80°C). Correlation for the optimal discharge pressure as the function of ambient temperatures and water outlet temperatures was reported. Boccardi et al. (2013),^{remove comma} reported results of an experimental investigation of a small capacity, air-forced refrigerating plant working with CO₂. The air inlet temperatures at gas cooler and evaporator was varied from 16°C to 31°C, and from -25°C to 25°C, respectively, to cover the range of temperatures under conditions typical of commercial refrigeration, during quasi-steady state operation. The thermodynamic analysis of the system performance was carried out by independently varying the pressure at the gas cooler and by overfeeding the liquid receiver to point out the effect of refrigerant charge. Sawalha (2013),^{remove comma} modeled a CO₂ trans-critical refrigeration system with heat recovery from the de-super heater. Cooling and heating COPs of the system were calculated at different ambient temperatures for floating condensing and heat recovery modes.

2.2 Components Design of Trans-Critical CO₂ Refrigeration System

The major components of the system are compressor, gas cooler, expansion device, and evaporator. Due to its trans-critical operation, unique properties of CO₂ and high operating pressure, CO₂ trans-critical systems and their components are different in design from the conventional vapour systems. Since the components are subjected to high pressure, a special attention is required while designing the components for a CO₂ system. Material selection, component design, their operation and maintenance are some of the critical issues involved in the design and selection of system components. Also the individual components should be compatible to each other.

2.2.1 Compressor

The compressor, one of the important component in a vapour compression system, has a strong influence on system performance. High pressure in a CO₂ trans-critical system makes the compressor more susceptible. With a background of substantial developmental

work carried out by several manufacturers, the technology has progressed fairly well lately. *Suss and Kruse*

Suss et al. (1998), showed that even in the presence of high pressure difference, high volumetric and energy efficiency can be achieved by reducing the leakage losses up to a reasonable amount with an appropriate design of the compressor. Later on, Neksa et al. (1999) showed that a two-stage compressor has the potential to improve the COP by 20%. Fukuta et al. (2000) showed the possibility of sliding vane mechanism in CO₂ compression and expansion employing a mathematical model and concluded that to get acceptable efficiency, leakage losses should be minimized. Kim et al. (2004a) presented numerically simulated results for scroll, two-stage twin rotary, and two cylinder reciprocating CO₂ compressors for water heat pump applications. Kim et al. (2004b), explored in their review, stand that due to the high density of CO₂, these compressors are compact compared to other refrigerants such as R134a. Efforts were made to develop a hermetic prototype machine of single cylinder 2.6 cm³ using some part of R-22 machine. It was found that isentropic and volumetric efficiency of CO₂ compressor were not drastically different; just 9-15% and 5% lower than the R22 machine, respectively. These findings were considered to be a milestone in the early development. Subsequently a series of semi-hermetic reciprocating CO₂ compressors were developed with the overall isentropic and volumetric efficiency of 0.69 and 0.77, respectively. Clearance volume ratio for a reciprocating compressor should not be more than 5% to have the volumetric efficiency at par with scroll compressor. Mechanical losses were unusually large at the thrust surface supporting the scroll orbit with CO₂ in case of scroll compressor. In addition, other experimental and theoretical studies were conducted on CO₂ scroll compressor.

Rigola et al. (2005) presented a comparative study of a CO₂ trans-critical refrigeration system and conventional subcritical refrigeration system of small capacity with an evaporative temperature of around 0°C, based on numerical and experimental results emphasizing behavior of hermetic reciprocating compressors used in these systems. Nieter (2006), described some of the challenges experienced in the application of a CO₂ reciprocating piston compressor (Dorin, TCS362) to a water heating heat pump. *delete comma* Due to the characteristics of CO₂ in a trans-critical cycle, including high pressures, high discharge temperatures, and high solubility in oil would results in operational particular

difficulties. They suggested design improvement as the way to overcome these challenges.

Yoshida et al. (2008), studied a higher compression efficiency scroll compressor for CO₂ heat pump water heaters, focusing on reduction of leakage loss. Gas leakage through radial and axial clearances was identifying to be caused by two predominant factors; “uneven thermal expansion on scroll members due to temperature difference between suction and discharge” and “difference of thermal expansion coefficient between fixed and orbiting scroll.” Temperature distributions on fixed and orbiting scrolls in operation was measured and several new scroll profiles were studied to reduce leakage loss in consideration of the uneven thermal expansion, and reported a higher efficiency CO₂ scroll compressor. Sanchez et al. (2010) evaluated, from an energy point of view, the effects of the superheat caused in the refrigerant by the electric motor cooling in a semi hermetic sealed compressor (SHSC) installed in an experimental refrigerating plant, for CO₂ trans-critical cycle. The tests were conducted for evaporating temperature (0, -10, and -17°C) at compressor speeds (1150, 1300, 1450, and 1600 rpm) over a range of discharge pressures from 74.2 to 104.9 bar. A empirical model of the compressor, its validation with the experimental measurements, and the effect of the SHSC on the energy efficiency of the plant were presented.

Yuan et al. (2012) experimentally investigated the discharge valve dynamics in a semi-hermetic reciprocating compressor for trans-critical CO₂ refrigeration cycle. The average valve speed was increased from 0.71 ms⁻¹ to 0.81 ms⁻¹ as the discharge pressure ranged from 7.8MPa to 12MPa. The experimental methods and results provide useful information for both valve testing and their reliability in trans-critical CO₂ system. Presently, a good number of manufacturing companies, like Dorin, Denso, Denfoss, GEA Bock etc, mostly from Japan and Europe, are manufacturing CO₂ compressors. Denso Corporation has brought out a single-stage semi-hermitic scroll compressor. Dorin developed high pressure semi-hermetic CO₂ compressor series comprising single and two- stage with nominal speed 1450 and 2900 rpm in the range of 1.7-10.7 m³/h swept volume as discussed by Casini D. in his article published in euro cooling. Bock compressor from GEA group is also one of the leading manufacturer of CO₂ compressor for wide range of trans-critical application.

2.2.2 Gas cooler

In a trans-critical CO₂ cycle, the heat rejection takes place by cooling of compressed CO₂ gas at supercritical high side pressure. The heat exchanger in which cooling of CO₂ gas takes place is called a gas cooler, which replaces the condenser of a conventional refrigeration cycle. Despite the single phase sensible heat transfer, high working pressure and favorable heat transfer properties of CO₂ enables compact heat exchanger design with suitable modification to handle the high pressure. The thermo-physical properties of CO₂ changes rapidly in supercritical region as detailed given in section 1.2.2, shows gas cooler as one of the most crucial component in a trans-critical CO₂ refrigeration system, and the overall system performance is very sensitive to the design of gas cooler.

Many researchers have theoretically and experimentally analyzed, and also have proposed various gas cooler design such as finned tube, tube in tube, and micro-channel, while finned tube and tube in tube design are conventional. Pettersen et al. (1998) first reported the possibility of using micro channel heat exchangers (both gas cooler and evaporator) for air conditioning systems. However, micro channels also have their weaknesses, such as large pressure drop, high cost of manufacture, ^{ing}dirt clogging, and flow mal-distribution, especially for two phase flows. The designer confidence and associated low cost is a motivation toward the modification of finned tube heat exchanger as gas cooler for trans-critical systems. The development stages of various gas cooler are summarized using heat transfer and pressure drop characteristics, heat transfer models followed by gas cooler design, in subsequent section.

2.2.2.1 Supercritical CO₂ heat transfer and pressure drop

Due to uneven behavior in properties of CO₂ in the supercritical region, the heat transfer and pressure drop characteristics are different from the conventional system. It also attract the researcher to study on these characteristics. Pitla et al. (1998) presented a review of heat transfer and pressure drop characteristics of supercritical CO₂ in-tube flow and found that none of the available studies were applicable to air-conditioning, heat pump and refrigeration applications. Compared to the heating of supercritical CO₂, much less work have been done in determining the heat transfer and pressure drop characteristics during cooling of supercritical CO₂, which is vitally essentially on the design of a gas cooler. Previous heat transfer correlations appropriate for constant

physical properties are generally not directly applicable to cooling of supercritical CO₂ and heat transfer without modification.

Pittersen et al. (2000) studied the gas cooling heat transfer & pressure drop of supercritical CO₂ and found that the influence of the heat flux on heat transfer coefficient was rather small. The experimental data showed a low average deviation compared with Gnielinski's correlation. However, moderate deviation was also seen at high temperatures (deviation as much as 45% at pressure of 81bar and mass flux of 900 kg m⁻²s⁻¹). Pitla et al. (2001) conducted experiments and numerical simulations for in-tube cooling of turbulent supercritical CO₂, which showed that supercritical CO₂ has excellent properties for operation in a gas cooler. A majority of the average heat-transfer coefficients predicted by the numerical model and the experimentally calculated ones were within 10% of each other. The tube inner diameter taken in the study was 4.72mm.

Fang et al. (2001a) did a comprehensive survey of the studies related to gas coolers, including single-phase in-tube heat transfer correlations and friction factor correlations under supercritical conditions. In recent studies, a number of researchers have proposed heat transfer correlations for supercritical CO₂ cooling by modifying previous correlations to fit their own data. However, there appears to be no generalized correlation for gas coolers which applies to both macro and micro-scale channels. Liao and Zhao (2002) investigated the heat transfer from supercritical CO₂ flowing in horizontal mini/micro circular tubes cooled at a constant temperature. Six circular tubes were tested with inner diameters of 0.5mm, 0.7mm, 1.1mm, 1.4mm, 1.55mm, and 2.16mm, respectively. Their experimental data deviated significantly from the existing correlations developed for large tubes. An empirical correlation was proposed based on their experimental data. Yoon et al. (2003) presented the experimental data for the heat transfer and pressure drop characteristics obtained during the gas cooling process of CO₂ in a horizontal tube with an inner diameter of 7.73mm. The experimental results were compared with the existing correlations for the supercritical heat transfer coefficient, which generally under-predicted the measured data by up to 67%.

Wang and Hihara (2002) derived an effective heat transfer temperature difference expression for variable fluid property and verified by numeric simulation of the tube in tube CO₂ water gas cooler. The author used the available correlated models for the cooled CO₂ supercritical heat transfer are used to simulate the gas cooler. Detail analysis were made for the deviations among the different models, and for the distributions of local

convective coefficient, heat flux, and local temperature of CO₂ along the flow path in the gas cooler.

Huai et al. (2005) conducted the experimental study for the heat transfer of supercritical CO₂ in horizontal, multi-port mini channel under cooling conditions. The inner diameter was 1.31mm. The measured average heat transfer coefficients was compared with other literature, and a large discrepancy was observed. A new correlation was developed based on their experimental data. Chang et al. (2008) presented a comprehensive analysis of heat transfer and pressure drop experimental data and correlations for supercritical CO₂ cooling in macro- and micro-channels. The effect of oil on both heat transfer and pressure drop for supercritical CO₂ was shown to significantly decrease the former and to increase the latter. A review of experimental studies on heat transfer and pressure drops of supercritical CO₂ cooling was provided and detailed comparisons and analysis relative to the available heat transfer and pressure drop correlations for supercritical CO₂ cooling were done. The author noted and remarked on the lack of all pertinent experimental details required to use the data published in many of these studies. Finally the author provided comments on how to reduce and present supercritical CO₂ experimental data properly in the future.

Large discrepancies exist between the experimental data of these studies on supercritical CO₂ gas cooling. There is no single correlation that predicts all the data accurately for supercritical CO₂ in the gas cooling process, a knowledge gap this study will attempt to fill.

2.2.2.2 Heat transfer correlations for supercritical CO₂ cooling

The thermo-physical properties of CO₂ in supercritical region show uneven variation and change drastically. The variations of the thermo-physical properties include two aspects: along and perpendicular to the fluid flow direction. The effect of the former can be diminished if the dimensional step in calculations is small enough, but that of the latter cannot. The conventional heat transfer correlations may not predict the heat transfer coefficient accurately. To evaluate the performance of a CO₂ gas cooling heat exchanger, it is necessary to develop an accurate heat transfer correlation that is valid in the supercritical region. The heat transfer correlations for supercritical fluids, proposed by different researchers from time to time are summarized below chronologically.

• **Krasnoshchekov's correlation**

Krasnoshchekov et al. (1969) conducted an experiment at supercritical pressures with CO₂ cooled in a long horizontal tube of an inner diameter = 2.22mm, and derived the following equation from the experimental data:

$$Nu_{wt} = Nu_{iso,wt} \left(\frac{\rho_{wt}}{\rho_{bt}} \right)^n \left(\frac{\bar{C}_p}{C_{p,wt}} \right)^m \quad (2.1)$$

$$m = B \left(\frac{\bar{C}_p}{C_{p,wt}} \right)^s \quad (2.2)$$

$$\bar{C}_p = \frac{H_{bt} - H_{wt}}{T_{bt} - T_{wt}} \quad (2.3)$$

where, n, B and s are constant and its values are given in Table 2.1. $Nu_{iso,w}$ is calculated with the following equation at wall temperature, given by Petukhov & Kirillov (1958) using Eq. (2.4) and ϕ is calculated using Eq. (2.5).

$$Nu = \frac{(\phi/8)RePr}{1.07 + 12.7(\phi/8)^{1/2} \left(Pr^{2/3} - 1 \right)} \quad (2.4)$$

$$\phi = (0.79 \ln Re - 1.64)^{-2} \quad (2.5)$$

Table 2.1: values of n, B, and s

P,MPa	7.845	8	8.5	9	10	12
n	0.30	0.38	0.54	0.61	0.68	0.80
B	0.68	0.75	0.85	0.91	0.97	1.00
s	0.21	0.18	0.104	0.066	0.04	0

The experimental Re range used in the Krasnoshchekov et al. equation was $Re_{bt} \in (9 \times 10^4, 3.2 \times 10^5)$ and $Re_{wt} \in (6.3 \times 10^4, 2.9 \times 10^5)$. Krasnoshchekov et al. compared their calculations with the Tanaka et al. (1967) experimental data of the CO₂ ascending flow cooled in a vertical tube of inner diameter 6mm, and found large over-predictions around the pseudo-critical region.

(1969) 1970
omit space

replace "x" by product symbol

- **Gnielinski's correlation**

Gnielinski (1976) developed a widely used correlation to predict the heat transfer coefficient for single-phase, forced convective, turbulent flow in a smooth single pipe/channel. Gnielinski's formula can be stated as:

$$Nu = \frac{(\varphi/8)(Re - 1000)Pr}{1.07 + 12.7(\varphi/8)^{1/2} \left(Pr^2 - 1 \right)} \quad (2.6)$$

Where friction factor is calculated from Eq. 2.4. Gnielinski's correlation is valid for $0.5 < Pr < 2000$ and $3000 < Re < 5 \times 10^6$, given constant thermo-physical properties.

- **Baskov's correlations**

Baskov et al. (1977) developed an equation specifically for the heat transfer and pressure loss of CO₂ cooled at supercritical pressures, limited to fully developed turbulent regime. The correlation is shown in Eq. (2.7).

$$Nu_{wt} = Nu_{iso,wt} \left(\frac{\bar{C}_p}{C_{p,wt}} \right)^m \left(\frac{\rho_{bt}}{\rho_m} \right)^n \quad (2.7)$$

where $m = 1.4$, $n = 0.15$ for $T_{bt}/T_{pc} \leq 1$, m and n are given in Table 2.2, for $T_{bt}/T_{pc} > 1$, T_{pc} is the pseudo-critical temperature, and $Nu_{iso,wt}$ is calculated with the following Petukhov et al. (1973) equation at wall temperature

$$Nu = \frac{(\varphi/8)RePr}{[1.07 + 900/Re - 0.63/(1 + 10Pr)] + 12.7(\varphi/8)^{1/2} \left(Pr^2 - 1 \right)} \quad (2.8)$$

Table 2.2: Value of 'm' and 'n' in the Baskov et al. equation for $T_{bt}/T_{pc} > 1$

	$\frac{\bar{C}_p}{C_{p,wt}} > 1$			$\frac{\bar{C}_p}{C_{p,wt}} < 1$		
P (MPa)	8	10	12	8	10	12
m	1.2	1.6	1.6	0.45	0.45	0.45
n	0.15	0.10	0	0.15	0.10	0

Here the friction factor f is calculated with Eq. (2.5). Comparing predictions of their equation with the experimental data of Tanaka et al. (1967) and Krasnoshchekov

et al. (1969), Baskov et al. (1977) found that their predictions were 25% lower than the former on average and most within $\pm 25\%$ of the latter. They speculated that the discrepancy might be connected with the difference in the orientation of the tubes and the schemes of the experimental units. However, after conducting experiments to compare ascending flow with descending flow, they concluded that in their experimental range ($0.95 \times 10^5 \leq Re_{bt} \leq 6.44 \times 10^5$), there was no effect of free convection on heat transfer.

- **Petrov-Popov's correlations**

Petrov and Popov (1985) studied the local frictional resistance coefficient of inertia in the supercritical region and presented a new heat transfer correlation. The correlation combines the cooling condition of heat flux and the fluid properties of specific heat and density, as shown in Eq. (2.9).

$$Nu_{wt} = Nu_{iso,wt} \left(1 + 0.001 \frac{\dot{q}}{G} \right) \left(\frac{\bar{C}_p}{C_{p,wt}} \right)^n \quad (2.9)$$

$$n = \begin{cases} 0.66 + 4 \times 10^{-4} (\dot{q}/G) & \text{if } \bar{C}_p / C_{p,wt} \leq 1, \\ 0.9 + 4 \times 10^{-4} (\dot{q}/G) & \text{if } \bar{C}_p / C_{p,wt} > 1 \end{cases}$$

where, $Nu_{iso,w}$ is calculated with the Petukhov-Popov equation (1963) Eq. (2.10) at wall temperature as shown below:

$$Nu = \frac{(\varphi/8) Re Pr}{(1 + 3.4\varphi) + \left(11.7 + 1.8/Pr^{1/3} \right) (\varphi/8)^{1/2} \left(Pr^{2/3} - 1 \right)} \quad (2.10)$$

where the friction factor φ was calculated using Eq. (2.5). The Petrov-Popov (1985) equation was developed based on the authors' theoretical calculations for CO₂ cooled in the supercritical region with $3.1 \times 10^4 \leq Re_{bt} \leq 8 \times 10^5$, $1.4 \times 10^4 \leq Re_{wt} \leq 7.9 \times 10^5$, and $29 \leq \frac{\dot{q}}{G} \leq 350 \text{ J kg}^{-1}$. Comparing the prediction of their correlation with those by Krasnoshchekov et al. (1970) and Baskov et al. (1977), Petrov and Popov (1985) found that their results were lower than those by the former, and not greater than $\pm 15\%$ of those by the latter in the range of $50 \leq \frac{\dot{q}}{G} \leq 240 \text{ J kg}^{-1}$.

- **Petrov-Popov's correlation**

Summarizing their calculations for CO₂, water and helium, Petrov and Popov (1988) obtained a generalized correlation for cooling heat transfer under supercritical pressure.

$$Nu_{bt} = \frac{\varphi Re_{bt} \bar{Pr}}{8 \sqrt{1.07 + 12.7 \sqrt{\frac{\varphi}{8} \left[\bar{Pr}^2 \sqrt{\frac{\rho_{wt}}{\rho_{bt}}} \left(1 - A_1 \sqrt{\frac{|\varphi_{ac}|}{\varphi}} \right) - \left(1 - A_2 \sqrt{\frac{|\varphi_{ac}|}{\varphi}} \right) \right]}}} \quad (2.11)$$

$$\bar{Pr} = \frac{\bar{C}_p \mu_{bt}}{K_{bt}} \quad (2.12)$$

where $A_1 = 0.9$ and $A_2 = 1.0$ for CO₂, $A_1 = 1.1$ and $A_2 = 1.0$ for water, $A_1 = 0.8$ and $A_2 = 0.5$ for helium, The friction factor φ and the acceleration factor φ_{ac} are calculated from the following equations;

$$\frac{\varphi}{\varphi_{iso,bt}} = \left(\frac{\mu_{wt}}{\mu_{bt}} \right)^{\frac{1}{4}} + 0.17 \left(\frac{\rho_{wt}}{\rho_{bt}} \right)^{\frac{1}{3}} \frac{|\varphi_{ac}|}{\varphi_{iso,bt}} \quad (2.13)$$

$$\varphi_{ac} = 2d_{in} \rho_{bt} \frac{d}{dL} \left(\frac{1}{\rho_{bt}} \right) = \frac{-8\dot{q}}{G} \left(\frac{\beta}{C_p} \right)_{bt} \quad (2.14)$$

where $\varphi_{iso,b}$ is calculated with the Eq. (2.5) at bulk temperature.

- **Fang's correlation**

↑ include bracket

Fang (1999) proposed the following equations for calculating heat transfer and pressure loss at supercritical pressures both in the fully developed turbulent regime and in the transitional regime:

$$Nu_{wt} = \frac{(\varphi_{wt}/8)(Re_{wt}-1000)Pr_{wt}}{A + 12.7(\varphi_{wt}/8)^{1/2}(Pr_{wt}^{2/3}-1)} \left(1 + 0.001 \frac{\dot{q}}{G} \right) \left(\frac{\bar{C}_p}{C_{p,wt}} \right)^n \quad (2.15)$$

where,

$$A = \begin{cases} 1 + 7 \times 10^{-8} Re_{wt} & \text{if } Re_{wt} < 10^6 \\ 1.07 & \text{if } Re_{wt} \geq 10^6 \end{cases}$$

$$n = \begin{cases} 0.66 + 4 \times 10^{-4} (\dot{q}/G) & \text{if } \bar{C}_p / C_{p,wt} \leq 1 \\ 0.9 + 4 \times 10^{-4} (\dot{q}/G) & \text{if } \bar{C}_p / C_{p,wt} > 1 \end{cases}$$

ϕ_{wt} is the friction factor evaluated at wall temperature by the Churchill (1977) equation as shown in Eq. (2.16)

$$\phi = 8 \left[\left(\frac{8}{Re} \right)^{12} + A^{-3} \right]^{1/12} \quad (2.16)$$

$$A = \left[2.457 \ln \frac{1}{(7/Re)^{0.9} + 0.27R_r} \right]^{16} + \left(\frac{37.530}{Re} \right)^{16}$$

where R_r is the channel relative roughness. $R_r = \varepsilon/d_{in}$ and ε is the channel roughness. Fang suggested that his equation could be used in the range of $3000 \leq Re_{wt} \leq 10^6$ and $0 \leq \frac{\dot{q}}{G} < 350 \text{ J kg}^{-1}$.

- **Liao-Zhao's correlation**

Liao and Zhao (2002) conducted experiments on convection heat transfer of supercritical carbon dioxide in heated horizontal and vertical miniature tubes. They concluded that both the buoyancy effect and the heat flux, or temperature difference, between the bulk fluid and the wall must be taken into account for developing a heat transfer correlation in the supercritical region. Based on a least-square fit of 68 experimental data points for the circular tubes of $d = 0.70, 1.40, \text{ and } 2.16\text{mm}$, they obtained the following correlation for convection of supercritical CO_2 in miniature tubes heated at an approximately constant temperature:

$$Nu_{wt} = 0.128 Re_{wt}^{0.8} Pr_{wt}^{0.3} \left(\frac{Gr}{Re_{bt}^2} \right)^{0.205} \left(\frac{\rho_{bt}}{\rho_{wt}} \right)^{0.437} \left(\frac{\bar{C}_p}{C_{p,wt}} \right)^{0.411} \quad (2.17)$$

where Gr is the Grashof number, defined as

$$Gr = \frac{g(\rho_{wt} - \rho_{bt})\rho_{bt} d_{in}^3}{\mu_{bt}^2} \quad (2.18)$$

d_{in}

- **Pitla's correlation**

insert dot
 Pitla et al. (2002) performed both numerical and experimental study on the heat transfer of a in-tube cooling of turbulent supercritical carbon dioxide. Using the obtained data as well as prior publications, the authors developed a new correlation to predict the heat transfer coefficient of supercritical carbon dioxide during in-tube cooling, as shown below:

$$Nu = \left(\frac{Nu_{wt} + Nu_{bt}}{2} \right) \frac{K_{wt}}{K_{bt}} \quad (2.19)$$

where, Eq. (2.20) was used to calculate both the Nusselt numbers. As seen, this correlation was based on mean Nusselt numbers that are calculated using the thermo-physical properties at the wall and the bulk temperatures, respectively. The friction factor was calculated with Eq. (2.5), in which the subscript f represent the film temperature, $T_f = (T_{bt} + T_{wt})/2$. *omit space*

$$Nu = \frac{(\varphi_f / 8)(Re_{bt} - 1000)Pr}{1.07 + 12.7(\varphi_f / 8)^{1/2} \left(Pr^{1/4} - 1 \right)} \quad (2.20)$$

- **Yoon's correlation**

Based on their experimental data on gas cooling of supercritical CO₂, Yoon et al. (2003) suggested an empirical correlation using the form of Dittus-Boelter's correlation and multiplying the density ratio. The correlation is given below: *needed*

$$Nu_{bt} = \begin{cases} 0.14 Re_{bt}^{0.69} Pr_{bt}^{0.66} & \text{for } T_{bt} / T_{pc} > 1 \\ 0.013 Re_{bt} Pr_{bt}^{-0.05} \left(\frac{\rho_{pc}}{\rho_{bt}} \right)^{1.6} & \text{for } T_{bt} / T_{pc} \leq 1 \end{cases} \quad (2.21)$$

where subscript pc refers to the pseudo-critical temperature T_{pc} .

- **Dang and Hibara's modification correlation**

Dang and Hibara (2004) modified the Gnielinski equation for more accuracy and suggested a modified correlation as following:

$$Nu = \frac{(\varphi_f / 8)(Re_{bt} - 1000)Pr}{1.07 + 12.7(\varphi_f / 8)^{1/2} \left(Pr^{1/4} - 1 \right)} \quad (2.22)$$

where,

$$Pr = \begin{cases} C_{p, bt} \mu_{bt} / K_{bt} & \text{for } c_{p, bt} \geq \bar{C}_p \\ \bar{C}_p \mu_{bt} / K_{bt} & \text{for } c_{p, bt} < \bar{C}_p \text{ and } \mu_{bt} / K_{bt} \geq \mu_f / K_f \\ \bar{C}_p \mu_f / K_f & \text{for } c_{p, bt} < \bar{C}_p \text{ and } \mu_{bt} / K_{bt} < \mu_f / K_f \end{cases}$$

and

$$\alpha = Nu K_f / D$$

Here the friction factor is calculated using Eq. (2.5).

- **Huai et al.'s correlation**

Based on their experimental data on gas cooling of supercritical carbon dioxide in multi-port mini channels, Huai et al. (2005) proposed a correlation for heat transfer coefficient, as shown in Equation below:

$$Nu_{wt} = 0.022186 Re_{wt}^{0.8} Pr_{wt}^{0.3} \left(\frac{\rho_{bt}}{\rho_{wt}} \right)^{-1.4652} \left(\frac{\bar{C}_p}{C_{p,wt}} \right)^{0.0832} \quad (2.23)$$

The experimental data ranges are $8.5 \text{ MPa} \geq P \geq 7.4 \text{ MPa}$, $53^\circ\text{C} \geq T \geq 22^\circ\text{C}$, $419 \text{ kg m}^{-2}\text{s}^{-1} \geq G \geq 114 \text{ kg m}^{-2}\text{s}^{-1}$, and $9 \text{ kW m}^{-2} \geq q \geq 0.8 \text{ kW m}^{-2}$. In this correlation, the effect of variances in density and specific heat was considered.

- **Son-Park's correlation**

Son and Park (2006) experimentally investigated the heat transfer coefficient and pressure drop during gas cooling process of CO_2 in a horizontal tube without oil in the refrigerant loop. A new correlation to predict the heat transfer coefficient of supercritical CO_2 during in-tube cooling was proposed as shown below;

$$Nu_{bt} = \begin{cases} Re_{bt}^{0.55} Pr_{bt}^{0.23} \left(\frac{C_{p,bt}}{C_{p,wt}} \right)^{0.15} & \text{for } T_{bt} / T_{pc} > 1 \\ Re_{bt}^{0.35} Pr_{bt}^{1.9} \left(\frac{\rho_{bt}}{\rho_{wt}} \right)^{-1.6} \left(\frac{C_{p,bt}}{C_{p,wt}} \right)^{-3.4} & \text{for } T_{bt} / T_{pc} \leq 1 \end{cases} \quad (2.24)$$

The majority of the experimental values are within 18% of the values predicted by the new correlation.

- **Kuang et al.'s correlation**

Kuang et al. (2008) experimentally measured heat transfer characteristics for supercritical heat transfer of CO_2 in microchannels, and a new semi-empirical correlation was developed to predict the gas cooling heat transfer coefficient of supercritical region. Experimental data were obtained for an 11-port microchannel tube with an internal diameter of 0.79mm and with a pressure range of 8 to 10MPa and mass flux range of 300 to 1200 $\text{kg s}^{-1}\text{m}^{-2}$. They suggested the following correlation:

$$Nu = 0.001546 Re^{1.054} Pr^{0.653} \left(\frac{\rho_{wt}}{\rho} \right)^{0.367} \left(\frac{\bar{C}_p}{C_p} \right)^{0.4} \quad (2.25)$$

make
normal
instead of
Italics

- **Oh-Son's correlations**

Oh & Son (2010) proposed a new correlation to predict more accurate heat transfer coefficient of supercritical CO₂ without lubricating oil in horizontal macro-tubes under cooling conditions. Experiments were done on two stainless steel circular tubes having inside-diameter of 4.55mm and 7.75mm with a mass flux of 200–600kg m⁻²s⁻¹, inlet fluid pressures of 7.5–10.0MPa, and the inlet fluid temperatures of 90–100°C.

$$Nu_{bt} = \begin{cases} 0.023 Re_{bt}^{0.7} Pr_{bt}^{2.5} \left(\frac{C_{p,bt}}{C_{p,wt}} \right)^{-3.5} & \text{for } T_{bt} / T_{pc} > 1 \\ 0.023 Re_{bt}^{0.6} Pr_{bt}^{3.2} \left(\frac{\rho_{bt}}{\rho_{wt}} \right)^{3.7} \left(\frac{C_{p,bt}}{C_{p,wt}} \right)^{-4.6} & \text{for } T_{bt} / T_{pc} \leq 1 \end{cases} \quad (2.26)$$

The above correlations were used for various range of operating and geometric parameters, for cooling of CO₂ in supercritical region. These ranges of parameters are summarized in the table below.

Table 2.3: Summary of heat transfer correlations of supercritical CO₂ cooling

Correlations	Flow parameter range				Flow geometry range			
	t _{in} (°C)	P _{in} (MPa)	G (kg m ⁻² s ⁻¹)	Q (kW m ⁻²)	D (mm)	L (mm)	Orientation	tube type
Krasnoshchekov et al. [1969]	28.7-199	8-12	2971	235-500	2.22	150	Horizontal	Single circular
Baskov et al. [1977]	17-212	8-12	1560-4170	Up to 640	4.12	375	Vertical	Single circular
Petrov-Popov [1985]	20-248	7.85-12	450-4000	14-1000	NA	NA	NA	NA
Petrov-Popov [1988]	20-248	7.85-12	450-4000	14-1000	NA	NA	NA	NA
Fang [1999]	25-65	8-12	200-1200	14-70	0.79	530	Horizontal	Multi-port extruded circular
Liao-Zhao [2002]	20-110	7.4-12	250-3500	NS	0.50-2.16	110	Horizontal	Single circular
Pitla et al. [2002]	100-124	8-13	1660-2200	NA	4.72	1.3-1.8	Horizontal	Single circular
Yoon et al. [2003]	50-80	7.5-8.8	225-450	NA	7.73	500	Horizontal	Single circular
Dan-Hibara [2004] modification	20-70	8-10	200-1200	6-33	1-6	500	Horizontal	Single circular
Huai et al. [2005,2007]	22-53	7.4-8.5	113.7-418.6	0.8-9	1.31	500	Horizontal	Multi-port extruded circular
Son-Park [2006]	90-100	7.5-10	200-400	NA	7.75	500	Horizontal	Single circular
Kuang et al. [2008]	45-55	8-10	300-1200	NA	0.79	635	Horizontal	Multi-port extruded circular
Oh-Son [2010]	90-100	7.5-10	200-600	NA	4.55, 7.75	400, 500	Horizontal	Single circular

Use circular bracket as used throughout the thesis

Most recently, Fang and Xu (2011) reported a comprehensive survey and evaluation of the available experimental results and existing correlations for in-tube heat transfer of supercritical CO₂ cooling. They compared all the correlations by calculating mean absolute relative deviation (MARD) and mean relative deviation (MRD), which are the deviation of correlations with the experimental results.

They found significant deviation for all correlation listed and proposed a new correlation having smaller deviation as compared to exiting correlations. The authors refers to the 297 experimental data for the comparative study of the existing heat transfer correlations for supercritical CO₂ cooling. The overall deviations of the model predictions are listed in Table 2.4.

Table 2.4: Prediction performances of the available correlations for supercritical CO₂ cooling

Model (in order of accuracy)	MARD%	MRD%
Modified Fang (2011)	8.9	1.4
Petrov-Popov (1988)	10.2	-2.2
Fang (1999)	11.5	-3.2
Krasnoshchekov et al. (1969)	11.5	0.6
Dang-Hibara (2004)	12.2	0.8
Petrov-Popov (1985)	12.6	-3.0
Baskov et al. (1977)	13.2	-1.3
Pitla et al. (2002)	17.2	-8.0
Huai et al. (2005, 2007)	30.4	1.9
Liao-Zhao (2002)	44.0	19.6
Kuang et al. (2008)	46.8	32.0
Son-Park (2006)	48.0	26.8
Yoon et al. (2003)	63.1	59.3
Oh-Son (2010)	>100.	>100.

Based on the comparison result the author concluded that there is a need of more accurate correlation to predict the heat transfer coefficients for supercritical CO₂ cooling.

Fang and Xu (2011) developed a new modified correlation which was more accurate among all the above listed correlation with the lowest deviation with 8.9% and 1.6% of DARM and DRM respectively. The correlation equation is given below:

$$Nu = \frac{(\varphi/8)(Re_{bt} - 20 Re_{bt}^{0.5})\bar{Pr}}{1 + 12.7(\varphi/8)^{1/2}(\bar{Pr}^{2/3} - 1)} \left(1 + 0.001 \frac{\dot{q}}{G}\right) \quad (2.27)$$

$$\varphi = \varphi_{noniso} - 1.36 \left(\frac{\mu_{wt}}{\mu_{bt}}\right)^{-1.92} \varphi_{ac} \quad (2.28)$$

where average Prandtl number as defined in Eq.(10), and φ_{noniso} and φ_{ac} are the non-isothermal single-phase friction factor and acceleration friction factor, respectively. The acceleration friction factor is calculated using

$$\varphi_{ac} = \frac{d_{in}}{\Delta L} (\rho_{bt,o} + \rho_{bt,in}) \left(\frac{1}{\rho_{bt,o}} - \frac{1}{\rho_{bt,in}}\right) \quad (2.29)$$

where the subscripts in and out mean the inlet and outlet of the tube section ΔL , respectively. The nonisothermal single-phase friction factor φ_{noniso} is calculated from

$$\varphi_{noniso} = \varphi_{iso,b} \left(\frac{\mu_{wt}}{\mu_{bt}}\right)^{0.49(\rho_f/\rho_{pc})^{.31}} \quad (2.30)$$

where ρ_f and ρ_{pc} are the density evaluated at the film temperature and the pseudo-critical temperature, respectively, and $f_{iso,b}$ is the isothermal single-phase friction factor calculated with the following equation at bulk temperature:

$$\varphi_{iso} = 1.613 \left[\ln \left(0.234 \left(\frac{\varepsilon}{d_{in}} \right)^{1.1007} \frac{60.525}{Re^{1.1105}} + \frac{56.291}{Re^{1.0712}} \right) \right]^{-2} \quad (2.31)$$

Eq. (2.31) represent the correlation for isothermal single-phase friction factors proposed by Fang et al.(2013) which has the MARD of 0.16% and the maximum relative deviation of 0.50% in the range of $Re = 3000$ to 10^8 and $\varepsilon/D = 0.0$ to 0.05 compared with the Colebrook equation

$$\frac{1}{\sqrt{\varphi}} = -2 \log \left(\frac{\varepsilon/d_{in}}{3.7} + \frac{2.51}{Re\sqrt{\varphi}} \right) \quad (2.32)$$

The modified Fang correlation is compared with the existing correlations, as shown in Table 6, from which it can be seen that it predicts the experimental data with the MARD of 8.9%. Comparing with the best existing correlation, the new model reduces MARD by 14.6%, increasing the accuracy remarkably.

write Yin et al (2011a) ←
or
Yin et al (2011b)

also see pg 180
for comments
given related
to this reference

2.2.2.3 Gas cooler design

Many researchers have proposed alternate design of gas cooler which are suitable for trans-critical CO₂ systems. From the construction point of view, three popular design exist i.e. finned tube, tube in tube, and micro-channel gas cooler. A brief study of the various theoretical and experimental studies on these gas cooler are given below:

Pettersen et al. (1998) explored the possibility of using micro channel based heat exchangers (both gas cooler and evaporator) for CO₂ air conditioning systems. The author reports a comparative study with flat fin and round tube heat exchanger and condenser used in conventional refrigeration system. The air inlet temperature was assumed as 25°C. Yin et al. (2001) modeled a multi-slab gas cooler using finite element method and reported that the modified gas cooler can improve the system capacity and COP by 3-5% at various operating conditions. The experimental validation was in a 10 kW split system residential heat pump, to operate with CO₂ on the trans-critical cycle. The final design was influenced by several factors, and tradeoffs were quantified by using simulation model, which was developed and validated using extensive experimental data from both residential and mobile ac systems. Several constraints prevented optimization of this particular design, including tube and fin dimensions and overall heat exchanger package dimensions. The numbers of passes were optimized by considering the total pressure drop and manufacturing processes.

Garimella (2002) presented a theoretical study on a novel near counter-flow serpentine flow for the tube side gas cooler for air conditioning system. The model used heat exchanger geometry and inlet conditions as the inputs to predict the overall duty as well as the temperature profiles of refrigerant and air. Neksa et al. (2004) proposed a fan less gas cooler in CO₂ system for heating purpose. A cross flow compact heat exchanger using finned tubes with internal micro channels was modeled to investigate the effects of heat conduction inside the metal on overall performance. Asinari et al. (2004) developed a numerical analysis using finite volume method for an accurate fully three-dimensional simulation of cross flow compact heat exchangers using finned flat tubes with internal micro-channels; as gas coolers in trans-critical refrigerating machines CO₂ operated.

The effects of thermal conduction inside metal on the overall performance of the gas coolers were investigated. Results showed that the conduction on fins along the direction of the air velocity and the longitudinal conduction on tubes produce a negligible effect.

2.2.2.3 Gas cooler design

Many researchers have proposed alternate design of gas cooler which are suitable for trans-critical CO₂ systems. From the construction point of view, three popular design exist i.e. finned tube, tube in tube, and micro-channel gas cooler. A brief study of the various theoretical and experimental studies on these gas cooler are given below:

Pettersen et al. (1998) explored the possibility of using micro channel based heat exchangers (both gas cooler and evaporator) for CO₂ air conditioning systems. The author reports a comparative study with flat fin and round tube heat exchanger and condenser used in conventional refrigeration system. The air inlet temperature was assumed as 25°C. Yin et al. (2001) modeled a multi-slab gas cooler using finite element method and reported that the modified gas cooler can improve the system capacity and COP by 3-5% at various operating conditions. The experimental validation was in a 10 kW split system residential heat pump, to operate with CO₂ on the trans-critical cycle. The final design was influenced by several factors, and tradeoffs were quantified by using simulation model, which was developed and validated using extensive experimental data from both residential and mobile ac systems. Several constraints prevented optimization of this particular design, including tube and fin dimensions and overall heat exchanger package dimensions. The numbers of passes were optimized by considering the total pressure drop and manufacturing processes.

Garimella (2002) presented a theoretical study on a novel near counter-flow serpentine flow for the tube side gas cooler for air conditioning system. The model used heat exchanger geometry and inlet conditions as the inputs to predict the overall duty as well as the temperature profiles of refrigerant and air. Neksa et al. (2004) proposed a fan less gas cooler in CO₂ system for heating purpose. A cross flow compact heat exchanger using finned tubes with internal micro channels was modeled to investigate the effects of heat conduction inside the metal on overall performance. Asinari et al. (2004) developed a numerical analysis using finite volume method for an accurate fully three-dimensional simulation of cross flow compact heat exchangers using finned flat tubes with internal micro-channels; as gas coolers in trans-critical refrigerating machines CO₂ operated.

The effects of thermal conduction inside metal on the overall performance of the gas coolers were investigated. Results showed that the conduction on fins along the direction of the air velocity and the longitudinal conduction on tubes produce a negligible effect.

Dang and Hihara (2004) experimentally investigated heat transfer of supercritical CO₂ cooled in circular tubes using water as coolant. The effect of mass flux, pressure, and heat flux on the heat transfer coefficient and pressure drop was measured for four horizontal cooling tubes with different inner diameters ranging from 1 to 6mm. A modified Gnielinski equation was put forward to predict the heat transfer coefficient of supercritical carbon dioxide under cooling conditions. Hwang et al. (2005) reported an experimental investigation on finned tube gas cooler used in trans-critical CO₂ cycle. Tests were conducted for air inlet temperature 29.4 and 35°C, gas cooler pressure 9, 10 and 11MPa, air frontal velocity 1, 2, and 3 ms⁻¹. Two refrigerant mass flow rate were considered viz. 36 and 76 gs⁻¹, while the gas cooler selected had 54 tube arranged in three pass and single circuit. Corradi et al. (2006) modeled and experimentally validated a commercial coil type gas cooler with copper tube and louvered fins gas cooler with air as a secondary fluid. Tests were focused on two different gas-coolers, with continuous and cut fins, and on two different circuit arrangements. Test on each heat exchanger were carried out at three different inlet conditions, both for CO₂ (87.0, 97.6 & 107.8 C) and air (20.3, 21.5, & 23.0°C) with air frontal velocity of 1.6 ms⁻¹.

Damseh (2006) investigated the influence of variable fluid properties on CO₂ in tube cooling process by a transient mathematical model for non thermally equilibrium fluid and solid domains, which was solved by means of finite difference technique. The effect of constant fluid properties assumption on cycle performance was studied. The validity of such assumption was investigated and it was found that it leads to higher gas cooler outlet temperature. The efficiency of the cooler was also affected which will tend the cycle to operate at a erroneous optimum cooling pressure. Chang and Kim MS (2007) modeled a fin and tube type gas cooler and proposed an air side heat ~~transfer~~ correlation. The model was validated experimentally. The effect of geometric parameters on performance of the gas cooler were investigated using the model. The gas cooler was optimized for air temperature of 15°C and air frontal velocity within range of 0.5 to 2.5 ms⁻¹.

Park and Hrnjak (2007) presented an experimental study to investigate the effect of conduction through the fins on the capacity of a gas cooler for trans-critical CO₂ system operated in A/C mode. The capacity of the gas cooler was carefully measured in the chamber which simulated the outdoor condition with the original heat exchanger. Some sections of the fins, where the conduction was most significant, were cut by

electrical discharge machining. It was shown by system simulation that system COP could be improved up to 5% by eliminating the conduction effect, as was done in the experiment. Ge and Cropper (2009) described a detailed mathematical model using distributed method and its application for air-cooled finned-tube CO₂ gas coolers. The focus of the work was to increase the heat capacity or minimize the approach temperature for a gas cooler. The validated model was used to carry out simulation and performance analysis with the circuit arrangement of the original heat exchanger is redesigned. It was found that the approach temperature and the heat capacity were both improved with the increase of heat exchanger circuit numbers. Result shows that the three circuit arrangement of gas cooler with air velocity gives the best performance. However the work was focused only on gas cooler performance, overall performance of the system and the effect of fan power consumption were not considered.

Waltrich et al. (2010) developed a novel first-principles mathematical model to simulate the thermo-hydraulic behavior of compact finned tube heat exchangers for light commercial refrigeration applications, for heat duties ranging from 0.5 to 2.0 kW. The model predictions were validated with experimental data taken at several operating and geometric conditions at air temperature ranging from 20°C to 30°C. Goodman et al. (2011a, 2011b) conducted an experimental and analytical study on the performance of CO₂ heat pumps for water heating. The performance of compact, micro-channel, water coupled gas cooler, evaporator, and suction line heat exchanger (SLHX) were evaluated experimentally. Isentropic and volumetric efficiency of compressor were found to range from 56% to 67% and 62% to 82%, respectively. The resulting component models are implemented in a system model in a companion paper Part II. The second part investigated the effects of a SLHX and once-through versus recirculating water heating schemes. The once-through systems outperformed the recirculating systems by 10% for the system without an SLHX and 15% with an SLHX. However, a gas cooler of twice as dimensions was needed.

Srinivasan et al. (2010) gave a thermodynamic basis for the evaluation of gas cooler pressure for the case of ideal compression using the compressors available in the market. They also provided an additional criterion that minimizes the cycle irreversibility which was predominantly due to gas throttling. The pressure limits for these two criteria for some typical evaporating temperatures and ambient conditions were also evaluated. The possible compressor discharge temperatures in each case was calculated and criteria

This is missing in references list \Leftarrow
Plz include it

for two-stage compression was identified. Kondou and Hrnjak (2011) presented an experimental investigation on heat rejection from CO₂ flow near the critical point, where commercial refrigerators spend most of their operating hours. Experimental results on the heat transfer coefficient and pressure drop of mass flux from 100 to 240 kg m⁻² s⁻¹ at pressures from 5 to 7.5MPa in a horizontal smooth tube of 6.1mm inner diameter were provided and compared with correlations. The results indicated that the heat transfer coefficient in superheat zone was significantly higher than correlations proposed for single-phase turbulent flow.

Fronk and Garimella (2011a, 2011b) studied both experimentally and analytically the performance of a compact, micro-channel water - CO₂ gas cooler. The gas cooler design under investigation used an array of refrigerant micro-channel tubes wrapped around water passages containing offset strip fins, resulting in a generally counter-flow configuration between the two fluids. Part I of the two-part paper addresses the experimental aspects. Data were obtained using an experimental heat pump facility at varying inlet conditions for three gas coolers with capacity range from 1.5 to 6.5 kW of the same design, but different sizes. The results were used to develop a predictive heat exchanger model to optimize gas cooler design over a wide range of operating conditions, eliminating the need for expensive prototype development and testing in the companion paper Part II. Ballester et al. (2011) presented a more fundamental numerical approach to heat exchanger modeling which takes into account the 2D longitudinal heat conduction in any element, and captured detailed representation of air properties. Using the fundamental numerical approach, the paper assesses the impact of the traditional heat exchanger model assumptions when modeling a micro-channel gas cooler working with CO₂. The study revealed significant differences in capacity predictions depending on the ϵ -NTU relationship adopted. Large errors in capacity prediction of individual tubes occurred due to the adiabatic-fin-tip assumption when the neighboring tubes were at different temperature.

Sarkar (2011) presented a theoretical analyses of the nanofluid cooled shell-and-tube gas cooler in trans-critical CO₂ refrigeration cycle to study the performance improvement of gas cooler as well as CO₂ cycle using various nanofluids and effects of various design and operating parameters. Study showed that the nanofluid may effectively be used as coolant in shell-and-tube gas cooler for improved performance. Yu et al. (2012), developed a tube-in-tube heat exchanger model applicable to supercritical

This is not available at the end of
thesis under references list.
Plz add it suitably.



CO₂ and water. The result shows that the effect of the inlet pressure on the variation of the CO₂ temperature was not as apparent as on the heat transfer rate, even the overall heat transfer coefficient was found to change significantly. Simulation results presented in the range of 15.9°C to 36.16°C water temperature at inlet.

Ballester et al. (2013) presented an extension of previous model published in 2011 for a micro-channel heat exchanger, For given working conditions, geometric data, heat transfer and face areas, with different circuit and aspect ratio, The presented model has reduced the simulation time by one order of magnitude and in terms of accuracy deviates less than 0.3%. Baek et al. (2013) investigated the control methods of the gas cooler pressure in a CO₂ heat pump. The cooling performance of the CO₂ heat pump was measured by varying the refrigerant charge amount, EEV opening, compressor frequency, and outdoor fan speed at various outdoor temperatures.

2.2.3 Evaporator

In the auto air-conditioning industry, during the 1980s, conventional copper tube-aluminum fin evaporators were replaced by lighter, more compact brazed aluminum designs. Refrigerant flows between plates patterned with chevrons or dimples to facilitate refrigerant distribution between the upwind and downwind sides; sets of parallel plates are in cross-flow, usually with several passes between headers, with a variable number of plates per pass to control pressure drop. With plate evaporators the auto industry adopted louvered fins, which re-start the boundary every millimeter, increasing air-side heat transfer coefficient by 50–100% over that of plain fins. Microchannel evaporators are currently the subject of research within the automotive air-conditioning industry because of the potential performance improvements obtainable from further increase in refrigerant-side area and higher face velocities. In both plate evaporators and microchannel evaporators, the challenge is to distribute the two-phase flow uniformly through the parallel circuits. A few important research work on evaporator are discussed below:

Kim and Bullard (2001) developed a detailed finite volume model for a multi-slab micro-channel evaporator for a CO₂ ACC system and validated the model for a two slab prototype evaporator to study air side phenomena such as the effects of condensate and inclination angle. Kim et al. (2003) critically reviewed the flow structure and its effect on the thermal hydraulic performance of folded louvered fins. They also described

the air-side heat transfer and pressure drop data and correlations of brazed aluminum heat exchangers under dry and wet conditions. Kim et al. (2004a) reported that the overall size required for CO₂ micro-channel evaporator with louvered fins is less than that of an R134a evaporator. To avoid misdistribution of the two phase flow in micro-channel of the evaporator, Elbel and Hrnjak (2004) proposed a flash gas by pass system. Cho and Kim (2007) experimentally investigated in-tube evaporation heat transfer characteristics of carbon dioxide and analyzed for evaporating temperature (0 °C to 20 °C), mass flux (212 to 656 kg m⁻²s⁻¹), heat flux (6 to 20 kWm⁻²) and tube geometry (5 m long smooth and micro-fin tubes with outer diameters of 5 and 9.52mm). It was found that the average evaporation heat transfer coefficients for a micro-fin tube improved from 150 to 200% for 9.52mm OD tube and from 170 to 210% for 5mm OD tube, at the same test conditions. Similar work is reported by Kim et al. (2008) for slightly different operating conditions and similar conclusion were drawn.

Cheng and Thome (2009) attempted to predict thermal performance of CO₂ in a silicon multi-micro-channel evaporator for cooling of a microprocessor. The effects of channel diameter, mass flux, saturation temperature and heat flux on flow boiling heat transfer coefficients and two-phase pressure drops were also addressed. It was concluded that the base temperatures using CO₂ are much lower than those using R236fa. CO₂ has much higher heat transfer coefficients and lower pressure drops in the multi-micro channel evaporator. However, the operation pressure of CO₂ is much higher. CO₂ appears to be a promising coolant for microprocessors at low operating temperatures but also has a great technological challenge. Onaka et al. (2010) measured heat transfer coefficient for horizontally installed smooth tube with 4mm internal diameter in-tube evaporation of pure dimethyl ether (DME) and mixtures with CO₂ for water heated double tube heat exchanger at mass flux of 100, 200, and 300 kg m⁻² s⁻¹ and inlet saturation temperature of 10°C. Results showed that heat transfer coefficient of mixture decreases with increasing CO₂, i.e. 20% for 10% CO₂ and 48% for 25% CO₂. However, existent correlations could not give reliable result for a mixture having more than 25% CO₂.

Jin et al. (2011) presented a model using finite volume method to predict the performance of an evaporator for a CO₂ mobile air-conditioning system, and the simulation results were supported by experimental data. The pressure losses both in the headers and at the port inlet of the microchannel tube were also considered. The in-tube refrigerant flow was divided into 2 region for study, i.e. two-phase and superheated

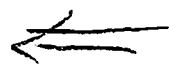
region, where both dry and wet conditions were considered. The effect of selecting various refrigerant-side heat transfer and pressure drop models on the performance of evaporator were discussed. Ayad et al. (2012) presented an experimental study of the CO₂ evaporation in conventional tubes as mini-channels and developed a model of heat transfer coefficient which was validated using a constructed experimental database for horizontal flows covering the operating conditions of a car air conditioning CO₂ evaporator. Fang et al. (2013) presented a comparative review of existing correlations for flow boiling heat transfer coefficient of CO₂. They analyzed 34 correlations ~~analyzed~~ using 2956 experimental data points. A correlation was reported as the best with a mean absolute deviation of 15.5%. The evaluation analysis sets a channel transition criterion for flow boiling heat transfer of CO₂. ✓

2.2.4 Expansion device - throttling process

The purpose of the expansion device in a conventional vapour compression systems are to reduce the pressure of the liquid refrigerant, and to regulate the flow of refrigerant to the evaporator. However, in case of trans-critical carbon dioxide vapour compression cycle where supercritical heat rejection takes place in gas cooler and the gas cooler pressure is independent of the refrigerant temperature at gas cooler exit, operationally expansion devices are different from conventional vapour compression system. An expansion device in a trans-critical CO₂ system is required to function, beyond its normal function to control the high side pressure to operate the system optimally and also reduce the expansion losses. However, expansion devices for CO₂ trans-critical system have been given less attention in the open literature. Research done focusing on expansion device as a throttling process in the literature are summarized below:

Casson et al. (2003) proposed a new expansion system, operating with a differential valve, a liquid receiver and a thermostatic valve. Simulation results showed that the proposed system had an intrinsic self-adjusting capability to operate the system optimally when a fixed value of differential pressure was chosen, even if the temperature of the secondary fluid varied to a large extent. Madsen et al. (2005) experimentally investigated the effects of capillary tubes in a trans-critical CO₂ refrigeration system. The behavior of an adiabatic capillary tube in a refrigeration cycle were investigated theoretically. Results showed that COP with capillary tubes was better than fixed high pressure, but not as good as variable optimal high pressure. Capillary tubes were found ✓

Silva et al (2009 & 2011)
none of above two are listed in
references list. The reviewer written
them on page 173. Plz check and
include them properly



suitable at constant evaporation pressure and gas cooler outlet temperature varies to no more than ± 10 K from the design condition. The reduction in COP is more significant at low temperatures outlet of the gas cooler.

Huang et al. (2006) reported development of an experimental setup to simulate the refrigerant flow through the valve and its downstream line in order to reveal the influence of the upstream vapour quality and the operation of the throttle valve on the freezing and blockage of CO₂ in the safety valve, and study was conducted under upstream pressure range 5.7–6.1MPa. It was recommended to avoid oversize of the downstream line of the safety valve and to install a device to eliminate static electricity in the downstream line. Agrawal and Bhattacharyya (2007a) investigated flow characteristics of an adiabatic capillary tube in a trans-critical CO₂ heat pump system employing the homogeneous model. Relationships between cooling capacity with capillary tube diameter, length and maximum mass flow rate were presented. A lower evaporating temperature yields, a larger cooling capacity due to the unique thermodynamic properties of CO₂. It was also observed that an optimum cooling capacity exists for a specified capillary tube. Subsequently, Agrawal and Bhattacharyya (2008) developed a steady state simulation model to evaluate the performance of a capillary tube based trans-critical CO₂ heat pump system for simultaneous heating and cooling against optimized expansion valve systems. Capillary tubes of various configurations and internal surface roughness have been tested to obtain the optimum design and operating conditions. It was found that the capillary tube system is quite flexible in response to changes in ambient temperature, almost behaving to offer an optimal pressure control. System performance was marginally better with a capillary tube at higher gas cooler exit temperature. A guideline for the selection of the optimum capillary tube was explored.

Silva et al. (2009) studied the trans-critical expansion of CO₂ through adiabatic capillary tubes. The influence of inlet and exit operating conditions and tube geometry on the CO₂ mass flow rate was experimentally evaluated with a strict control of the measured variables. A dimensionless correlation to predict the refrigerant mass flow rate as a function of tube geometry and operating conditions was developed. Silva et al. (2011) presented extensively the influence of both operating conditions and tube geometry on the heat and mass flow rate. Tests were carried out with heat flux spanning from 1 to 11 kW m⁻² and refrigerant mass flow rates ranging from 12 to 26 kg h⁻¹. Wang et al. (2012) presented a separated flow model of coiled adiabatic capillary tube for CO₂ considering meta stable flow

region. For a straight capillary, different friction factors are compared with each other. The result helped formulating modified friction factor for the best reasonable prediction.

Now a days, to improve performance of the overall system, throttling expansion is replaced by ejector expansion and also by using work recovery turbines in modified cycle. The research development of these modified systems are summarized in subsequent sections.

2.3 Cycle Modification on Trans-Critical CO₂ Refrigeration System

A large number of modifications are feasible in the basic trans-critical CO₂ cycle to improve the performance and to adopt the conditions as per requirements and applications. A few studies that have reviewed multiple modifications to improve system performance are Lorentzen (1994), Kim et al. (2004b), and Sarkar (2010). Research progress related to such modifications is summarized below.

2.3.1 System with internal heat exchanger

The function of an internal heat exchanger (IHX) in a trans-critical CO₂ cycle is the same as the liquid suction heat exchanger in a subcritical vapour compression cycle with conventional refrigerants. Effectiveness of the IHX depends on the working fluids and operating conditions. The influence of an IHX on CO₂ trans-critical cycles is however found to be nominal. Robinson and Groll (1998) showed in their thermodynamic study that employing an IHX can increase the COP by a maximum of 7%. In such systems, both the optimum pressure corresponding to a given capacity and efficiency can still be maintained with simple control system. Boewe et al. (2001) experimentally investigated the effects of internal heat exchange on the performance of a prototype trans-critical mobile air conditioning and showed that the contribution of the IHX is significant, and reported an efficiency improvement of nearly 25% on account of relatively high irreversibility in the expansion device in a CO₂ trans-critical cycle. Simulation work, validated based on experimental results followed by identifying an optimal design for a COP maximizing IHX.

Sarkar et al. (2004) concluded from their experimental study that the performance of IHX has a minor influence on system optimization at low and moderate gas cooler exit temperature. Later Sarkar et al. (2005) reported that the exergy destruction is minimum for an IHX compared to that in other components in a trans-critical CO₂ system reported.

Check the year

No reference. ~~at a~~ give
at the end for the year

Chen and Gu (2005) analyzed the relationship between the optimum high pressure and other systematic parameters. They observed that evaporator temperature has little influence on optimum high pressure; and IHX can minimize the sensitivity of the system to the refrigerant quality at the evaporator outlet. Based on simulation data, a correlation of optimum high pressure was developed to predict the simulation values with a deviation of less than 3.6% in the whole range and 0.94% when the evaporating temperature was 5.3°C. Kim et al. (2005) investigated the performance of a trans-critical CO₂ cycle with an IHX for hot water heating by test and simulation. It was found that as length of the IHX increases, COP is enhanced but heating capacity tends to decrease due to the trade-offs between the effectiveness and pressure drop in IHX. Cho et al. (2007) analyzed the cooling performance of a variable speed CO₂ cycle by varying the refrigerant charge amount, compressor frequency, EEV opening, and length of an IHX. The optimum EEV opening increased with compressor frequency, Simultaneous control of EEV opening and compressor frequency allowed optimum control of the compressor discharge pressure. Results showed that the optimal compressor discharge pressure of the modified CO₂ cycle with IHX was reduced by 0.5MPa, and the cooling capacity and COP increased by 6.2-11.9% and 7.1 - 9.1% respectively.

Aprea and Maiorino (2008) evaluated the energy performances of a trans-critical CO₂ cycle working as a classical “split system” to cool air in residential applications, with an IHX. An increase of the coefficient of performance have been found using IHX. Finally the authors compared the coefficients of performance of two cycles, working with and without IHX. Rigola et al. (2010) presented a numerical and experimental study of the whole vapour compression refrigerating cycle and focused on the influence of using an IHX. The study concluded improvement of cooling capacity and COP with IHX especially when ambient temperature increases. Here the ambient temperature considered was 35°C and 43°C.

Zhang et al. (2011) presented a detailed analysis of the IHXs effect in CO₂ trans-critical cycles and found suitable operating conditions for the IHX from a thermodynamic performance point of view. The results indicate that the COP slightly reduces by an IHX in a CO₂ subcritical inverse cycle, which makes the IHX is unjustified. However, for trans-critical CO₂ cycles, the compressor discharge pressures and CO₂ gas cooler outlet temperatures both have significant impacts on system performance. The result showed that a transition discharge pressure and a transition CO₂

gas cooler outlet temperature are limiting conditions above which, the IHX improves the cycle performance. Nakagawa et al. (2011) analyzed experimentally the effect of IHX in the performance of ejector refrigeration system. Experiments were conducted at different operating pressure and temperature for the cases of without, 30 cm, and 60 cm IHX. The results showed that IHX significantly increased COP of ejector system. The ejector system with 60 cm IHX provided the maximum COP improvement of up to 27% compared to similar conventional system. Cabello et al. (2012) presented the experimental evaluation of the energy performance of a modified CO₂ trans-critical refrigeration plant with an IHX based on vapour injection in suction line. Three different injection points were evaluated experimentally: before and after IHX, and just before the suction chamber of the compressor. The experimental study claims 9.81% and 7.01% of enhancement in cooling capacity and COP respectively.

2.3.2 Multi-stage system

Multistage is commonly employed with halocarbon and ammonia refrigerants in industrial refrigeration systems where plants operate with a large difference between evaporating and condensing temperatures approximately 50°C to 80°C. Although employing multi-staging increases the initial cost over single-stage systems, it alleviates a few problems and can save on total compressor work. In multistage compression, the refrigerant flows in series through two or more compressors with a special process performed on the refrigerant between stages. Intermediate pressure is an important and critical parameter which affects the performance of a multistage system. A significant number of work have been reported on the optimization of the multistage systems.

Chen and Wu (1996), Khan and Zubair (1998) investigated the optimum inter-stage pressure on the basis of minimum work requirement. A fair agreement is reported on the optimum intermediate pressure in a two-stage refrigeration system, which is quite close to the classical estimate, given by the geometric mean of gas cooler and evaporator pressure. CO₂ trans-critical heat pump systems have an inherent advantage of a large temperature lift. However, high discharge temperature is the penalty for system COP which can be overcome by employing a two-stage or multistage system with an intercooler in between compression stages in parallel with the gas cooler. Kim et al. (2004) presented a comprehensive review of two-stage trans-critical CO₂ systems. Bell

↳ a or b

the optimal values of both the upper and the intermediate pressures. Heo et al. (2012) proposed an optimum cycle control method for a refrigerant injection heat pump with a double expansion sub-cooler based on the intermediate pressure and the injection ratio. The optimum sub-cooler pressure ratio was proposed within range of 0.4 to 0.7 from the point of view of the heating capacity, and from 0.7 to 0.8 in view of the COP. A trend of rise in optimum injection ratio was reported from 0.1 to 0.3 with an increase in the compression ratio.

2.3.3 Ejector-expansion

In principle, by reducing the expansion losses, the COP of the basic trans-critical cycle can be improved. An ejector-expansion device causes significant reduction in expansion losses of the basic trans-critical cycle.

Li and Groll (2005) presented simulation results of trans-critical R744 air-conditioning systems with a two-phase ejector. Their analysis was also based on Kornhauser's approach. COP improvements of up to 16% were reported without IHX. In a subsequent publication by Li (2006), experimental R744 ejector data were presented as well, although the emphasis of the work was on modeling a trans-critical CO₂ two-phase ejector system and studying of the effects of different geometries and operational conditions. Elbel and Hrnjak (2004a) ^{delete} also used Kornhauser's approach to numerically investigate the effect of using an IHX on the performance of a trans-critical R744 ejector system. They showed that the highest COPs can be achieved with ejector and IHX, even though both devices compete in the reduction of throttling losses. Another finding of their numerical study was that the high side pressure of the trans-critical ejector system can still be used to maximize system performance. Later, Elbel and Hrnjak (2006a, 2008) were able to verify their numerical predictions by experimental results. Their prototype was equipped with a needle extending into the throat of the motive nozzle, allowing for high side pressure control. They also pointed out that the use of an ejector may result in reduced evaporator pressure drop, increased evaporative heat transfer coefficient, and an improved refrigerant distribution in the evaporator, in accordance with their earlier results they obtained with a concept termed as flash gas bypass (Elbel and Hrnjak, 2004b). Elbel and Hrnjak (2006b) used T-s diagrams to visualize the interference between expansion work recovery and internal heat exchange. They showed that both of these mechanisms are competing for the same temperature difference. They predicted

that an ejector having 70% efficient nozzle and diffuser can replace an IHX with 60% effectiveness to achieve the same COP at a given cooling capacity.

Elbel and Hrnjak (2007) presented the first high-side pressure control equation used to maximize the COP of a trans-critical CO₂ two-phase ejector system. Furthermore, they identified the existence of mixing shock waves which they detected through static wall pressure distributions along the axis of the ejector. Images of the ejector mixing section were obtained through high-speed flow visualization under realistic operating conditions by using a semi-transparent ejector. Dubey et al. (2007) presented simulation model using ejector expansion considering Indian condition. Deng et al. (2007) presented a theoretical analysis of trans-critical CO₂ ejector expansion refrigeration cycle. The performance was strongly coupled to the ejector entrainment ratio which is necessary to produce the proper CO₂ quality at the ejector exit. Maximum COP improvement of 8.2% is reported over IHX and 11.5% over simple cycle. Liu and Groll (2008) presented an analysis through simulation and experimentation of a two phase flow ejector for the trans-critical CO₂ cycle applied to an air conditioning system. Results were obtained at different operating conditions and various ejector geometries and it was found that motive nozzle efficiency decreases as ejector throat area decreases and that the suction nozzle efficiency is affected by the outdoor temperature and ejector throat area.

Guangming et al. (2010) presented an experimental and theoretical study of an ejector used in the CO₂ heat pump water heater system. Effects of primary flow pressure, entrained flow pressure and back pressure on the entrainment ratio in off-design conditions were analyzed and Optimized. Elbel (2011) presented an overview of historical and present developments on how ejectors can be utilized to improve the performance of air-conditioning and refrigeration systems. Research on ejector refrigeration cycles that utilize low-grade energy sources to produce cooling was also summarized. Fangtian and Yitai (2011) presented a second law analysis to compare the trans-critical carbon dioxide refrigeration cycle with ejector and throttling valve. It was found that ejector reduce exergy loss by 25% and increase COP by 30% compare to throttling valve. In addition, critical entrainment ratio of the ejector, optimal heat rejection pressure and critical outlet temperature of gas cooler affects COP greatly for the trans-critical CO₂ refrigeration cycle with ejector.

Nakagawa et al. (2011) experimentally analyzed the effect of internal heat exchanger (IHX) in the performance of ejector refrigeration system and compare the same with conventional expansion refrigeration system. Experiments were performed at different operating pressure and temperature for the cases of without IHX, 30cm IHX and 60cm IHX. The ejector system with 60 cm IHX was found to have maximum COP improvement of up to 27%. Lee et al. (2011) studied a practical improvement on two-phase ejector for CO₂ air conditioning system. The experiments of performance with respect to variation of ejector geometry such as the motive nozzle throat diameter, mixing section diameter and the distance between motive nozzle and diffuser were carried out. Experiments showed that the coefficient of performance of the system using an ejector was about 15% higher than that of the conventional system.

Cen et al. (2012) proposed and modeled a novel cycle with two ejectors and compared with conventional ejector-expansion CO₂ cycle with only one ejector. This novel cycle with two ejectors showed more improvement of system performance. Effects of parameters, such as ejector nozzle efficiency, gas cooler pressure, entrainment ratios of the two ejectors, gas cooler outlet temperature, on the cycle performance were analyzed by using the model. Banasiak et al. (2012) performed an experimental and numerical investigation of the optimum ejector geometry for a small capacity CO₂ heat pump. Based on a simplified, one-dimensional ejector model, an optimization of the ejector geometry was obtained and the ejector efficiency found to be notably dependent on the mixer length and the diameter, as well as on the diffuser divergence angle. The maximum increase in COP was 8% over a system with a conventional expansion valve.

Liu et al. (2012) presented performance enhancement of a trans-critical CO₂ air conditioner with a controllable ejector at variable operating conditions and variable compressor frequencies. It was concluded that the enhancement became more significant as the outdoor air temperature increased (COP increase by 36%), further the effect on COP is reported, as compressor frequency decreased (COP increase by 147% compared to conventional cycle with compressor frequency at 50 Hz), and the motive nozzle throat diameter decreased (COP increase by 60%). Manjili and Yavari (2012) investigated a new two-stage multi-inter cooling trans-critical CO₂ refrigeration cycle with ejector expansion device including two intercoolers. It was reported that the new cycle exhibited COP improvement in the range of 15.3% - 19.6 %.

Lucas and Koehler (2012) presented an experimental comparison between the standard CO₂ expansion valve refrigeration cycle and the ejector refrigeration cycle. Effect of large pressure variations for different evaporation pressure condition and gas cooler outlet temperatures were analyzed. It was found that as compared to the maximal COP of the expansion valve cycle, COP improvements of the ejector cycle by 17% with ejector efficiency 22%. Chen et al. (2013) proposed a new one dimensional model to predict ejector performance at critical and subcritical operational modes, with constant pressure mixing inside the constant area section of the ejector at critical and sub-critical mode operation. The analysis showed that the proposed model accurately predicts ejector performance over all ranges of operation, and is a useful tool for predicting ejector performance within larger refrigeration cycle models.

Lucas et al. (2013) presented an ejector operation characteristic for a CO₂ ejector based on experimental data. Correlations for the ejector efficiency and the driving mass flow rate were used for the analysis and found these correlations are used to simulate a simple CO₂ ejector cycle in order to demonstrate their feasibility. Zhang et al. (2013) theoretically analyzed the effect of IHX on the performance of the ejector expansion trans-critical CO₂ refrigeration system. They reported that IHX in the CO₂ ejector refrigeration cycle increases the ejector entrainment ratio and the ejector efficiency, while decreasing the pressure recovery. Therefore they concluded that IHX addition does not always improve the system performance in the ejector expansion cycle, and is only applicable in cases of lower ejector isentropic efficiencies or higher gas cooler exit/evaporator temperatures for the ejector expansion system from the view of energy efficiency.

Recently, Lawrence and Elbel (2013) compared the standard two-phase ejector refrigeration cycle having a liquid-vapour separator with two alternates, one two-phase ejector refrigeration cycles and a conventional cycle with an expansion valve. The analysis showed that the standard two-phase ejector cycle has lower availability destruction and higher Second Law efficiency than the alternate ejector cycles despite having the same theoretical COP.

2.3.4 Expansion turbine

Single phase expansion and high pressure operation of a CO₂ trans-critical cycle lead to the possibility of employing a work producing device such as an expansion turbine which will reduce expansion losses significantly. Employing the work recovery turbine

with an isentropic efficiency of 60% causes the reduction of total cycle irreversibility by 35% as reported by Robinson and Groll (1998).

The design and related issues of various possible CO₂ cycles with expanders have been discussed at length by Heyl and Quack (1999). It has been shown that using the work recovery turbine in a trans-critical CO₂ system reduces irreversibility and improves the system performance, although such arrangements may not be economical and practically viable for small capacity systems. As in conventional vapour compression systems, capillary tube may also be a viable option to use as an expansion device in the CO₂ trans-critical system. In this section, detailed research and developments with expansion turbine as work recovery are reviewed. Beak et al. (2002) designed, constructed and tested a piston-cylinder type work output expansion device for a trans-critical CO₂ cycle. The device was based on a modified small four-cycle, two-piston engine with a displacement of 2 x 13.26cm³ that was commercially available. The expansion device replaced the expansion valve in an experimental trans-critical CO₂ cycle and increased the system performance by 10%.

Huff and Radermacher (2003) modeled three types of expanders and presented a comparative study with a base line R22 system and concluded that CO₂ system COP is strongly influenced by expander efficiency while the effect is almost negligible for an R22 system. Westphalen and Dieckmann (2004) developed a scroll expander design for use in CO₂ air-conditioning cycles operating at high ambient conditions. Cycle analysis, used to establish expander operating conditions indicated that external system power input can be reduced by 20% for a system using a 60% efficient expander. Nickl et al. (2005) proposed a three stage expander with a vapour-liquid separator between the second and third stage of expansion for optimum integration. Baek et al. (2005, 2005a) showed in their experimental and theoretical study that by replacing piston-cylinder work producing device with an isentropic efficiency of only 11% can improve the COP by about 10%. 2005a, 2005

Yang et al. (2005) presented a comparative study of a throttling valve and with an expander in a trans-critical CO₂ cycles, based on the first and second laws of thermodynamics. It was reported that in the throttling valve cycle, the largest exergy loss occurs in the throttling valve, that is about 38% of the total cycle irreversibility. While in the expander cycle, the irreversibility mainly comes from the gas cooler (38%) and the compressor (35%). The COP and exergy efficiency of the expander cycle are on average 33% and 30% higher than those of the throttling valve cycle,

respectively. Kohsokabe et al. (2006) developed an expander-compressor unit with an expander to improve COP of a small capacity air-cooled chiller. A scroll type expander and a rolling-piston type rotary sub-compressor was adopted. The expander-compressor unit was shown to be stable and can be used to improve the COP of the CO₂ chiller cycle under both cooling and heating conditions. The test results indicated that the COP improvement of the cycle was more than 30%, while the total efficiency of the expander-compressor unit was 57%.

Haiqing et al. (2006) developed a swing piston expander prototype for replacing the throttling valve based on the thermodynamic analysis of the operating conditions of a CO₂ trans-critical heat pump cycle. The performance of the CO₂ swing expander prototype was tested in a CO₂ trans-critical cycle water-to-water heat pump and the test results illustrate that the isentropic efficiency of the prototype can be enhanced from 28% to 44%. Fukuta et al. (2006) investigated the performance of CO₂ scroll expander both theoretically and experimentally. The investigation showed that the total efficiency of the scroll expander becomes about 60% when the leakage gap size is 10 μ m and the rotational speed is 3600 rpm. The volumetric efficiency of 80 % was obtained and the total efficiency reached about 55% although the scroll element of the compressor was used without any major modifications. Kim et al. (2008) presented an analysis of a two-stage compression CO₂ trans-critical cycle, using a combined scroll expander-compressor. Numerical simulation of performance showed that for suction pressure of 3.5MPa and discharge pressure of 10MPa with expander inlet temperature at 35°C, the main compressor power input could be reduced up to 12.1% by the expander output. Further, increase in the cooling capacity by the expander was 8.6%. As a consequence, COP improvement of the cycle was estimated to be 23.5%.

Yang et al. (2009) presented an experimental investigation of the internal working process of a rotary vane expander prototype for trans-critical CO₂ refrigeration cycle. Performance test of modified expander prototype showed that the volumetric efficiency increased from 17% to 30% and the isentropic efficiency from 9% to 23% at the speed of 800 rpm. Subiantoro and Ooi (2010) examined, four possible design variants of the Revolving Vane expander in relation to their application when using CO₂ as refrigerant. They showed that the revolving vane expander RV-I design configuration with the vane attached to the rotor, where the rotor was also used as the driving component was the most superior design. Yang et al. (2010) developed a mathematical model to simulate, optimize

and control trans-critical CO₂ refrigeration cycle. The simulation results showed that maximum COP was obtained at the optimal heat rejection pressure not only for throttle valve cycle but also for expander cycle. Two types of polynomial correlations were obtained, one in cubic form, having an average deviation of less than 0.5% while the other, which is a simplified form, has an average deviation of less than 1%.

Nagata et al. (2010) developed a scroll expander to recover the throttling loss in CO₂ cycles with an intercooler, the expander directly drives the second-stage compressor using the energy recovered from the expansion process. Experimental results showed that in the prototype device, the sub-compressor increased the pressure by 1.30MPa, while the pressure drop between the inlet and outlet of the expander was 3.19MPa. Sarkar (2010) presented a study of various important cycle modifications on the trans-critical CO₂ cycle. A detailed comparisons as well as the optimum system high side pressure were discussed. Studies showed that the highest improvement of the trans-critical CO₂ vapor compression cycle can be achieved by replacing the expansion device with a work recovery expansion or by using multi-staging. The optimum high side pressure in case of using turbine or multi-staging is also lower compared to that of other modifications. However, these are costly improvement compared to others.

Jia et al. (2011) presented an experimental investigation of the improved prototype expander for trans-critical CO₂ cycle. The investigation showed that, by introducing the high-pressure gas into the vane slots, it was possible to improve the volumetric efficiency from 17% to 35%, and the isentropic efficiency improved from 15% to 45%, resulting in a maximum COP improvement of 27.2% compared to the throttling cycle under the same working conditions. Hua et al. (2011) reported an investigation carried out on the influence of a non-condensable gas to expander performance of a CO₂ trans-critical heat pump. The result indicated that at 35°C the inlet temperature of expander and 8MPa inlet pressure, the efficiency of expander used in the system with non condensable gas become 25% higher on average. The results showed that with increase in the addition quantity of non-condensable gas increases expander efficiency.

Subiantoro and Ooi (2013) presented an economic analysis of the installation of expanders on to existing vapor compression cooling systems, for medium scale air conditioners. It was reported that the payback periods are shorter for systems with highly efficient expanders, high cooling loads, high ambient temperatures and for low refrigerating temperature applications. Li et al. (2013) investigated the influence of a

non-condensable gas, nitrogen on the performance of the expander in a CO₂ trans-critical heat pump. The experimental results showed that the recovery work of the expander in the presence of nitrogen is higher than that without nitrogen. However, the efficiency of the expander decreases with increasing nitrogen concentration.

2.4 Summary of Literature Review

A detailed discussion on the research and development of the various aspects of the CO₂ trans-critical systems has been presented. A broad spectrum of the gas cooler studies are also included. Some specific observations were made during the literature survey based on different aspects i.e. applications, component design and cycle modification are shown in Fig. 2.2 to Fig. 2.4 respectively. Fig. 2.2 shows that majority of the work reported for heating application and Fig. 2.3 shows that most of work are focused on gas cooler. Similarly it is clear from Fig. 2.4, that system modification with ejector and work recovery turbine are more popular.

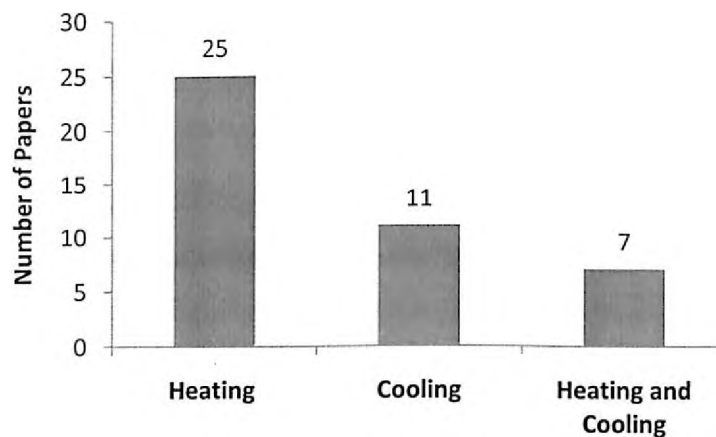


Figure 2.2: Summary of literature based on application

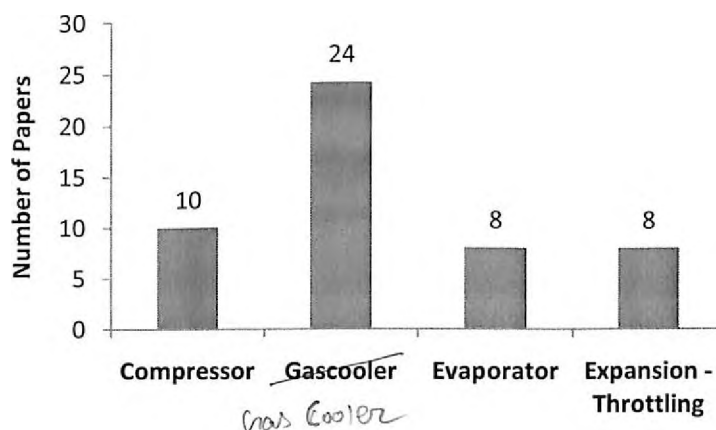


Figure 2.3: Summary of literature based on component design

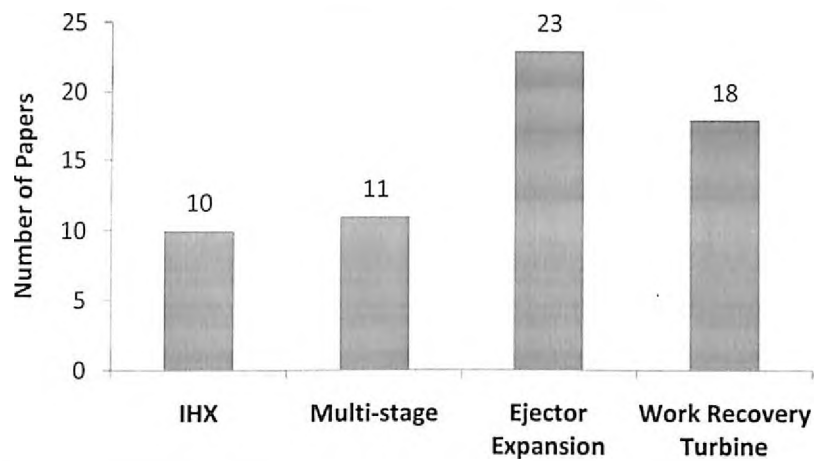


Figure 2.4: Summary of literature with system modification

In a trans-critical CO₂ vapour compression cycle, owing to the presence of two independent parameters such as pressure and temperature, employing a gas cooler leads to distinctly different situations. There exist an opportunity to investigate the heat transfer, design of gas cooler, and the overall performance of the system in typical environmental conditions with carbon dioxide as a refrigerant.

2.5 Gap Areas in Existing Research

From the literature survey, it was found that the following significant issues need to be addressed which will also be the focus of this research work.

1. The commercial success in trans-critical CO₂ system is so far mostly observed in heat pump applications. Some research work have been reported on cooling and simultaneous cooling & heating applications, however such work were carried out at comparatively lower environmental temperature.
2. Most of the published work on theoretical or experimental research reported in the trans-critical CO₂ domain assumes low ambient temperature. Use of the same system in tropical regions particularly like India requires taking care of the challenge of high temperature of heat rejection.
3. In trans-critical regions, heat transfer characteristics are also highly sensitive. It calls for appropriate parameter optimization of gas cooler so as to increase in rate of heat rejection to the surrounding.
4. Most of the work have been reported on micro channel type gas cooler, However, micro channels also have their weaknesses, such as large pressure drop, higher manufacturing cost, dirt clogging, and flow mal-distribution, especially for two phase flows. The designer confidence and associated low

disadvantages

cost is a motivation toward the modification of finned tube heat exchanger as gas cooler for trans-critical systems.

5. Majority of the work is either focused on gas cooler design or on overall system performance with particular gas cooler at a specified environmental temperature. Very few work is reported that focuses on gas cooler optimization, together optimizing with the overall performance of the modified system at different environmental temperatures.

Based on the above literature survey and existing gap in the research, this work ^{is} ~~was~~ carried out. The details of which are elaborated and summarized in the subsequent chapters.

Problem Identification and Description

Literature review related to trans-critical CO₂ systems presented in chapter 2, a theoretical analysis and steady state modeling of an ideal CO₂ trans-critical cycle have been presented in this chapter. In order to describe and ^{Identify} (indentify) the challenges associated with trans-critical CO₂ systems, in tropical countries like India, an analysis is done which included the effect of environmental temperature on the system performance and also on design of the system. Since India has a wide range of variation in environmental temperature, hence the design conditions for a refrigeration system at various part of the country are different. Ambient temperature affects the performance of the system and required to select a suitable component design and specific operating conditions at specific environmental conditions. This chapter also help to formulate the guideline for selecting the operating condition and specific design conditions at particular environmental conditions.

3.1 CO₂ Refrigeration System in Indian Conditions

Based on literature review, it is found that most of work reported was for heating application, while some cooling applications were also reported for the lower ambient temperature. Since the ambient temperature in India varies from place to place, and are comparatively higher than reported in the literature, hence the performance of the system also is expected to vary.

It was also found during literature review that, gas cooler is one of the main component of the system which is affected most by the ambient temperature. According to the environmental condition the operating conditions of gas cooler and other components are selected. Present study is focused on the performance of the trans-critical CO₂ refrigeration system especially in Indian condition. The design temperature conditions of different locations of India are taken from ASHRAE Handbook (2009). The performance of gas and the system are analyzed based on ideal trans-critical CO₂ cycle for these range of design conditions. Table 3.1 shows the design condition of major

include a
 9-10-2010
 10/5

locations in India. Since the major concern is about the refrigerant temperature at the outlet of the gas cooler, the effect of humidity is not considered during the analysis.

Table 3.1: Outside design conditions of major cities in India

City	Outside DBT (°F)	Outside DBT (°C)	Outside DBT (°C)
Agra	108	42.22	42
Ahmedabad	110	43.33	43
Ahmednagar	108	42.22	42
Ajmer	108	42.22	42
Aligarh	108	42.22	42
Allahabad	110	43.33	43
Ambala	110	43.33	43
Assansol	108	42.22	42
Bangalore	96	35.56	36
Belgaum	100	37.78	38
Bellary	105	40.56	41
Bhopal	106	41.11	41
Bhubaneswar	100	37.78	38
Calicut	96	35.56	36
Chennai	103	39.44	39
Coimbatore	98	36.67	37
Cuttack	105	40.56	41
Dehradun	105	40.56	41
Dibrugarh	90	32.22	32
Durgapur	108	42.22	42
Gauhati	90	32.22	32
Gaya	110	43.33	43
Goa	90	32.22	32
Hyderabad	106	41.11	41
Indore	106	41.11	41
Jaipur	110	43.33	43
Jamnagar	100	37.78	38
Jamshedpur	110	43.33	43
Jhansi	111	43.89	44
Jodhpur	110	43.33	43

100 are same here check it
is the same column
don't give value of its previous column

omit h
Calicut

City	Outside DBT (°F)	Outside DBT (°C)	Outside DBT (°C)
Kanpur	109	42.78	43
Kochi	95	35.00	35
Kolkata <i>Kolkata</i>	100	37.78	38
Kotah	113	45.00	45
Kurnool	108	42.22	42
Lucknow	109	42.78	43
Madurai	101	38.33	38
Mangalore	96	35.56	36
Meerut	110	43.33	43
Mumbai	95	35.00	35
Mysore	100	37.78	38
Nagpur	112	44.44	44
Nellore	108	42.22	42
New Delhi	110	43.33	43
Ootacmund	73	22.78	23
Patna	108	42.22	42
Pune	104	40.00	40
Raichur	107	41.67	42
Raipur	110	43.33	43
Ranchi	100	37.78	38
Salem	103	39.44	39
Sambalpur	110	43.33	43
Shillong	85	29.44	29
Sholapur	108	42.22	42
<u>Thana-Kalyam</u>	100	37.78	38
Thiruvandrum	92	33.33	33
Trichy	104	40.00	40
Varanasi	109	42.78	43
Vijayawada	110	43.33	43
Visakhapatnam	92	33.33	33

check 2t

ASHRAE Handbook fundamentals (2009), Inch-Pound Edition, American Society of Heating, Refrigerating and Air-Conditioning Engineers, Inc. 1791 Tullie Circle, N.E., Atlanta, GA 30329.

Base on the above temperature range, an analysis of trans-critical CO₂ system with ideal cycle is carried out, as reported in subsections 3.2.

3.2 Effect of Gas Cooler Outlet Temperature and Operating Pressure

A steady state study of a CO₂ trans-critical refrigeration cycle is done base on the temperature range given in Table 3.1. The study state model is described in Eq. 3.1 to Eq. 3.3, which represent the compressor work input, refrigeration capacity and COP of the system respectively and Fig. 3.1 is used as a basic trans-critical cycle for the above steady state modeling of the system.

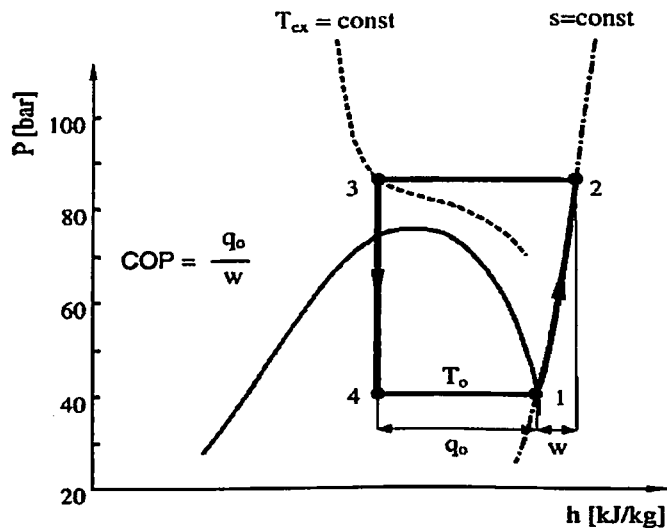


Figure 3.1: Trans-critical cycle for CO₂

Referring Fig. 3.1, Where, $H_r = H_r(P, T)$ and $H_{rgco} = H_{rei}$

Work done for compression,

$$w_{\text{comp}} = \{H_{rco}(P_{co}, T_{co}) - H_{rci}\} \quad (3.1)$$

Refrigeration capacity

$$q_0 = \{H_{reo} - H_{rei}(P_{gco}, T_{gco})\} \quad (3.2)$$

Coefficient of performance of the system

$$COP = \frac{\{H_{reo} - H_{rei}(P_{gco}, T_{gco})\}}{\{H_{rco}(P_{co}, T_{co}) - H_{rci}\}} \quad (3.3)$$

The range of design temperature is from 23°C to 45°C, hence the analysis is carried out for the system operating at 20°C to 55°C environmental temperature at different operating pressure range of 9.5MPa to 12.5MPa with interval of 0.5MPa.

In this analysis the effect of gas cooler outlet temperature and operating pressure, on compressor work, cooling capacity and COP is carried out. All the properties of CO₂ at different state are found by using NIST REFPROP[®] 9.0. The compressor ~~condition~~ ^{inlet} condition is assumed to be saturated vapour and evaporator temperature is maintained at 0°C without pressure drop.

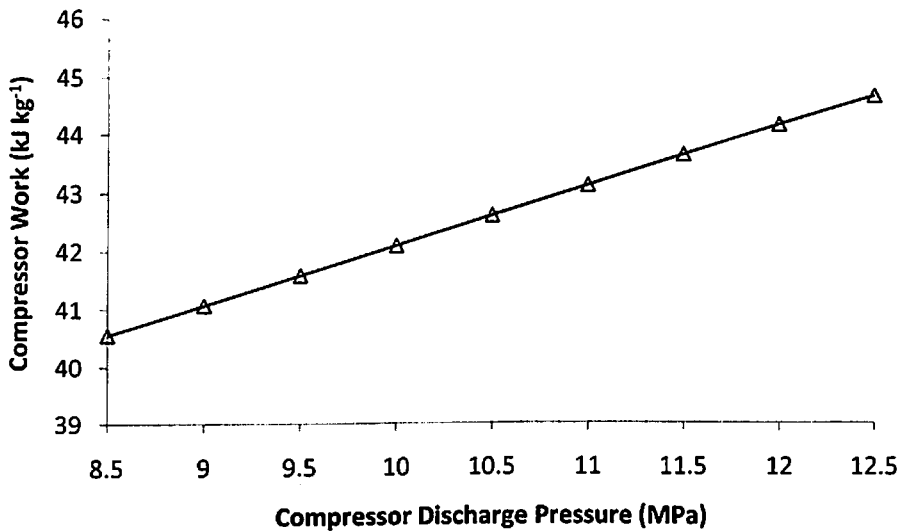


Figure 3.2: Variation of compression work with compressor discharge pressure

Refer to Eq. 3.1 - Eq. 3.3, for different value of gas cooler outlet temperature and operating pressure, the variation of compression work, refrigeration capacity and COP are obtained using MATLAB[®] simulation. Fig. 3.2 show the variation of compression work with operating pressure, it is observed that the compression work increase with increase in pressure as expected.

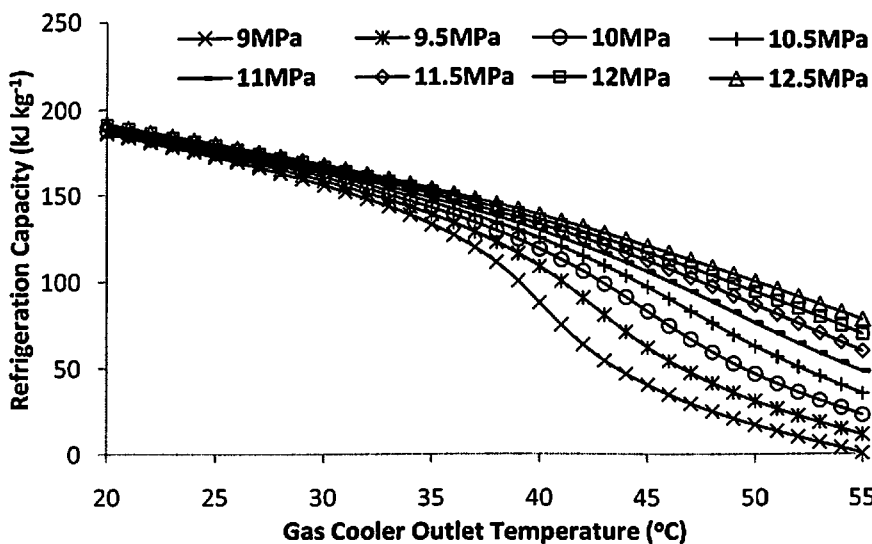


Figure 3.3: Variation of refrigeration capacity with gas cooler outlet temperature at different operating pressure

Fig. 3.3 represent the variation of refrigeration capacity with gas cooler outlet temperature at different operating pressure. It shows that the variation of refrigeration capacity is more prominent at higher gas cooler outlet temperature, especially above critical point. In order to investigate the cumulative effect of above two parameters, the variation of COP with respect to gas cooler outlet temperature for different pressure is studied as shown in Fig. 3.4. It is observed that, with increase in gas cooler outlet temperature, COP of the system initially decreases. With increase in operating pressure, COP decreases up to certain gas cooler outlet temperature, then COP increases with pressure. It is also observed that the variation of COP with pressure is significant at higher gas cooler outlet temperature (e.g. 32°C to 55°C, above the critical point). This is due to fact that the thermo-physical properties of CO₂ changes rapidly during the constant pressure cooling in supercritical region observable in the P-h chart shown Fig. 3.1 for CO₂ as refrigerant.

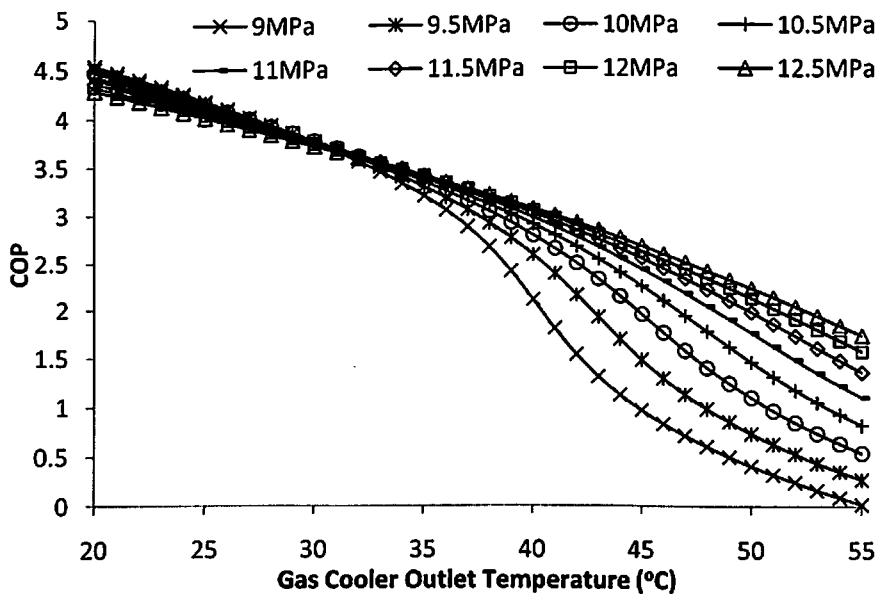


Figure 3.4: Variation of COP with gas cooler outlet temperature at different operating pressure

From above study it is concluded that in Indian context, where the required operating temperature is generally high, the gas cooler design is very critical in order to obtain reasonable COP. While in the colder countries a simpler design of gas cooler with slack control over pressure will give lesser performance variation in terms of COP. Also, as the operating temperature increases, we get lower overall COP. At the same time the effect of pressure is also an important factor affecting the COP. The major factors which affect the performance of CO₂ based trans-critical refrigeration system are: design of gas

cooler, its pressure & outlet temperature and ambient condition. Overall, the gas cooler outlet temperature will depend on the ambient temperature and it will vary with the location and seasons.

3.3 Temperature Zones in Indian Conditions

It is found from the result of the study described in previous section, that in tropical or Indian climate condition, where the ambient temperature is higher, the performance of the gas cooler is highly sensitive to ambient temperature and operating pressure. Further the performance of the overall system depends on the gas cooler performance, therefore ambient temperature has a significant effect on the system performance.

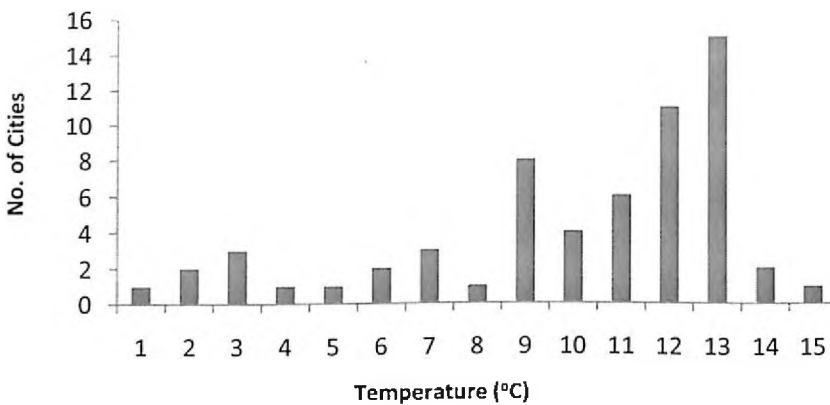


Figure 3.5: Number of cities in India and its design temperatures

It is also found from Table 3.1 that the design temperature at most of the locations in India are more than 38°C. Fig. 3.5 shows the detail of this design temperature with number major cities in India. It is not possible to design a specific component and select specific operating conditions for all design temperature, keeping this point in mind, clusters of temperature (i.e. 20 to 30°C, 30 to 40°C and above 40°C) are selected and named as temperature zone I, zone II and zone III as shown in Table 3.2. It is also clear in Fig. 3.6 that the major percentage of Indian cities comes under the temperature zone three, hence the design of gas cooler is more crucial in Indian conditions.

Table 3.2: Temperature zones and its range of temperature

Temperature Zones	No. of major cities	Design Temperature
Zone I	3	$\leq 29.4^\circ\text{C}$
Zone II	19	$> 29.4^\circ\text{C} \leq 40^\circ\text{C}$
Zone III	41	$> 40^\circ\text{C} \leq 45^\circ\text{C}$

Insert all space

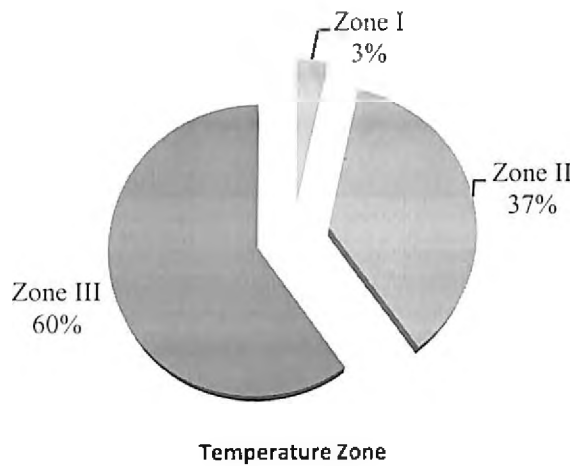


Figure 3.6: Percentage of cities in India at selected temperatures zones

3.4 Ideal Cycle Based Performance Analysis at Different Temperature Zones

In this section an ideal cycle based performance of a trans-critical CO₂ refrigeration system are studied at different temperature zones in India as described in previous section. The study is focused on the performance of air cooled gas cooler at different temperature zone and operating pressure. During the study, following assumption are taken; a) No pressure drop in gas cooler and the exit of compressor to gas cooler b) Evaporator temperature is constant of 273.15K. c) Throttling process is consider for the expansion. The temperature difference between the refrigerant outlet and incoming ambient air for an air cooled gas cooler is called approach temperature (AT) and their effect (within the range of 0°C to 5°C) on the performance of the system is also analyzed.

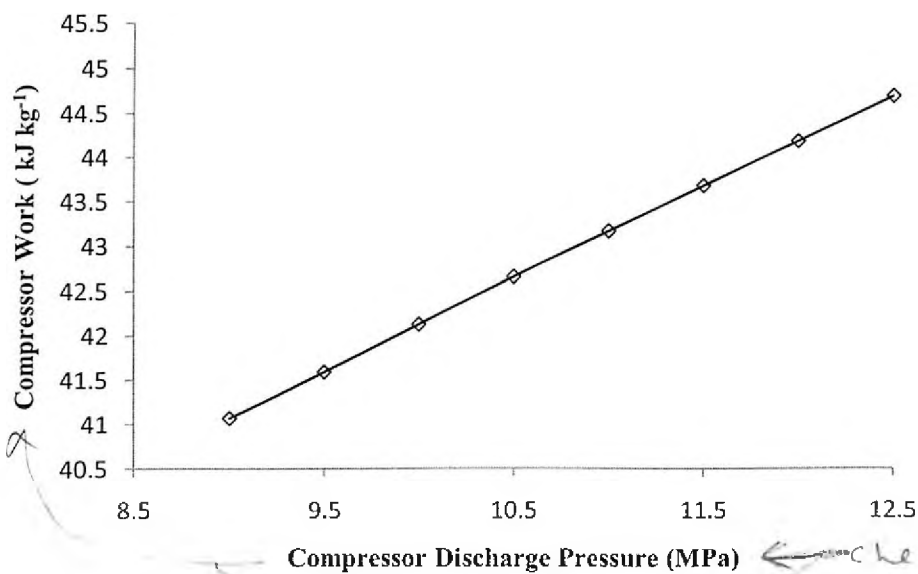


Figure 3.7 Variation of compressor work with the compressor discharge pressure

Fig. 3.7 shows the variation of compressor work with the compressor discharge pressure, keeping evaporator pressure constant. Compressor work does not depend on ΔT , and it increases with increase in the compressor discharge pressure as in a conventional system.

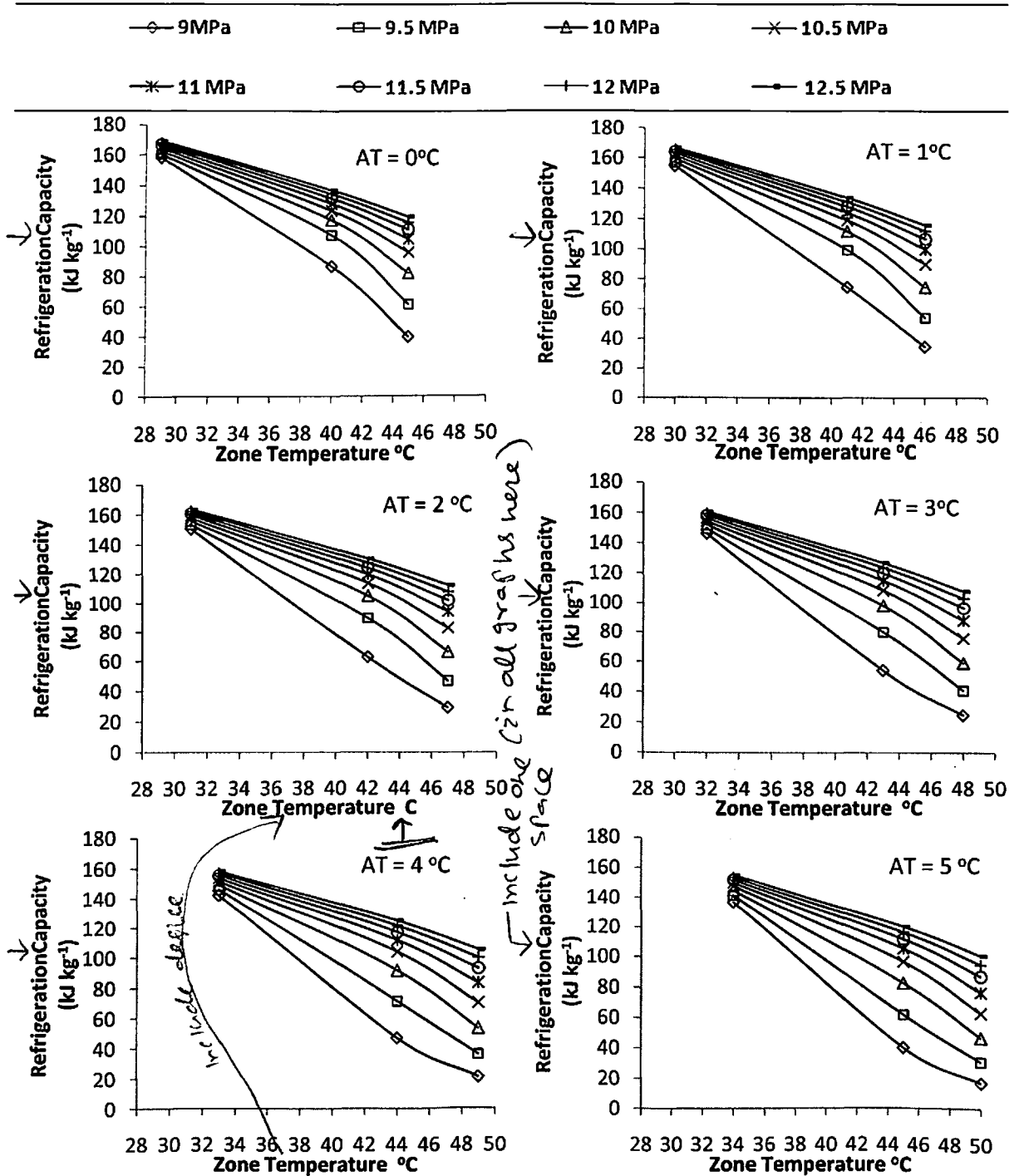


Figure 3.8: Variation of refrigeration capacity with gas cooler outlet temperature at different ΔT

Fig. 3.8 shows the variation of refrigeration capacity with gas cooler outlet temperature at different temperature zone and different value of AT. It is found during the study that the refrigeration capacity variation with operating pressure is more prominent at higher gas cooler outlet temperature, however these variation is insignificant at lower gas cooler outlet temperature.

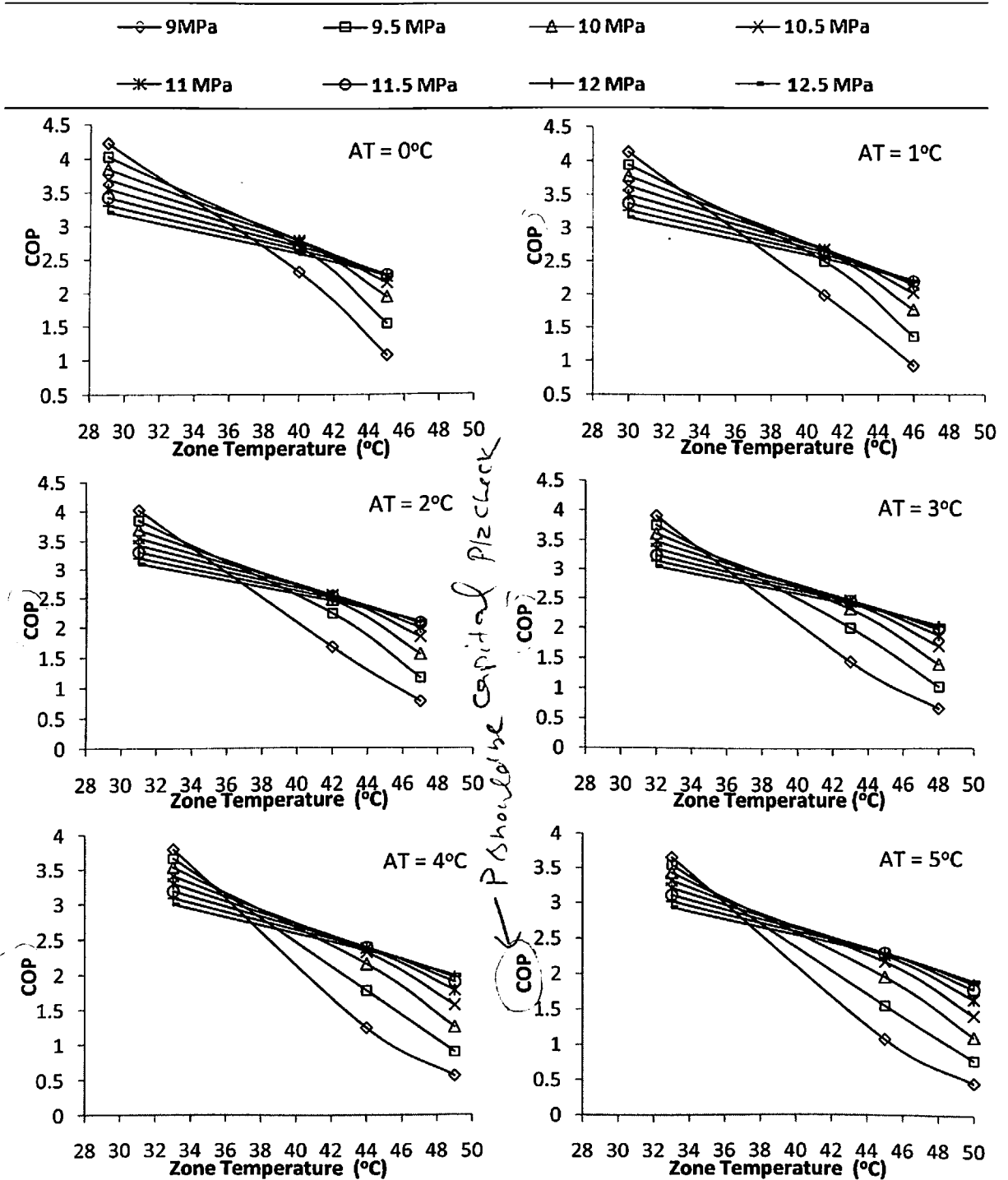


Figure 3.9: Variation of COP with gas cooler outlet temperature at different AT

A cumulative effect of compression work and refrigeration capacity are studied next as shown in Fig. 3.9 which shows the variation of COP with gas cooler approach temperature and operating pressure at different AT. Approach temperature is found to be a very important parameter in the design of gas cooler and literature on gas cooler clearly indicates the feasibility of designing with a low value of approach temperature even with air cooled coils. To obtain optimum operating pressure (design pressure) for gas cooler for maximum COP at different climatic zones for different approach temperatures are presented here in Fig. 3.9 as determined using the simulated energy model.

3.5 Ideal Cycle Based Guideline for Operating Conditions

The selection of operating pressure of gas cooler for higher COP is a crucial issue which is clearly demonstrated from Fig. 3.8. It not only depends on the environmental condition but also depends on AT of the gas cooler. The above results are summarized in Fig. 3.10 and Fig. 3.11.

Fig. 3.10 shows the pressure at which the maximum COP can be achieved for different approach temperature. With increasing approach temperature, operating pressure also increases for maximum COP in zone I and III, whereas for zone II, COP will be maximum at same pressure for all approach temperature.

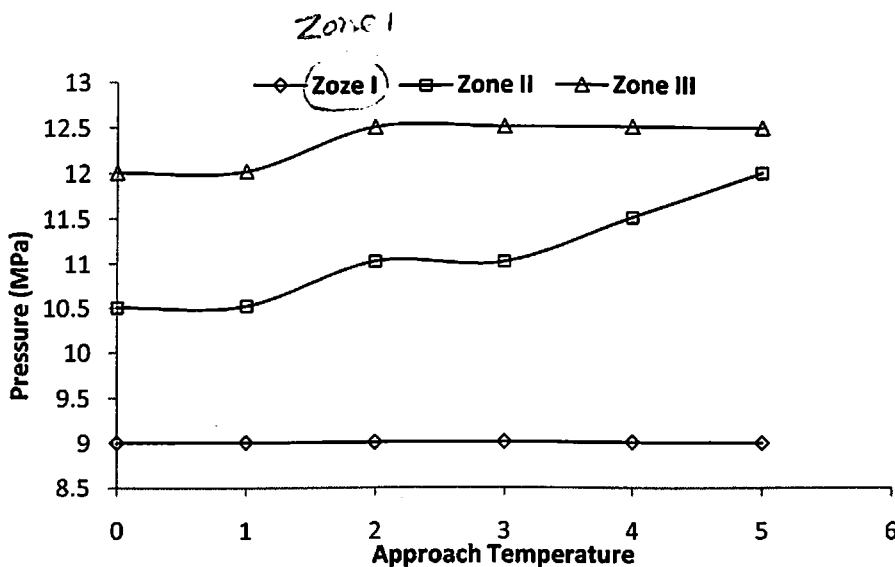


Figure 3.10: Pressure at which the maximum COP achievable at different AT

A cumulative effect of compression work and refrigeration capacity are studied next as shown in Fig. 3.9 which shows the variation of COP with gas cooler approach temperature and operating pressure at different AT. Approach temperature is found to be a very important parameter in the design of gas cooler and literature on gas cooler clearly indicates the feasibility of designing with a low value of approach temperature even with air cooled coils. To obtain optimum operating pressure (design pressure) for gas cooler for maximum COP at different climatic zones for different approach temperatures are presented here ⁱⁿ Fig. 3.9 as determined using the simulated energy model.

3.5 Ideal Cycle Based Guideline for Operating Conditions

The selection of operating pressure of gas cooler for higher COP is a crucial issue which is clearly demonstrated from Fig. 3.8. It not only depends on the environmental condition but also depends on AT of the gas cooler. The above results are summarized in Fig. 3.10 and Fig. 3.11.

Fig. 3.10 shows the pressure at which the maximum COP can be achieved for different approach temperature. With increasing approach temperature, operating pressure also increases for maximum COP in zone I and III, whereas for zone I, COP will be maximum at same pressure for all approach temperature.

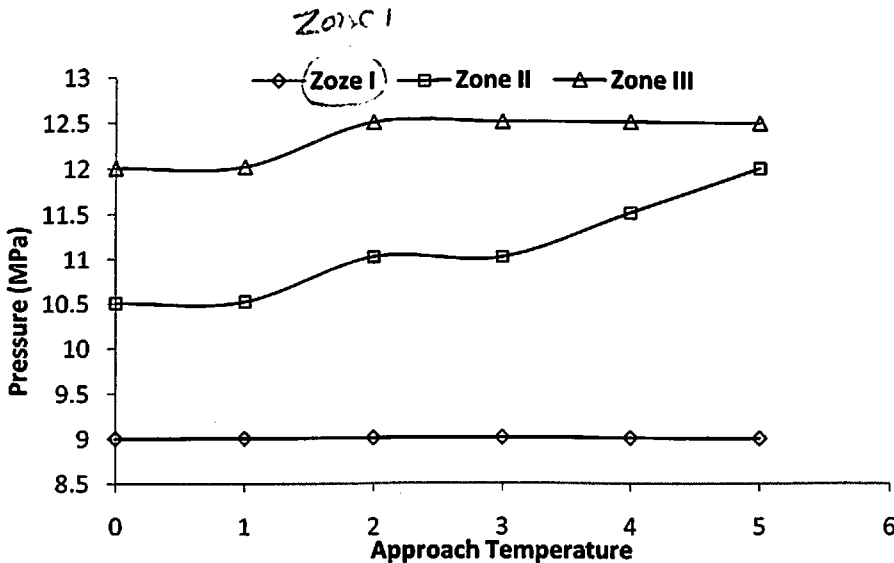


Figure 3.10: Pressure at which the maximum COP achievable at different AT

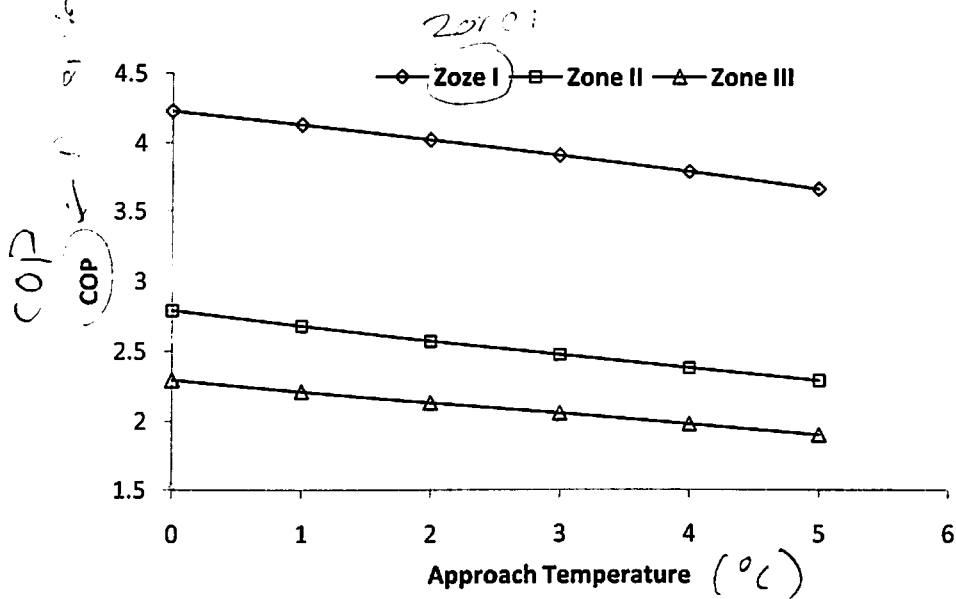


Figure 3.11: Variation of maximum possible COP with AT at different zones

Fig.3.11 shows the variation of maximum possible COP with approach temperature in different zones. It is found that the variation of COP with approach temperature is more sensitive in zone II and III than in ~~Zone~~^{Zone} I. Hence design of gas cooler is more crucial in ~~Zone~~^{Zone} II and III. Most of the Indian cities belongs to these regions. The operating condition recommended for different zones in India are summarized in Table 3.3, which shows the operating pressure and maximum COP obtainable at different zones for a range of approach temperatures.

Table 3.3: Operating pressure and maximum COP at different approach temperature

Zones		Approach Temperature (°C)					
		0	1	2	3	4	5
I	Pressure (MPa)	9	9	9	9	9	9
	COP	4.22	4.12	4.02	3.91	3.79	3.66
II	Pressure (MPa)	10.5	10.5	11	11	11.5	12
	COP	2.79	2.68	2.57	2.47	2.38	2.29
III	Pressure (MPa)	12	12	12.5	12.5	12.5	12.5
	COP	2.29	2.21	2.13	2.05	1.98	1.90

In tropical or Indian climate condition, where the ambient temperature is higher, the performance of the gas cooler is highly sensitive to operating temperature and pressure. And while designing a plant for higher COP, the gas cooler design is one of the most important parameters, which affect COP. With increase in the ambient temperature, the dependence of COP on gas cooler operating pressure increases, therefore the pressure

drop in the gas cooler, which is generally neglected, may become an important factor. Finally, the gas cooler operating conditions for maximum obtainable COP are presented for different region within India and for different approach temperature of gas cooler design.

Based on the above studies, it was found that the gas cooler is the most crucial component which affect the system COP, especially in tropical country like India. It is due to the gas cooler operates in supercritical region where the CO₂ properties varies drastically. Therefore, a detail study and optimum design of gas coolers are required for the best performance of the system. In subsequent chapter, a detail mathematical modeling, simulation and validation are presented.

Modeling and Simulation

The literature related to trans-critical CO₂ systems is reviewed in chapter 2 and the importance of gas cooler design for the performance of the system is established in chapter 3. Subsequently the work is now completely focused on gas cooler performance to evaluate the overall performance of the system. In this chapter the mathematical model of a finned tube air cooled CO₂ gas cooler is developed by means of distribution method. Updated correlations of heat transfer coefficients and pressure drops for both refrigerant and air sides are utilized and an efficient solving method is proposed for the simulation. The model is validated with the help of published experimental results. Further, this model is expanded to include the complete cycle and overall performance of the system is studied using the same.

4.1 Gas Cooler Geometry

The three dimensional geometry of the selected gas cooler along with its dimensional parameters is shown in Fig. 4.1 and the detail specification of the gas cooler is given in Table 4.1.

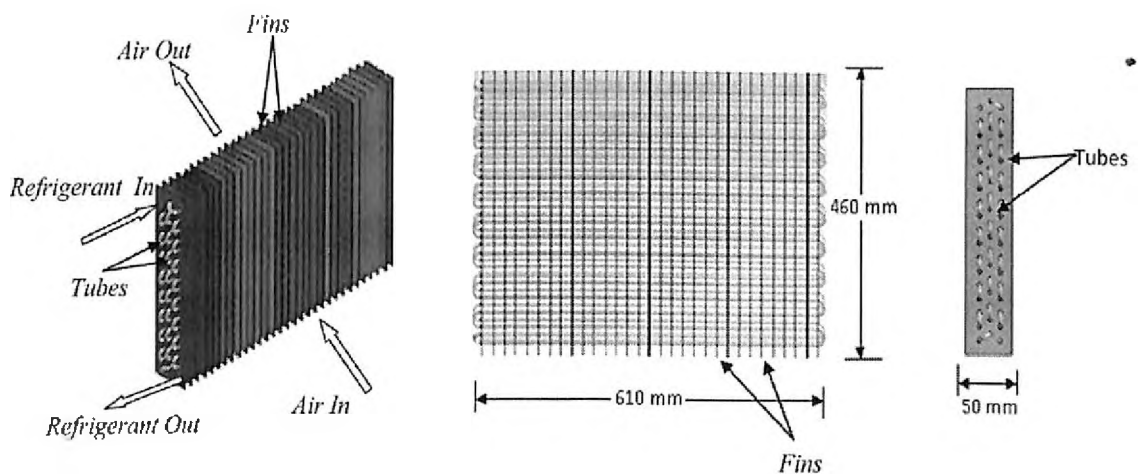


Figure 4.1: Three dimensional geometry of gas cooler

Table 4.1: Specification of Tested Gas Cooler

Width × Height × Depth	610 × 460 × 50 mm ³
Front area	610 × 460 mm ²
Fin (Plate type)	
Material	Aluminum ($K = 250 \text{ W m}^{-1}\text{K}^{-1}$)
Pitch	1.5 mm
Thickness	0.13 mm
Tube (Circular and Smooth)	
Number of Row	3
Number of Tube Per Row	18
Outside Diameter	7.9 mm
Inside Diameter	7.5 mm
Material	Copper ($K = 385 \text{ W m}^{-1}\text{K}^{-1}$)

A counter cross flow type finned tube air cooled gas cooler is selected from the published literature ^{i.e.} Hwang et al. (2005), ^{had} was used for experiment. Gas cooler is having copper tube with thin aluminum fins. Mathematical modeling effort of the above gas cooler is described in subsequent sections.

4.2 Mathematical Modeling

The thermo-physical properties of CO₂ changes rapidly during the constant pressure cooling in supercritical region as discussed in the literature review chapter 4; therefore, the conventional method for calculating heat transfer i.e. effectiveness-NTU and LMTD are not applicable for refrigerant side, however it is applicable for air side heat transfer. Hence, a one dimensional flow of heat and fluid for both air and refrigerant side is modeled separately for gas cooler.

4.2.1 Discretization

The three dimensional geometry of the gas cooler is discretized into number of small elements (as a small volume), detailed schematic diagram with elements of the gas cooler is shown in Fig. 4.2. The tubes are arranged parallel to i direction and j - k is the plane of fins. Air flows in k direction and CO₂ flows in i direction. An element for analysis has a dimension Δx_i , Δx_j , Δx_k in i , j , k directions respectively. The coordinate of each divided element in the 3D space can accordingly be determined. Subsequently, the detail of an

element volume with co-ordinates and its flow direction is shown in Fig. 4.3, where each element consists of small tube section with number of fins depending upon the size of element in the direction of flow of CO₂.

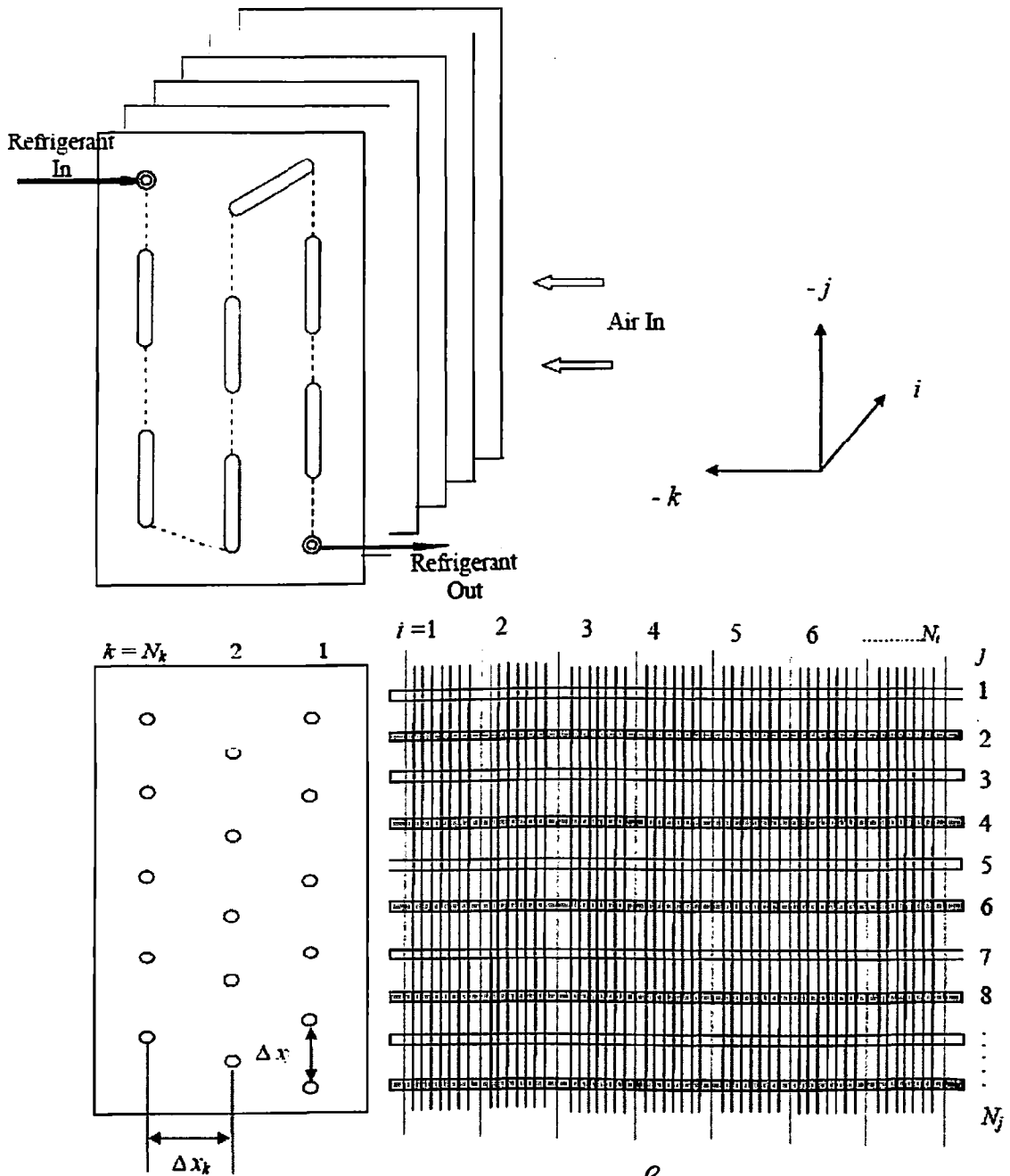


Figure 4.2: Co-ordinates of the elements in the discretized geometry of the gas cooler

The coordinate value i represent the number of elements for each pipe, selected by the model, j corresponds to the tube numbers in transverse path originating from the bottom and inlet of the refrigerant, while k corresponds to pipe numbers in longitudinal path starting from the air inlet.

Therefore, the state of either refrigerant or air at each specified sub-element in the 3D space can be uniquely identified with its corresponding coordinate values $i, j,$ and $k,$ which vary according to the circuit number and pipe number. The selection of number of small elements in i direction is arbitrary from one to infinity. The larger this value is, the more accurate the simulation will be, but expensive computational load will be there. The mathematical model is first solved for one element and then the solution is extended for complete geometry element by element.

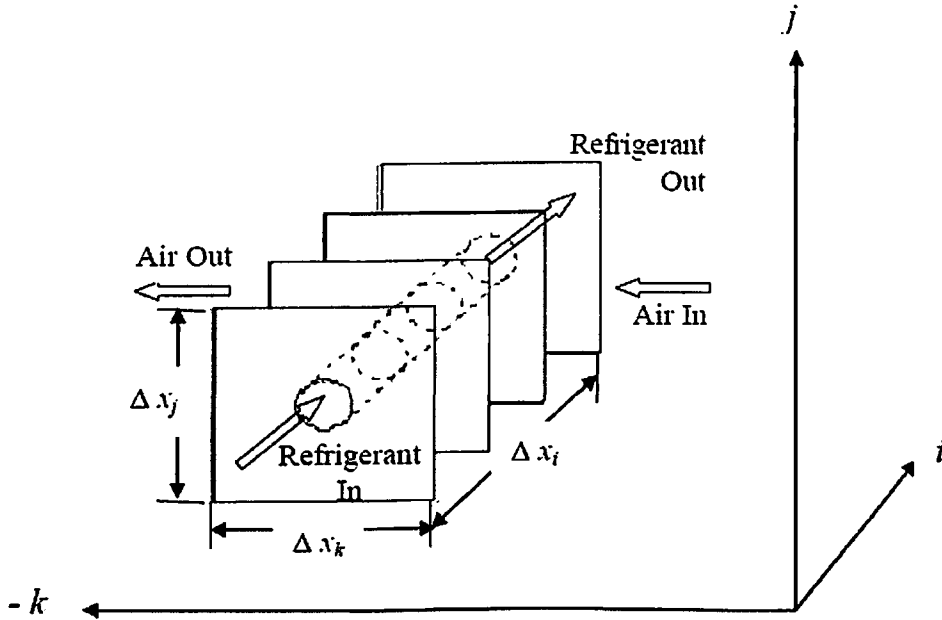


Figure 4.3: Control volume element with flow directions

4.2.1.1 Refrigerant side modeling

Fundamental conservation equations of mass, momentum and energy as given in equation 4.1 to 4.3 are solved simultaneously to compute the heat transfer in gas cooler.

$$\frac{d(\dot{M}_r)}{dx} = 0 \quad (4.1)$$

$$\frac{d(\dot{M}_r u_r)}{dx} + \left(\frac{dP}{dx} + \frac{\sigma_{iw} p_{tw}}{A_{siw}} \right) A_{in} = 0 \quad (4.2)$$

$$\frac{d(\dot{M}_r H_r)}{dx} + \pi d_o \dot{q} = 0 \quad (4.3)$$

These conservation equations are based on following assumptions: a) Flow and heat transfer are one dimensional steady state, b) Heat conduction along pipe axis and within fin are negligible, c) Homogeneous distribution of air d) Contact resistance at the joint of the fin and pipe wall are negligible e) Refrigerant is in thermal equilibrium at each point.

The conservation equations are discretized by finite difference scheme for an element from coordinates (i, j, k) to $(i+1, j, k)$ as shown in Eq. (4.4) - (4.6).

$$(\dot{M}_r)_{(i+1,j,k)} - (\dot{M}_r)_{(i,j,k)} = 0 \tag{4.4}$$

$$\frac{1}{A_{in}} \left[(\dot{M}_r u_r)_{(i+1,j,k)} - (\dot{M}_r u_r)_{(i,j,k)} \right] + \Delta P_r = 0 \tag{4.5}$$

$$\frac{[(\dot{M}_r H_r)_{(i+1,j,k)} - (\dot{M}_r H_r)_{(i,j,k)}]}{\Delta x_i} + \pi d_o \dot{q} = 0 \tag{4.6}$$

In addition, there is a heat balance between air and refrigerant side for each element. Heat transfer coefficient of refrigerant side is calculated from the mean Nusselt number reported by Pitla et al. (2001), Eq. (4.7).

$$Nu = \left(\frac{Nu_{wt} + Nu_{bt}}{2} \right) \left(\frac{K_{wt}}{K_{bt}} \right) \tag{4.7}$$

where, Nu_{wt} and Nu_{bt} are the Nusselt number evaluated based on thermo-physical properties at wall and bulk temperature respectively. Wall and bulk temperatures are calculated using iterative method by initially assuming them as the temperature of refrigerant and air respectively. In each case the respective Nusselt number and other required parameters are calculated using the correlation given by Gnielinski (1976), Eq. (4.8).

$$Nu = \frac{\frac{\phi}{8}(Re - 1000)Pr}{12.7 \sqrt{\frac{\phi}{8} \left(Pr^{\frac{2}{3}} - 1 \right)} + 1.07} \tag{4.8}$$

where ϕ is the friction coefficient, as expressed in Eq. (4.9). Heat transfer coefficient h_r and refrigerant side pressure loss ΔP_r are obtained using Eq. (4.10) and Eq. (4.11).

$$\phi = \frac{1}{(0.79 \ln(Re) - 1.64)^2} \tag{4.9}$$

$$h_r = \frac{Nu}{d_i} K_{bt} \tag{4.10}$$

$$\Delta P_{fr} = \frac{\phi G^2 \Delta x_i}{2 \rho d_i} \tag{4.11}$$

4.2.1.2 Air side modeling

The heat transfer in the air side at grid points are calculated by the effectiveness - NTU method. For one grid, the heat transfer equation is expressed as Eq. (4.12).

$$Q_{ta} = \varepsilon C_{min} (T_r(i, j, k) - T_a(i, j, k)) \tag{4.12}$$

where ε is effectiveness of the element and is calculated as per published literature by Ge, et. al. (2009), given by Eq. (4.13) for $C_{max} = C_h$ and Eq. (14) for $C_{min} = C_h$.

↑ remove comma remove dot
-80-

Wang et al. (1995) is not listed
in the References section
include it in references section.



$$\varepsilon = 1 - e^{(-\gamma C_r)} \quad (4.13)$$

where $\gamma = 1 - e^{(-\frac{UA}{C_{max}})}$ and $C_r = \frac{C_{max}}{C_{min}}$

$$\varepsilon = C_r (1 - e^{(-\gamma \frac{1}{C_r})}) \quad (4.14)$$

where $\gamma = 1 - e^{(-\frac{UA}{C_{min}})}$

Air side heat transfer coefficient is calculated from the Nusselt number correlation from Incropera (1996) as shown in Eq. (4.15) and Eq. (4.16). η_o is overall surface efficiency, calculated using the correlation given by Wang et al. (1999), equation Eq. (4.17). $\sum R_{ct}$ is the conduction resistance through tube wall to fins. Pressure drop in air side is calculated using the correlation given by Hwang et. al. (2005) as shown in Eq. (4.18).

$$Nu_a = 0.683 Re_a^{0.466} Pr_a^{0.33} \quad (4.15)$$

$$h_a = \frac{Nu_a K_{bt}}{de} \quad (4.16)$$

$$\eta_o = [1 - \frac{A_{fin}}{A_t} (1 - \eta_{fin})] \quad (4.17)$$

$$\Delta P_a = 19.70 u_a^{1.481} \quad (4.18)$$

Overall heat transfer coefficient of the gas cooler is thus given by Eq. (4.19)

$$U_o A = \left(\frac{1}{h_a \eta_o A_{ta}} + \sum R_{ct} + \frac{1}{h_r A_{in}} \right) \quad (4.19)$$

The heat transfer equation in the discretized form of a small element is given in Eq. (4.20) for finding the value of air outlet temperature at next grid element $k+1$. Further it will be used to calculate the refrigerant properties at next grid element $i+1$.

$$\begin{aligned} Q_{ta} &= [\dot{M}_a(i, j, k) C_{pa}(i, j, k) \{T_a(i, j, k+1) - T_a(i, j, k)\}] \\ &= U_o A(i, j, k) [T_r(i, j, k) - T_a(i, j, k)] \end{aligned} \quad (4.20)$$

4.2.2 Numerical implementation through MATLAB code

Air side and refrigerant side equations are solved simultaneously using an iterative method for $i+1$ and $k+1$. Air and refrigerant properties are obtained by connecting subroutine with NIST REFPROP[®] 9.0. The pipe number starts from refrigerant inlet to refrigerant outlet for each circuit and the simulation run through each numbered pipe starting from refrigerant inlet and then the element loop for each pipe. The gas cooler is counter cross flow and only one temperature is known out of four

temperatures at a particular element as shown in Fig. 4.4, therefore, one more temperature is to be assumed. The air outlet temperature of the gas cooler is assumed, which should be higher than the air inlet temperature and equations are solved iteratively to find the inlet air temperature and refrigerant outlet temperature for one element.

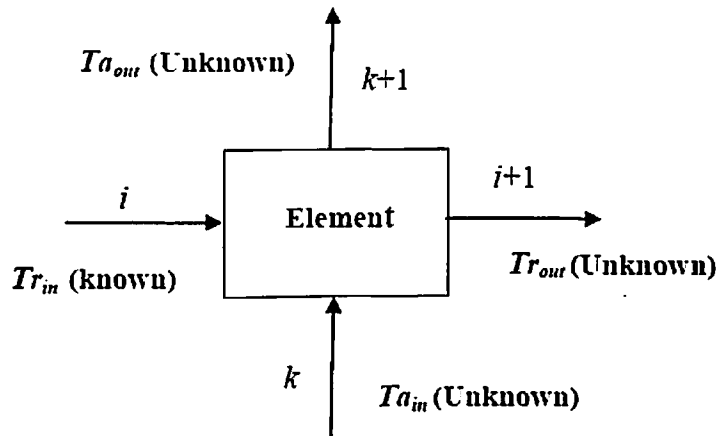


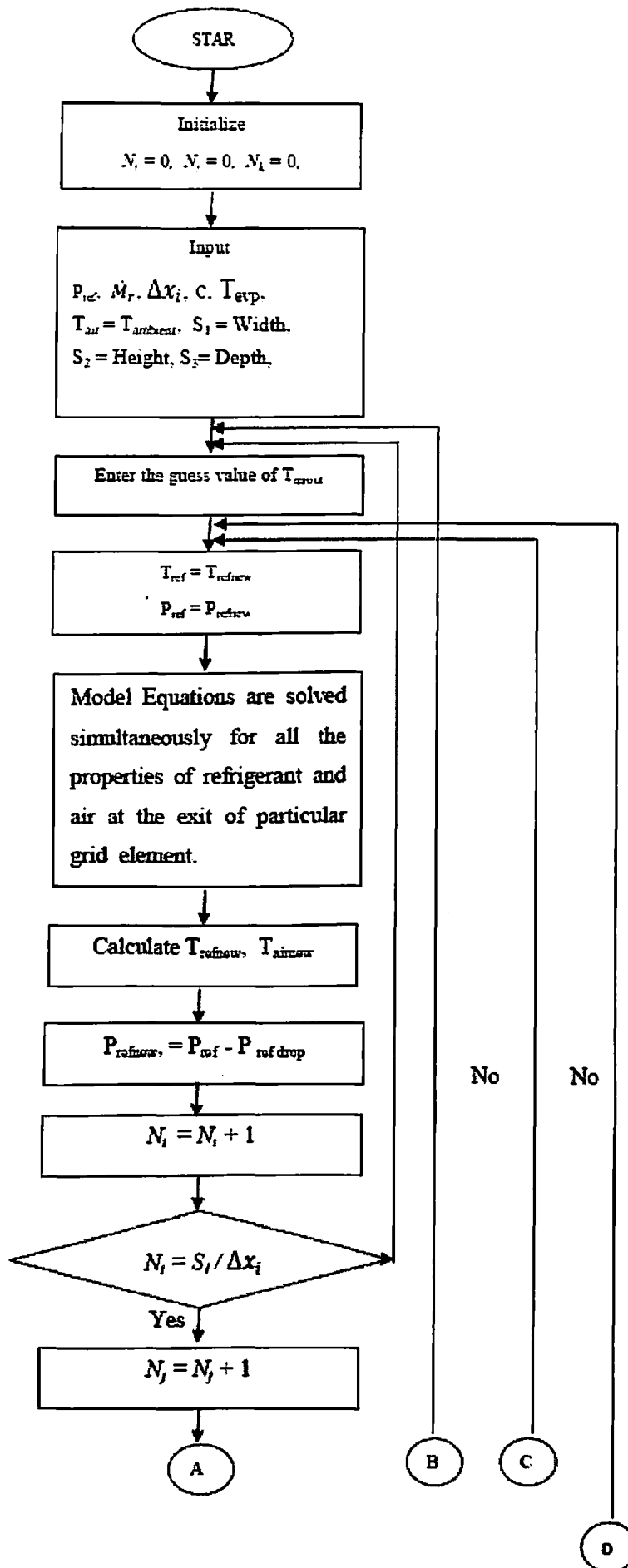
Figure 4.4: Temperatures at grid points in an element

The solution proceeds with the outlet of one element as inlet for an adjacent element with the same guess value of air temperature. The total gas cooler load is calculated at the end of each iteration and the iteration process continues till all the loops are completed with error level of the order of 10^{-3} . A MATLAB[®] code is developed using the above mathematical model and describes the method to solve the same. A detail of MATLAB[®] code, its computer implementation is shown below as a flow chart in Fig. 4.5.

4.4 Model validation

The above mathematical model is simulated for the same gas cooler with the specified boundary conditions at which experimental results were reported by Hwang et al. (2005). The experimental setup was equipped with an air duct and two environmental chambers that house an evaporator, a gas cooler, an expansion valve and a compressor. By means of this test rig, a set of parametric measurements at various inlet air temperatures and velocities, refrigerant inlet temperatures, mass flow rates and operating pressures were carried out on a specified CO₂ gas cooler as listed in table 4.2.

T



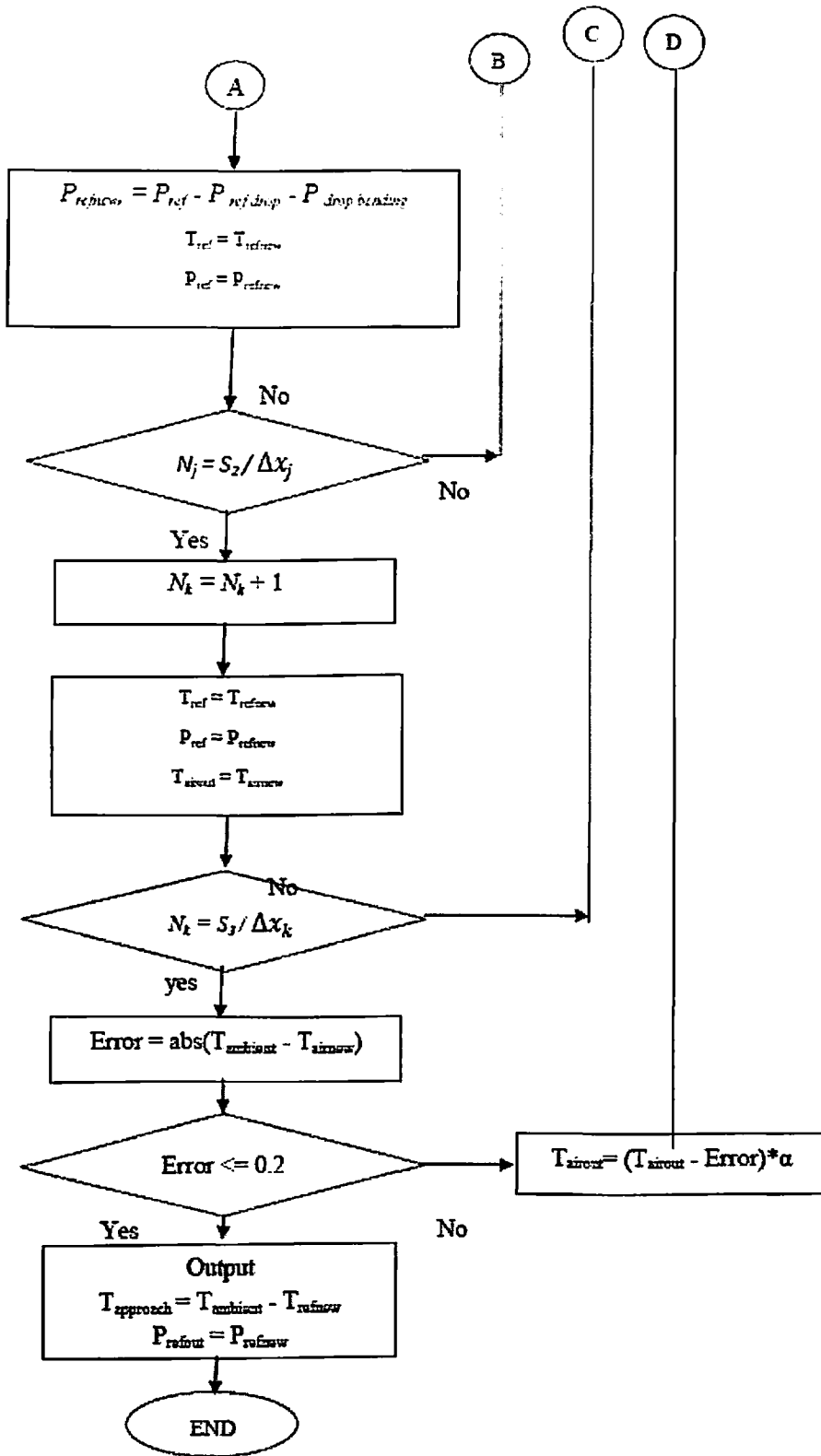


Figure 4.5: Detail flow chart of MATLAB® code, its computer implementation

Each test condition contains the measurements of air inlet temperature, air velocity, refrigerant inlet temperature, refrigerant inlet pressure and refrigerant mass flow rate. These measurements and the coil structural parameters are used as model inputs and parameters, respectively in present case. The predicted refrigerant temperature profile at each test condition is therefore compared with the corresponding test result in order to validate the model.

Table 4.2: Tested input operating conditions

Test Conditions	$T_{a(in)}$ ($^{\circ}\text{C}$)	u_a (m s^{-1})	$T_{r(in)}$ ($^{\circ}\text{C}$)	P (MPa)	Refrigerant flow (kg s^{-1})	$T_{r(out)}$ ($^{\circ}\text{C}$)
1	29.4	1	118.1	9	0.038	40.4
2	29.4	2	109.5	9	0.038	33.5
3	29.4	3	113.5	9	0.038	31.3
4	29.4	1	124	10	0.038	41.5
5	29.4	2	118	10	0.038	32.3
6	29.4	3	117.1	10	0.038	31.1
7	29.4	1	128.8	11	0.038	40.4
8	29.4	2	123.5	11	0.038	31.7
9	29.4	3	123.1	11	0.038	30.9
10	35	1	121.3	9	0.038	43.1
11	35	2	119.4	9	0.038	39.8
12	35	3	118.8	9	0.038	38.2
13	35	1	127.7	10	0.038	45.5
14	35	2	122.6	10	0.038	38.7
15	35	3	122.2	10	0.038	37.2
16	35	1	133.3	11	0.038	46
17	35	2	128.9	11	0.038	38
18	35	3	128.4	11	0.038	36.7
19	29.4	1	94.8	9	0.076	41.1
20	29.4	2	90.8	9	0.076	38.4
21	29.4	3	86.9	9	0.076	37.2
22	29.4	1	103.3	10	0.076	45.8
23	29.4	2	94.8	10	0.076	39.1
24	29.4	3	90.7	10	0.076	35.3
25	29.4	1	110.6	11	0.076	49.3
26	29.4	2	100.7	11	0.076	38.4
27	29.4	3	97.1	11	0.076	33.9
28	35	1	92.5	9	0.076	43.8
29	35	2	90	9	0.076	40.2
30	35	3	88.4	9	0.076	39.4
31	35	1	104.1	10	0.076	48
32	35	2	98.4	10	0.076	43.4
33	35	3	93.9	10	0.076	41.1
34	35	1	109.6	11	0.076	51.5
35	35	2	101.9	11	0.076	43.6
36	35	3	98.4	11	0.076	40.5

Fig. 4.6, 4.7, 4.8 and 4.9 represent the simulation result based on the mathematical model discussed earlier in ~~previous~~ section 4.3 giving input as simulation condition given in Table 4.2. The refrigerant temperature at each tube outlet and at the final gas cooler outlet are plotted.

Fig. 4.6, shows the comparison between simulated and experimental results of refrigerant temperature profile during the cooling in gas cooler, operating at lower range of pressure 9MPa and air velocity 1, 2 and 3 ms^{-1} respectively. Fig. 4.6a and 4.6b, show the trend of the temperature profile with air inlet temperature 29.4°C and 35°C keeping refrigerant flow rate constant as 0.038 kg s^{-1} at same operating pressure. Fig. 4.6c and 4.6d, show the similar simulated results with refrigerant flow rate of 0.076 kg s^{-1} .

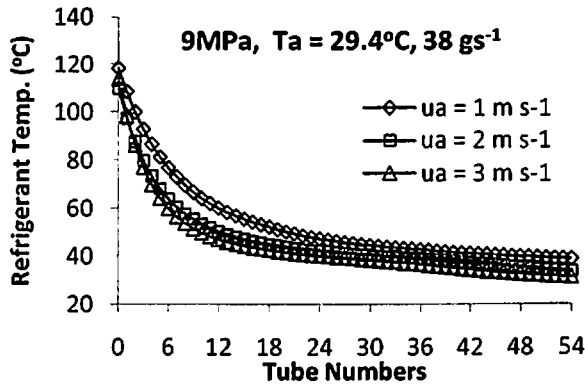
Similarly Fig. 4.7 shows the comparison between simulated and experimental results of refrigerant temperature profile during the cooling of refrigerant in gas cooler operating at the higher range of pressure 11MPa. However, Fig. 4.8 shows only the simulation results for the temperature profile at 10MPa, because the corresponding experimental results are not available. The simulated results of temperature profiles are in agreement with the general experimental trends. It is noted that in the experimental result graphs were plotted with respect to the position of thermocouples, which is placed at the end to each alternative number of tubes, whereas in simulation, graphs are plotted with respect to the each tube number.

Comparing above results it is observed that, as the refrigerant flow rate increases (doubled) the refrigerant inlet temperature decrease significantly. At the same time the refrigerant temperature at the outlet across the gas cooler increases, as expected.

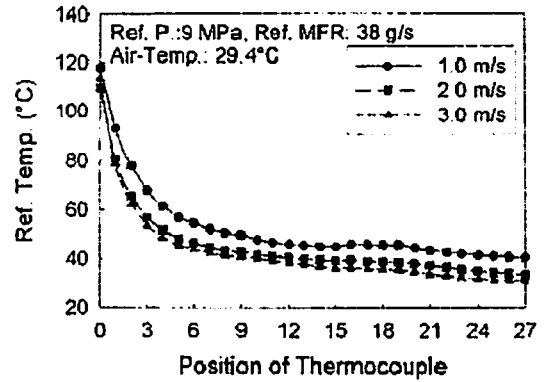
Further, as the operating pressure increases, keeping the mass flow rate constant; the refrigerant temperature at the inlet of gas cooler increases for all air velocities. However, the refrigerant temperature at the gas cooler outlet decreases due to higher temperature gradient. The effect is more pronounced at lower operating pressure.

Simulation results

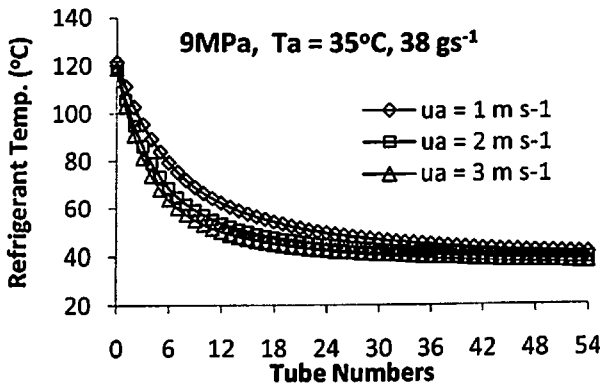
Experimental results



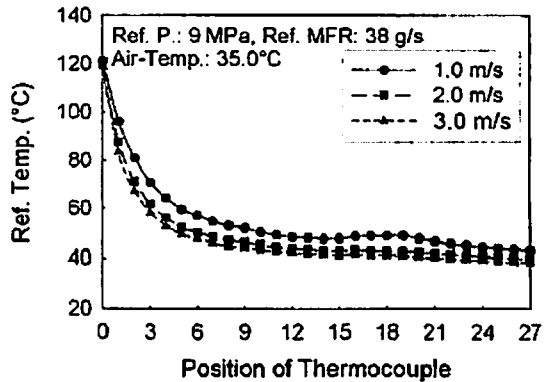
(a)



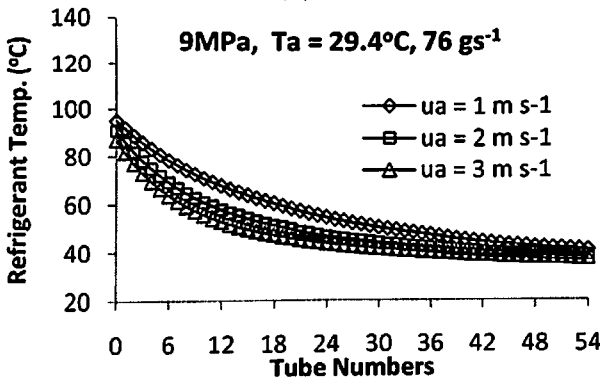
(a)



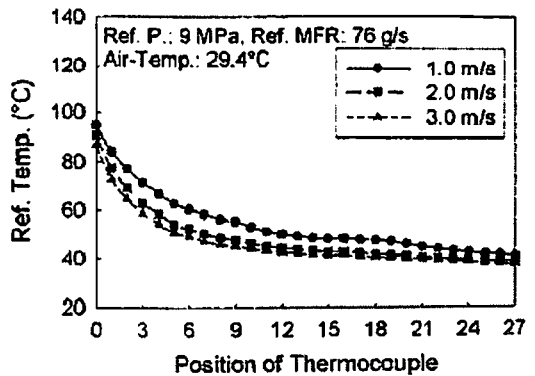
(b)



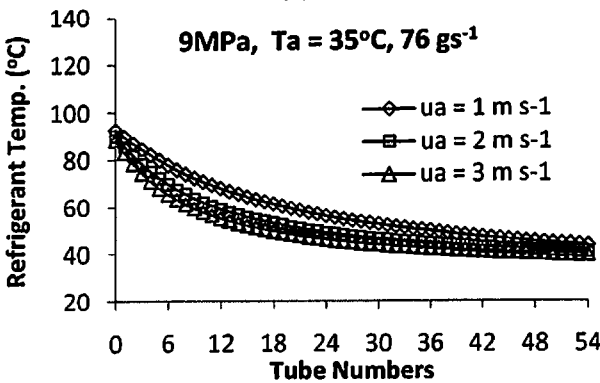
(b)



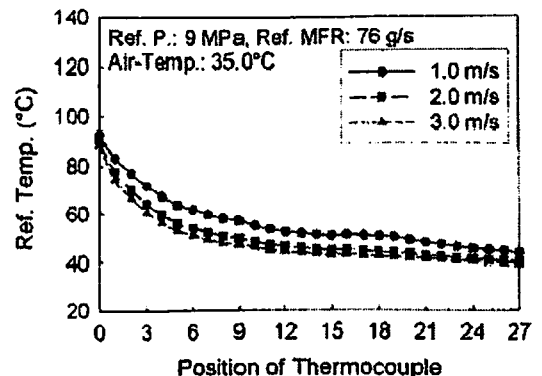
(c)



(c)



(d)

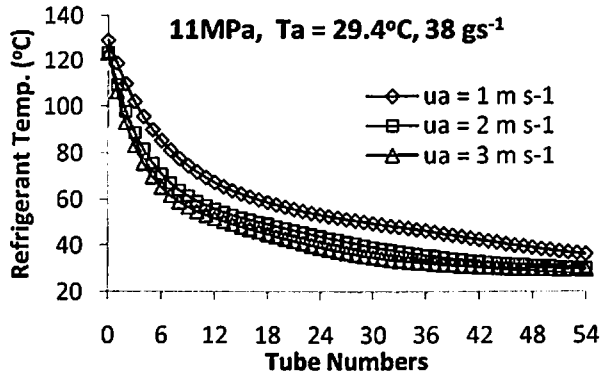


(d)

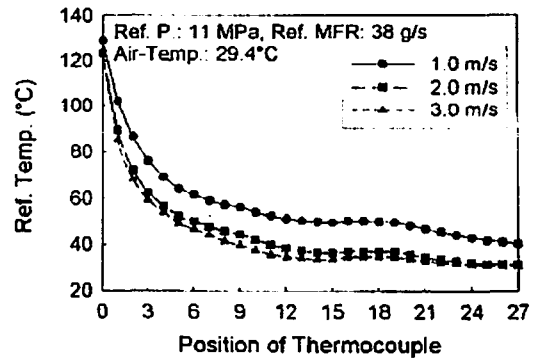
Figure 4.6: Temperature profile of refrigerant with operating pressure 9MPa

Simulation results

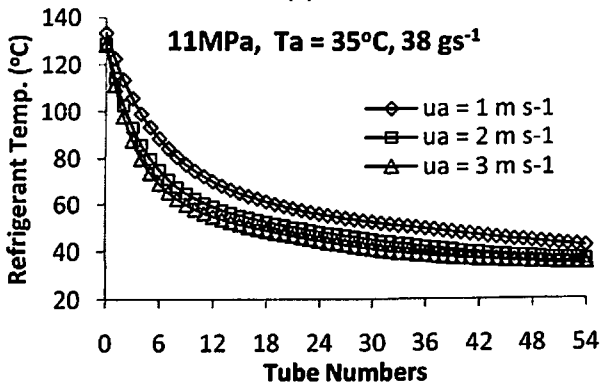
Experimental results



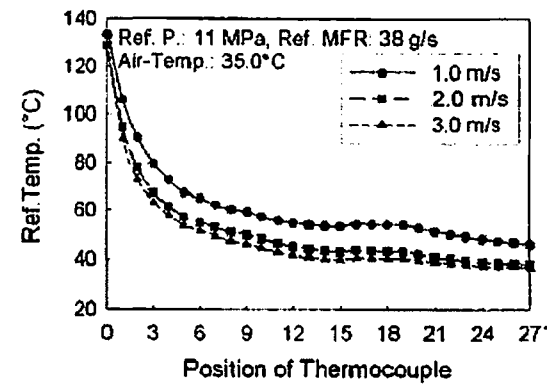
(a)



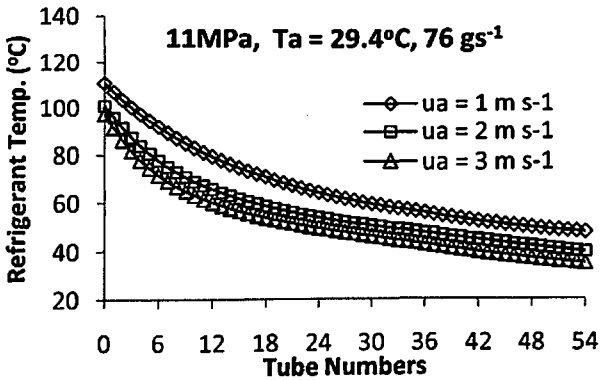
(a)



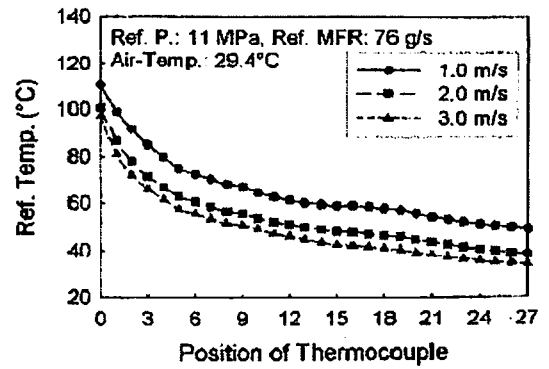
(b)



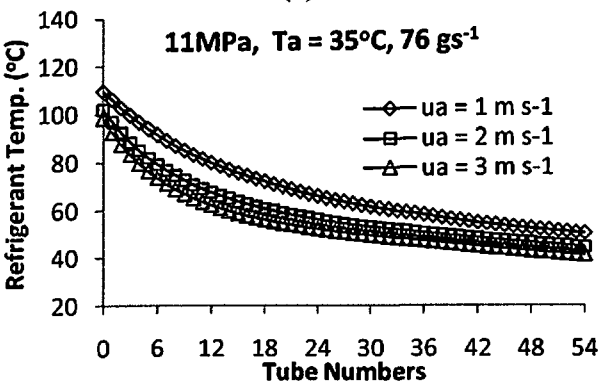
(b)



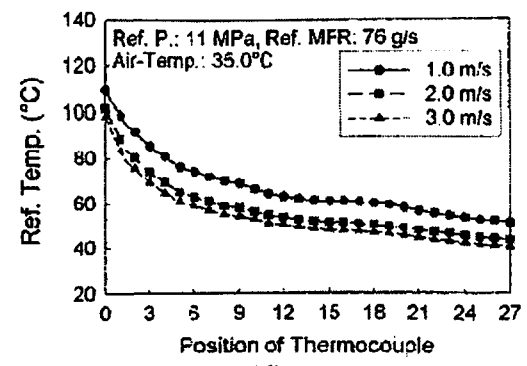
(c)



(c)



(d)



(d)

Figure 4.7: Temperature profile of refrigerant with operating pressure 11MPa

The temperature profiles are observed to be very similar at two different air inlet temperatures (i.e. 29.4°C and 35°C) for same operating pressure and refrigerant flow rate. However, due to smaller temperature gradient between refrigerant and air, the temperature of each tube outlet is higher at higher air inlet temperature.

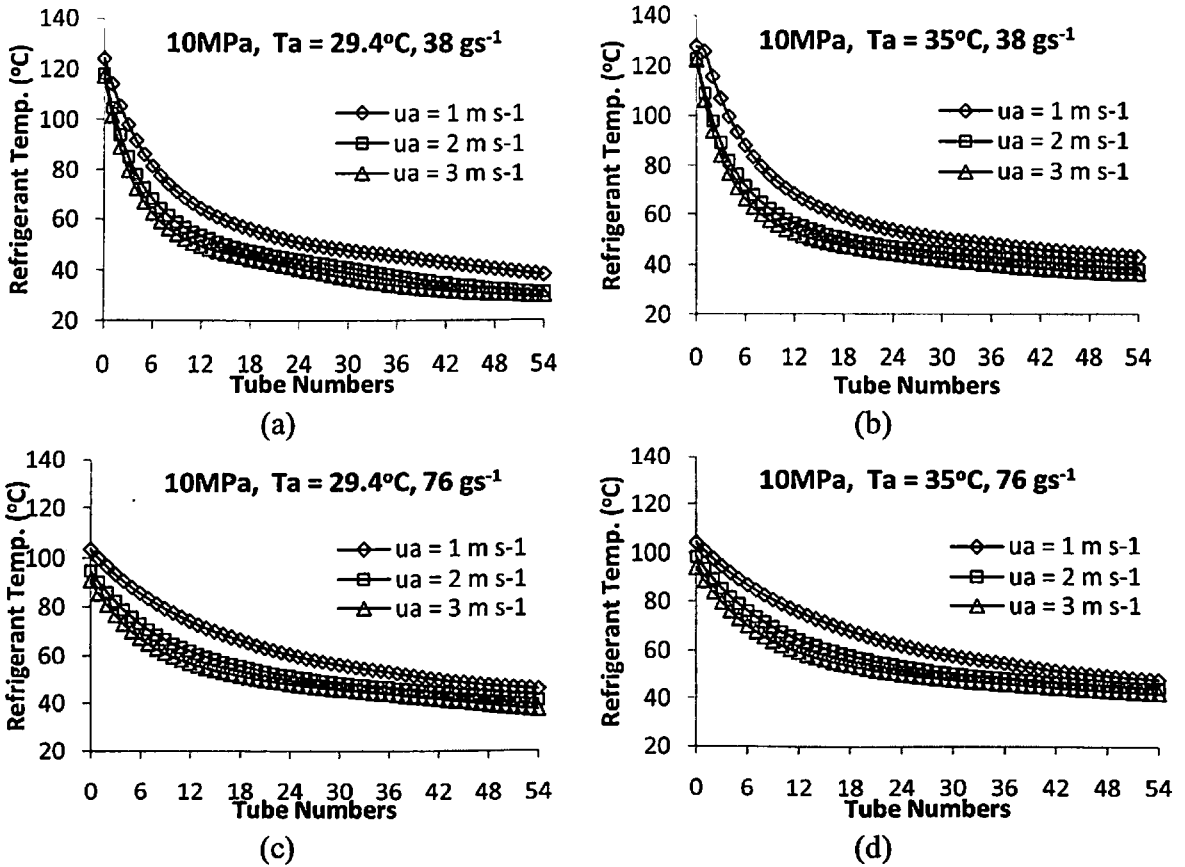


Figure 4.8: Temperature profile of refrigerant with operating pressure 10MPa

It is also observed that for each set of graph ^{as the} the air velocity increases from 1 ms⁻¹ to 2 ms⁻¹ and then to 3 ms⁻¹, the refrigerant temperature at each tube outlet falls due to higher heat transfer rate in air side. The benefit from the increase in air velocity however wanes out and hence simulation is not conducted beyond 3 ms⁻¹ air velocity. Only at refrigerant flow rate at and beyond 0.076 kgs⁻¹ and higher pressure 11MPa, it may be justifiable to consider air velocity higher than 3 ms⁻¹.

Overall there is a very good agreement in results, tube by tube, with the published data. A minor deviation in temperatures is observed between tube number 35 to 40. The deviation is perceived to be due to neglecting the conduction within fin in the modeling. However this does not significantly affect the final temperature of the refrigerant at the outlet of the gas cooler. Fig. 4.9 shows the comparison of experimental and simulated results for refrigerant temperature at gas cooler outlet for three different operating pressure 9MPa, 10MPa and 11MPa and for three different air velocities i.e. 1 ms⁻¹, 2 ms⁻¹ and 3 ms⁻¹.

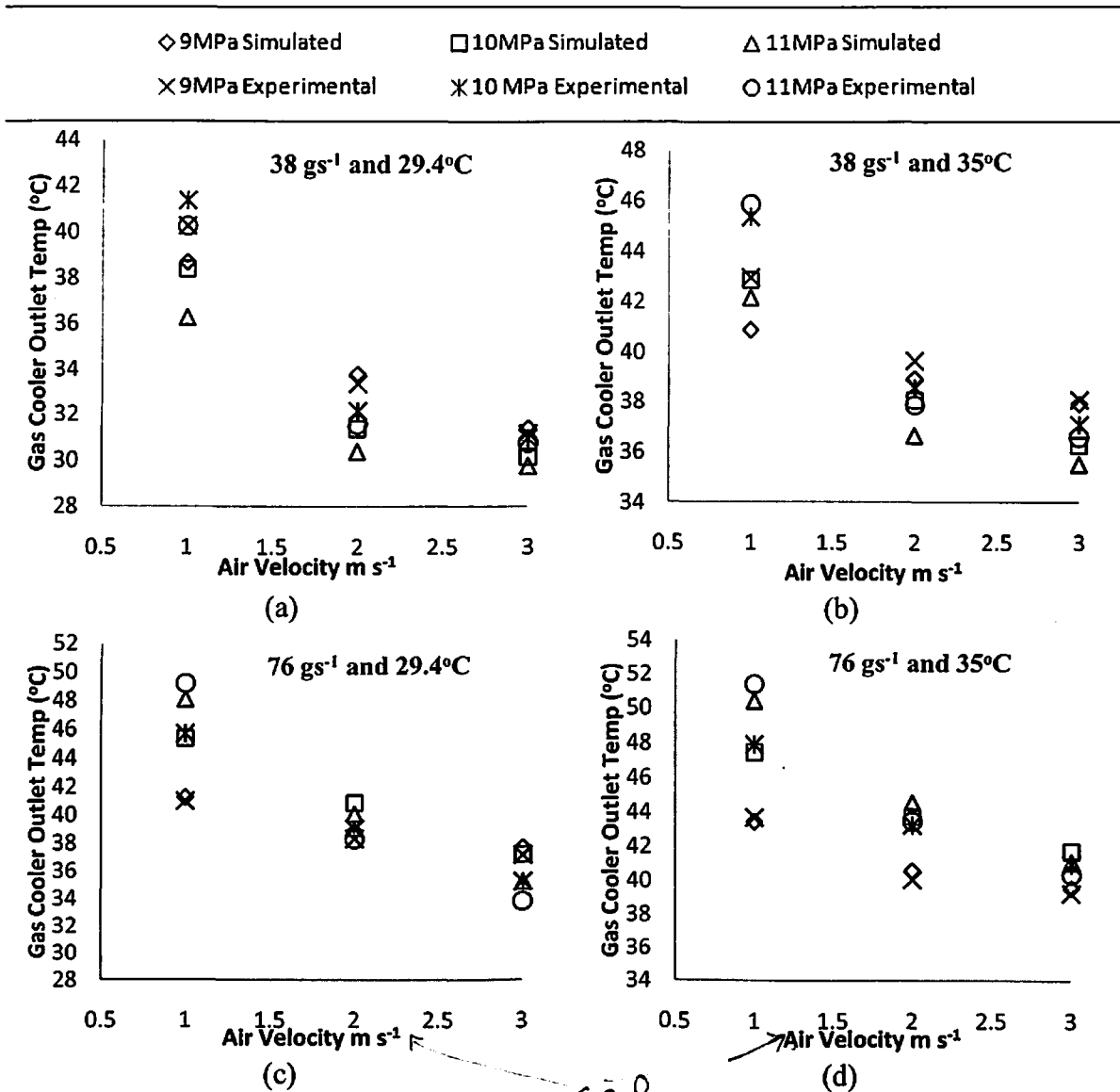


Figure 4.9: Comparison of experimental and simulated result of the gas cooler outlet temperature

A very good agreement between the experimental and simulated results are observed at all operating ranges, with a maximum deviation of 4°C. The maximum deviation is observed at lower air velocity and higher operating pressure i.e. 1 ms⁻¹ and 11MPa. However the deviations are very small between the experimental and simulated results for rest of the conditions. It is concluded that the simulation can fairly represent the test results and the model is therefore validated.

The above model developed and validated is used to evaluate the performance of the same and modified design of gas cooler for various approach temperature, exit temperature of refrigerant, refrigerant side pressure drop in gas cooler, heat transfer capacity and heat transfer coefficient etc. The work is then extended to evaluated the performance of overall system i.e. refrigeration capacity, power required and COP, in subsequent chapters.

Analysis of Gas Cooler and CO₂ Trans-critical Refrigeration System

In this chapter the analysis of gas cooler and overall CO₂ trans-critical refrigeration systems using the respective gas cooler design are discussed. The mathematical model developed and validated as described in chapter 4, is now used to analyze the performance of gas cooler and its modified design of gas coolers. Further this model is extended to steady state model of the overall system for evaluating the performance of overall system. The same is then used to study performance of different design of gas cooler at different temperature zones. In this part of the thesis the gas cooler geometry and its flow arrangement of refrigerant are modified and performance of gas coolers and the overall system with the respective gas cooler are studied. Extension of mathematical model, modified gas cooler geometry, its flow arrangement, operating conditions, and the simulated results at different temperature in Indian conditions are discussed in subsections of this chapter.

5.1 Modified Design of Gas Cooler and Operating Conditions

The gas cooler geometry selected for the mathematical modeling and simulation as discussed in chapter 4, a counter cross flow air cooler finned tube type compact heat exchanger, in which the refrigerant flow is in a single circuit and tubes are arranged in three passes. It is seen from both simulation and test results that a sharp decrease in refrigerant temperature occurs in the first pipe row, (as pipes numbered 1 to 18 as shown in Fig. 5.1(a)). The rate of temperature change in the subsequent rows are gradually reduced, and even become insignificant after few rows. Lowering the approach temperature of gas cooler is desirable for improved performance of gas cooler and higher COP of the system. Increasing the size of gas cooler is an obvious option to lower the approach temperature but COP of the system may even decrease, when the size of gas cooler is larger than certain size due to internal pressure drop as reported by Rozhentsev et al. (2001). Therefore, it is important to optimize the gas cooler not only in terms of lower approach temperature but also for higher performance of the overall system. To

→ Rozhentsev and Wang (2001)

utilize the surface area available for heat transfer in gas cooler as well as to maintain a small size of gas cooler, modification of gas cooler geometry and its flow circuit arrangements are done. There are three circuit arrangement namely 1-circuit, 2-circuit and 3-circuit, where 1-circuit is the tested gas cooler by Hwang et al. (2005) as discussed in chapter 4. In the gas cooler with 2-circuit and 3-circuit, the flow rate of the refrigerant at inlet of the gas cooler is divided into two and three equal branches and final outlet of the refrigerant mixes at the exit of the gas cooler as shown in Fig. 5.1. A modified geometry with three different circuit arrangements i.e. 1-circuit with 48 tubes, 2-circuit with 48 tube, and 3-circuit with 45 tubes are shown in Fig. 5.2. it is having only 45 tubes. The performance of gas cooler and the overall system are evaluated at existing and some modified operating condition as well.

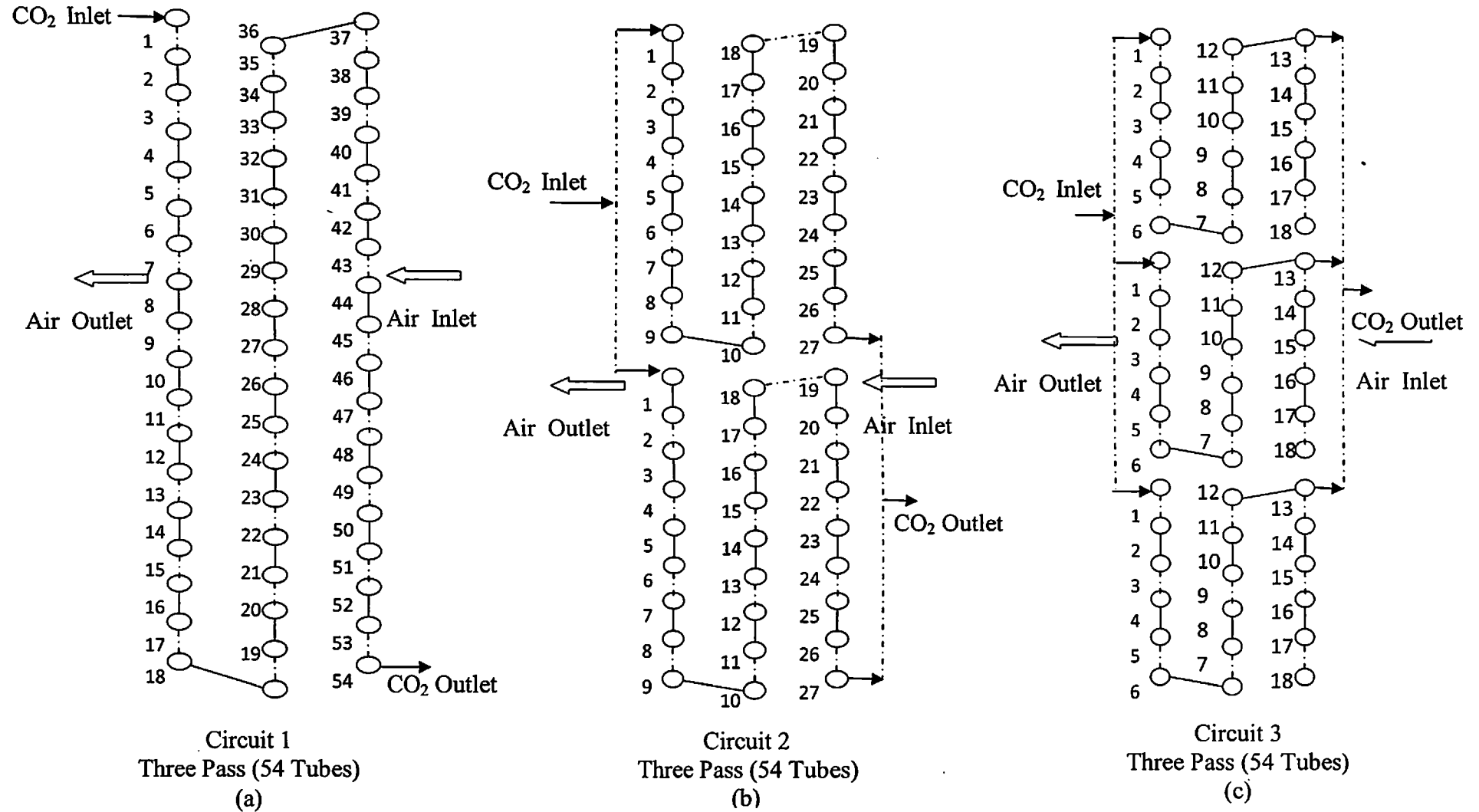
write unit (m/s)

Table 5.1: Combination of simulation conditions

Simulation Condition	Air inlet velocity	No. of Tube	No. of Circuit	Simulation Condition	Air inlet velocity	No. of Tube	No. of Circuit
1	1	54	1	10	1	48	1
2	2	54	1	11	2	48	1
3	3	54	1	12	3	48	1
4	1	54	2	13	1	48	2
5	2	54	2	14	2	48	2
6	3	54	2	15	3	48	2
7	1	54	3	16	1	45	3
8	2	54	3	17	2	45	3
9	3	54	3	18	3	45	3

These operating conditions are the combination of number of tubes, number of circuit arrangement, air velocity, refrigerant side gas cooler inlet pressure, and different temperature zones.

The range of operating pressure, taken for the analysis is from 9 MPa to 13 MPa at an interval of 0.5 MPa, and air velocity ranges are from 1 m s⁻¹ to 3 m s⁻¹ with an interval of 0.5 m s⁻¹. Apart from the two limiting end value of mass flow rate of refrigerant i.e. 0.038 kg s⁻¹ and 0.076 kg s⁻¹ for which the theoretical model was validated, a mid range of mass flow rate 0.045 kg s⁻¹ is also ~~is~~ taken up for further analysis. The simulations are carried out for the above operating condition with different design of gas cooler at all three temperature zones in Indian context i.e. 29.4°C (zone I), 40°C (zone II), and 45°C (zone III). The combination of simulation conditions are listed in Table 5.1.


Figure 5.1: Modified circuit arrangement of gas cooler

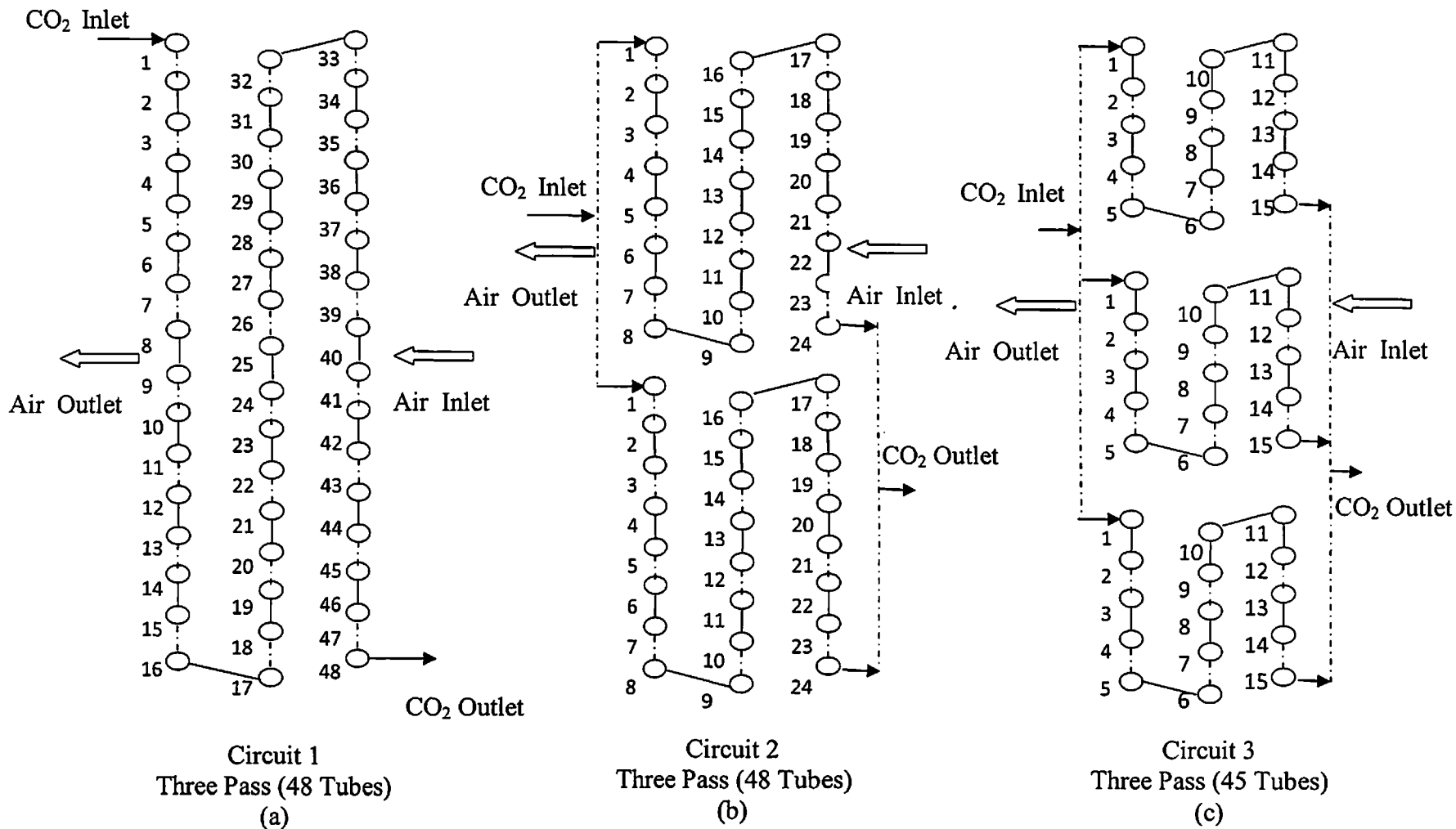


Figure 5.2: Modified geometry with different circuit arrangement of gas cooler

5.2 Model Application

The mathematical model developed and validated in chapter 4, is now utilized to evaluate the performance of gas cooler and the model is extended for the performance of overall system. The gas cooler model is extended with a steady state model to calculate the refrigeration capacity in kW, compressor work in kW, and COP of the overall system. The model is represented mathematically in Eq. 5.1 to Eq. 5.3.

$$W_{\text{comp}} = \frac{\{H_{\text{rco}}(P_{\text{co}}, T_{\text{co}}) - H_{\text{rci}}\}}{\eta_{\text{isen}}} \quad (5.1)$$

$$\text{RE} = \{H_{\text{reo}} - H_{\text{rei}}(P_{\text{gco}}, T_{\text{gco}})\} \quad (5.2)$$

$$\text{COP} = \frac{\{H_{\text{reo}} - H_{\text{rei}}(P_{\text{gco}}, T_{\text{gco}})\}}{\frac{\{H_{\text{rco}}(P_{\text{co}}, T_{\text{co}}) - H_{\text{rci}}\}}{\eta_{\text{isen}}}} \quad (5.3)$$

where, $H = H(P, T)$ and $H_{\text{gco}} = H_{\text{ei}}$,

Solving the above steady state model, performances of system are analyzed for different operating and geometric conditions for different temperature zones and selected combinations of model input parameters. All the performance are analyzed for maintaining 0°C as constant evaporator side temperature and saturated vapour at the inlet of the compressor.

The isentropic efficiency of the compressor for the operating condition is calculated using the Eq. 5.4, reported by Wang et. al (2009).

$$\eta_{\text{isen}} = -0.26 + 0.7952(P_{\text{co}}/P_{\text{ci}}) - 0.2803(P_{\text{co}}/P_{\text{ci}})^2 + 0.0414(P_{\text{co}}/P_{\text{ci}})^3 - 0.0022(P_{\text{co}}/P_{\text{ci}})^4 \quad (5.4)$$

Further, in order to enhance heat transfer and achieve low approach temperature, increasing the size of a gas cooler may be an obvious choice. However size increase is found to be inefficient not only from the point of view of excess material use but also from energy consumption and performance point of view. Increase in size of gas cooler increases pressure drop in the refrigerant side, bringing down the overall performance of the system. Moreover, in the air side, it implies need of high capacity fan and increased power consumption.

The performance of the system is evaluated for three zones for air inlet temperature. 29.4°C, 40°C, and 45°C, at different simulation condition of gas cooler as shown in Table 5.1 for Indian climatic conditions and different compressor discharge

pressure ranges from 9MPa to 13MPa. Pressure drop between the compressor discharge and gas cooler inlet is neglected. Evaporator pressure is taken as constant for maintaining 0°C evaporator temperature and constant mass flow rate 0.045 kg s⁻¹ for all cases. The modified gas cooler geometry is arranged in three different manner, viz 54-tubes 1-circuit, 48-tubes 2-circuit and 45 tubes 3-circuit.

5.3 Results and Discussion

The performance of gas cooler using the validated model from chapter 4 and the overall system performance using the extended model with the respective gas cooler are discussed in subsequent sections. The results are shown and discussed separately for all three temperature zones in Indian climatic conditions.

5.3.1 Performance of gas cooler

The performances of gas cooler are evaluated in terms of approach temperature, gas cooler capacity and pressure drop in refrigerant side inside the gas cooler at environmental temperature zone I, Zone II and Zone III. These performance result are plotted for the combinations of various operating conditions and geometric design of the gas cooler as given in Table 5.1.

5.3.1.1 Temperature zone I

Fig. 5.3 represents the simulation result of gas cooler for temperature zone I (Air Temperature 29.4°C) in terms of approach temperature, Gas cooler heat rejection capacity and pressure drop inside the gas cooler at different operating pressure and simulation conditions.

Fig. 5.3(a) shows the variation of approach temperature with the simulation conditions, it is observed that the approach temperature having significantly higher value at simulation condition 1-3 and 10-12 (i.e. air velocity 1,2,3 at 1-circuit) as compare to remaining conditions. This is due to in single circuit arrangement, the gradient diminishes as heat transfer progresses.

Simulation conditions 4-9 and 13-18 have insignificant variation of approach temperature, however in simulation condition 4 and 13 have slightly higher approach temperature but is comparatively lower than 1-3 and 10-12.

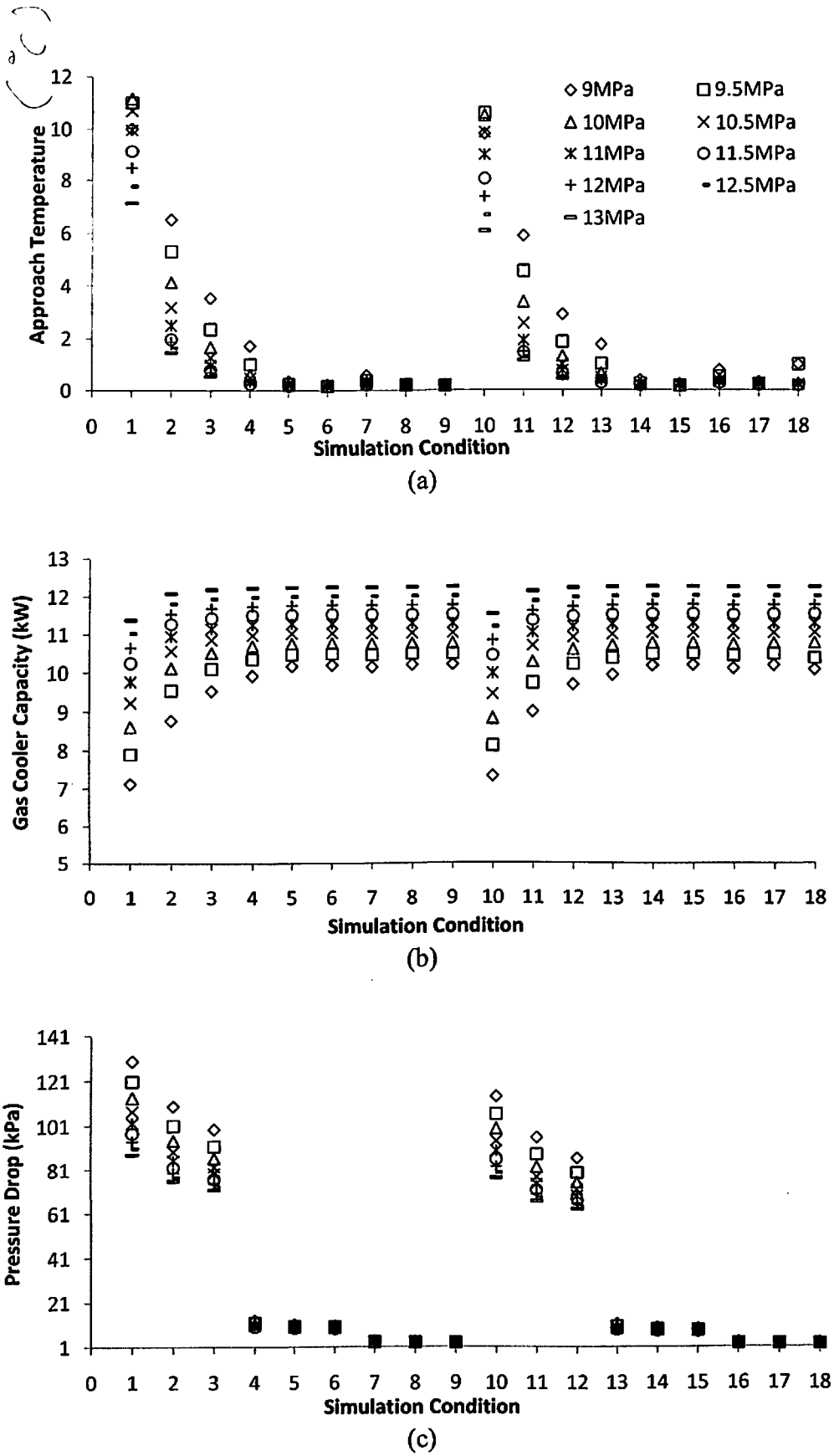


Figure 5.3: Performance of gas cooler at temperature zone I

It is also observed that the approach temperature decreases with increase in operating pressure for each simulation condition, the effect is more prominent at simulation condition 1-4 and 10-13. However the effect is insignificant for simulation condition 5-9 and 14-18.

For each circuit arrangement, value of approach temperature decreases with increasing the air velocity and for each value of air velocity, approach temperature decreases with increase in the number of circuit. However the effect of increase in number of circuit is insignificant for 2-circuit to 3-circuit arrangements, hence only arrangement is selected up to 3- circuit.

Approach temperature are close to zero for simulation conditions 5, 6, 8, 9, 15, and 17. It is achieved with the gas cooler arrangement in 2-circuit and 3-circuit. Again approximately same value of approach temperature are observed for gas cooler having 54, 48, and 45 tubes at different circuit arrangement and air velocity, hence the smaller size of gas cooler should be preferred for material and energy point of view.

Fig. 5.3 (b) shows the variation of gas cooler heat rejection capacity with different simulation conditions and operating pressures. It is observed that for each simulation condition, gas cooler heat rejection capacity increases with an increase in operating pressure, as expected due to the larger temperature gradient at higher operating pressure.

Except simulation condition 1 and 10, in remaining simulation conditions, the changes in gas cooler heat rejection capacities are insignificant with change of simulation conditions other than operating pressure. Hence it is concluded that it only depends on operating pressure in these conditions.

The highest value of the heat rejection capacity of gas cooler is achieved at 13MPa operating pressure, as expected because of the higher temperature gradient. It increases with increase in the operating pressure for each simulation conditions, However its absolute value may vary with simulation combinations at a particular operating pressure because of the higher surface area available in large size of gas cooler.

Fig. 5.3(c) shows the variation of refrigerant side pressure drop in gas cooler; it is observed that for simulation condition 1-3 and 10-12 (i.e. 1-circuit) have significant pressure drop as compare to remaining conditions. However, these variations diminishes in 2-circuit and 3-circuit arrangement of gas cooler.

For the same circuit arrangement the value of pressure drop reduces with the increase in air velocity. In 1-circuit arrangement, pressure drop significantly vary with operating pressure for each simulation condition, however, it is insignificant in 2-circuit and 3-circuit arrangements. The lowest pressure drop is observed at 3-circuit arrangement at higher air velocity.

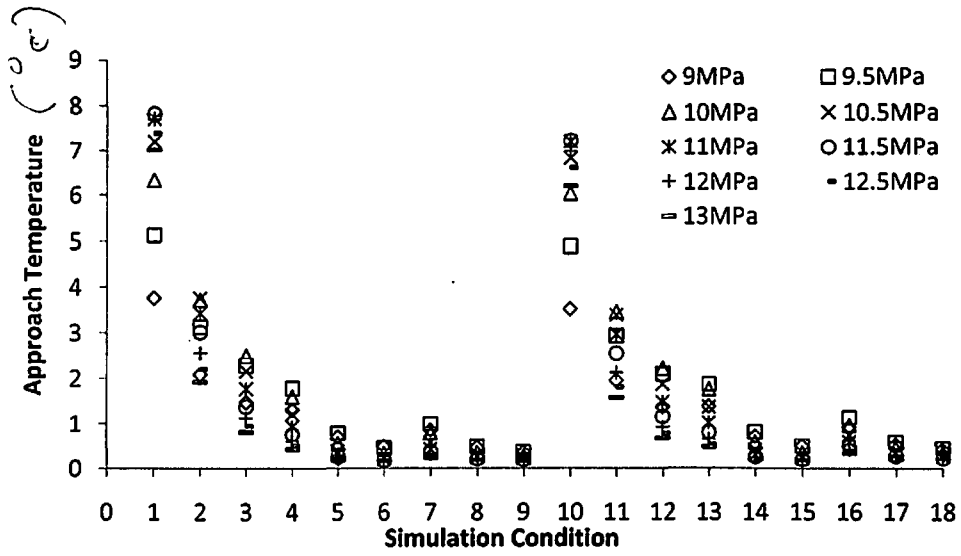
5.3.1.2 Temperature zone II

Similar to temperature zone I, the performances of gas cooler i.e. approach temperature, gas cooler capacity and refrigerant pressure drop inside the gas cooler, are evaluated for environmental temperature zone II (Air Temperature 40°C), simulation results are shown in Fig. 5.4.

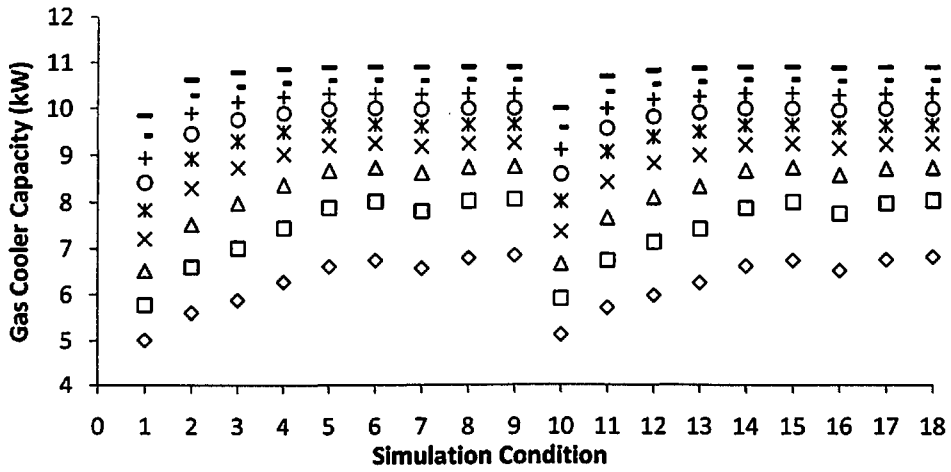
Fig. 5.4(a); *move comma* shows the variation of approach temperature, with different simulation condition at different operating pressure. Unlike in zone I, it is observed that, approach temperature is having an uneven variation with operating pressure. The variation is more pronounced at lower air velocities. For each operating pressure and each circuit arrangement, approach temperature decreases with increase in air velocities.

For simulation condition 6, 8, 9 and 15, 17, 18; approach temperatures variation are almost negligible for all operating pressures and these conditions are having very low approach temperature i.e. closed to zero. Note that the simulation condition 15 consists of 48 tube and 17 & 18 has 45 tubes, which are lower than the original gas cooler design i.e. 54 tubes. Hence the size of gas cooler is smaller for same approach temperature.

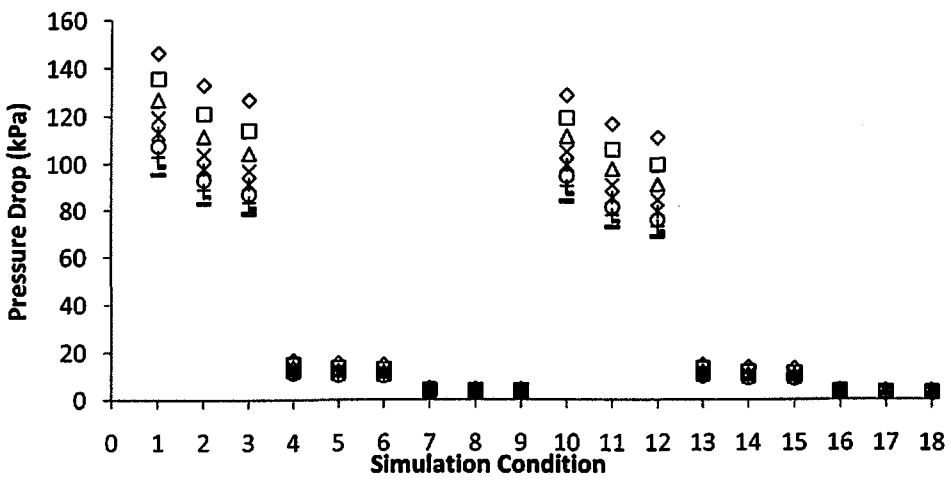
insert one space
Fig.5.4(b) shows the variation of gas cooler heat rejection capacities with simulation conditions at different operating pressure for temperature zone II. Similar results are observed as temperature zone I. In this case also gas cooler capacity increase with operating pressure for each simulation conditions. However for each pressure, the variation of gas cooler capacity are insignificant, except simulation condition 1 and 10, and it is obvious to prefer lower size of gas cooler for same heat rejection capacity.



(a)



(b)



(c)

Figure 5.4: Performance of gas cooler at temperature zone II

Fig. 5.4 (c) show the variation of refrigerant pressure drop inside the gas cooler and similar to zone I, it is observed that pressure drop is more significant for 1-circuit arrangement compare to 2-circuit and 3-circuit arrangement. However these variations are insignificant for 2-circuit and 3-circuit arrangement.

It is also observed that for each circuit, the pressure drop decreases with increase in air velocity, and for each value of air velocity it decrease with increase in the number of circuits. These effect diminishes at simulation condition 7-9 and 16-18, Hence for each 3-circuit arrangement the pressure drop is lowest at higher velocity of air.

5.3.1.3 Temperature Zone III

Similar to temperature zone I and zone II, the performances of gas cooler i.e. approach temperature, gas cooler capacity and pressure drop in refrigerant side inside the gas cooler, are evaluated for environmental temperature zone III (Air Temperature 45°C), simulation results are shown in Fig. 5.5.

Fig. 5.5(a) depict the variation of approach temperature with various simulation conditions at different operating pressure. It is observed that the variation trends are very much similar to zone II, except the simulation condition 1 and 10, where variations are more sensitive to operating pressure as compare to zone I and II. Again the behavior is uneven with pressure at each simulation conditions in zone II, but unlike zone I.

Simulation conditions 6, 9 and 15, 18 have lowest value of approach temperature and its variation with operating pressure is insignificant. For zone III, air velocity 3 ms⁻¹ has lowest approach temperature and is approximately same for 2-circuit and 3-circuit arrangement. Therefore, further preference will be based on smaller number of tubes.

Fig. 5.5(b) and (c) shows the variation of gas cooler capacity and refrigerant pressure drop inside the gas cooler, it is observed that trends are very similar to zone I and zone II, however the absolute value may vary.

Results are favorable for 3-circuit arrangement and gas cooler with smaller number of tubes. Since the results do not shown much variation for 2-circuit and 3-circuit, especially at higher air velocity. Therefore it is concluded that the same will not analyzed for further number of circuit arrangements.

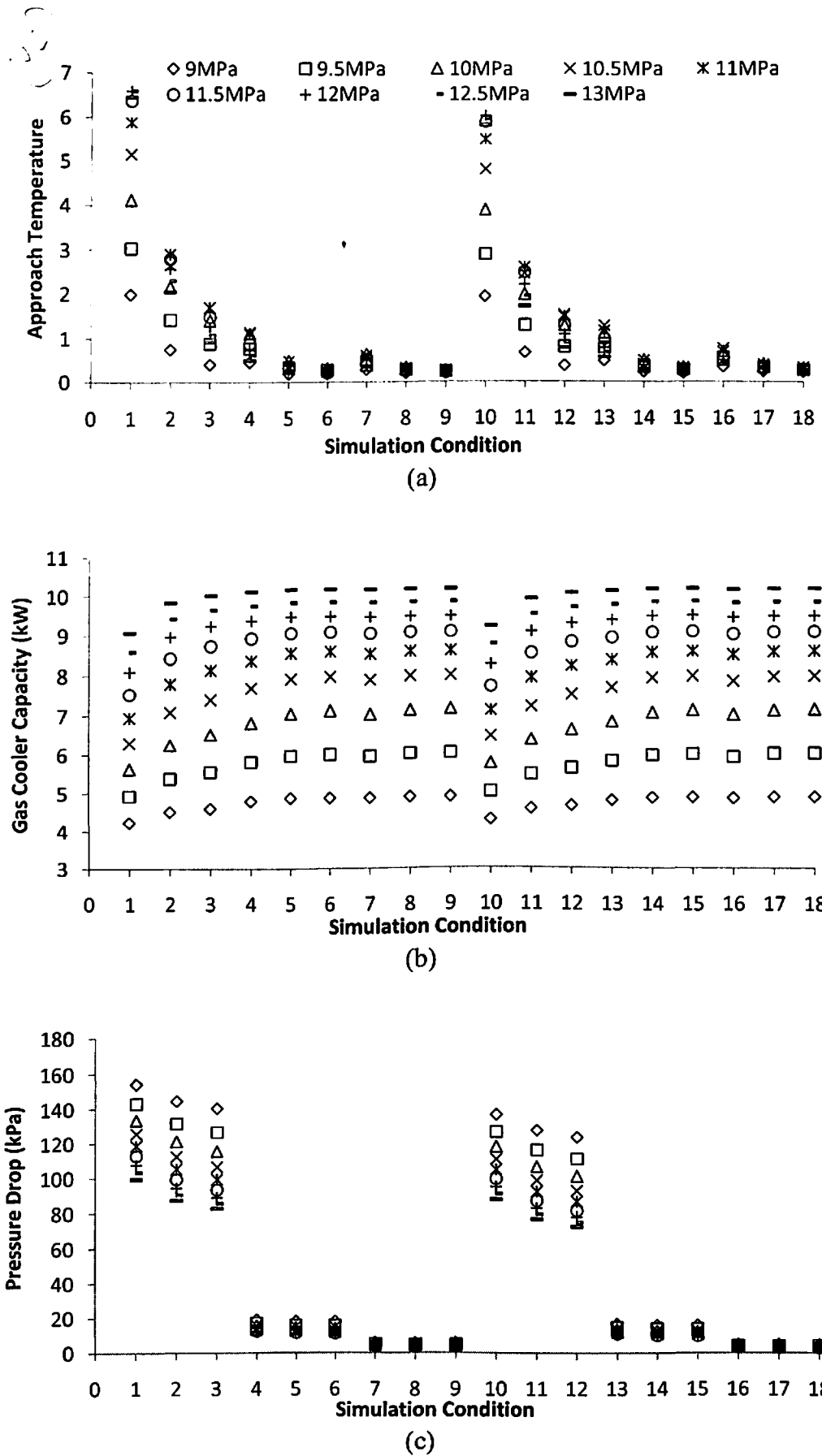


Figure 5.5: Performance of gas cooler at temperature zone III

It is concluded from the above results shown in Fig. 5.1 to 5.3 and their discussion that the overall results of temperature zone I (i.e. 29.4°C) are similar to the conventional system, but once the operating temperature increases beyond the critical point of CO₂ (i.e. 31.3°C); the trends of approach temperature shows the uneven variation with operating pressure at each simulation condition. This is due to the rapid change in thermo-physical properties of CO₂ in supercritical region, moreover the design of gas cooler and its operating condition to achieve the best possible performance of gas cooler are more sensitive at higher temperature zones i.e. zone 2 and zone 3. Above discussion also indicate the need for study of cumulative effect of gas cooler performance parameters on the performance of overall system.

II

III

5.3.2 Performance of trans-critical CO₂ refrigeration system

In this section, the performance of overall system is analyzed through simulation with the respective design of gas cooler and operating conditions as discussed in section 5.3.1. The cumulative effect of gas cooler performance parameters on the performance of overall system are studied and results are summarized in Fig. 5.6 to Fig 5.8 for temperature zone I, II and III respectively.

5.3.2.1 Temperature Zone I

Fig. 5.6 show the performance of the overall system in terms of cooling capacity, compressor work and COP with different simulation conditions (Table 5.1.) at different operating pressure for temperature zone I (i.e. 29.4°C).

↑ error a lot

Fig. 5.6(a) shows the variation of refrigeration capacity with different simulation conditions at different operating pressure for temperature zone I. It is observed that the refrigeration capacity increases with decrease in the operating pressure for each simulation conditions and is similar to conventional systems. however the simulation condition 1 and 10 (i.e. 1-circuit and air velocity 1 ms⁻¹) exhibit slightly uneven variation, this may be due to relatively higher error found during the model validation in this conditions (refer section 4.4, Fig. 4.9).

Further simulation conditions 1-3 and 10-12 have significant variation in refrigeration capacity for each operating pressure but refrigeration capacity does not vary significantly for remaining conditions. Higher value of refrigeration capacities are found to be at higher air velocities and for circuit 2 and circuit 3.

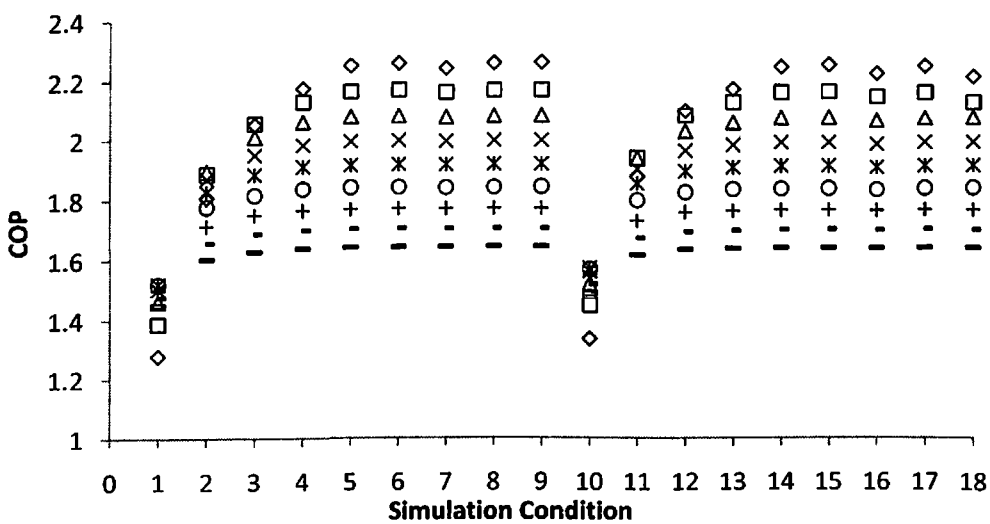
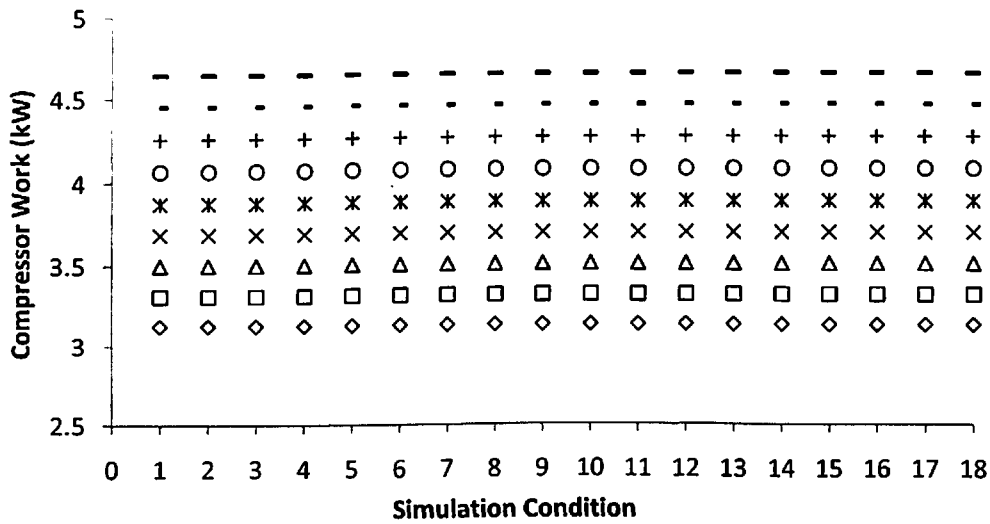
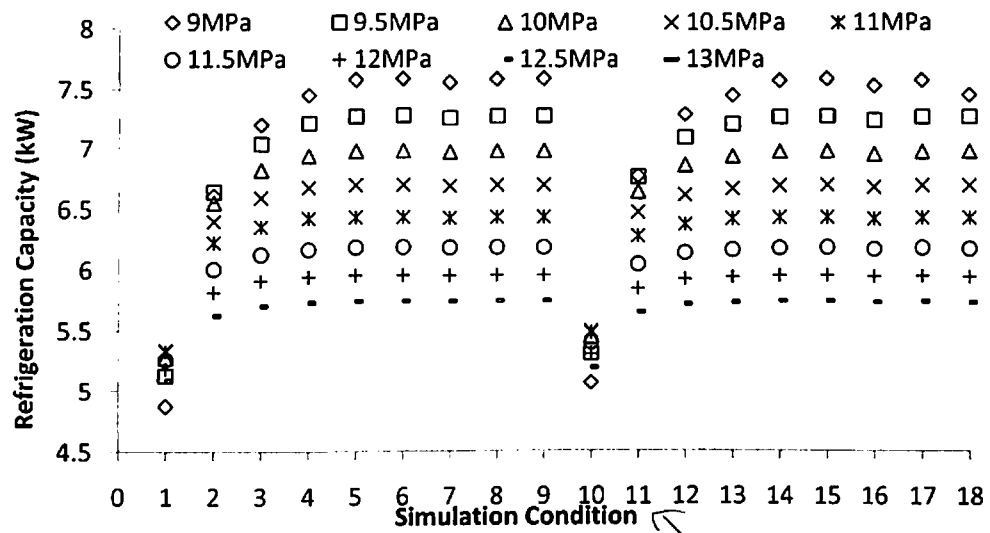


Figure 5.6: Performance of overall system at temperature zone I

Fig. 5.6(b) shows that the compressor work required at different operating pressure, it increases with increase in pressure, however it is not dependent on other factor like air velocities, ambient temperature, gas cooler geometry etc.

Fig. 5.6(c) shows the cumulative effect of refrigeration capacity and operating pressure on the performance of overall system as COP. It is also following the same trend as conventional system, because the operating temperature is below the critical temperature. The COP is higher for low operating pressure at each simulation condition and results are slightly uneven for simulation condition 1 and 10, due to the higher error that is found in these conditions. Higher value of COPs are found to be at higher air velocities and for 2-circuit and 3-circuit arrangements.

COP at simulation condition 6, 8, 9, 14, and 15, 16, 17 and 18 have very small difference; so from the optimum design point of view simulation condition number 17 is recommended to be the best possible combination giving both material and energy saving at the same time giving an equal level of performance. subsequently for all pressure. These result also help us to select the compressor discharge pressure at different temperature zone for the best performance. Form above analysis for temperature zone I, 9 MPa is found to be the discharge pressure for the maximum COP Fig.5.6(c).

5.3.2.2 Temperature zone II

↑
gap

Fig. 5.7 show the performance of the overall system in terms of cooling capacity, compressor work and COP with different simulation conditions (Table 5.1.) at different operating pressure for temperature zone II (i.e. 40°C).

Fig. 5.7(a) shows the variation of refrigeration capacity with different simulation conditions at different operating pressure for temperature zone II. It is observed that unlike temperature zone I, the refrigeration capacity increase with increase in the operating pressure for each simulation conditions, the trends are opposite to the conventional systems. It is because of the property variation of CO₂ above the critical point as discussed in section 3.2 (Fig. 3.4). The effect of operating pressure on refrigeration capacity gradually reduces as system operating at higher pressure.

The variation of refrigeration capacity with simulation condition are found to be nil with operating pressure, except at the simulation conditions 1 and 10, and the values are lowest at these conditions. However these effects are more prominent at lower operating pressures.

For each circuit arrangement, the value of refrigeration capacities are increases with increase in air velocity and vice versa, at lower operating pressure, it is due to the lower approach temperature and pressure drop as discussed in section 5.3.1.2 Fig. 5.4. However these effects are insignificant at higher operating pressures. It is also observed that the higher refrigeration capacity from above simulation conditions are achieved at 13 MPa operating pressure. However, it is having very small difference at simulation conditions 6, 8, 9, 14, and 15, 16, 17 and 18.

Fig. 5.7(b) shows the variation of compressor work required at different operating pressure, compression work increases with increase in pressure same as earlier. The work requirement increases more significantly at higher operating pressures. Fig. 5.7(c) shows the cumulative effect of refrigeration capacity and compressor work on the performance of overall system as COP. It is observed that unlike to temperature zone I, the variation of COP with different operating pressure at each simulation conditions.

The value of COP are found to be similar at simulation condition 6, 8, 9 and 15, 17, 18 for each operating pressure. Based on the logic discussed earlier the best possible value are found to be for simulation condition 17 having 45 tubes, 2 m/s air velocity and 3-circuit with operating condition 10.5MPa compressor discharge pressure for temperature zone II.

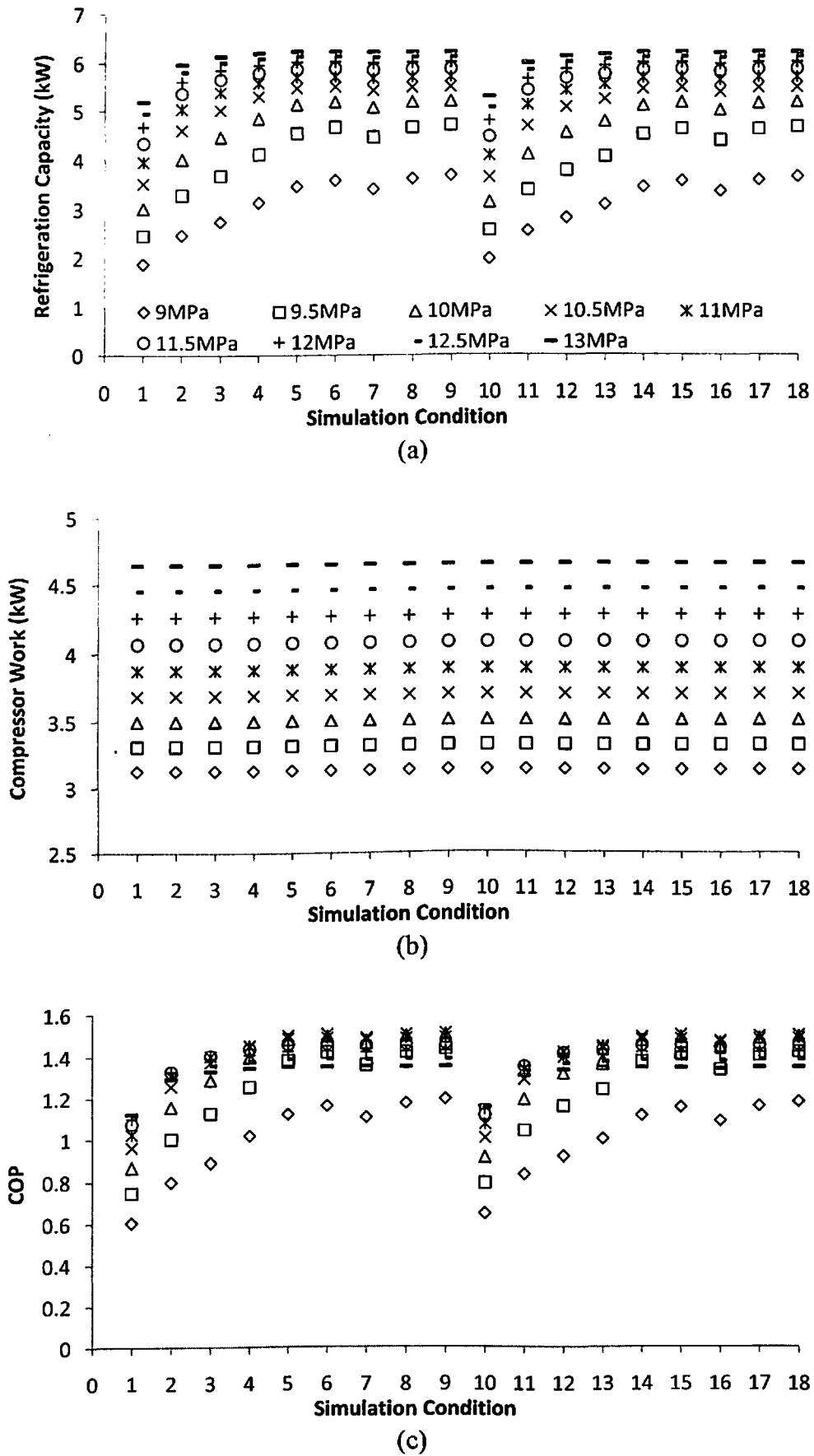


Figure 5.7: Performance of overall system at temperature zone II

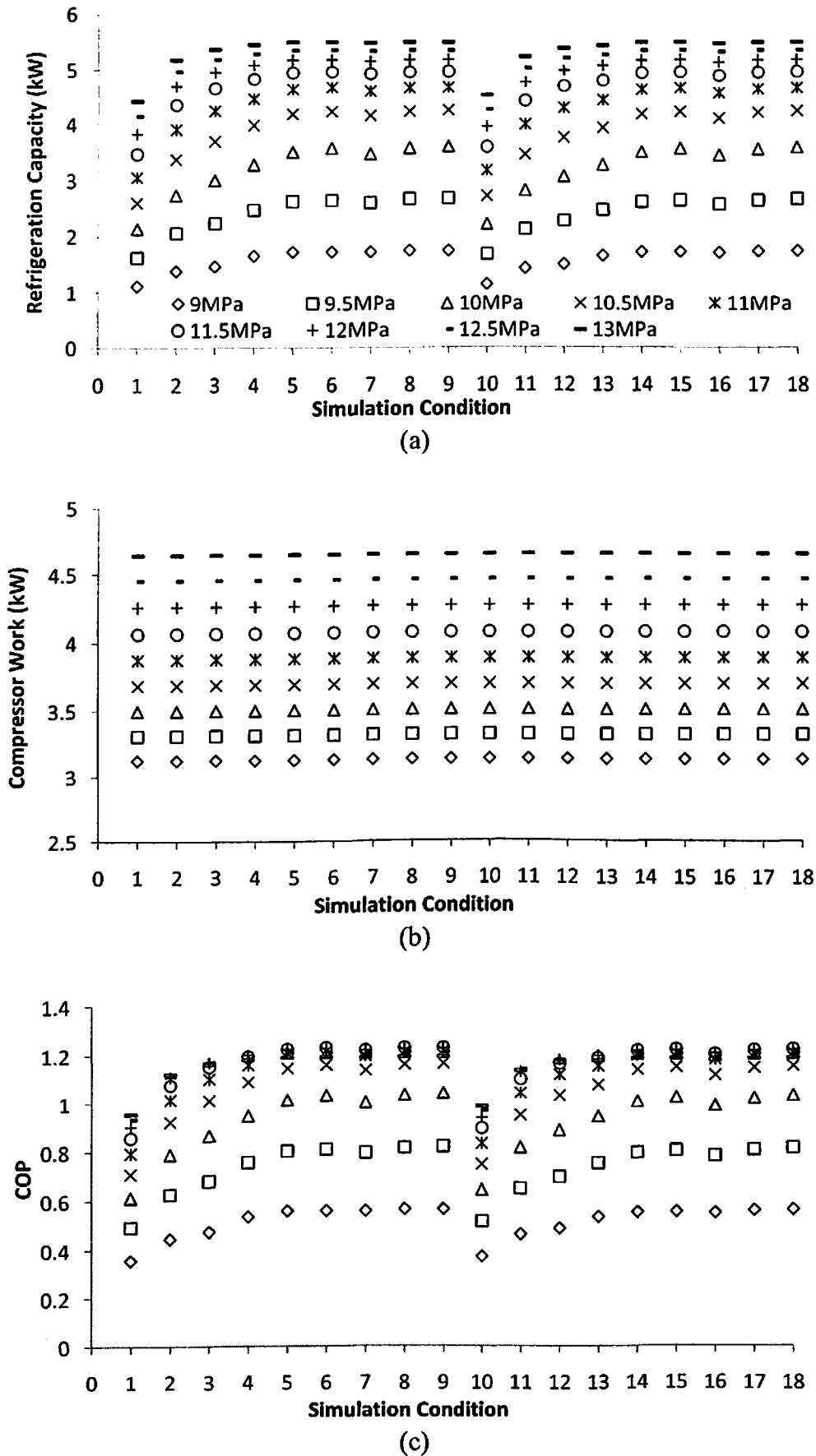


Figure 5.8: Performance of overall system at temperature zone III

5.3.2.3 Temperature zone III

Fig. 5.6 show the performance of the overall system in terms of cooling capacity, compressor work and COP with different simulation conditions (Table 5.1.) at different operating pressure for temperature zone III (i.e. 45°C).

Fig. 5.8(a) to 5.8(c) shows the variation of refrigeration capacity, compressor work and COP with different simulation conditions at different operating pressure for temperature zone III. It is observed that trends are unlike temperature zone I but are similar to zone II.

The value of COP are found to be insignificant variation in simulation condition 6, 8, 9 and 15, 17, 18 for each operating pressure. The best possible value is found for simulation condition 17 having 45 tubes, 2 ms⁻¹ air velocity and 3-circuit with operating condition 11.5MPa compressor discharge pressure giving both material and energy saving at equal level of performance for temperature zone III.

With the help of detail and flexible model of a finned tube gas cooler discussed in chapter 4, simulation based study is carried out for the gas cooler performance and its impact on the overall system performance against the variation in operating temperature, pressure, air velocity and various other physical design parameters are discussed. Importance of selection of optimum combination of parameters are explored.

Further the performance of the trans-critical CO₂ refrigeration system is evaluated using the operating conditions in warm climate like in India. Formulating design guidelines for operating such gas cooler and overall refrigeration system is explored. It is also observed that, unlike the conventional refrigeration system, the COP of the systems may increase with the increase in the gas cooler pressure. The results are more favorable at higher air velocity and number of circuit, but it need to optimized based on the possible improvement of performance with number of circuit and fan power consumption to maintain higher air velocity. Therefore in subsequent chapter a simulation based analysis is carried out for optimization of gas cooler to achieve best possible performance of gas cooler and overall system considering fan power consumption as well.

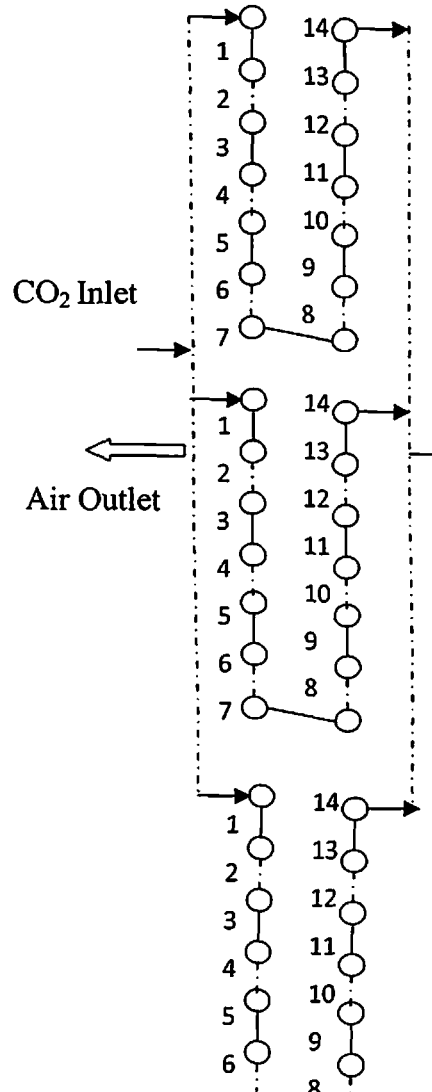
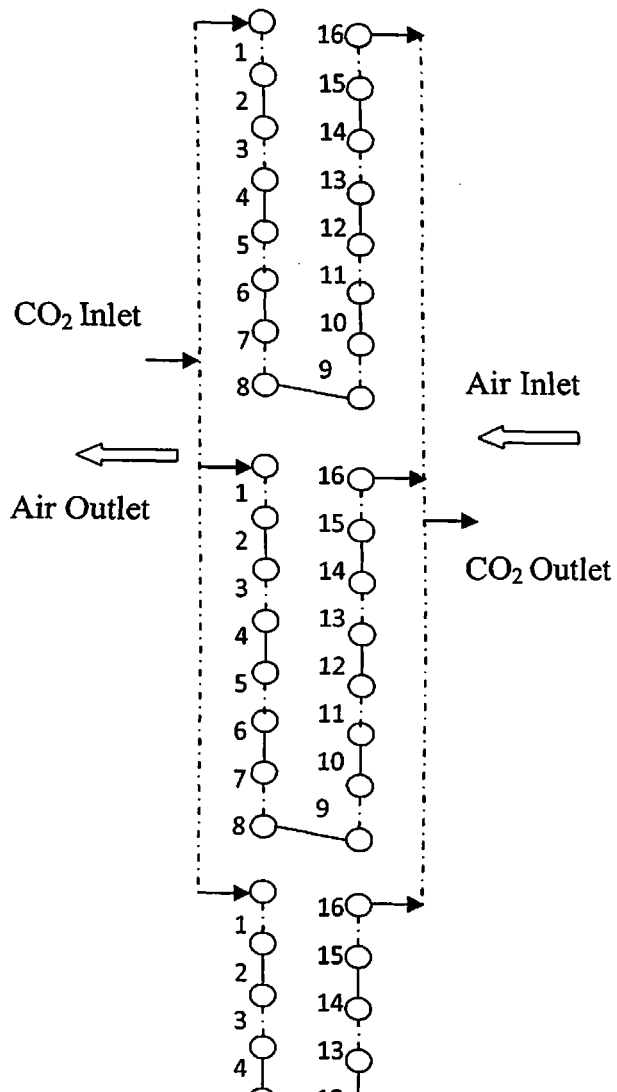
Optimization of Gas Cooler

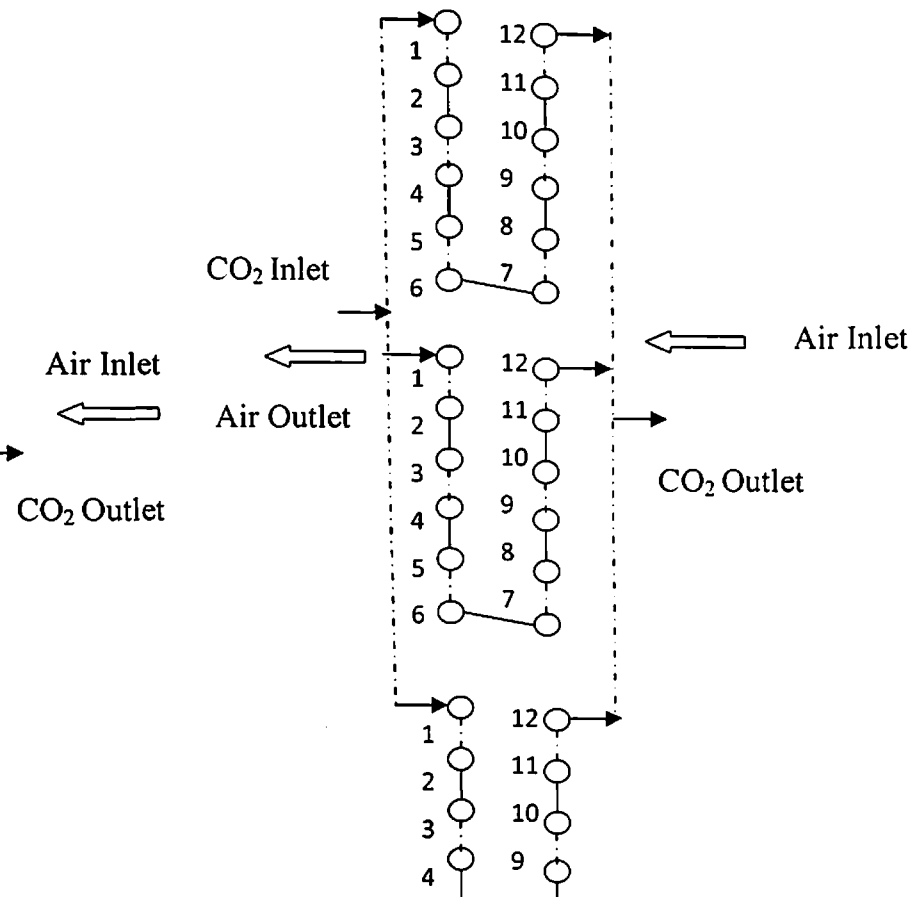
In previous chapter the performance analysis of gas cooler and overall CO₂ trans-critical refrigeration systems are discussed using the validated model described in chapter 4 along with extension of the model at different temperature zones in India conditions. It was found that the consequences are more favorable at higher air velocity and higher number of circuit, however higher air velocity needs high capacity fan and ~~there is corresponding~~ energy consumption. Therefore, it is required to optimized the gas cooler based on ^{the higher} the possible improvement of performance of overall system with number of circuit and fan power consumption to maintain higher air velocity. In this chapter an attempt is made to optimize the gas cooler design and the operating parameters to achieve best possible performance of gas cooler and overall system considering fan power consumption. Mathematical model is extended to include the fan power consumption, and the simulation based studies are carried out with modified gas cooler geometry, its flow arrangement, and operating conditions. The simulation results at different temperature zones in India conditions are discussed in subsections of this chapter.

↳ Indian

6.1 Selection of Input Combinations of Geometric and Operating Parameters

Based on the observation of simulation results in chapter 5, the low performance input combinations, detailed below are discarded and only the sensible range of operating parameters is taken up for further analysis. Gas cooler performance increase with increase in number of circuit, however 3-circuit arrangements is found to have marginal improvement in COP over 2-circuit. Therefore, number of circuits are further not increased and only 3-circuit arrangement is taken in this study. Similarly the operating pressure in which the system performance was having lower COP are also removed from the study. Different operating pressure ranges are selected based on the temperature zones. Since the effect of fan power consumption on the COP is one of the focuses of the study, finer steps of air velocities are taken for analysis. The compactness of the gas cooler may also affect the fan power consumption therefore the performance is analyzed for two, three and four passes arrangement of gas cooler designs as shown in Fig. 6.1 to Fig. 6.3. The number of input combination is now refined for each temperature zones and the ranges of input parameters are summarized in Table 6.1.





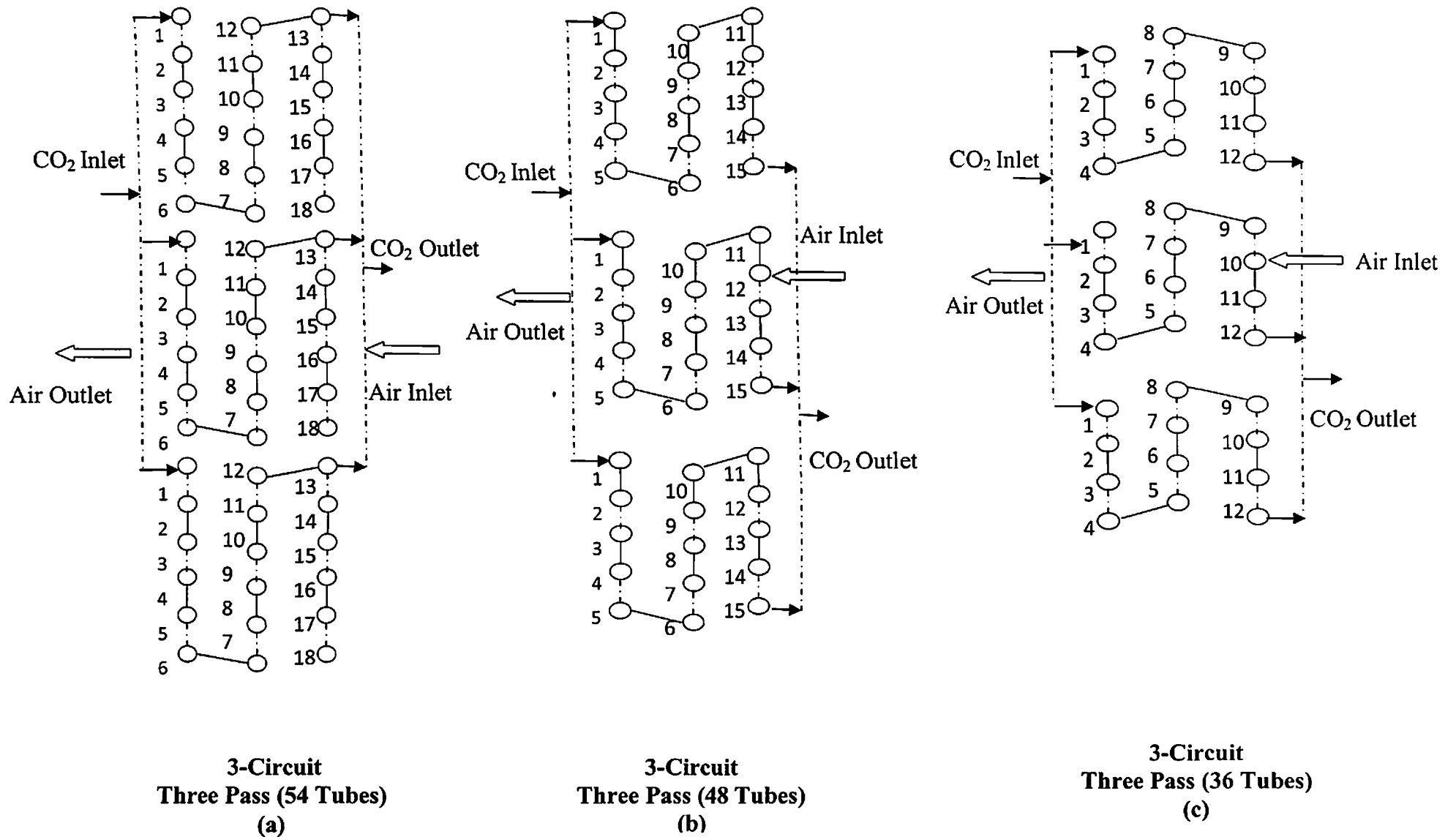


Figure 6.2: Modified geometry with different circuit arrangement of (three pass) gas cooler

remove inlet!

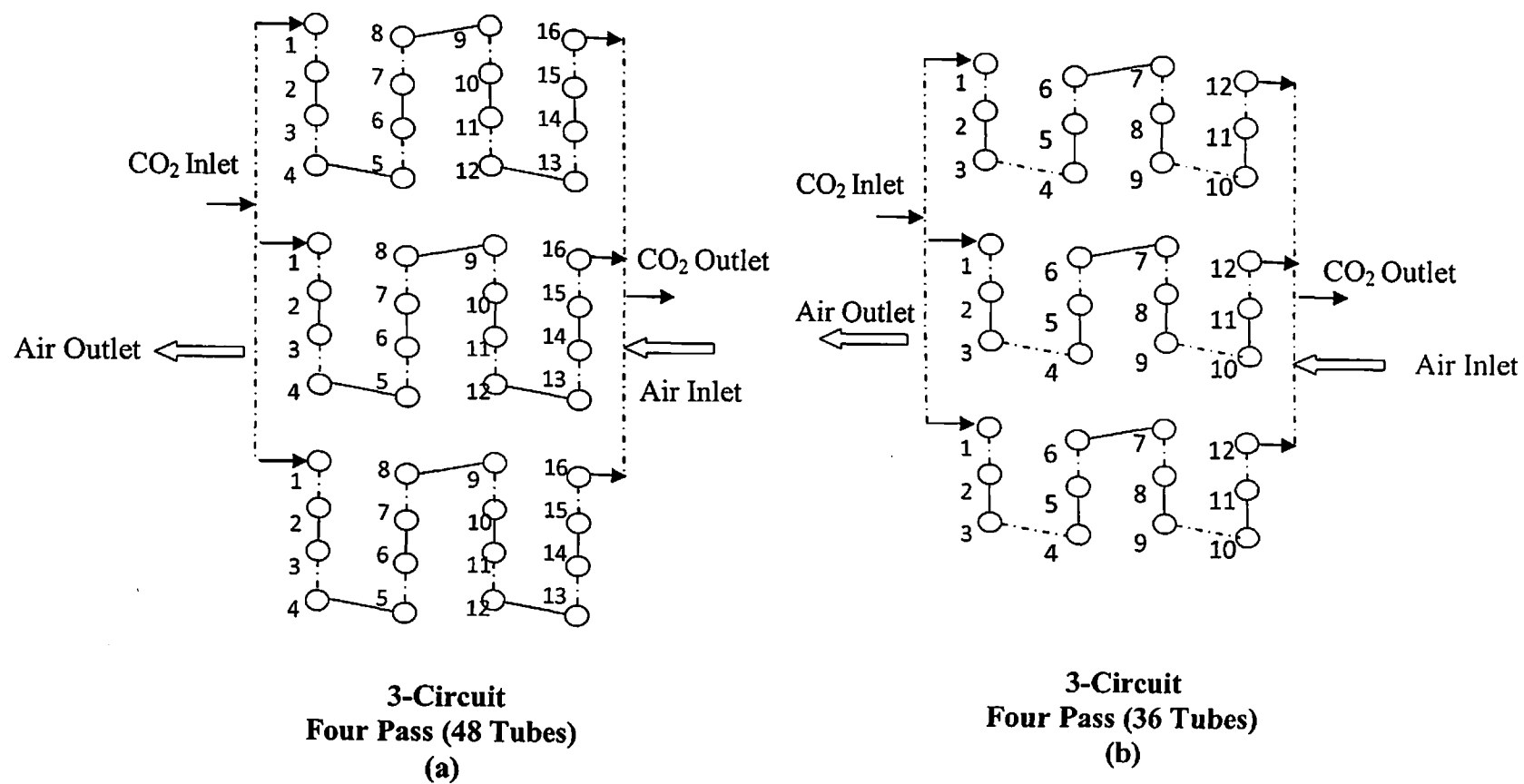


Figure 6.3: Modified geometry with different circuit arrangement of (*four pass*) gas cooler

Table 6.1: Modified operating conditions and simulation parameters for optimization

Parameters	Operating Pressure (MPa)	Air Velocities (ms ⁻¹)	Number of Tubes		
			2 pass	3 pass	4 pass
Zone I	8	1			
	8.5	1.5	48	54	48
	9	2	42	45	36
		2.5	36	36	
Zone II		3			
	10	1			
	10.5	1.5	48	54	48
	11	2	42	45	36
Zone III		2.5	36	36	
		3			
	11.5	1			
	12	1.5	48	54	48
	12.5	2	42	45	36
		2.5	36	36	
		3			

Pressure drop between compressor discharge and gas cooler inlet is neglected, evaporator pressure is taken as constant for maintaining 0°C temperature and mass flow rate of refrigerant is taken as 0.045 kg s⁻¹, which is within the validated range.

6.2 Model Application

The mathematical model developed and validated in chapter 4, is now utilized to evaluate the performance of gas cooler and the model is extended for the performance of overall system including fan power consumption. The model is represented mathematically in Eq. 6.1 to Eq. 6.4. Fan power consumption is calculated assuming 90% fan efficiency using Eq. 6.3.

$$W_{\text{comp}} = \frac{\{H_{\text{rco}}(P_{\text{co}}, T_{\text{co}}) - H_{\text{rci}}\}}{\eta_{\text{isen}}} \quad (6.1)$$

$$RE = \{H_{\text{reo}} - H_{\text{rei}}(P_{\text{gco}}, T_{\text{gco}})\} \quad (6.2)$$

$$W_{\text{fan}} = \frac{Q_v \Delta P_{\text{air}}}{\eta_{\text{fan}}} \quad (6.3)$$

$$\text{COP} = \frac{RE}{W_{\text{comp}} + W_{\text{fan}}} = \frac{\{H_{\text{reo}} - H_{\text{rei}}(P_{\text{gco}}, T_{\text{gco}})\}}{\frac{\{H_{\text{rco}}(P_{\text{co}}, T_{\text{co}}) - H_{\text{rci}}\}}{\eta_{\text{isen}}} + \frac{Q_v \Delta P_{\text{air}}}{\eta_{\text{fan}}}} \quad (6.4)$$

where, H is function of P and T , and enthalpy at gas cooler outlet is equal to the enthalpy at evaporator inlet. Using the above steady state model, performances of the system is analyzed for different operating and geometric conditions for different temperature zones and selected combinations of model input parameters. Using the updated model, the refrigeration capacity in kW, compressor work in kW, and COP of the overall system is calculated.

6.3 Results and Discussion

The performance of gas cooler using the validated model from chapter 4 and the overall system performance using the extended model with the respective gas cooler at various combinations of input parameters (Table 6.1.) are discussed in subsequent articles. The results are shown and discussed separately for all three temperature zones in Indian climatic conditions in subsequent sections.

remove dot

6.3.1 Performance of gas cooler and overall system

The performances of gas cooler in terms of approach temperature, gas cooler capacity, and pressure drop in refrigerant side, in gas cooler and the performance of overall system in terms of cooling capacity in kW, power input including fan power consumption in kW and COP are tracked through simulation with the respective design of gas cooler and various operating conditions as discussed in section 6.1. The cumulative effect of gas cooler performance parameters on the performance of overall system at environmental temperature zone I, zone II and zone III are studied and results are summarized.

6.3.1.1 Temperature zone I

The simulation results are present in this section to analyze the performance of the gas cooler and overall system for temperature zone I (Air ^aTemperature 29.4°C) at different operating pressure and simulation conditions. Fig. 6.4 to Fig. 6.6 show the simulation result with two, three and four pass gas cooler respectively and 3-circuit arrangement.

Fig. 6.4 shows the performance with two pass gas cooler with 48, 42 and 36 tubes in 3-circuit arrangement. Fig. 6.4(a) depict the variation of approach temperature with operating pressure and air velocity using different design of gas cooler. It is observed that the approach temperature is significantly high in two pass arrangement of the gas

cooler, it is due to the lower surface area and temperature gradients available for heat transfer. The lowest value of approach temperature ~~is~~ achieved is at 9MPa operating pressure, 48 tubes and 3 ms^{-1} air velocity. *2022*

Fig. 6.4(b) shows the variation of gas cooler heat rejection capacity with air velocity, the results indicate that the gas cooler capacity increases with increase in air velocity and operating pressure. Further for the same operating pressure gas cooler capacity increase with increase in number of tubes in gas cooler. It is due ^{to} the lower approach temperature at these condition shown in Fig. 6.4(a), hence gas cooler capacity is higher at the condition where lower AT achieved.

Fig. 6.4(c) depicts the variation of pressure drop with air velocity at different operating and design conditions. It is found that the pressure drop decrease with decrease in number of tubes in gas cooler and for same number of tubes in gas cooler, pressure drop decreases as operating pressure increases. This observation can be ~~explain~~ ^{explained} from the fact that lower surface area available for frictional pressure drop with less number of tubes. Overall the pressure drop slightly decreases with increase in air velocity for each gas cooler design and operating conditions.

Fig. 6.4(d) shows that refrigeration capacity increases with increase in air velocity and operating pressure for same number of tubes. However these variations are more prominent at lower air velocity. It is due to lower AT and higher gas cooler capacity at this condition. It is also found that refrigeration capacity increases with increase in number of tubes at each operating conditions.

Fig. 6.4(e) show the COP variation with air velocity at different operating and design conditions, it is observed that COP first increases with air velocity then decreases. Value of COP depends on refrigeration capacity, compressor work and fan power consumption. Therefore the trends of COP variation are uneven and the maximum COP of the system operating at zone I with two pass gas cooler is found to be at 9MPa, 2 ms^{-1} air velocity and 48 tubes.

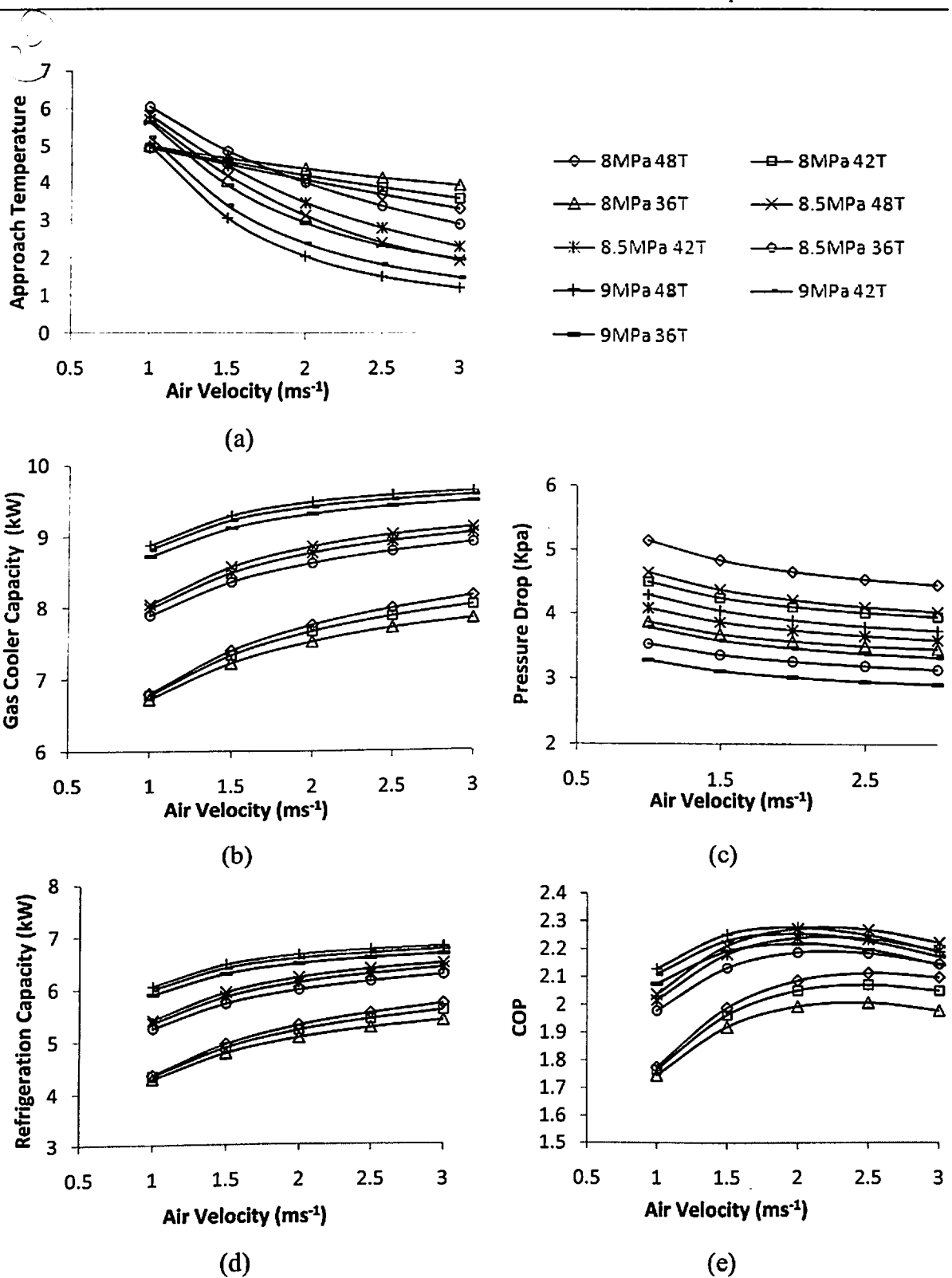
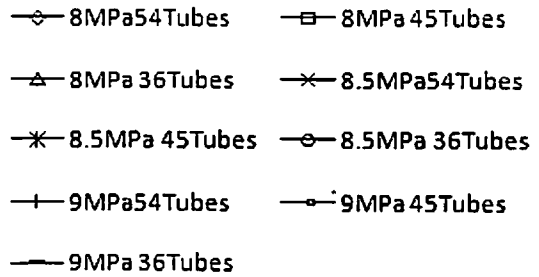
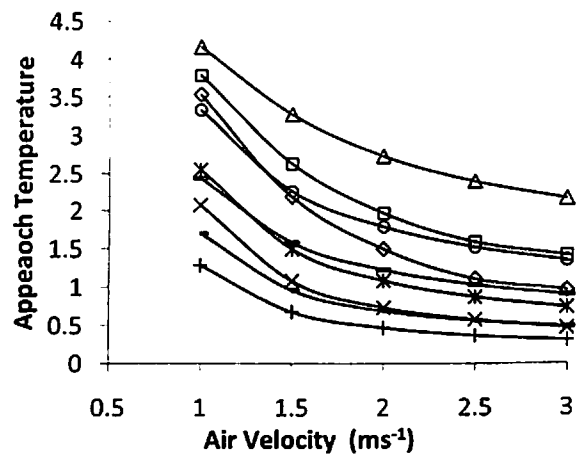


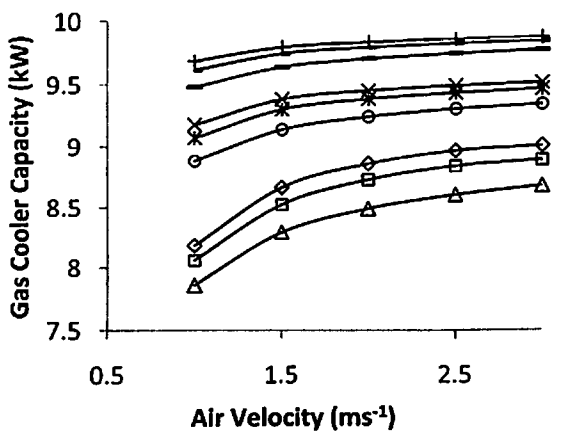
Figure 6.4: Performance of (*two pass*) gas cooler and overall system at zone I

Fig. 6.5 shows the performance of three pass gas cooler and overall system at temperature zone I. Fig. 6.5(a) depict the variation of approach temperature with air velocity at different operating and design of gas cooler. It is observed that the approach temperature decreases with increase in air velocity, operating pressure and number of tube, and the absolute values are lower than that of two pass gas cooler at each

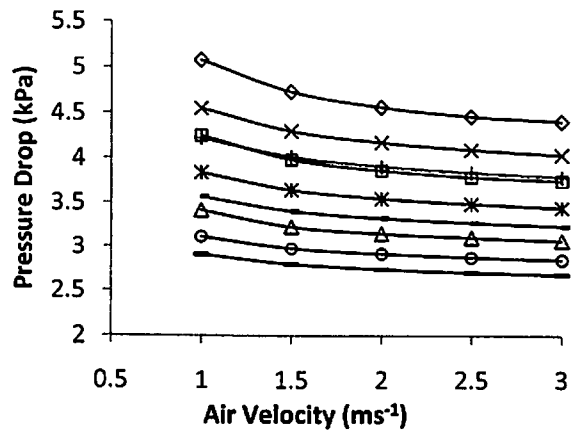
conditions. It is perceived to be due to the higher surface area available for heat transfer. Approach temperature is found to be lower at higher operating pressure i.e. 9MPa with 54 tubes and 3 ms⁻¹ air velocity.



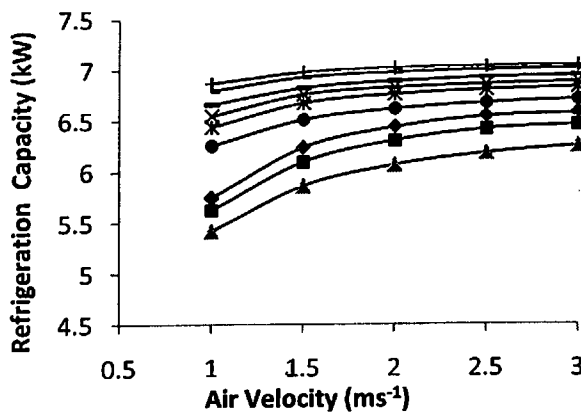
(a)



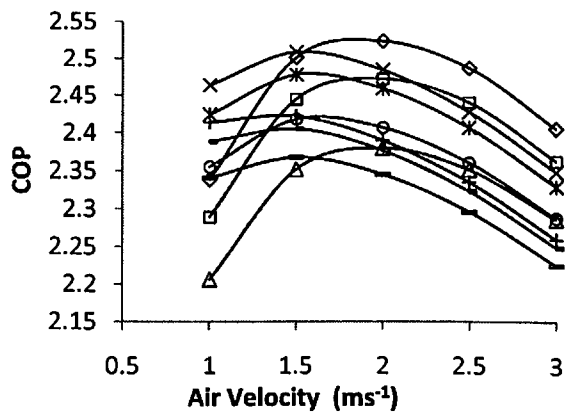
(b)



(c)



(d)



(e)

Figure 6.5: Performance of (three pass) gas cooler and overall system at zone I

Fig. 6.5(b) shows the variation of gas cooler heat rejection capacity, similar trends as two pass gas cooler are observed in this case. The gas cooler capacity increase with air velocity but this increment ceases at higher velocities. The capacity of gas cooler increase with increase in operating pressure, increased in number of tubes and with increase in air velocity. However, at higher operating pressure the effect of air velocity in increasing the gas cooler capacity is found to be insignificant.

Fig. 6.5(c) shows the variation of pressure drop, very small variations are observed with air velocity at each operating pressure and gas cooler designs. For each operating pressure, pressure drop decreases with less number of tubes, due to less surface area available for frictional pressure drop. Lowest pressure drop occurs at higher operating pressure, for less number of tubes and at higher air velocity.

Fig. 6.5(d) shows the variation of refrigeration capacity, it increases with increase in air velocity and operating pressure with large number of tubes in gas cooler. However these variation diminishes at higher operating pressure.

Fig. 6.5(e) depict the variation of COP of the system with air velocity at different operating pressure and gas cooler. An uneven trends of variation of COP are observed, this is due to several factors that are competing with each other. It is found that the maximum COP is achieved at lower operating pressure 8 MPa with 54 tubes and 2 ms^{-1} air velocity. The COP with three pass gas cooler is found higher than that of two pass gas cooler.

Fig. 6.6 depicts the performance of four pass gas cooler and overall system at temperature zone I (environment temperature 29.4°C). Fig. 6.6(a-e) shows the variation of approach temperature, gas cooler capacity, pressure drop, refrigeration capacity and COP respectively with air velocity at different operating pressure and design of gas cooler.

Trends of approach temperature Fig. 6.6(a) in case of four pass gas cooler is similar to three pass gas cooler but has slightly lower value as compare to three pass gas cooler and significant lower as compare to two pass gas cooler.

Gas cooler heat rejection capacity Fig. 6.6(b), pressure drop Fig. 6.6(c) and refrigeration capacity Fig. 6.6(d) are also showing similar trend as three pass gas cooler, however COP is having slightly different trends.

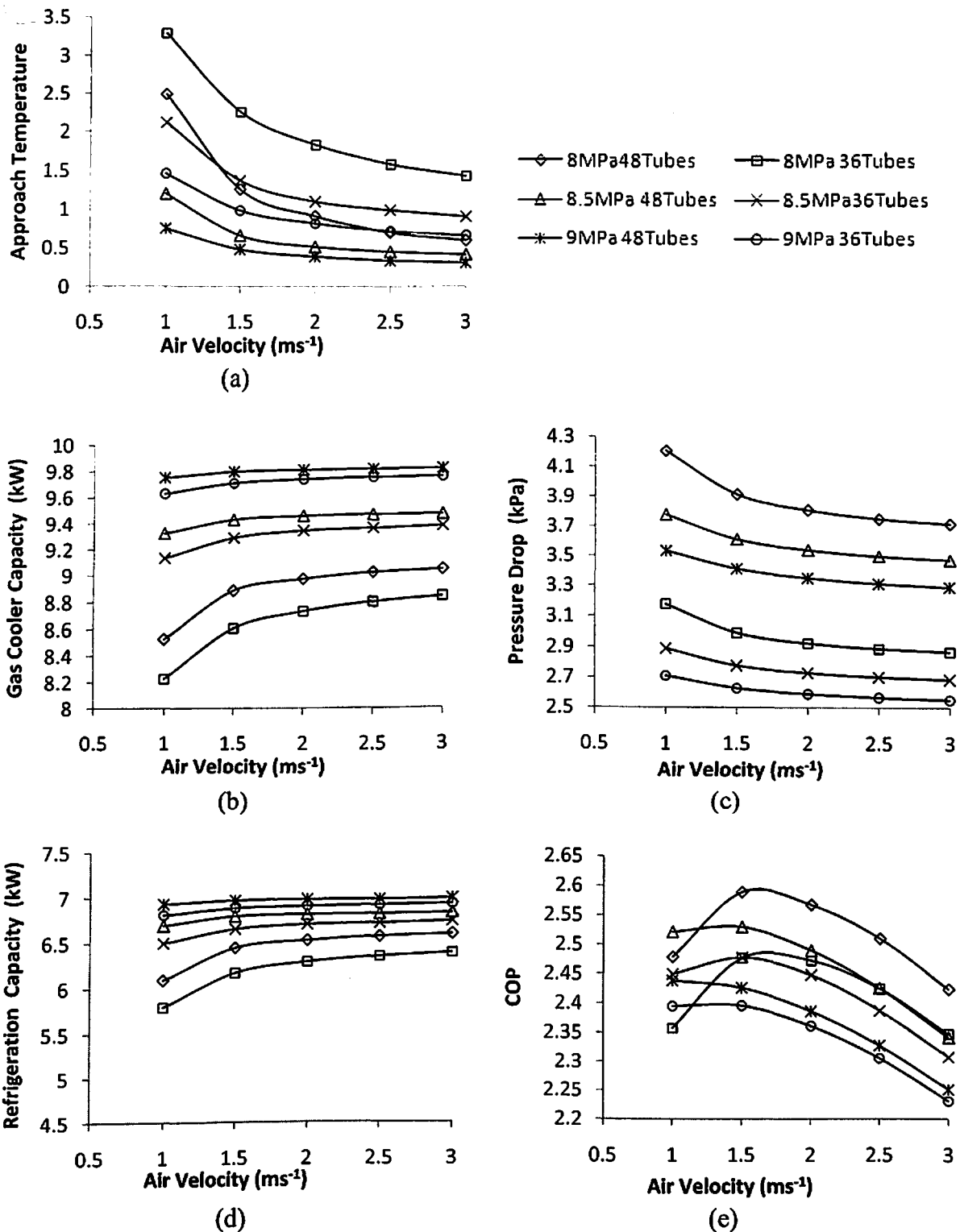


Figure 6.6: Performance of (*four pass*) gas cooler and overall system at zone I

The maximum COP is found at lower operating pressure 8MPa and air velocity 1.5 ms^{-1} with 54 tubes in gas cooler. Referring to Fig. 6.5(e) and Fig. 6.6(e) it is observed that the maximum COP is having insignificant different between three pass and four pass

cooler design, however there is a significant difference with two pass gas cooler as shown in Fig. 6.4(e).

Overall, it is found that the performance of the system with four pass and three pass gas are very close but with two pass gas cooler it has poorer performance.

6.3.1.2 Temperature zone II

Fig. 6.7 - Fig. 6.9 shows the performance analysis of gas cooler and overall system at temperature zone II (i.e. environment temperature 40°C) with two pass, three pass and four pass gas cooler respectively. These all parameter variations are plotted against the air velocity at different operating pressure with different design of gas coolers.

Fig. 6.7(a) shows the variation of approach temperatures of a two pass gas cooler, where it is observed that AT decrease with increase in air velocity. Further AT is lower for the gas cooler having larger number of tubes at each operating pressure, it is due to the higher heat transfer area available. Similarly AT is lower at higher operating pressure for gas cooler having same number of tubes, because of the higher temperature gradient at high operating pressure. Lowest value of AT is found at higher operating pressure and air velocity i.e. 11MPa and 3 ms⁻¹ with 48 tubes in gas cooler.

The variation of gas cooler heat rejection capacity of a two pass gas cooler is plotted in Fig. 6.7(b). The variation of gas cooler capacity is observed to be very similar as in temperature zone I and the maximum value of heat rejection capacity is achieved at higher operating pressure, higher air velocity and large size of gas cooler (i.e. where the approach temperature is lowest), however, the effect of the air velocity on gas cooler capacity is negligible at higher air velocity.

Fig. 6.7(c) shows the variation of pressure drop in a two pass gas cooler, trends of the variation are very much similar to that in temperature zone I. Lowest pressure drop is achieved at higher pressure, higher air velocity and for large size of gas cooler because of large surface available for frictional pressure drop.

The variation of refrigeration capacity is plotted in against air velocity Fig. 6.7(d), similar trends as zone I are observed, however the absolute value of refrigeration capacities are found to be slightly lower and the variations with operating pressures are significant as compare to zone I.

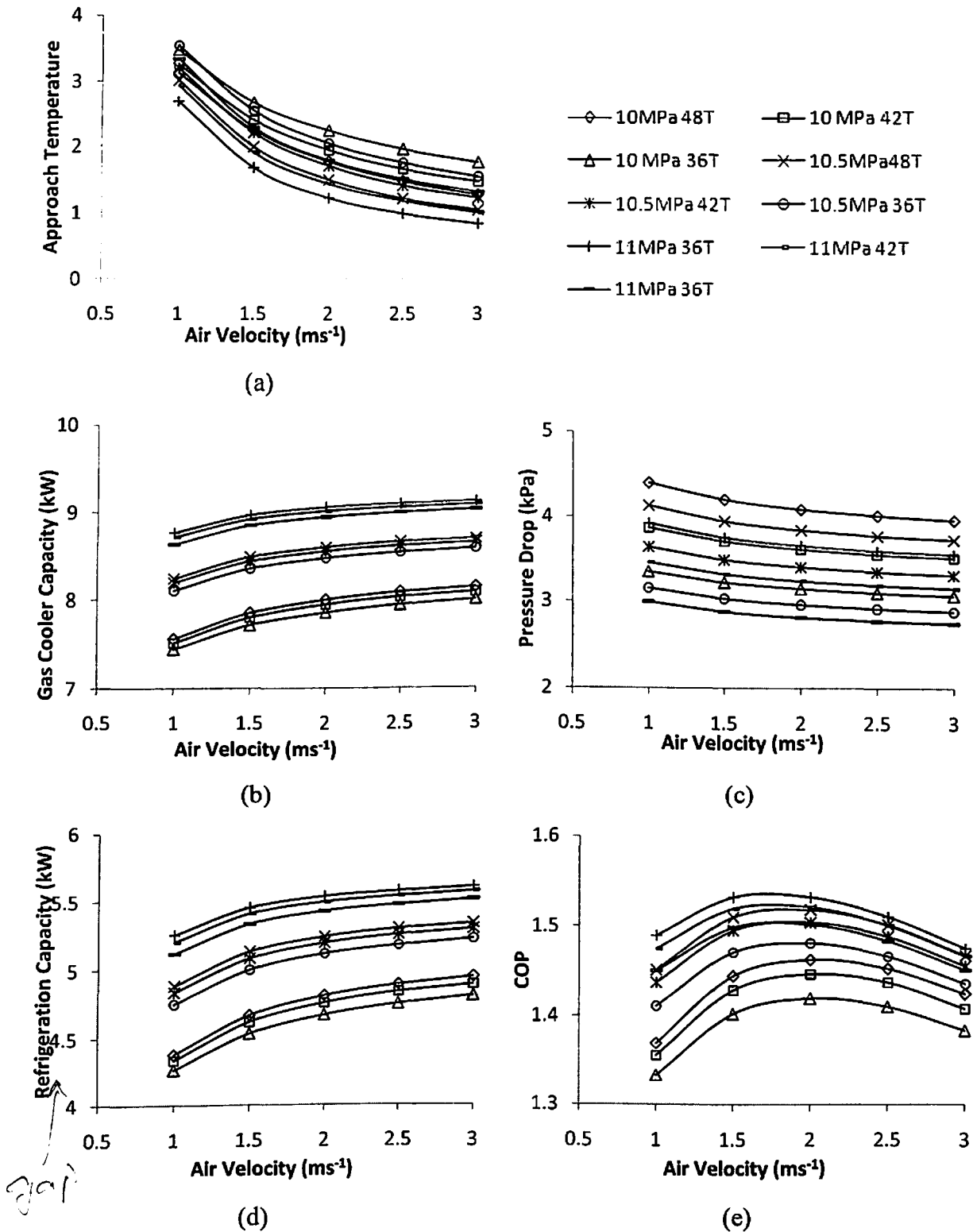


Figure 6.7: Performance of (two pass) gas cooler and overall system at zone II

The highest value of refrigeration capacity is found to be at high pressure and large size of gas cooler. It is also observed that the refrigeration capacity variation is insignificant at higher air velocities.

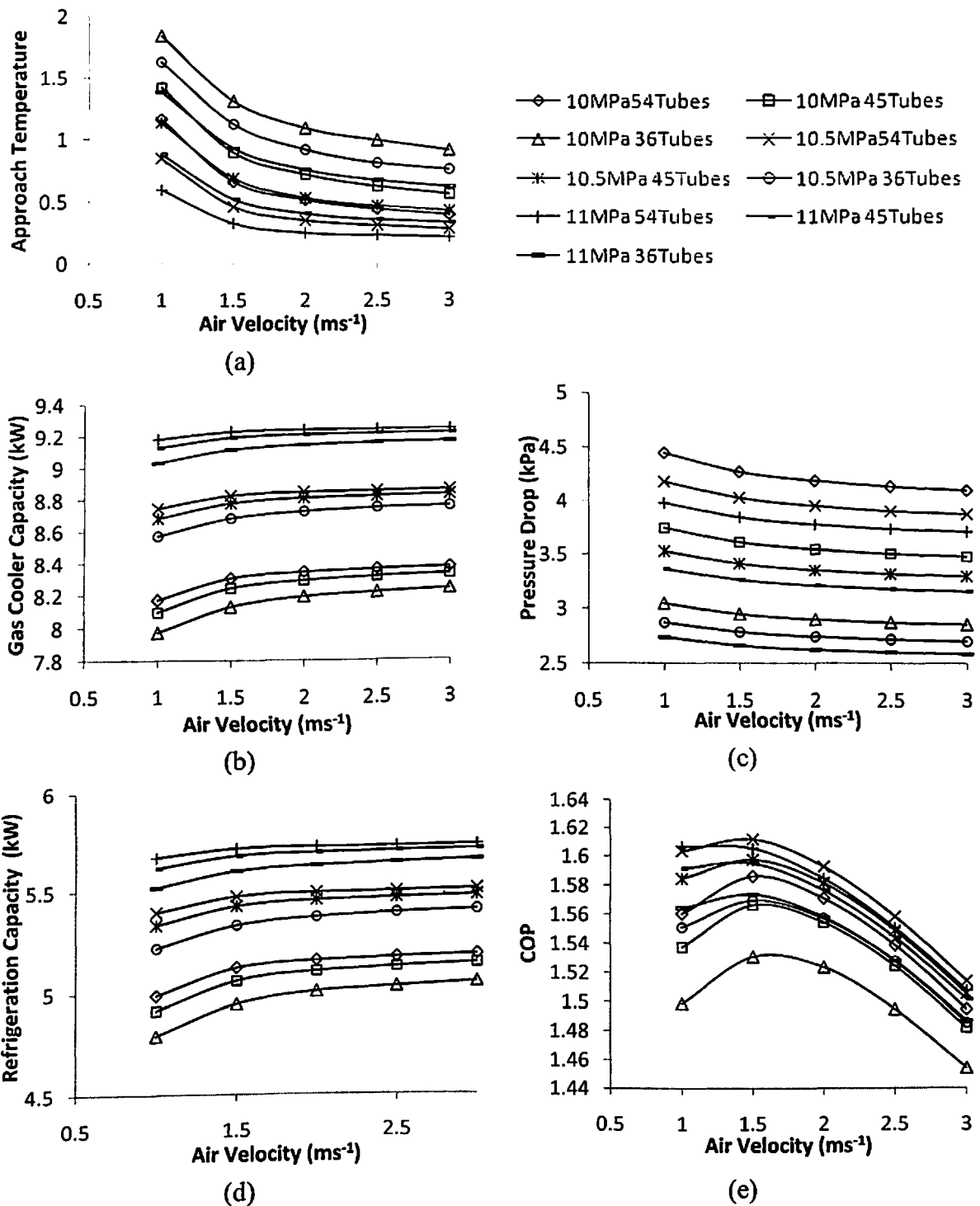


Figure 6.8: Performance of (three pass) gas cooler and overall system at zone II

The cumulative effect of refrigerating capacity, compressor work and fan power consumption on COP of the system are plotted in Fig. 6.7(e). Somewhat uneven variation of COP with air velocity is observed and the highest value of COP is achieved at higher operating pressure and higher number of tubes i.e. 11MPa and 48 Tubes with air velocity 2 ms^{-1} .

Fig. 6.8 shows similar performance analysis of three pass gas cooler and overall system at temperature zone II. Most of the parameter variation exhibits similar trend as two pass gas cooler, however some observations are made which differ from the previous results. It is found that the absolute of AT is significantly lower as compared to two pass gas cooler and for some operating pressure and gas cooler design, very lower AT less than 0.5 as shown in Fig. 6.8(a).

Therefore, referring Fig. 6.8(b), the gas cooler capacity obtained is higher and Fig. 6.8(c) pressure drop is lower in these conditions.

It is observed from Fig. 6.8(d) that the variation of refrigeration capacity with air velocity is similar as zone II with two pass gas cooler but absolute value is slightly higher as compared to two pass gas cooler because gas cooler performance is better. Again the variation is insignificant with air velocity at each operating pressure and gas cooler design, and for each air velocity it has significant variations.

The variation of the system COP plotted in Fig. 6.8(e), it is found that COP first increases with air velocity then decreases drastically with the same, it is due to the fan power consumption that plays an important role in higher temperature zone with larger size of gas cooler. The best possible COP at these conditions are achieved with 10.5MPa operating pressure, with 54 tubes in gas cooler and 1.5 ms^{-1} air velocity.

With four pass gas cooler at temperature zone II, the results are similar that of three pass. Referring to Fig. 6.9, the trends of approach temperature [Fig. 6.9(a)], gas cooling heat rejection capacity [Fig. 6.9(b)], pressure drop [Fig. 6.9(c)], and refrigeration capacity [Fig. 6.9(d)] are similar with three pass gas cooler, however few differences are found in COP trends as shown in Fig. 6.9(e). The maximum COP point is achieved at lower air velocity i.e. 1 ms^{-1} . It is due to results the fan power consumption is more in case of higher number of passes. The optimum condition is 10.5MPa operating pressure with 48 tubes and the value of the maximum COP attained is approximately same. Since the magnitude of maximum COP is same for both using three pass and four gas cooler, any of the gas cooler can be selected for the further analysis in zone II.

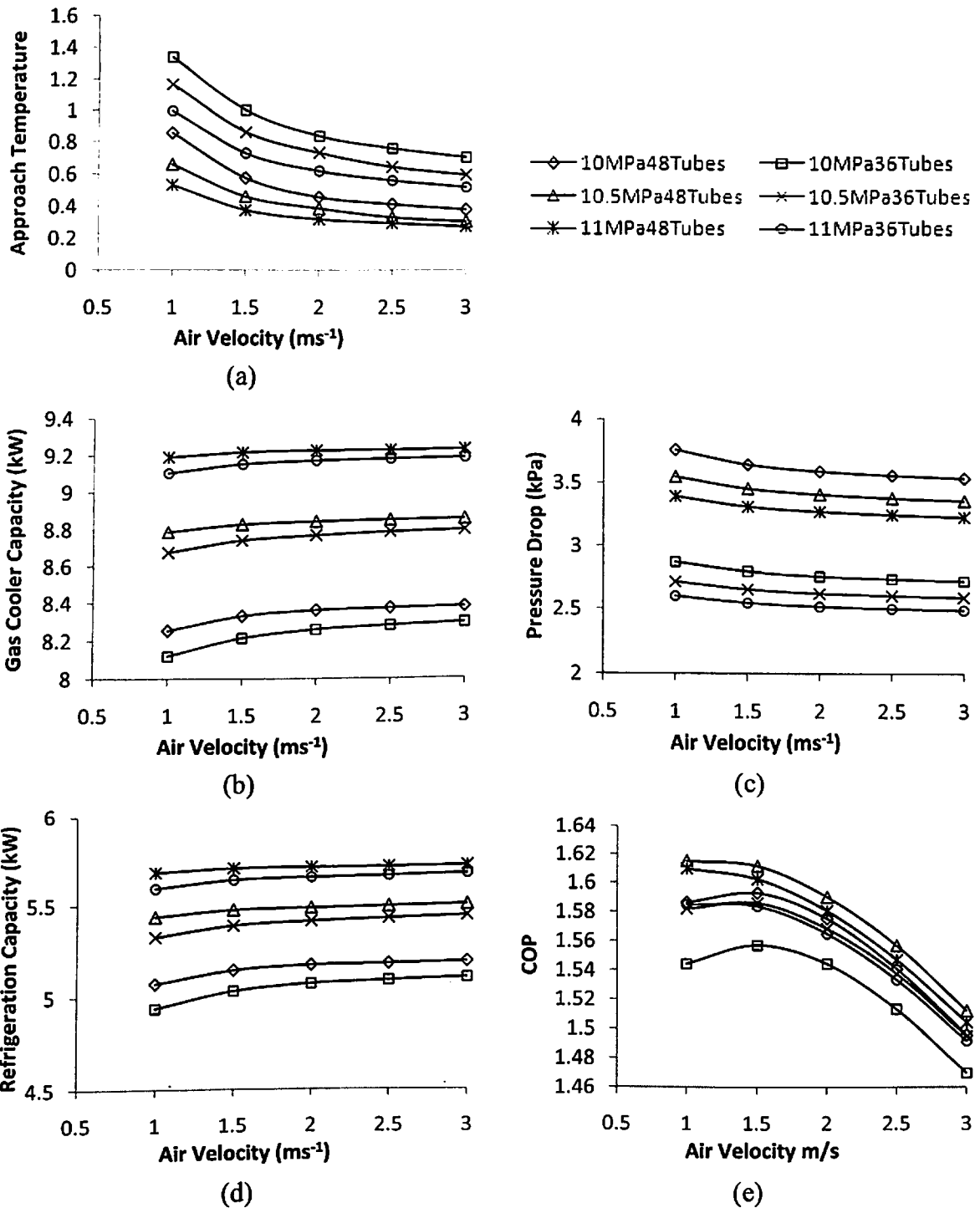


Figure 6.9: Performance of (*four pass*) gas cooler and overall system at zone II

6.3.1.3 Temperature zone III

The performance analysis of gas cooler and overall system at temperature zone III (i.e. environment temperature 45°C) with two pass, three pass and four pass gas cooler are represented in Fig. 6.10 - Fig. 6.12 respectively. The performance variations are plotted against the air velocity at different operating pressure with different design of gas coolers.

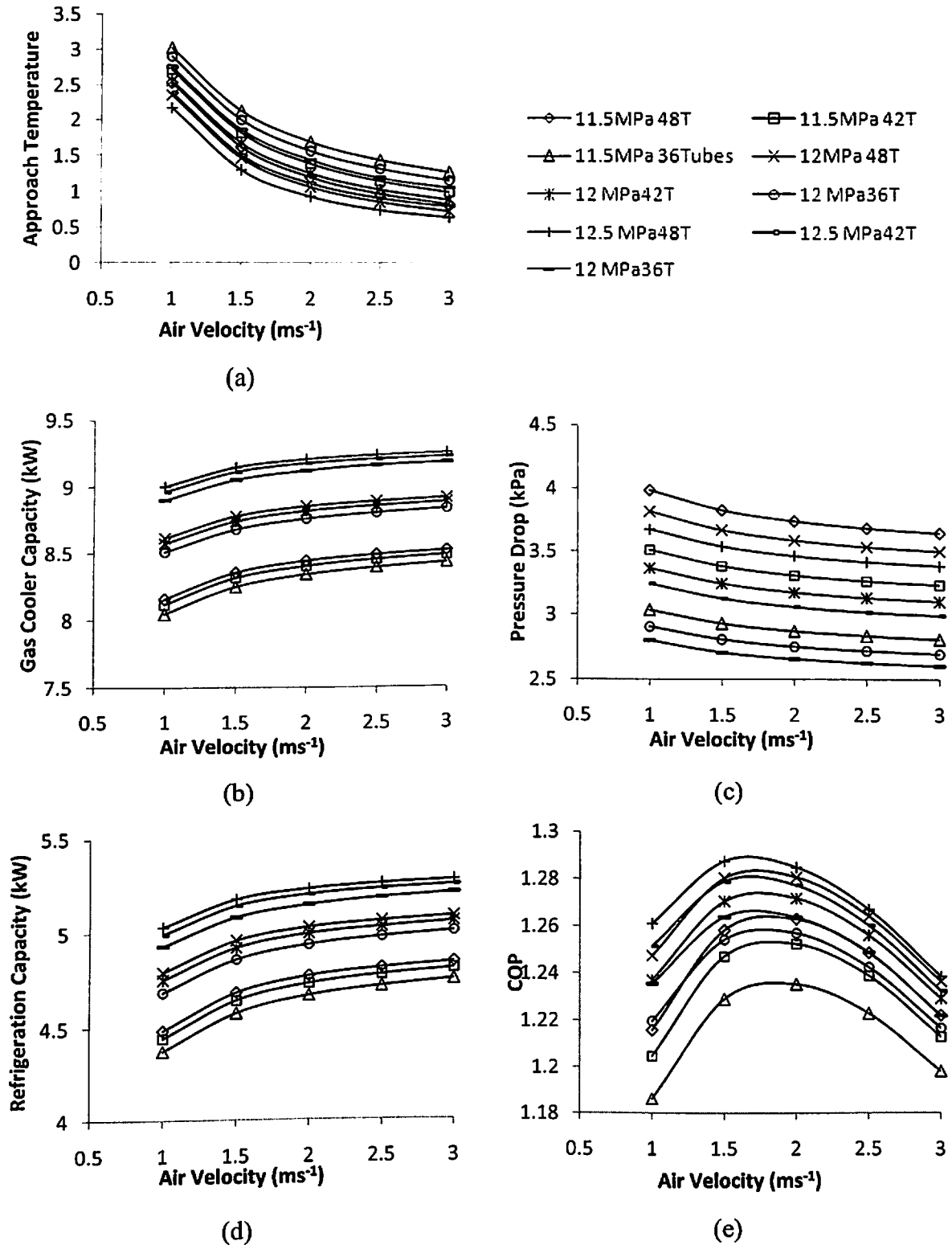


Figure 6.10: Performance of (two pass) gas cooler and overall system at zone III

Fig. 6.10 shows the performance results of two pass gas cooler and overall system, where Fig. 6(a) depicts the variation of ATs at zone III, it is observed that the AT have similar trends as zone I and Zone II, however the magnitudes are more close to zone II. The trends of the variation of gas cooler heat rejection in Fig. 6.10(b), pressure

drop in Fig. 6.10(c) and refrigeration capacity in Fig. 6.10(d) are also same as zone I and zone II but absolute values are close to zone II. Lower value of AT, higher value of gas cooler heat rejection capacity, lower pressure drop are achieved in this zone as compare to zone I and zone II. It due to the large surface area and temperature gradient is available for heat transfer in this higher temperature zone. The variation of COP is shown in Fig. 6.10(e) with air velocity at different operating pressure and two pass gas cooler design, it is observed that the trends of variation are close to zone II. The maximum COP achieved at 12.5MPa operating pressure, 1.5 ms^{-1} air velocity with gas cooler of 48 tubes.

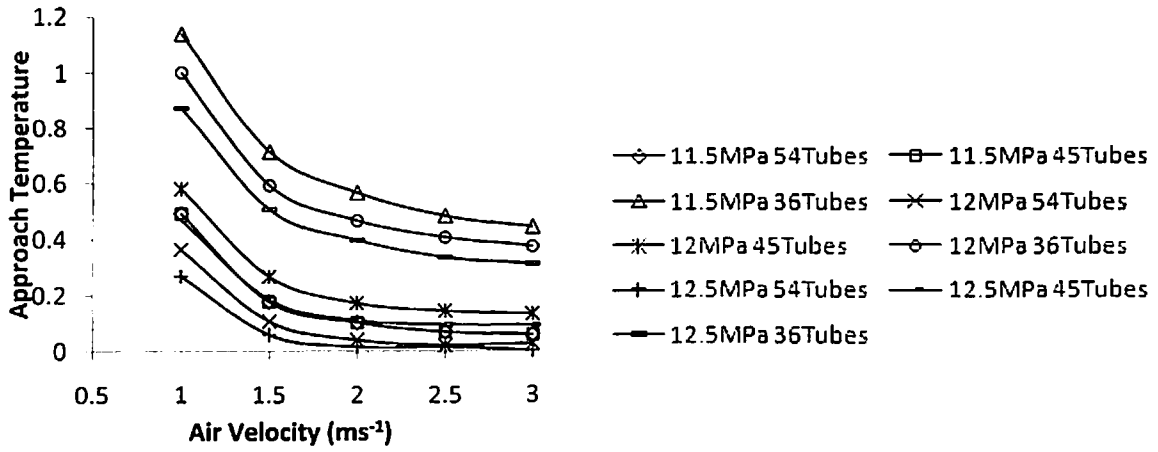
Fig. 6.11 shows the results with three pass gas cooler at temperature zone III. Unlike to two pass gas cooler it is observed that ATs Fig. 6.11(a) have significant small value for each design and operating conditions. The variation of gas cooler heat rejection capacity in Fig. 6.11(b) and pressure drop in Fig. 6.11(c) shows the similar variation as pass two gas cooler.

However due the larger surface and temperature gradient, higher gas cooler capacity and pressure drops are observed. The variation of refrigeration capacity Fig. 6.11(d) are same as the previous case but the values are comparatively larger because of better gas cooler performance.

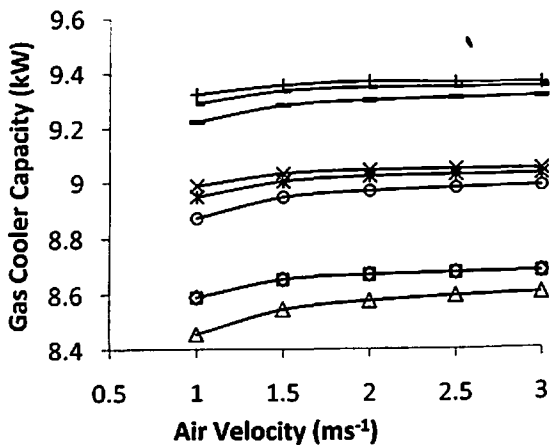
The cumulative effect of refrigeration capacity, compressor work and fan power consumption are shown as COP in Fig. 6.11(e). It is observed that there are slightly different trend of COP with operating pressure and gas cooler size. The maximum COP is found at 12MPa, 1.5 ms^{-1} air velocity with 54 tubes in gas cooler.

Fig. 6.12 shows the performance results of four pass gas cooler and overall system, All the performance parameter having similar trends as three pass gas cooler. However approximately same value of maximum COP is found at different conditions i.e. 12MPa, 1 ms^{-1} air velocity with 48 tube.

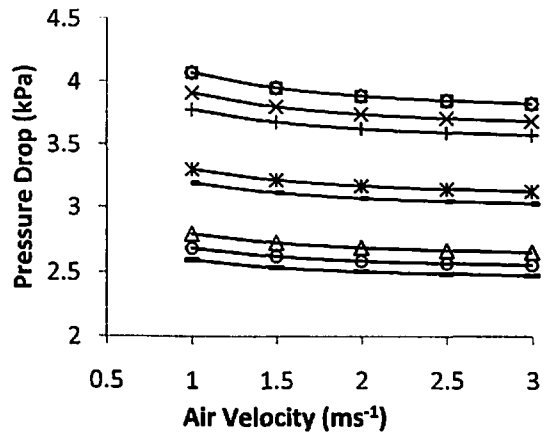
The simulation results and discussion on performance of gas cooler (two, three and four) and overall system at temperature zone I, II and III.



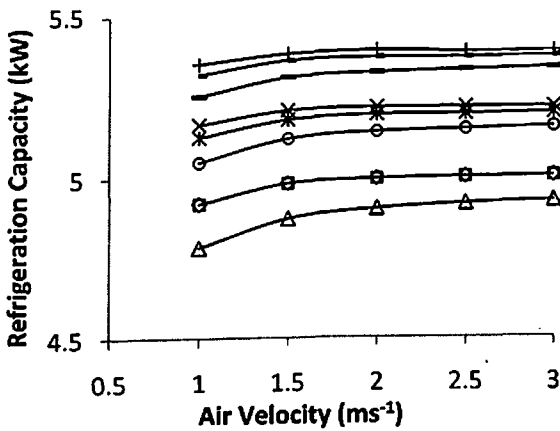
(a)



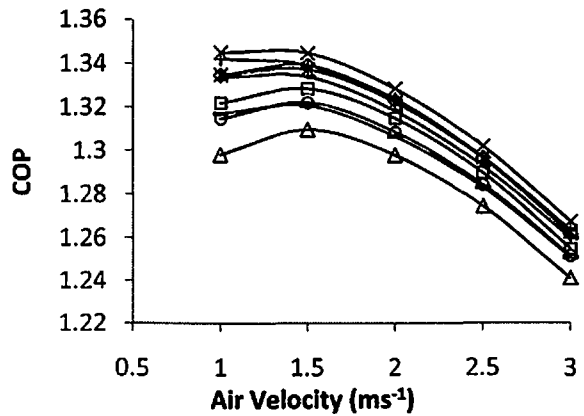
(b)



(c)



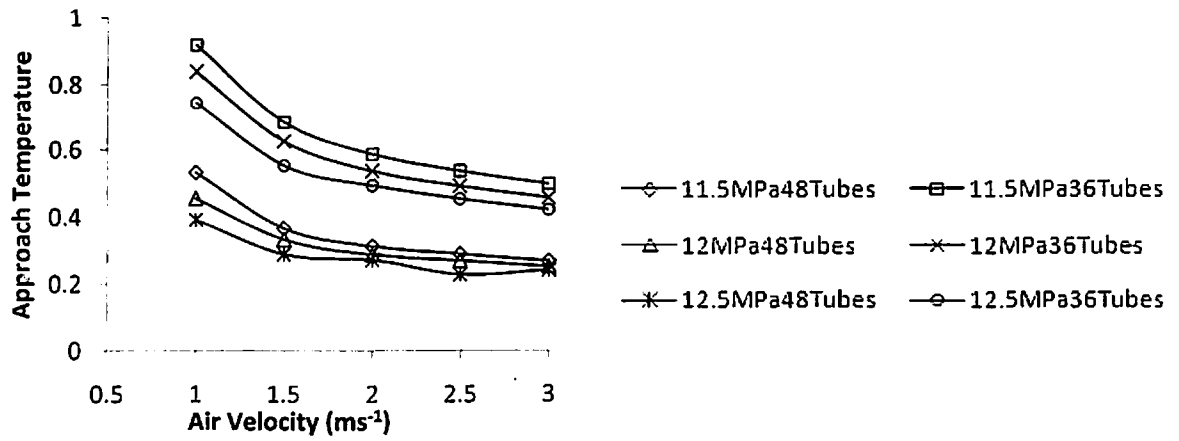
(d)



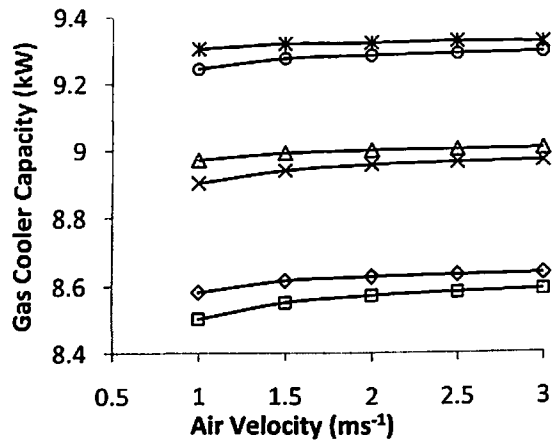
(e)

Figure 6.11: Performance (*three pass*) of gas cooler and overall system at zone III

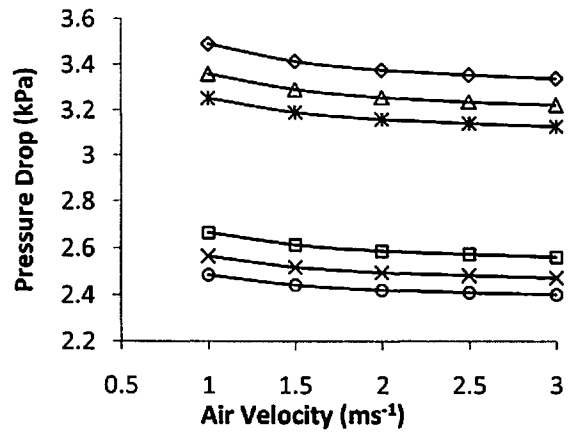
It is found that there are certain operating and design condition exists for each zone with the system using different gas cooler. The overall performance of two pass gas cooler are poor as compare to three pass and four pass gas cooler, however there is insignificant difference with three pass and four gas cooler.



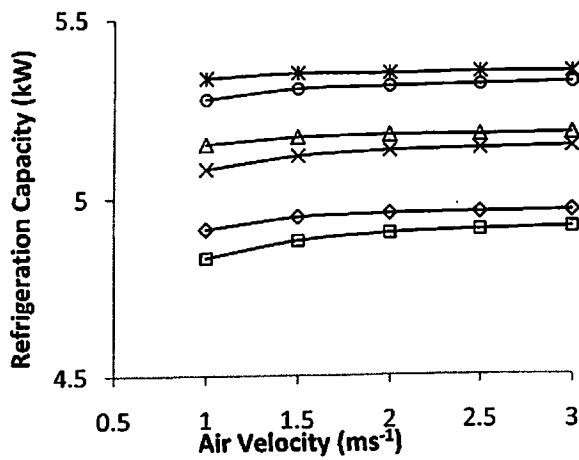
(a)



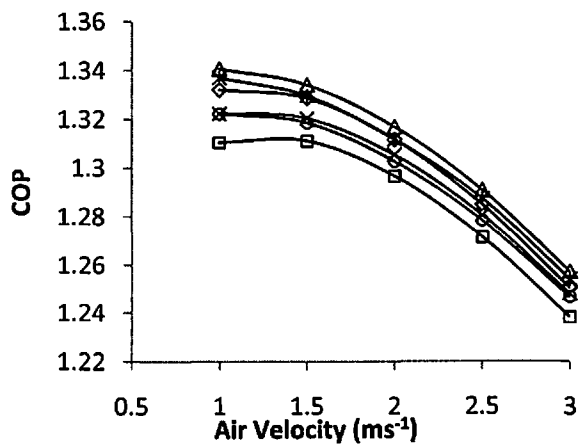
(b)



(c)



(d)



(e)

Figure 6.12: Performance of (four pass) gas cooler and overall system at zone III

6.3.2 Effect of compressor isentropic efficiency and evaporator temperature

In addition to the analysis of different design of gas cooler and the overall performance of the system using these gas cooler with different operating condition at different temperature zone, the effect of performance parameters of other components like compressor and evaporator etc. are also analyzed. In this section the effect of compressor isentropic efficiency (as 0.6, 0.7 and 0.8) and evaporator temperature (268K, 273K and 278K) on the performance are discussed at the optimum condition at which maximum COPs are achieved for each temperature zones with two, three and four pass gas coolers.

6.3.2.1 Two pass gas cooler

A comparison of the effect of evaporator temperatures and the compressor isentropic efficiencies on the performance of overall system with two pass gas cooler at temperature three temperature zones are shown in Fig. 6.13.

Fig. 6.13(a) shows the variation of compressor work with different evaporator temperatures and isentropic efficiencies at all three temperature zones. It is observed that with increase in evaporator temperature and isentropic efficiency reduces the compressor requirement of the system as expected. For each evaporator temperature and isentropic efficiency, compressor work is lowest for zone I, then zone II and then zone III.

The variation of refrigeration capacity with different evaporator temperatures and isentropic efficiencies at all three temperature zones are shown in Fig. 6.13(b). It is observed that for each temperature zone, the refrigeration capacities have insignificant variation with evaporator temperature and isentropic efficiency, However there is significant variations are found at zone I with evaporator temperature, even the variations negligible with isentropic efficiency. The magnitude of refrigeration capacities are decrease at higher temperature zones.

Fig. 6.13(c) depicts the variation of COP with different evaporator temperatures and isentropic efficiencies at all three temperature zones. It is observed that the COP of increases with increase in evaporator temperature and isentropic efficiency of the compressor at each temperature zone.

For each evaporator temperature and isentropic efficiency, COP is highest for zone I, then zone II and then zone III.

Fig. 6.13(d) shows the percentage of COP with respected to lowest evaporator temperature i.e. 268K to increment to 273K and 278K, and different isentropic efficiency at

three temperature zones. It is found that percentage change of COP with increment of 268K to 273K and 273K to 278K are almost same for each evaporator temperature at all zones.

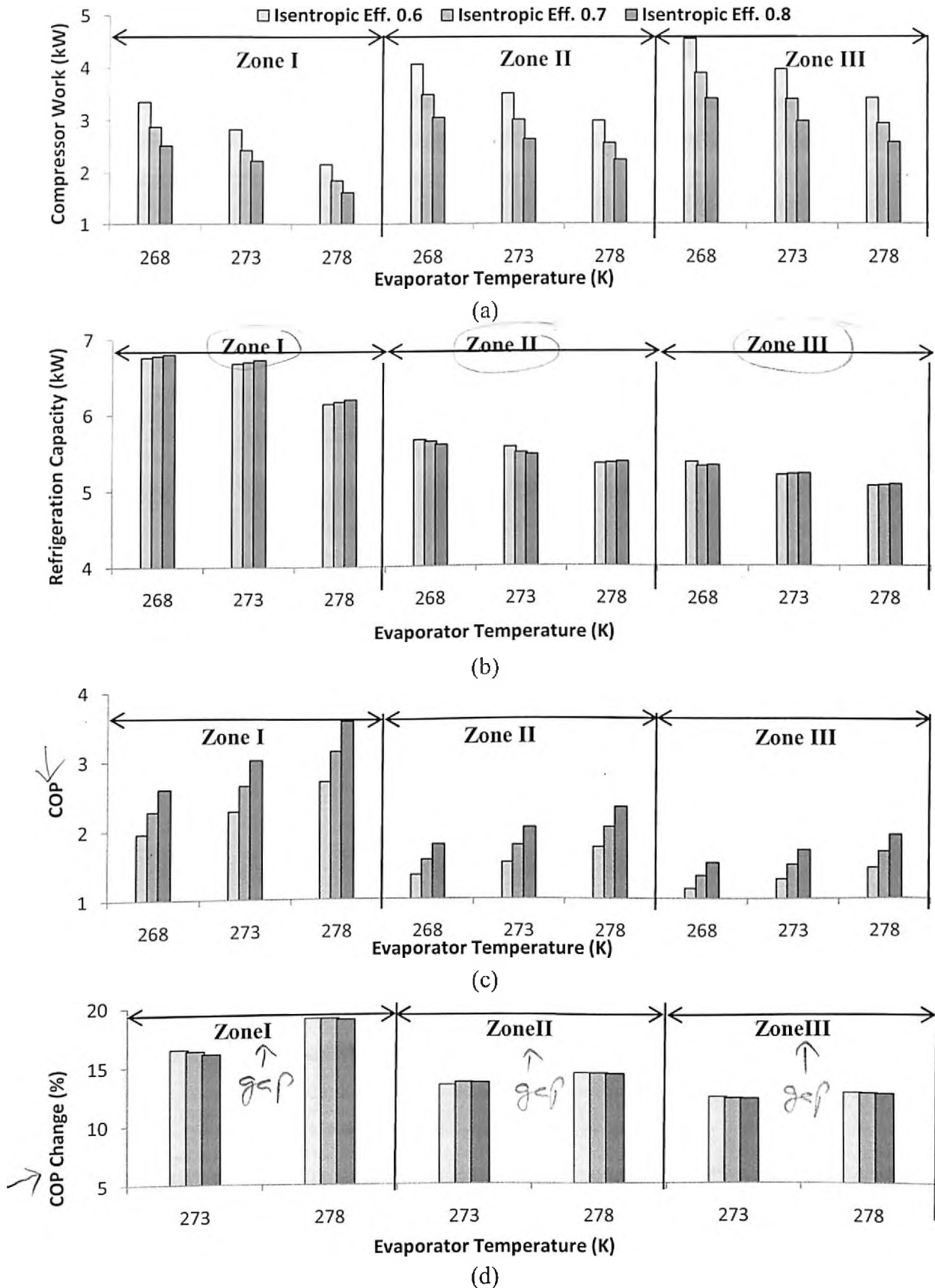
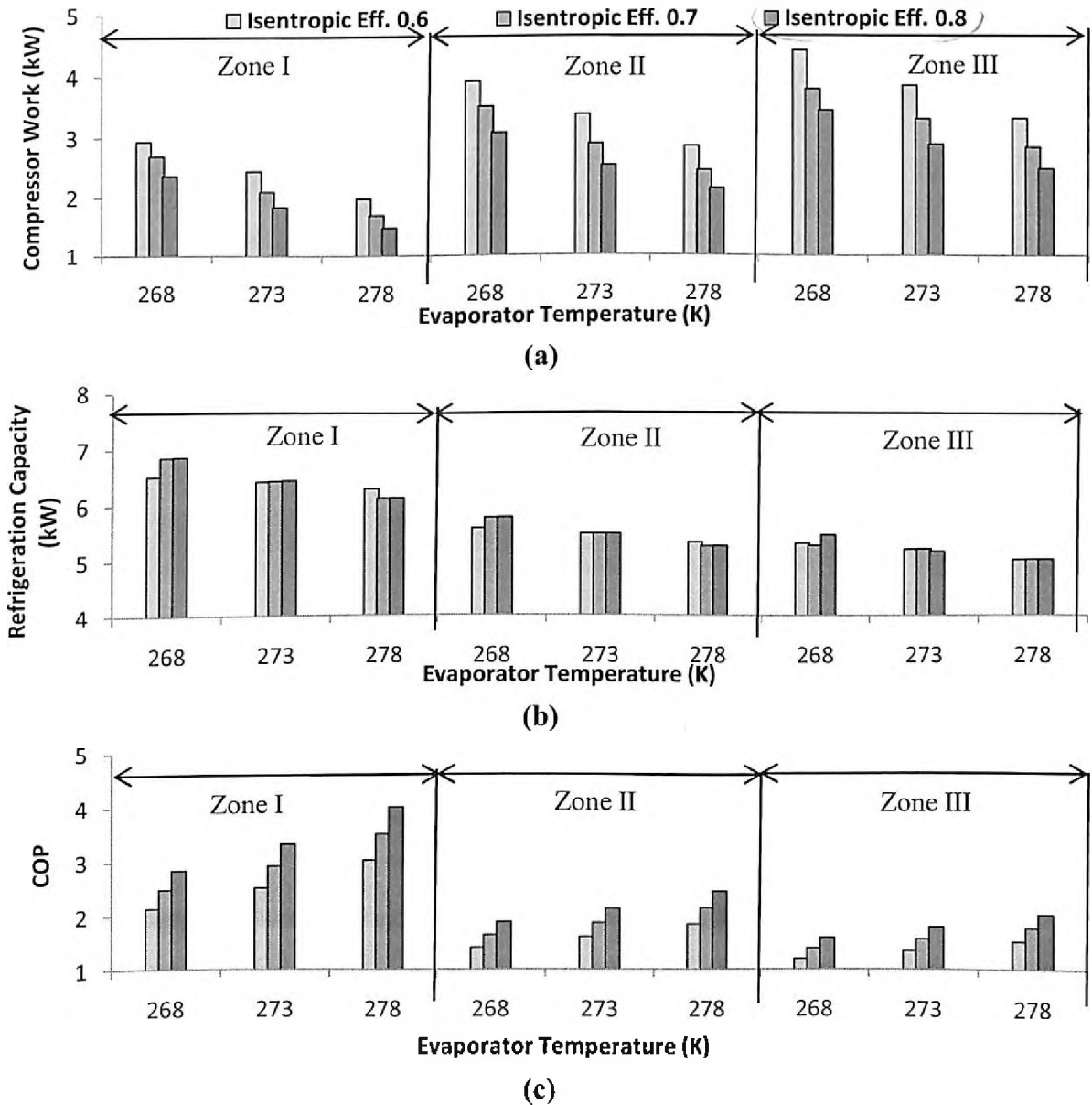


Figure 6.13: Comparison of performance of overall system with (two pass) gas cooler

It is observed that in zone II and zone III, rate of improvement is constant with evaporator temperatures, however in zone I, it has slightly more increment at higher evaporator temperatures. It is due the thermo-physical properties of CO₂ above critical point, as the system need to operate at high supercritical range for zone II and zone III. Poor performance of two pass gas cooler as discussed in sub section 6.3.1 may also be one of the reason for above differences. Moreover, it is found that the evaporator temperature has significant effect on the system COP.

6.3.2.2 Three pass gas cooler

A comparative analysis to see the effect of evaporator temperatures and the compressor isentropic efficiencies on the performance of overall system with three pass gas cooler at temperature three temperature zones are shown in Fig. 6.14.



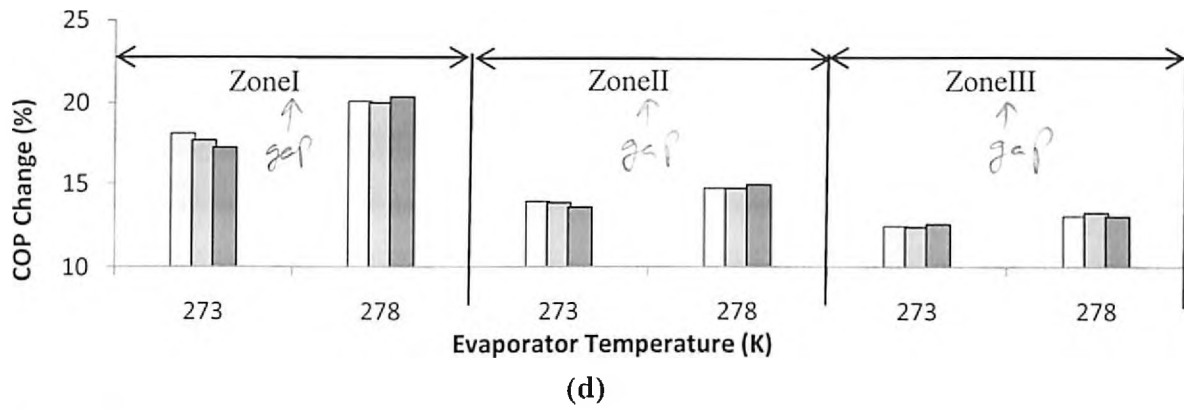


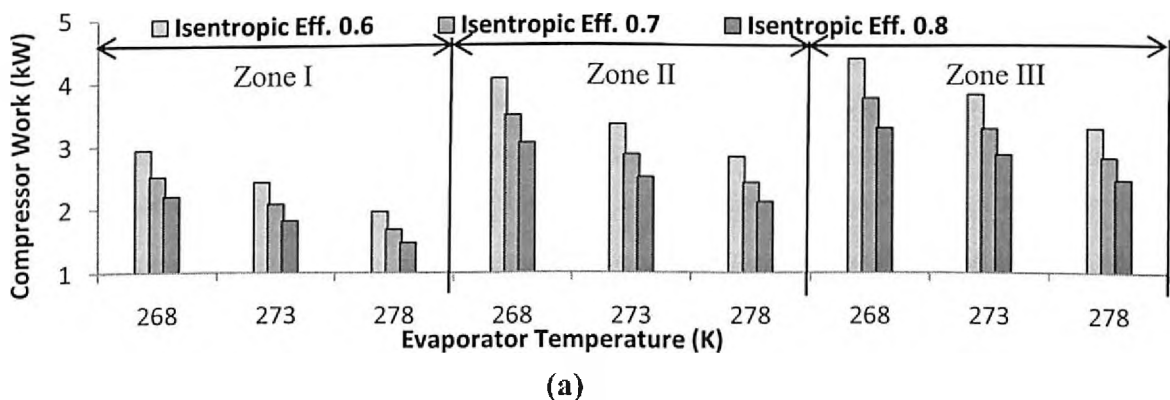
Figure 6.14: Comparison of performance of overall system with (three pass) gas cooler

Similar trends as two pass gas cooler for compressor work, refrigeration capacity and COP are found. Comparing Fig. 6.13(d) and Fig. 6.14(d) it is observed that the COP improvement is significant at each zones, however at zone II and zone III, the variations rate are approximately constant with evaporator temperatures, and isentropic efficiency. The magnitude of these results are more favorable with three pass as compare to two pass gas cooler.

6.3.2.3 Four pass gas cooler

A comparative analysis to see the effect of evaporator temperatures and the compressor isentropic efficiencies on the performance of overall system with four pass gas cooler at temperature three temperature zones are shown in Fig. 6.15.

Again as two pass and three pass gas cooler, the similar trends of compressor work, refrigeration capacity and COP are found with four pass cooler. Magnitude of these performance results are significantly differ from the system using two pass gas cooler but insignificant deference from the system using three pass cooler at each zones.



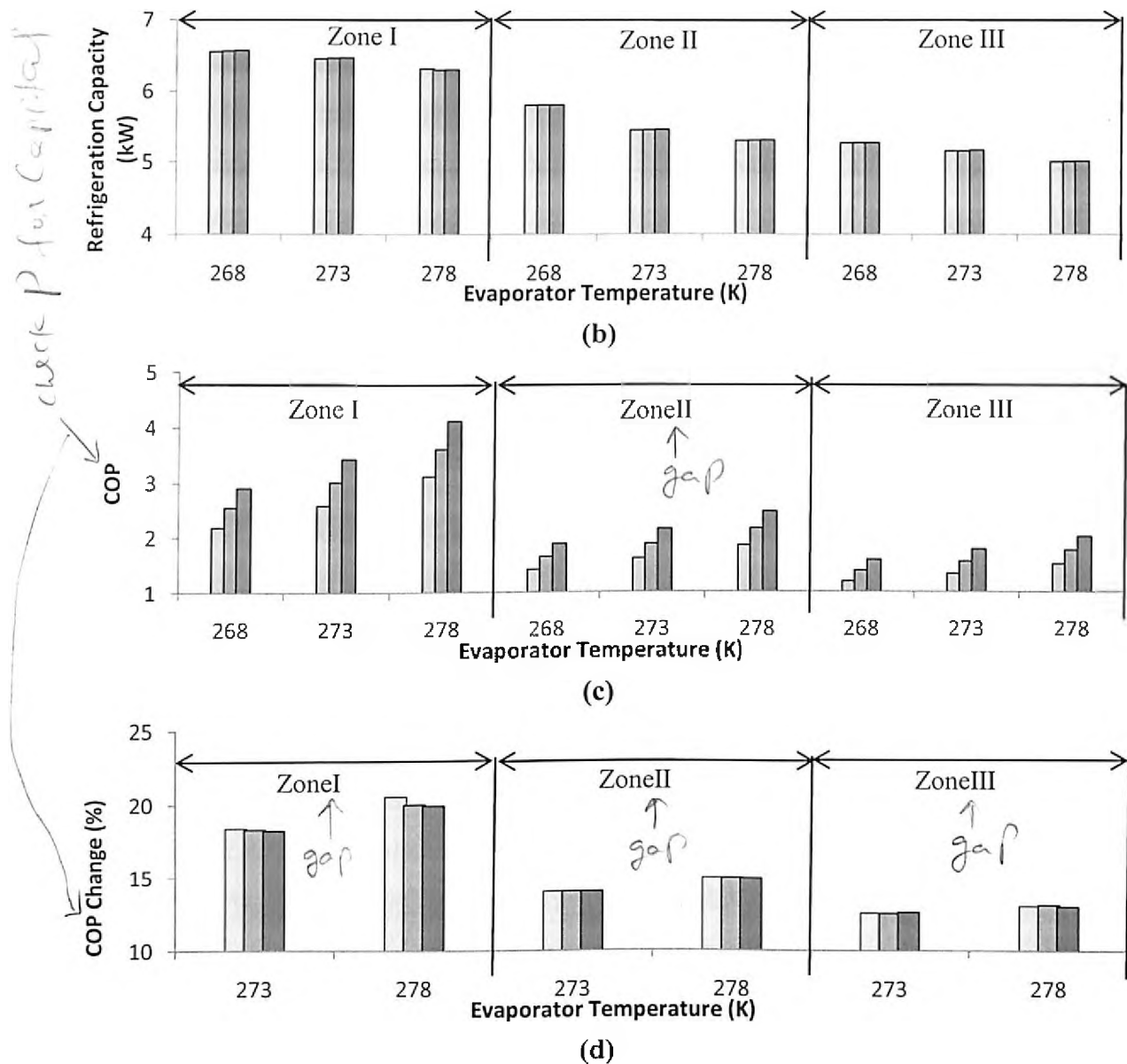


Figure 6.15: Comparison of performance of overall system with (four pass) gas cooler

It is due the performance of two pass and three pass gas cooler are very closed to each other as discussed in subsection 6.3.1.3. The performance improvement rate with evaporator temperature are approximately constant for zone II and zone III, however it has some significantly different in zone I. The above results and discussion in this subsection indicate that higher isentropic efficiency and evaporator temperature, leads to higher performance of the system, however there are always practical limitations like desire temperature based on the application of the system and the design of the compressor to achieve higher isentropic efficiency.

In this chapter of the thesis, the performance of gas cooler and overall system using respective gas cooler are analyzed at three temperature zones in Indian conditions. Further an attempt is made to optimize the gas cooler design and various operating conditions to achieve the best possible performance of the overall system. The optimum gas cooler design and operating conditions have been used to further analyze the effect of compressor isentropic efficiency and evaporator temperature on the system performance.

It is found that two pass gas cooler performances are poor, hence the system performances using two pass gas cooler are inferior. Three pass and four pass gas cooler have better performance as compare to two pass, however three pass and four pass gas cooler have approximately similar performance results, therefore the system performances are also similar in these two gas cooler and the overall system using these gas cooler. As for as the selection of gas cooler is concern, three pass or four pass can be selected for the equal performance. The list of optimum design and operating conditions with their performance results are given in Appendix A.

Since the COP of the overall system is still lower after the optimization of gas cooler design and operating condition, it is required to modified the system to improve the performance. In next chapter, a steady is made with modified system.

Study

modified
system is
studied

Performance of CO₂ Trans-Critical Refrigeration System with work recovery Turbine

In previous chapter an attempt was made to optimizing the gas cooler design and operating parameters to achieve best possible performance of gas cooler and overall system considering fan power consumption. Mathematical model was modified to include the fan power consumption, and the simulation based studies are carried out with several modifications of gas cooler geometry, its flow arrangement, and operating conditions. The result shows that the overall performance of the system is low and still need improvement. In this chapter a simulation based study with modified system is carried out to further analyze the performance of the gas cooler and overall system, including a work recovery turbine.

There are many modifications feasible in the basic trans-critical CO₂ cycle to improve the performance and to adopt the conditions as per requirements and applications. A few studies that have reviewed multiple suggested modifications to improve system performance are Lorentzen (1994), Kim ~~MH~~ et al. (2004)^b, and Sarkar (2010). Research progress related to such modifications are summarized in chapter 2 in section 2.3.

Sarkar (2010) made a comparative study on the performance improvement with six possible modifications in the system. Due to the trans-critical nature of CO₂ refrigeration cycle, there are significantly higher expansion losses compared to that of conventional system. therefore, the various cycle modifications such as multi-staging, internal heat exchanger, expansion turbine, ejector and vortex tube can be incorporated to improve the system performance. Fig. 7.1 shows the reported possible improvement percentage using various modifications. Study results indicate that the highest improvement of the trans-critical CO₂ vapor compression cycle can be achieved by replacing the expansion device with a work recovery expansion machine or by using multi-staging. The optimum high side pressure in case of using work recovery turbine or

check whether
2004a
or
2004b

multi-staging is lower compared to that of other modifications as shown in Fig. 7.2. These are cost intensive improvement compared to others and more effective at higher temperature environment.

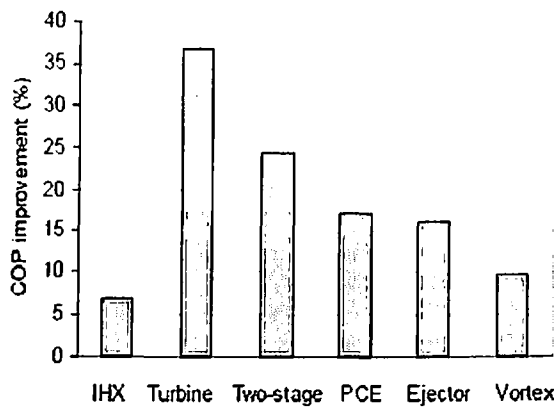
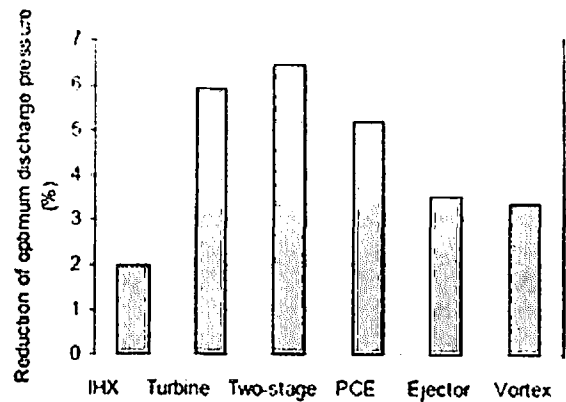


Figure 7.1: Improvement in COP with modification (Sarkar, 2010)



Figures 7.2: Reduction in optimum operating pressure with modification (Sarkar, 2010)

Based on the above data, expansion with work recovery turbine is selected for the study and further the performances of the system is analyzed to find the optimum design of gas cooler and operating condition for best possible COP with modified system. The simulation results at different temperature zones in India conditions are discussed in subsequent sections of this chapter.

7.1 Selection of Input Combinations of Geometric and Operating parameters

The simulation results discussed in chapter 6, two pass gas coolers have poorer performance and system using these gas cooler performances are inferior. It was also found that the performances of three and four pass gas cooler, and the system using these gas cooler are not significantly different. However, these results are better than two pass gas cooler and the system using two pass gas cooler. For all the optimum condition, gas coolers with 54 tubes has been found to have best performance and in some cases, performance of gas cooler with 45 tubes are comparable, but gas coolers with 36 tubes are always found to have poor performance. Therefore, for further analysis, two pass gas coolers and the gas coolers with 36 tubes are removed from the study.

If no of tubes higher than 54 considered then 45 tube likely to give worst performance among them. Is this statement correct?

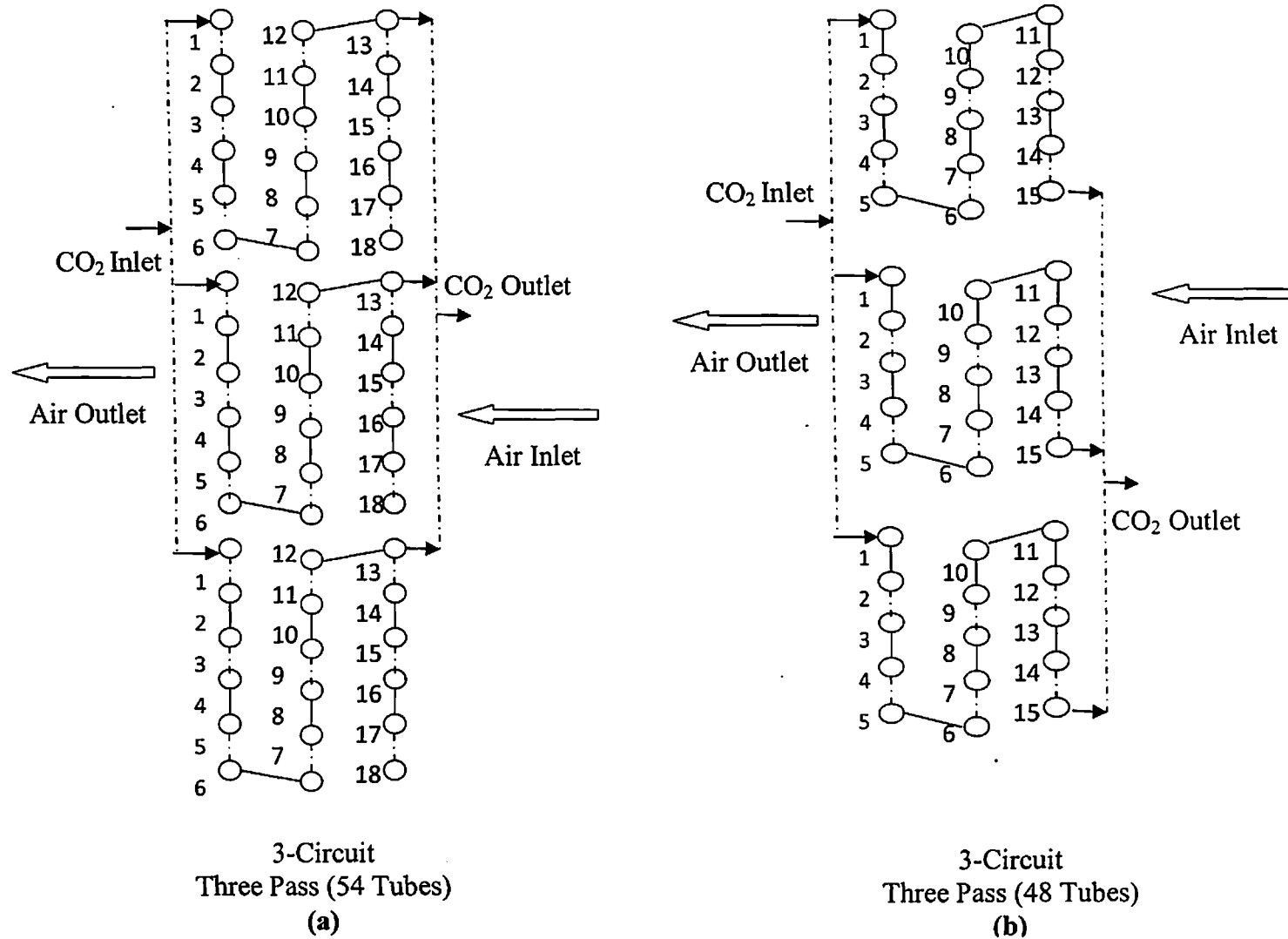


Fig. 7.3 Modified geometry with different circuit arrangement of gas cooler

Further the study is extended for one step lower operating pressure to accommodate the use of work recovery turbine as expansion device. The operating pressure reduces when work recovery turbine used as per the literature (Sarkar 2010). Only three pass gas coolers are consider for further analysis as the model is already validated for three pass gas cooler. Circuit design of gas coolers are shown in Fig. 7.3, and number of input combinations are now refined for each temperature zones and the ranges of input parameters are summarized in Table 7.1.

Table 7.1: Modified operating conditions and simulation parameters for optimization

Parameters	Operating Pressure (MPa)	Air Velocities (ms ⁻¹)	3 pass (Tubes)
Zone I	7.5	1	54
	8	1.5	45
	8.5	2	
	9		
Zone II	9.5	1	54
	10	1.5	45
	10.5	2	
	11		
Zone III	11	1	54
	11.5	1.5	45
	12	2	
	12.5		

It is to be noted that the overall system performance falls with increase in air velocity for all conditions hence higher range of the air velocities beyond 2 ms⁻¹ have not been taken for this study. Pressure drop between compressor discharge and gas cooler inlet is neglected, evaporator pressure is taken as constant for maintaining 0°C evaporator temperature and mass flow rate of refrigerant is taken as 0.045 kg s⁻¹, which is within the validated range.

7.2 Model Application

The mathematical model that was developed and validated in chapter 4, and extended for the performance of overall system including fan power consumption in chapter 5 and 6 are utilized for exploring application of work recovery turbine. Using the updated model, the refrigeration capacity in kW, compressor work in kW, and COP of the overall system is computed. The model is represented mathematically in Eq. 6.1 to Eq. 6.4. Fan power consumption is calculated assuming 90% fan efficiency using Eq. 6.3. The net

What is the basis for this assumption?

compressor work in modified system is calculated as the difference of compressor and turbine work. The set equations are;

$$W_{\text{comp}} = \frac{\{H_{\text{rco}}(P_{\text{co}}, T_{\text{co}}) - H_{\text{rci}}\}}{\eta_{\text{isen}}} \quad (6.1)$$

$$RE = \{H_{\text{reo}} - H_{\text{rei}}(P_{\text{gco}}, T_{\text{gco}})\} \quad (6.2)$$

$$W_{\text{fan}} = \frac{\dot{Q}_v \Delta P_{\text{air}}}{\eta_{\text{fan}}} \quad (6.3)$$

$$W_{\text{Turbine}} = \{H_{\text{rco}}(P_{\text{co}}, T_{\text{co}}) - H_{\text{rei}}(P_{\text{ei}}, T_{\text{ei}})\} \eta_{\text{isen}, T} \quad (6.4)$$

$$COP = \frac{\{H_{\text{reo}} - H_{\text{rei}}(P_{\text{gco}}, T_{\text{gco}})\}}{\frac{\{H_{\text{rco}}(P_{\text{co}}, T_{\text{co}}) - H_{\text{rci}}\}}{\eta_{\text{isen}}} + \frac{\dot{Q}_v \Delta P_{\text{air}}}{\eta_{\text{fan}}} - \{H_{\text{rco}}(P_{\text{co}}, T_{\text{co}}) - H_{\text{rei}}(P_{\text{ei}}, T_{\text{ei}})\} \eta_{\text{isen}, T}} \quad (6.5)$$

where, H is function of P and T , and enthalpy at gas cooler outlet is equal to the enthalpy at evaporator inlet. Using the above steady state model, performances of the system is analyzed for different operating and geometric conditions for different temperature zones and selected combinations of the model input parameters.

7.3 Results and Discussion

The performance of gas cooler using the validated model from chapter 4 and using above modified extended model, study is carried out for overall system performance with respective gas cooler. The various combinations of input parameters are as given in Table 6.1. The results are shown and discussed subsequently for all three temperature zones in Indian climatic conditions (assuming isentropic efficiency of 0.6 for compressor and turbine).

include references to support this assumption

7.3.1 Performance of trans-critical CO₂ refrigeration system

Fig. 7.4 to Fig. 7.6 shows performance of gas cooler and overall system at temperature zone I, zone II and zone III respectively. Gas cooler approach temperature and pressure drop variation, and the variation of refrigeration capacity, compressor and COP of the overall system are analyzed at different operating and gas cooler design conditions. Finally, percentage improvement of COP with work recovery turbine is compared to that without turbine.

7.3.1.1 Temperature zone I

Fig. 7.4 shows the simulation results at temperature zone I with the variation in air velocity, for different operating conditions and gas cooler design. Fig. 7.4(a) depicts the variation of approach temperature, with air velocity at operating conditions and gas cooler design. It is observed that approach temperature decreases with increase in air velocity for each conditions and at each air velocity, there are mixed variation depending on the operating pressure and number of tubes. It is due to the fact that at higher operating pressure, there is large temperature gradient whereas the gas cooler with large number of tubes has more surface area available for heat transfer.

as
→ Job
It is to be note that ^{the} ~~The~~ value of approach temperatures is significantly higher at this temperature zone, Fig. 7.4(b) shows the variation of pressure drop in gas cooler, it is observed that the pressure drop is slightly reduced with increase in air velocity and it is higher for large size gas cooler (i.e. 54 tubes) and at lower range of operating pressure. It is due to a similar reason that large size of gas cooler have more surface area whereas at lower operating pressure, the refrigerant velocity is lower. Fig. 7.4(c) shows the variation of refrigeration capacity, it is found that the refrigeration capacity is highest at the conditions where approach temperature is lowest. It has upward trends with air velocity, however these variations are insignificant at higher operating pressure. Refrigeration capacity variations are found to be dependent more on pressure instead of gas cooler size at each air velocity, further effect of pressure also reduce^d at higher operating pressure.

Fig. 7.4(d) shows the variation of compressor work, it is observed that compressor work mainly depends upon operating pressure and weakly depends on air velocities. The work increases with increase in operating pressure and air velocities. It was discussed in chapter 6 (section 6.3.1) that for simple system, compressor work is independent of air velocity, however in modified system with work recovery turbine, small variation with air velocity is observed. It is due to the fact that air velocity affect the gas cooler exit conditions which in term affect the turbine performance.

turb

Compressor Efficiency = 0.6 Turbine Efficiency = 0.6 Evaporator Temperature = 273.15K

◇ 7.5MPa 54Tubes □ 7.5MPa 45Tubes △ 8MPa 54Tubes × 8MPa 45Tubes
 * 8.5MPa 54Tubes ○ 8.5MPa 45Tubes + 9MPa 54Tubes ● 9MPa 45Tubes

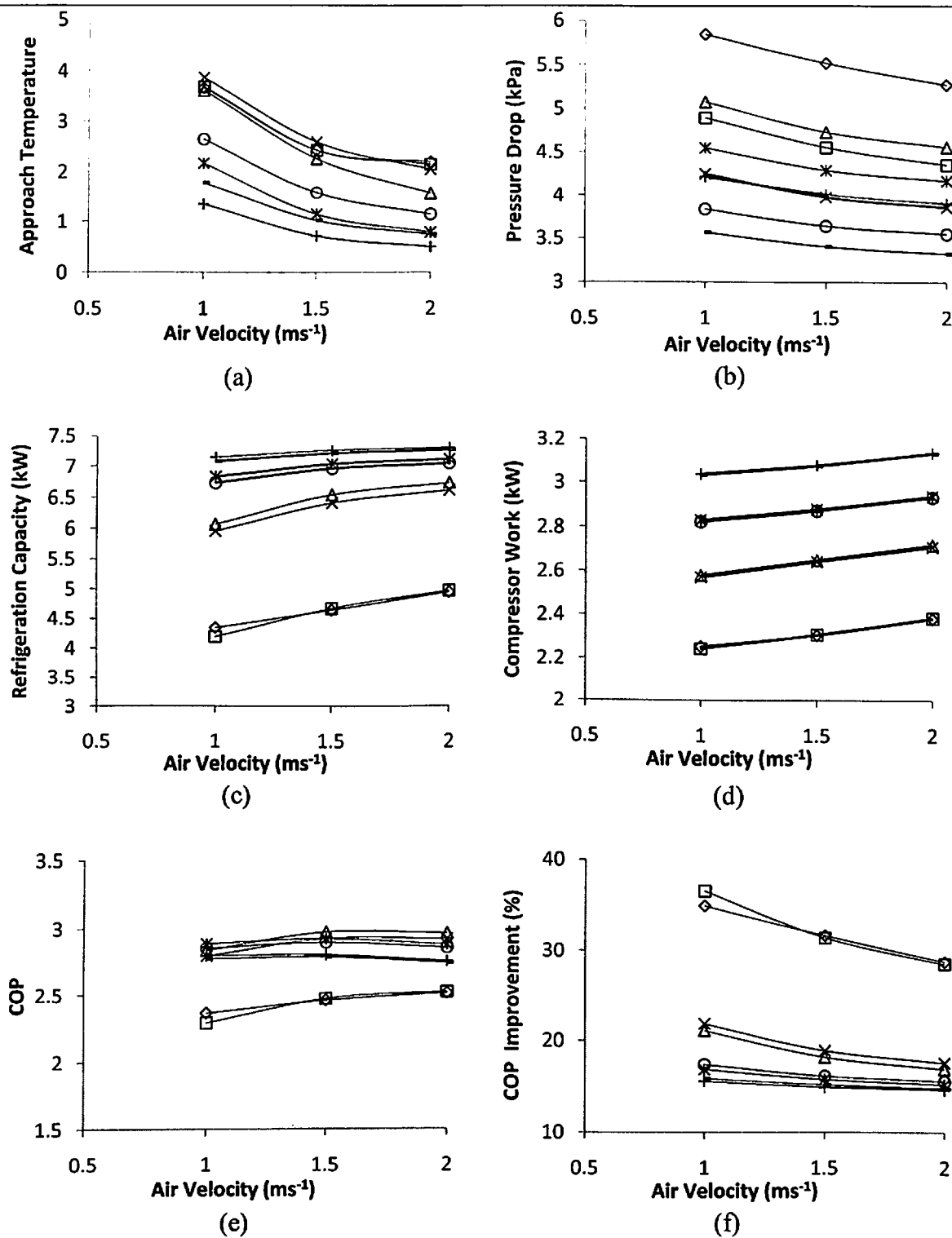


Figure 7.4: Performance of gas cooler and overall system with expander expansion at zone I

The cumulative effect of the above results are plotted as COP of the system and its variation is shown in Fig. 7.4(e). It is observed that the COP has significant variation with operating pressure and gas cooler designs whereas insignificant variation with air velocities. The optimum condition for the best COP at zone I is found to be with 8MPa operating pressure, 2 ms⁻¹ air velocity and 54 tubes in gas cooler. Further, the percentage improvement of COP using work recovery turbine for expansion is plotted in Fig. 7.4(f). The highest improvement is found to be 37.78% at lower air velocity (1 ms⁻¹) and lower operating pressures (7.5MPa), however the maximum COP is not achieved at that condition. It is due to the fact that work produced by the turbine also depends on operating pressure. Therefore, while selecting the operating condition and design of gas cooler, the maximum COP condition will be preferred where the improvement is 17.8%.

7.3.1.2 Temperature zone II

Fig. 7.5 shows the simulation results at temperature zone II (i.e. ambient temperature 40°C) with air velocity for different operating conditions and gas cooler design. Overall there are trends as in zone I as shown in Fig. 7.5(a), however the value of approach temperatures are significantly lower at zone II and again the maximum approach temperature is obtained at lower pressure and air velocity where as minimum value is obtained at higher pressure and velocity. It is observed from Fig. 7.5(b) that the minimum pressure drop are at higher air velocity and operating pressure but the values of pressure at different conditions are lower as compare to zone I.

Fig. 7.5(c) and Fig. 7.5(d) show the variation of refrigeration capacity and net compressor work with air velocities and operating condition with various gas cooler design. Trends of these parameter variations are similar to zone I, however in zone II refrigeration capacity values are lower and net compressor work are higher, at the respective simulation conditions.

Fig. 7.5(e) shows the variation of COP with air velocities and operating condition with various gas cooler design. It is observed that there are significant variation of COP with air velocity and slightly uneven trends are observed with different operating and design conditions of gas cooler. The maximum COP is found at operating pressure 10.5MPa, air velocity 1.5 ms⁻¹ and gas cooler with 54 tubes.

Compressor Efficiency = 0.6 Turbine Efficiency = 0.6 Evaporator Temperature = 273.15K

◇ 9.5MPa 54Tubes □ 9.5MPa 45Tubes △ 10MPa 54Tubes × 10MPa 45Tubes
 * 10.5MPa 54Tubes ○ 10.5MPa 45Tubes + 11MPa 54Tubes ■ 11MPa 45Tubes

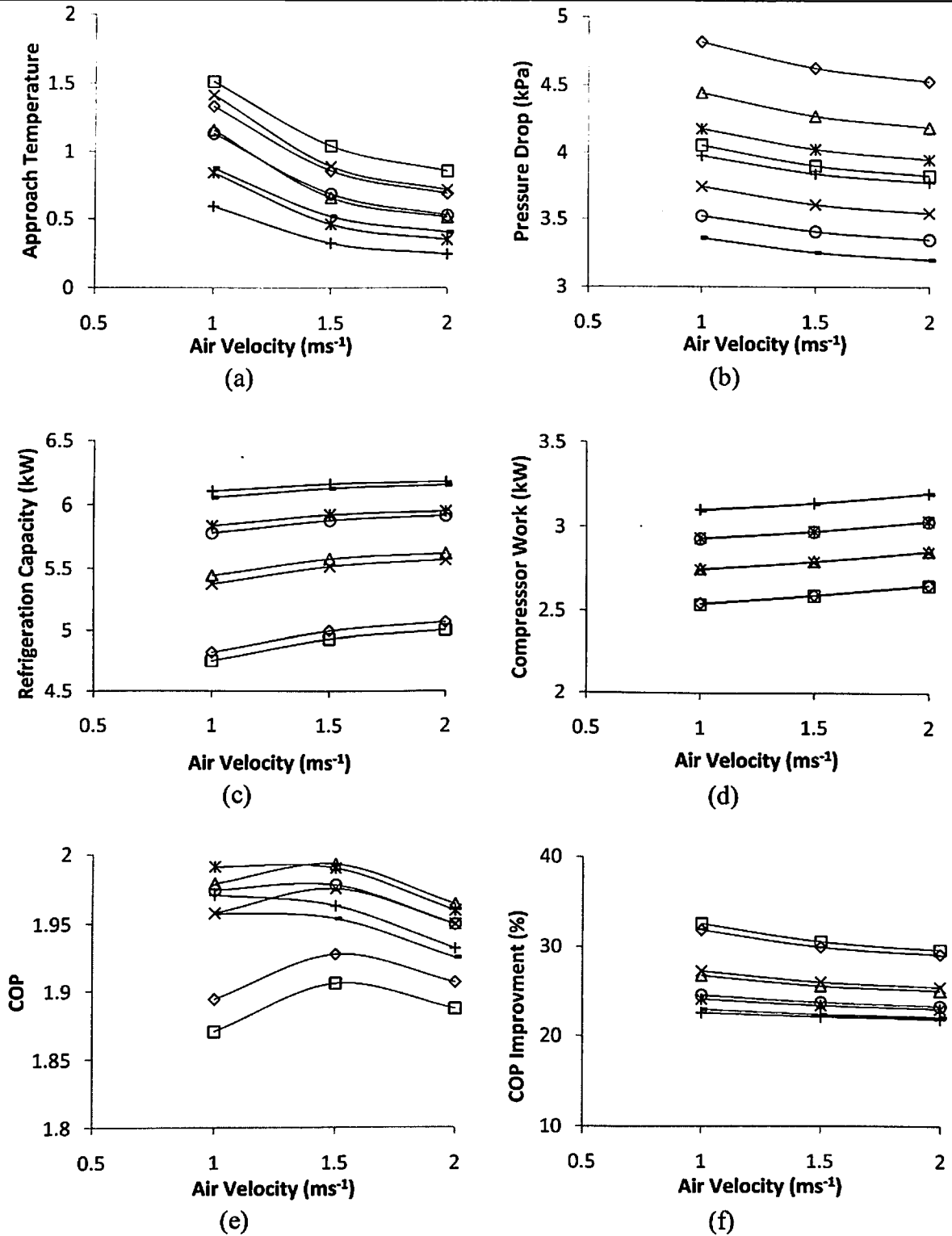


Figure 7.5: Performance of gas cooler and overall system with expander expansion at zone II

Further the COP improvements using work recovery turbine are plotted in Fig. 7.5(f), it is found that the maximum COP improvement achieved (i.e. 32.95%) at lower pressure 9.5MPa and velocity 1 ms⁻¹ with 54 tubes of gas cooler, however maximum COP condition is different where the improvement is 25.26%. Therefore for maximum COP condition is to be adopted even improvement rate is slightly lower than maximum.

Comparing with results from zone I and zone II, it is observed that the maximum improvement at zone I is higher than zone II. However, the improvement rate with optimum condition is more in zone II. Hence use of work recovery turbine as expansion device will be more effective at higher temperature zone.

7.3.1.3 Temperature zone III

Fig. 7.6 shows the simulation results at temperature zone III (i.e. ambient temperature 45°C) with air velocity for different operating conditions and gas cooler design. The trends are similar to that found in zone I and zone II as shown in Fig. 7.6(a), however the value of approach temperatures are significantly lower at zone III and again the maximum approach temperature is obtained at low pressure and air velocity where as minimum value is at higher pressure and velocity.

Fig. 7.6 (b, c, & d) shows the similar variation in trends, for pressure drop in gas cooler, refrigeration capacity, and the net compressor work respectively. The cumulative effect of these parameters are plotted in Fig. 7.6(e) as variation of overall COP system at zone III. It is observed that the COP has comparatively less variations with different conditions and maximum COP is achieved at operating pressure 11.5MPa, air velocity 1 ms⁻¹ with 54 tubes in gas cooler.

Fig. 7.6(f) shows the variation in COP improvement, it is found that maximum COP improvement (i.e. 31.10%) occurs at lower pressure and velocity conditions. However at the optimum condition the COP improvement is 28.13%, therefore the optimum condition should be adopted as maximum COP achieved at this condition. The percentage improvement in COP achieved at this zone is higher as compare to zone I and zone II.

Compressor Efficiency = 0.6 Turbine Efficiency = 0.6 Evaporator Temperature = 273.15K

◇ 11MPa 54Tubes □ 11MPa 45Tubes ▲ 11.5MPa 54Tubes × 11.5MPa 45Tubes
 * 12MPa 54Tubes ○ 12MPa 45Tubes + 12.5MPa 54Tubes — 12.5MPa 45Tubes

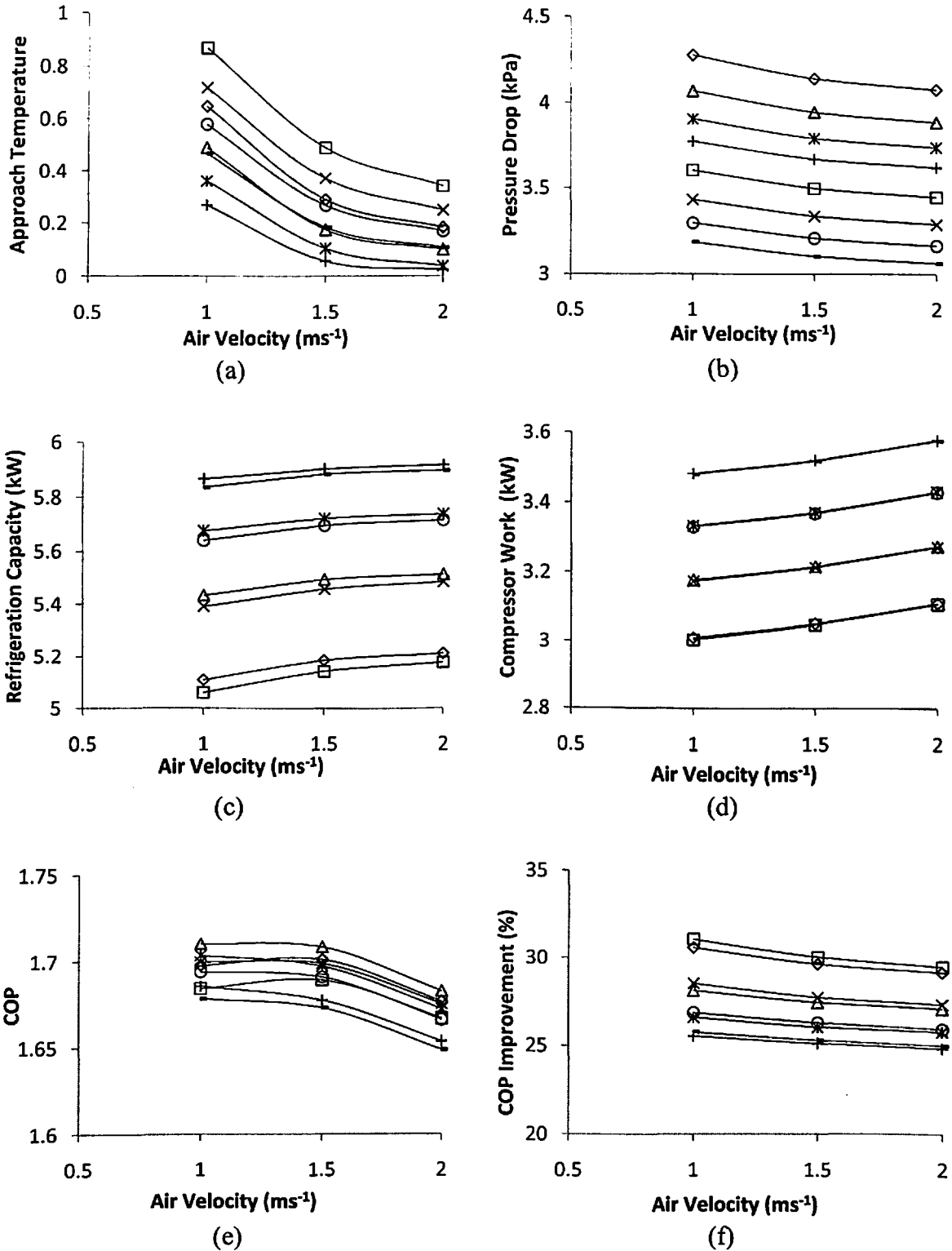


Figure 7.6: Performance of gas cooler and overall system with expander expansion at zone III

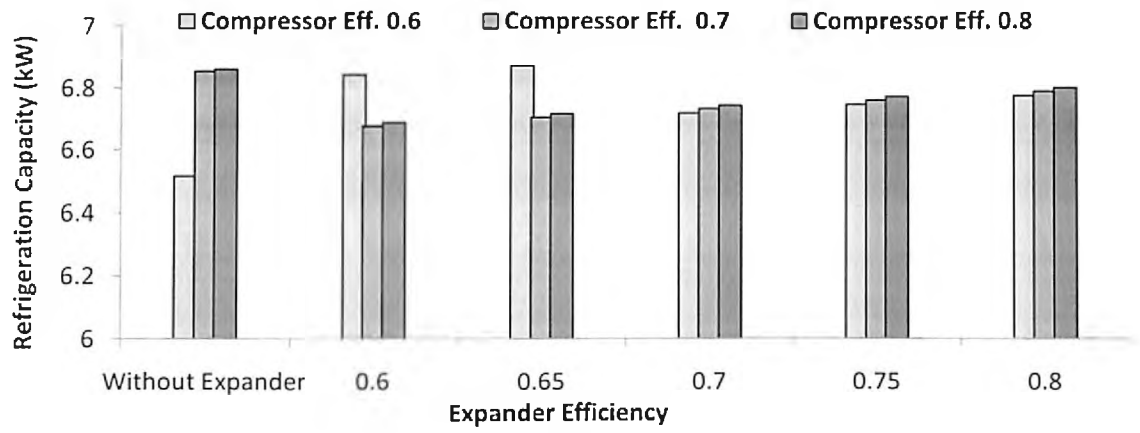
From the above discussion of simulation results, it is established that by using work recovery turbine, the COP of the system improves significantly. The maximum improvement among all temperature zones are found to be for a combination of lower operating pressure and lower temperature zone. However with optimum operating conditions, COP improvement is higher at higher temperature zones. These modification of the system reduces the optimum operating pressure, which is more prominent at higher temperature zones.

7.3.2 Effect of isentropic efficiency and evaporator temperature

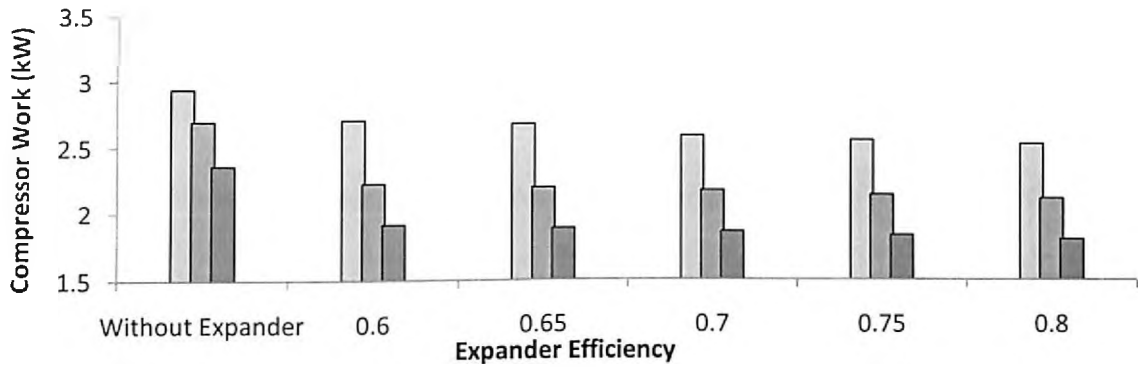
From the analysis of different design of gas cooler and the overall performance of the system using work recovery turbine as expansion device, the effect of isentropic efficiencies of turbine and compressor are kept constant. As discussed in chapter 6, system COP is effected by evaporator temperature. In these subsection the system performances are analyzed at different compressor and turbine isentropic efficiencies, and evaporator temperatures. In this analysis three level of compressor isentropic efficiencies (0.6, 0.7, and 0.8), turbine isentropic efficiencies (0.6, 0.65, 0.7, 0.75, and 0.8) and evaporator temperature (268K, 273K and 278K) are taken for all three temperature zones. All these results are shown for the optimum design and operating conditions as found in section 7.3.1. The comparisons are between the system with and without work recovery turbine.

7.3.2.1 Temperature zone I

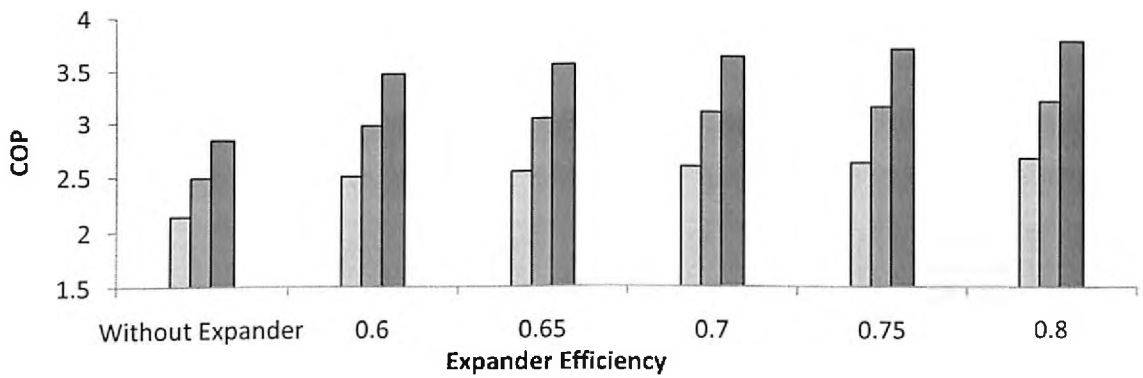
Fig. 7.7 - Fig. 7.9 shows the comparative results of overall system performance in terms of refrigeration capacity, net compressor work, COP and COP improvement at temperature zone I (i.e. ambient temperature 29.4°C) with evaporator temperature 268K, 273K and 278K respectively. All the results are plotted with expander efficiency at different compressor efficiency. Fig. 7.7(a) shows the variation of refrigeration capacity with expander isentropic efficiency at different isentropic efficiency of compressor. It is observed that, there are insignificant variation in refrigeration capacity. Fig. 7.7(b) shows the variation of net compression work. It is found that net compressor work decrease with increase in isentropic efficiency of the compressor for each value of turbine isentropic efficiency. This is due to the fact that compression losses are lower at higher efficiency. It is also found that there are small reduction of net compression work with increase in expander isentropic efficiency.



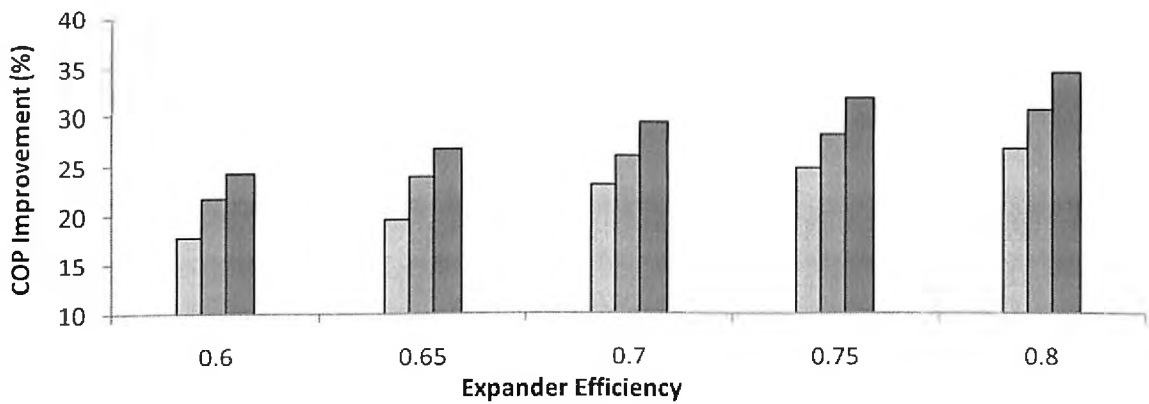
(a)



(b)



(c)



(d)

Figure 7.7: Performance of overall system at zone I (evaporator temperature 268K)

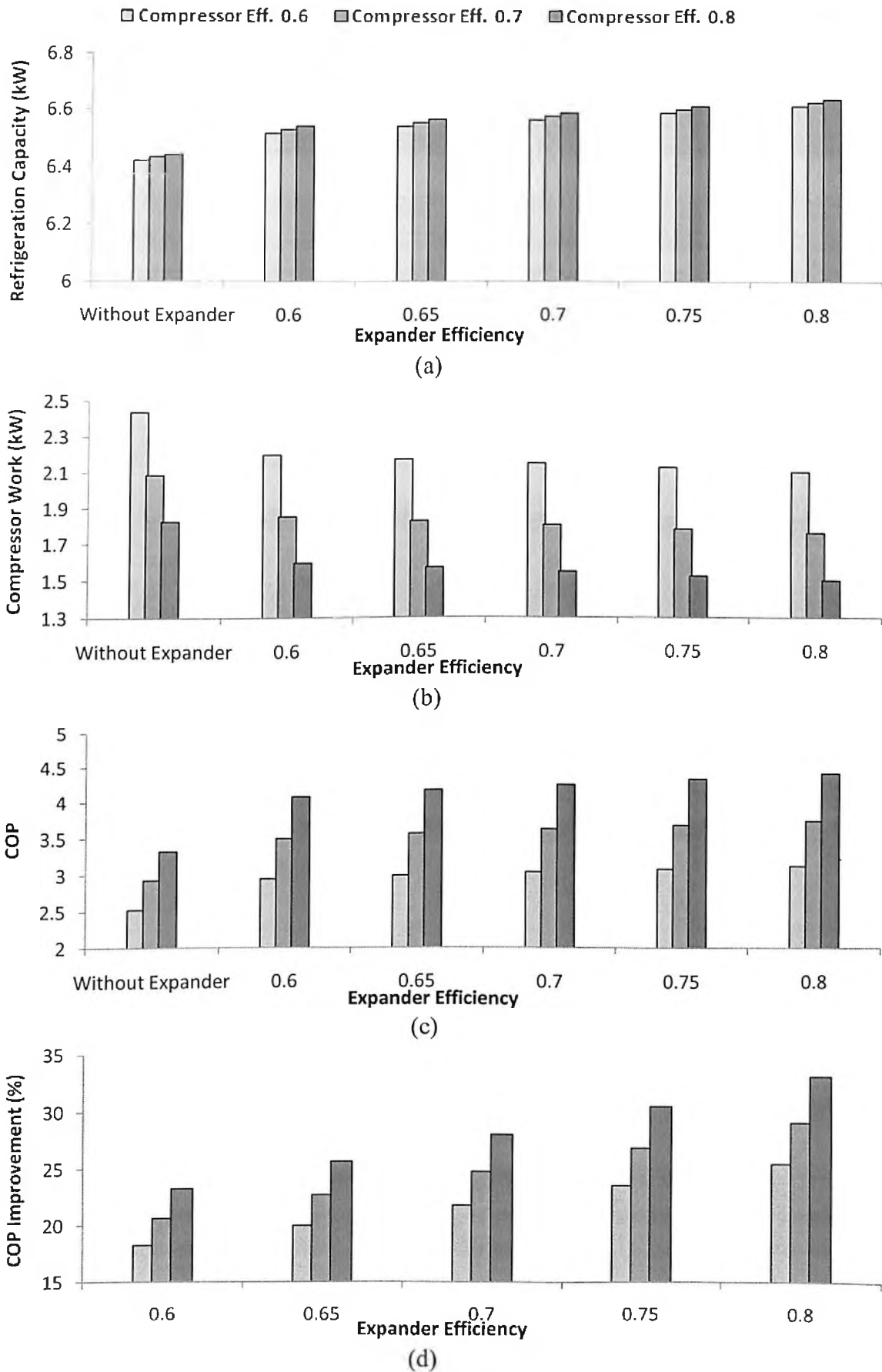


Figure 7.8: Performance of overall system at zone I (evaporator temperature 273K)

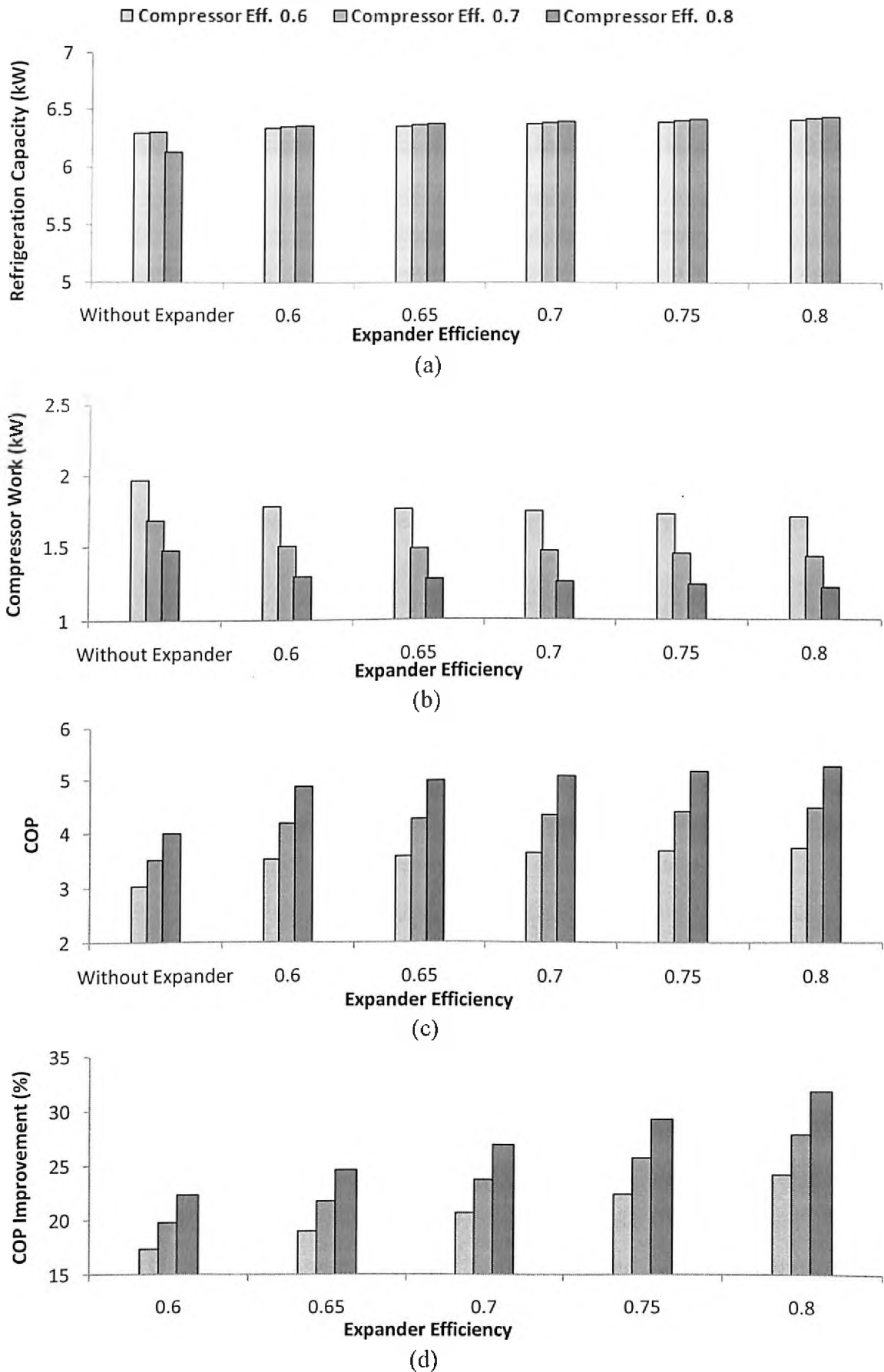


Figure 7.9: Performance of overall system at zone I (evaporator temperature 278K)

The cumulative effect of above two parameters are shown in Fig. 7.7(c) on COP of the system. It is observed that COP increases significantly with work recovery turbine, further it is found that COP increase with increase in compressor isentropic efficiency at each value of expander efficiency. It is also observed that at each value of compressor efficiency, the COP increase is small for increase in expander efficiency. It is due to the fact that variation of COP ^{is} depends mainly on the net compression work, as the variation of refrigeration capacity is relatively smaller.

Fig. 7.7(d) shows the percentage improvement of COP as compare^d to the system without work recovery turbine, where it is observed that COP improvement increases significantly with both compressor and turbine isentropic efficiencies. However these rate of increment decrease with increase in compressor and turbine isentropic efficiencies, it is because higher compressor isentropic efficiency has low operating pressure which reduces the work recovery in turbines.

The similar analysis is presented in Fig. 7.8 and Fig. 7.9, maintaining evaporator temperature as 273K and 278K respectively at temperature zone I. It is found that the performance parameters has similar variation trends like that found when evaporator temperature is maintained as 268K. However form Fig. 7.7 - Fig. 7.9(c & d) it is observed that the value of COP increases with increase in evaporator temperatures and the rate of improvement slightly decrease with the evaporator temperature at each simulation conditions. It is due the fact that the effect of evaporator temperatures are comparatively more prominent without expander. The detail of the performance results and their optimum conditions for zone I are shown in Appendix B with maintaining evaporator temperatures 268K, 273K and 278K respectively.

7.3.2.2 Temperature zone II

Fig. 7.10 - Fig. 7.12 shows the comparative results of overall system performance in terms of refrigeration capacity, net compressor work, COP and COP improvement at temperature zone II with evaporator temperature 268K, 273K and 278K respectively. All the results are plotted with expander efficiency at different compressor efficiency.

Small variation on refrigeration capacity with isentropic efficiencies of compressor and turbine at optimum operating conditions for 268K evaporator

temperature is as shown in Fig. 7.10(a), and Fig. 7.10(b) shows the net compressor work, which has significantly variation with the isentropic efficiencies. Therefore, the COP variation mainly depends on the compressor work as shown in Fig. 7.10(c), it is observed that similar to zone I, COP varies significantly with compressor isentropic efficiency and comparatively less with expander efficiency. Further, percentage improvement of COP as compare to the system without work recovery turbine as expansion are shown in Fig. 7.10(d), it is found that increment of COP is higher at higher isentropic efficiency of both compressor and turbine, these rate of improvement is more significant as compare to zone I, however the COP values at all the respective simulation conditions are lower as compare to zone I. Now the analysis is further extended for evaporator temperatures 273K and 278K.

Fig. 7.11 and Fig. 7.12 shows the performance results of the overall system with maintaining evaporator temperature 273K and 278K respectively at zone II. It is observed that refrigeration capacities have again insignificant variation as shown in Fig. 7.11(a) and Fig. 7.12(a). The net compressor work reduces with increase in evaporator temperature and compressor isentropic efficiency at each value of expander efficiency as shown in Fig. 7.11(b) and Fig. 7.12(b).

However these variations are small with expander efficiencies. The magnitude of these net compression work are found to be higher as compare to zone I at each respective simulation conditions. It is due to the fact that the optimum pressures for zone II are significantly higher than zone I.

Fig. 7.11(c) and Fig. 7.12(c) depict COP of the system and it is found that ~~it~~ COP increases significantly with increase in compressor efficiencies but only slightly increase with increase in expander isentropic efficiency. The value of COP also increase with increase in evaporator temperatures at each simulation conditions. However, these increment are more prominent at lower evaporator temperatures.

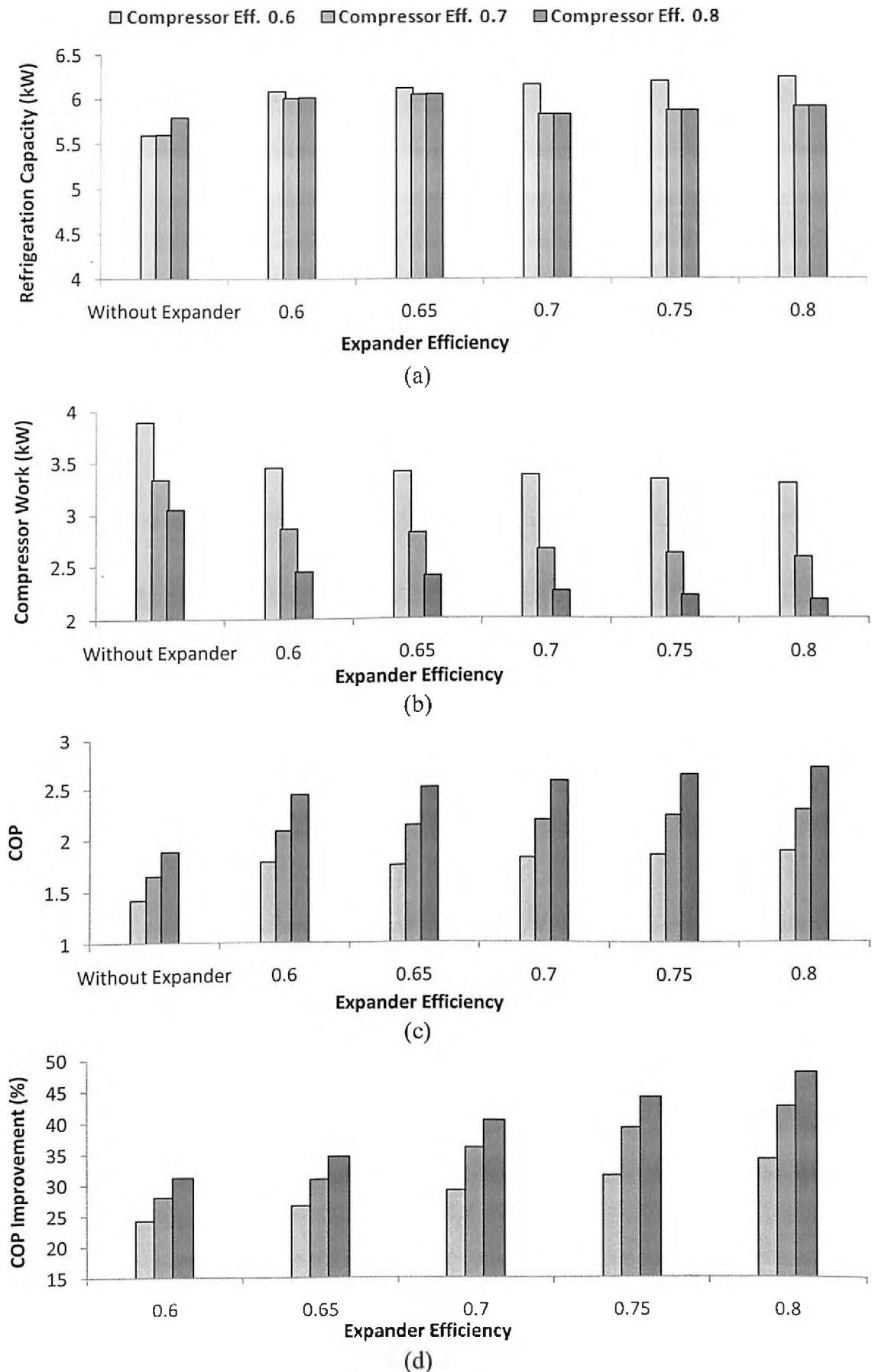


Figure 7.10: Performance of overall system at zone II (evaporator temperature 268K)

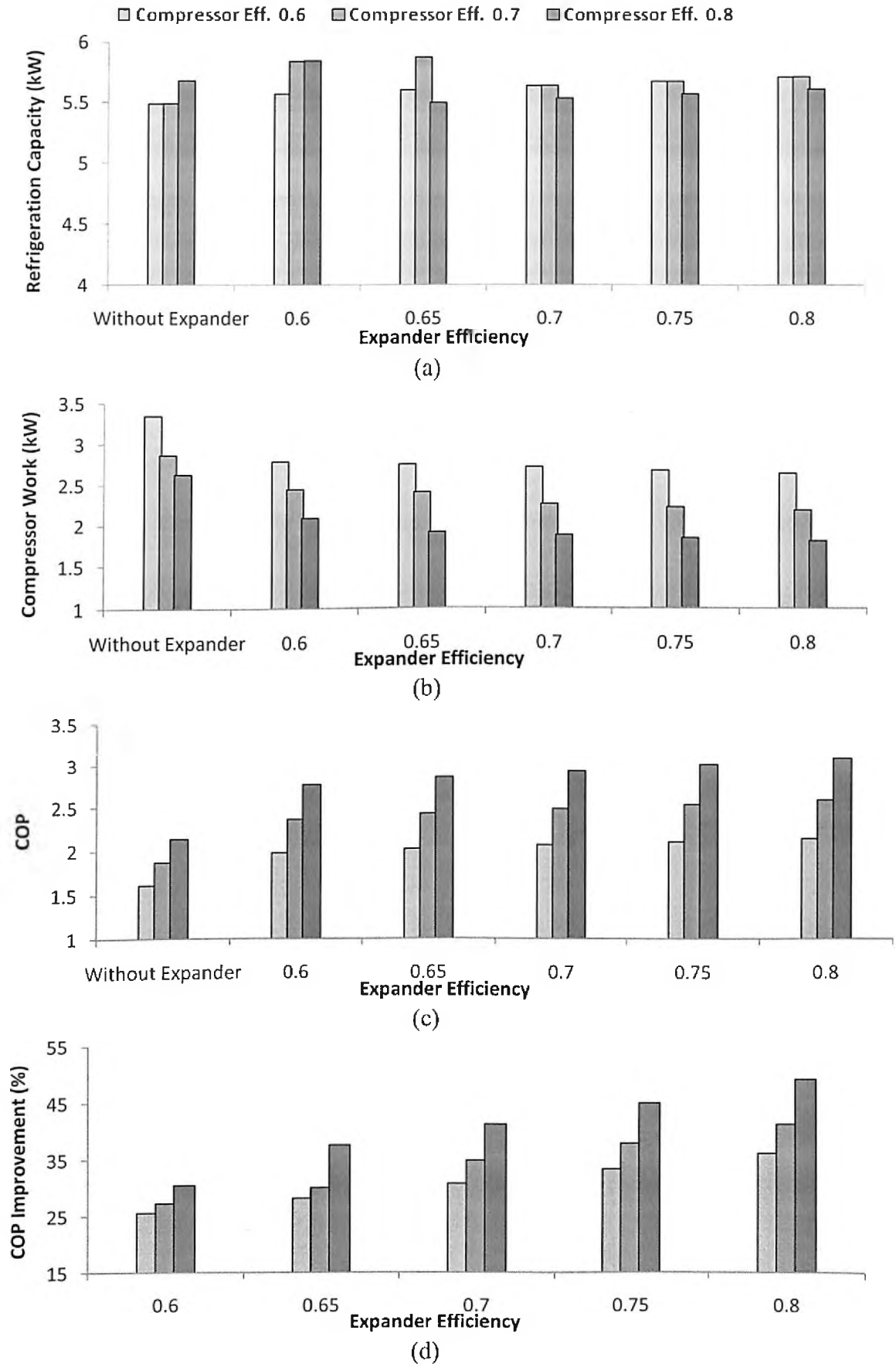


Figure 7.11: Performance of overall system at zone II (evaporator temperature 273K)

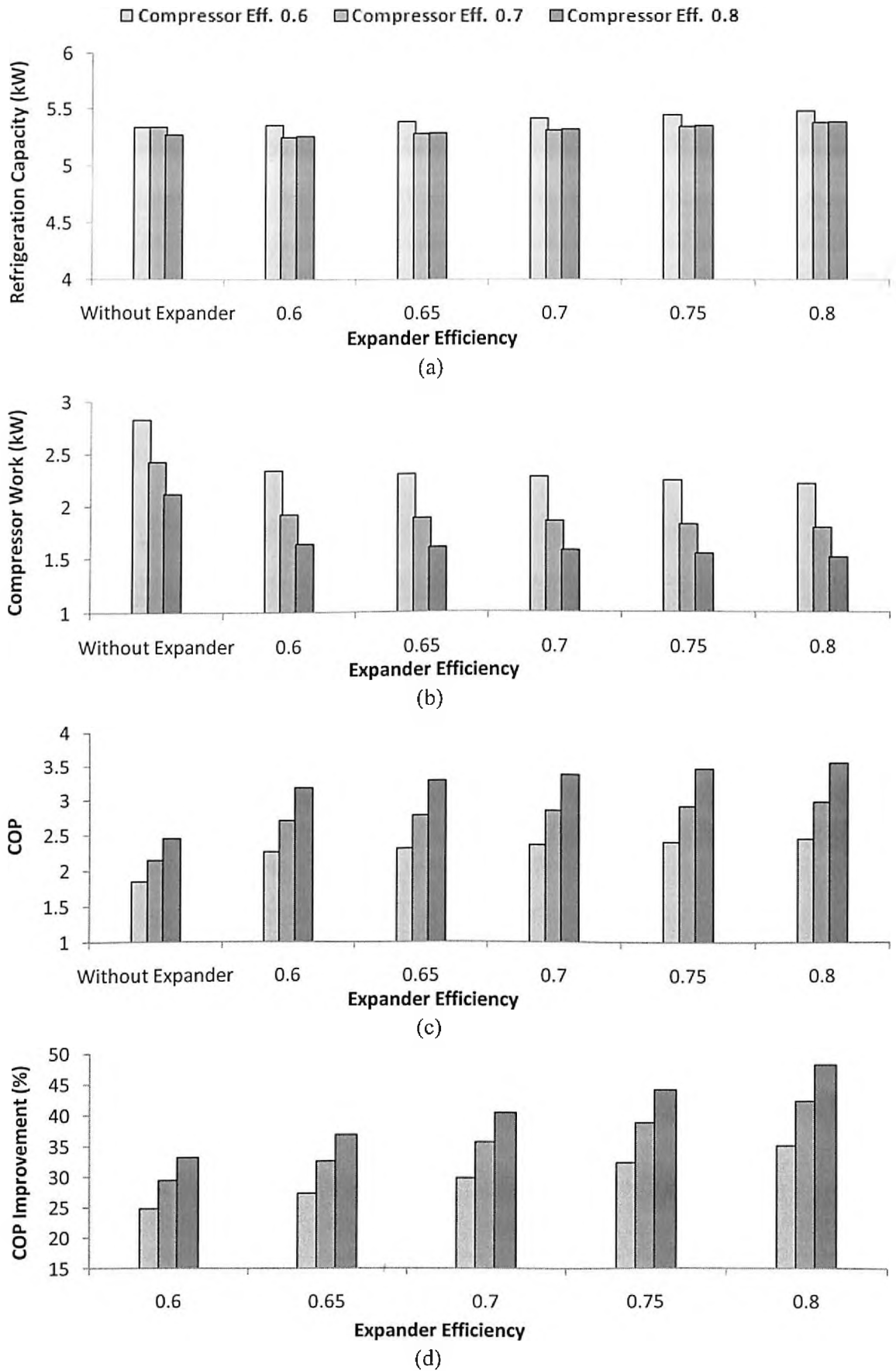


Figure 7.12: Performance of overall system at zone II (evaporator temperature 278K)

Fig. 7.11(d) and Fig. 7.12(d) compares show percentage of COP improvement with and without expander at different simulation conditions. It is found that the rate of improvements are approximately same with different evaporator temperature at each simulation conditions. Finally it is found that even the value of COP at zone II is lower compare to zone I, and the magnitude of rate of increment are higher.

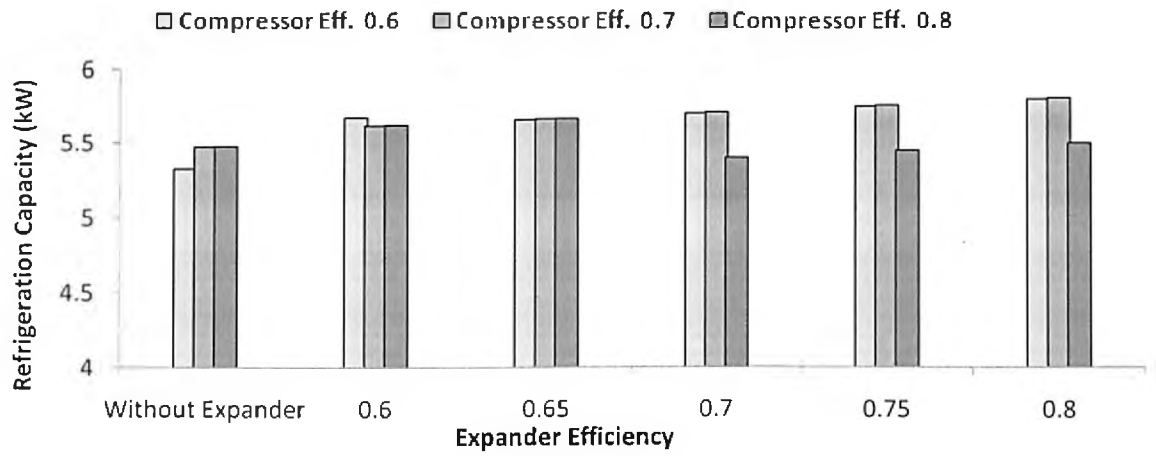
7.3.2.3 Temperature zone III

Fig. 7.13 - Fig. 7.15 shows the comparative results of overall system performance in terms of refrigeration capacity, net compressor work, COP and COP improvement percentage at temperature zone III with evaporator temperature 268K, 273K and 278K respectively. All the results are plotted with expander efficiency at different compressor efficiency. Very similar trends are observed at zone II and zone III. There are few point to be noted in part (c) of Fig. 7.13 - Fig. 7.15 the maximum value of COP at each optimum condition are found to be decreasing for zone I, zone II and then zone III. However the rate of improvement in COP increases from zone I, zone II to zone III.

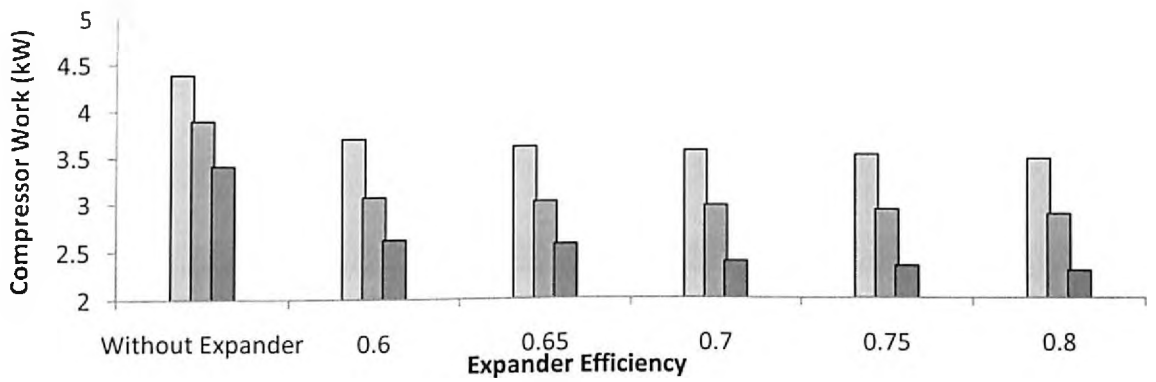
The overall performances of the modified system using work recovery turbine as expansion are extensively analyzed at three temperature zones in Indian conditions. Further, an attempt is made to find the optimum operating conditions with the modified system using refined simulation conditions.

It was discussed in article 6.3.2 that the isentropic efficiency also affects the overall performance of the system, the effect of isentropic efficiency of compressor and expander are studied and compared for different evaporator temperatures at all temperature zones.

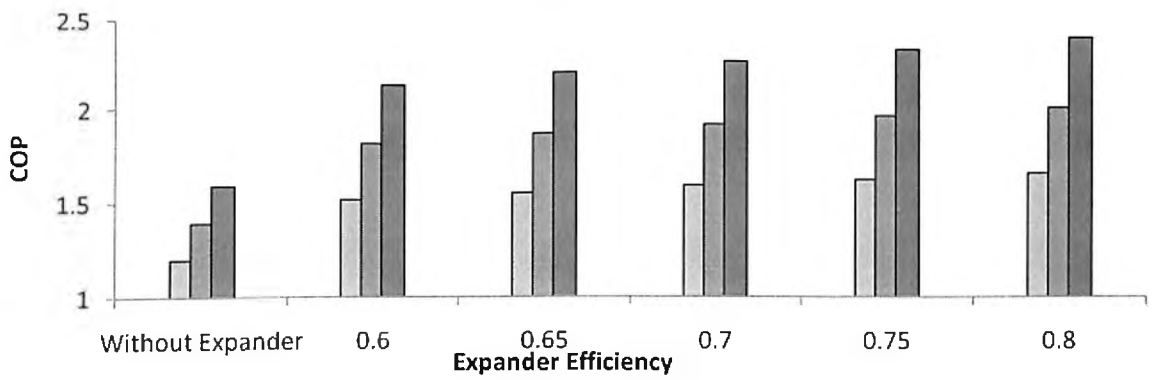
It was found during the analysis that the system using work recovery turbine shows significant improvement as compared to the system without turbine. The rate of improvements are more significant at temperature zone II and zone III as compared to zone I. The effect of evaporator temperature on COP of the system are prominent at zone I, however these effects are lower at zone II and zone III. It is also observed that the optimum operating pressure was slightly lower specially at zone II and III, as compared to the system without modification.



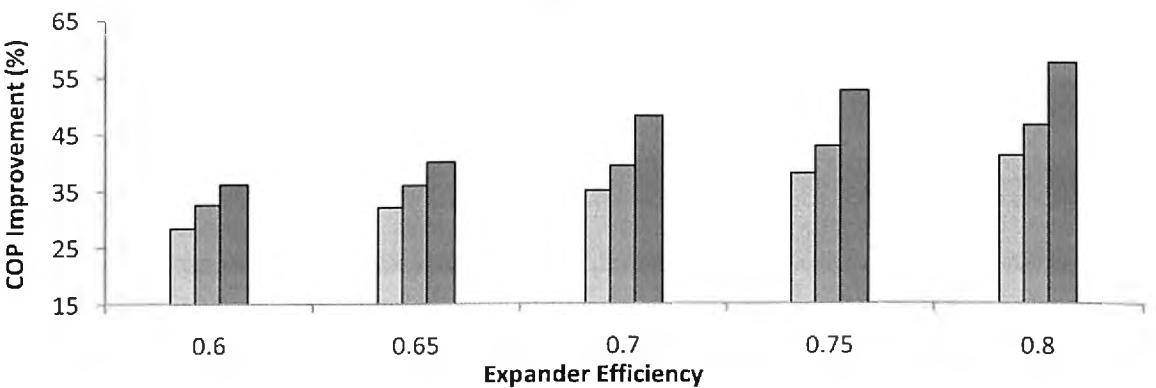
(a)



(b)



(c)



(d)

Figure 7.13: Performance of overall system at zone III (evaporator temperature 268K)

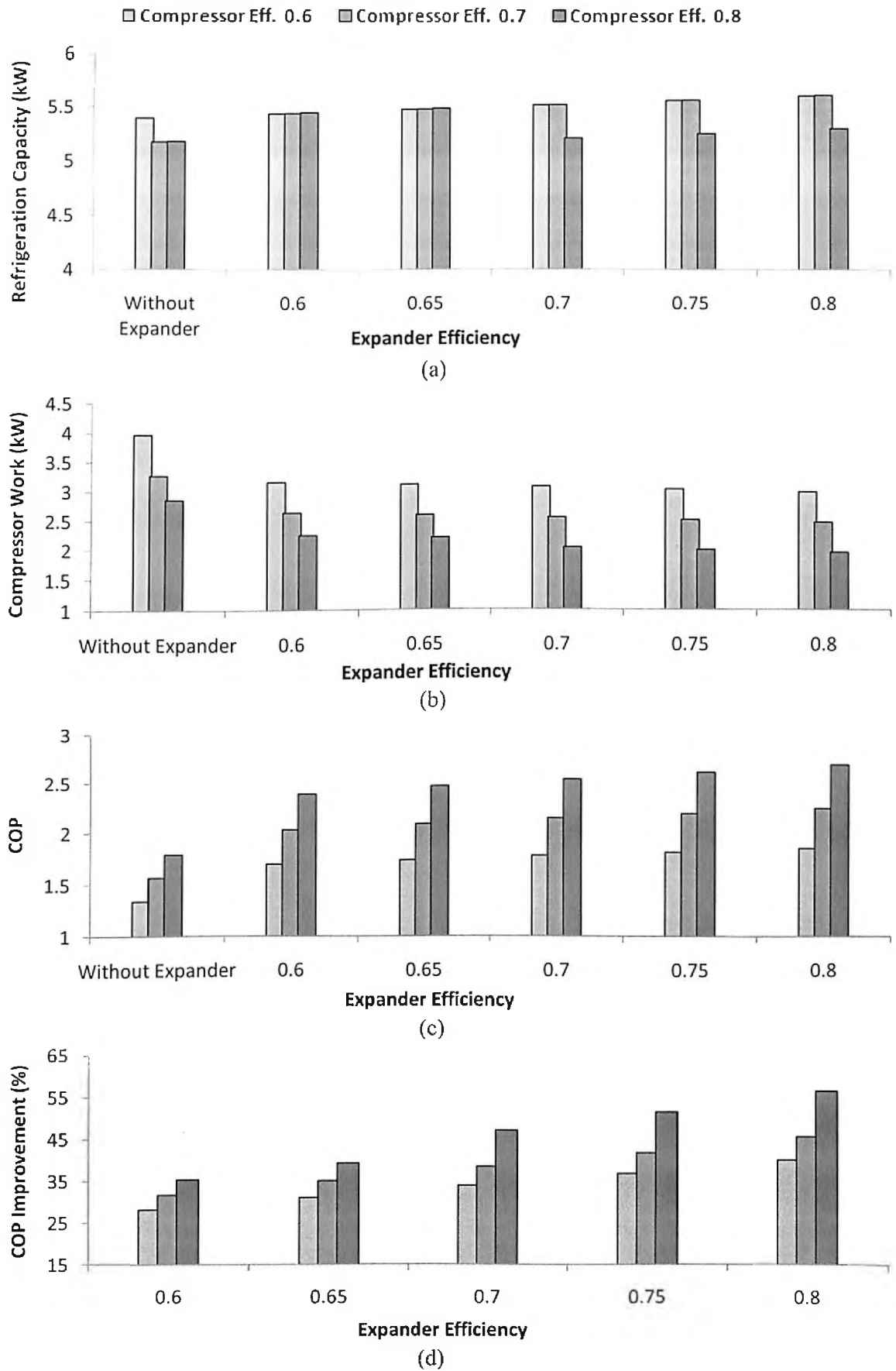


Figure 7.14: Performance of overall system at zone III (evaporator temperature 273K)

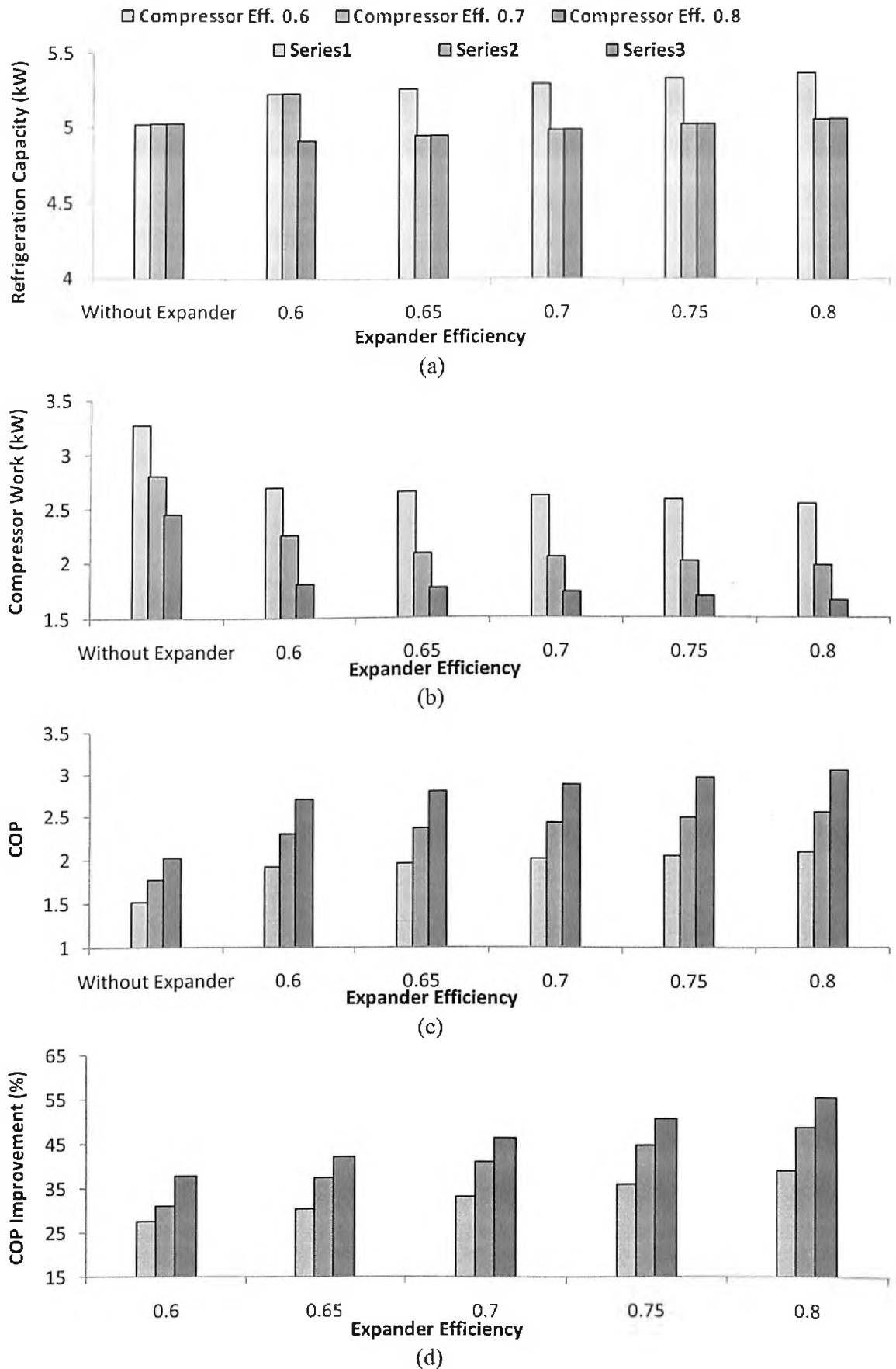


Figure 7.15: Performance of overall system at zone III (evaporator temperature 278K)

The above results and discussion indicate that higher isentropic efficiency and evaporator temperature, leads to higher performance of the system, however there are always practical limitations like desire temperature based on the application of the system and the design of the compressor and turbine to achieve higher isentropic efficiency. The detailed results with the different isentropic efficiencies and evaporator temperature for optimum conditions are shown in Appendix B.

Conclusion and Future Scope of The Work

A detailed theoretical analysis of trans-critical CO₂ vapour compression refrigeration system and its components in Indian climatic conditions have been presented. Work involves formulation of a detailed and flexible mathematical model of a finned tube gas cooler in MATLAB platform. The same has been developed and validated using published literature. The model is further extended for the overall system. The performance of the trans-critical CO₂ refrigeration system has been analyzed at various combinations of operating conditions relevant to Indian conditions. Further various design of the gas cooler with and without the inclusion of fan power consumption has been analyzed considering three temperature zones. Temperature zones are defined as zone I, zone II, and zone III with consideration of ambient temperature 29.4°C, 40°C, and 45°C respectively. An attempt has been made to optimize the performance of the gas cooler, the most crucial component based on its geometric and operating parameters, to achieve the best possible COP of the overall system at each zone. The system modification using work recovery turbine has also been explored and the operating conditions are optimized to achieve the best possible COP of the system in conjunction of suitable gas cooler designs. The outcome of the theoretical and simulation based studies, and its major conclusions are summarized below.

8.1 Conclusions

Chapter 3

- ✓ Due to the near critical operation, CO₂ exhibits some distinct feature compared to other conventional refrigerants and these properties change rapidly in supercritical region. Therefore, the design of gas cooler is found to be one of the most sensitive factors which affect the system COP. This factor becomes more sensitive at higher environmental temperatures (i.e. zone II and zone III) as compare to low environmental temperature (i.e. zone I) in Indian conditions.

- ✓ The approach temperature (AT) is a measure of gas cooler performance i.e. a lower approach temperature indicate the better performance of the gas cooler. The system performance is found to be maximum at the lowest approach temperature for each zone and also different optimum operating pressure was determined for each zone to achieve a maximum COP of the system. Based on analysis of ideal cycle, maximum COP achieved was at 10.5 MPa with lower AT and at 11.5MPa with higher AT for zone II, and at 12MPa with lower AT, and at 12.5MPa with higher AT for zone III. However, for zone I, maximum COP was achieved at lower operating pressure for the approach temperature range. Hence the maximum COP value increases with a decrease in both the environmental temperature and the approach temperature.

Chapter 4

- ✓ A detailed and flexible model of a gas cooler has been constructed using distribution method and validated against published literature. Simulation result showed very good agreement with the published experimental results at different test conditions. Further the model has been extended to analyze overall system performance using the respective design of the gas cooler and various operating conditions.

Chapter 5

- ✓ The simulation shows that the rate of decrease of temperature of CO₂ is higher in the beginning along the pipe, from refrigerant inlet to outlet. Therefore, there is a scope of proper utilization of the heat transfer area that can be achieved by modifying the gas cooler circuit arrangements. These different circuit arrangements have been analyzed in this work. Simulation results with modified design of gas cooler, shows that, in general, the gas cooler with higher number of circuit arrangement and higher air velocity have a low approach temperature. However, the drop in approach temperature is insignificant when number of circuit increase beyond two and air velocity exceed 2 ms⁻¹. Hence, overall system performance remains approximately constant in these conditions at each zone. At the same time the power consumed by the fan to maintain air velocity increases significantly with the increase in air velocity. There is also increment in initial material and fabrication cost as the gas cooler design gets complex. It also

increases the air flow resistance. Therefore, the consideration of fan power consumption is established to be an important parameter to optimize overall performance of the system.

- ✓ This is a novel approach to consider the gas cooler and overall performance of the system, including fan power consumption.

Chapter 6

- ✓ The performances of the gas cooler and overall system have been analyzed with different design and operating conditions of gas cooler, considering fan power consumption. It was found that two pass gas cooler shows poor performance; as compared to three pass and four pass gas cooler, which has approximately the same performance. Further, the system performance was also found favorable with three and four pass gas cooler. These performances have been achieved with three circuit arrangement of gas cooler and at the middle range of air velocity which differs with temperature zones.
- ✓ The maximum COP of the systems have been found to be 2.525, 1.612, and 1.345 at zone I, zone II and zone III respectively. These results are achieved with isentropic efficiency of compressor 0.6, evaporator temperature 273K and air velocity 1.5 ms^{-1} .
- ✓ The system performance is also found to vary with different evaporator temperature and compressor isentropic efficiencies. It is found that higher evaporator temperature and higher isentropic efficiency give better COP. Analysis with higher evaporator temperature (278 K) and higher isentropic efficiency (0.8) have been considered for analysis using three pass gas cooler having the maximum COP of 4.0 (at 8MPa, 1.5 ms^{-1}), 2.459 (at 10.5MPa, 1 ms^{-1}), and 2.027 (at 12MPa, 1 ms^{-1}) in temperature zone I, zone II and Zone III respectively. This indicates that the consideration of fan power becomes more prominent at higher temperature zones.
- ✓ A comparative analysis of the system performance has been presented for all three zones with different evaporator temperature and isentropic efficiencies. The results show that the effect of evaporator temperature on maximum COP are

more in zone I, however such effect reduces from zone II to zone III for all values of Isentropic efficiency. Approximately equal level effects were observed with isentropic efficiency for all conditions.

- ✓ It is found that the system performances using two pass gas cooler are inferior as compared to system using three and four pass gas cooler. However, system performance with three pass and four pass gas cooler have approximately similar performance results. As far as the selection of gas cooler is concerned, three pass or four pass can be selected for achieving similar performance. However the compactness of the gas cooler can also be a selection criteria for these two gas cooler. The list of optimum design and operating conditions with their performance results are given in Appendix A.
- ✓ Since the COP of the overall system is still lower after the optimization of gas cooler design and operating condition, it is required to modify the system to improve the performance.

Chapter 7

- ✓ In this chapter, the performance analysis have been done for the modified system using work recovery turbine as expansion device. In this analysis, only three pass cooler with 54 and 45 tubes in three circuit arrangements are taken based on previous results.
- ✓ It was found during the analysis that the system using work recovery turbine shows significant improvements (i.e. 17-34% in zone I, 24-47% in zone II, and 28-56% in zone III) as compare to the system without turbine. The rate of improvements are more significant at temperature zone II and zone III as compare to zone I. The effect of evaporator temperature on COP of the system are prominent at zone I , however, these effects are lower at zone II and zone III.
- ✓ It was also observed that the optimum operating pressure was slightly lower, especially at zone II and III, as compare to without modification.
- ✓ Maximum COP achieved for the modified system was 2.958 (at 8MPa and 2 ms⁻¹), 1.991 (at 10.5MPa and 1.5 ms⁻¹), 1.709 (at 11.5MPa and 1 ms⁻¹) for temperature zone I, zone II and zone III respectively. These results were achieved

with assuming isentropic efficiency of compressor and turbine as 0.6 and evaporator temperature 273K.

- ✓ The above results and discussions indicate that higher isentropic efficiency and evaporator temperature, leads to higher performance of the system, however there are always practical limitations like desired temperature, which depends on the application of the system and the design of the compressor and turbine to achieve higher isentropic efficiency.
- ✓ Analysis with higher evaporator temperature (278 K) and higher isentropic efficiency of the compressor and turbine (0.8) were considered for the analysis using three pass gas cooler having maximum COP of 5.280 (at 8MPa and 1.5 ms⁻¹), 3.563 (at 10MPa and 1 ms⁻¹), and 3.061 (at 11MPa and 1 ms⁻¹) at temperature zone I, zone II and zone III respectively. The detailed results with the different isentropic efficiencies and evaporator temperature for optimum conditions are shown in Appendix B
- ✓ If these isentropic efficiencies can be maintained practically with improved system design, the value of COP of trans-critical CO₂ systems are comparable with commercial available conventional systems and CO₂ based system looks feasible.
- ✓ Finally it was found that individual combination of design and operating conditions can give better performance for each temperature zones in Indian conditions. This work will also help the designer to formulate a guidelines of design and operating conditions to achieve the best possible COP of the system at different temperature zones.

8.2 Suggestions for Future Work

Several unique applications together with various advantages of CO₂ based systems have motivated large volume of research work and industrial innovations as reported in the literature. Several studies related to cycle modification, system component design and applications can be recommended. Detailed multistage cycle analysis to optimize the gas cooler pressure and intermediate pressures can be done from both the first law and second law points of view.

The life cycle analysis or economic analysis can be recommended for future work, which will be required before commercialization of the products. Although various theoretical and experimental investigations on supercritical heat transfer and pressure drop, boiling heat transfer and pressure drop, two phase flow have been done, pseudo-critical region of gas cooling is still one of the interesting areas, where one can rigorously study heat transfer and fluid flow. CO₂ compressors should be designed appropriately for each temperature zones and improve the design to achieve higher performance. Prototype developments and experimental CO₂ system development can be analyze for Indian climatic conditions and its applications like, dual heating and cooling for dairy and drying applications and in food industry are some of the very promising applications that can be pursued.

REFERENCES

move up

Adriansyah, W. (2004). Combined air conditioning and tap water heating plant using CO₂ as refrigerant. *Energy and Buildings*, 36(7), 690–695.

Adeyefa, S., Schade, O., & Carl, U. (2006). ^{B.} COP-optimized pressure control for a centralized CO₂ cooling system in aircraft applications. *7th IIR Gustav Lorentzen Conference on Natural Working Fluids, Trondheim, Norway, May 28–31, 2006*.
 → COP (add capital letter)

Agrawal, N., & Bhattacharyya, S. (2007a). Adiabatic/capillary tube flow of carbon dioxide in a transcritical heat pump cycle. *Int. J. Energy Res.* 2007; 31:1016–1030.
 → 31(11), 1016–1030.

Agrawal, N., & Bhattacharyya, S. (2007b). Studies on a two-stage transcritical carbon dioxide heat pump cycle with flash intercooling. *Applied Thermal Engineering* 27, 299–305.
 → write in full. International Journal of Energy Research

Agrawal, N., & Bhattacharyya, S. (2008). Optimized transcritical CO₂ heat pumps: Performance comparison of capillary tubes against expansion valves. *International Journal of Refrigeration* 31, 388–395.
 → 27(2-3) ← delete this symbol
 → remove
 → delete ← 31(3)

Apra, C., & Maiorino, A. (2008). An experimental evaluation of the transcritical CO₂ refrigerator performances using an internal heat exchanger. *International Journal of Refrigeration* 31, 1006–1011.
 → 31(6)

Asinari, P., Cecchinato, L., & Fornasieri, E. (2004). Effects of thermal conduction in microchannel gas coolers for carbon dioxide. *International Journal of Refrigeration*, 27(6), 577–586. ✓

Ayad, F., Benelmir, R., & Souayed, A. (2012). CO₂ evaporators design for vehicle HVAC operation. *Applied Thermal Engineering*, 36, 330–344. ✓

Baek, C., Heo, J., Jung, J., Cho, H., & Kim, Y. (2013). Optimal control of the gas cooler pressure of a CO₂ heat pump using EEV opening and outdoor fan speed in the cooling mode. *International Journal of Refrigeration*, 36(4), 1276–1284.

Baek, J. S.; Groll, E. A.; & Lawless, P. B. (2002). Development of a piston-cylinder expansion device for the transcritical carbon dioxide cycle. *International Refrigeration and Air Conditioning Conference. Paper 584*.
 → remove

Baek, J. S., Groll, E. A., & Lawless, P. B. (2005a). Piston-cylinder work producing expansion device in a transcritical carbon dioxide cycle, Part I: experimental investigation. *International Journal of Refrigeration* 28, 141–151.
 → delete
 → omit gap

Baek, J. S., Groll, E. A., & Lawless, P. B. (2005b). Piston-cylinder work producing expansion device in a transcritical carbon dioxide cycle, Part II: theoretical model. *International Journal of Refrigeration* 28, 152–164.
 → delete
 → 28(2)

Banasiak, K., Hafner, A., & Andresen, T. (2012). Experimental and numerical investigation of the influence of the two-phase ejector geometry on the performance of the R744 heat pump. *International Journal of Refrigeration*, 35(6), 1617–1625. ✓

Delete

Baskov, V.L., Kuraeva, I.V., & Protopopov, V.S. (1977). Heat transfer with the turbulent flow of a liquid under supercritical pressure in tubes under cooling conditions. *High Temperature* 15 (1), 81-86.

Bell, I. (2004). Performance increase of carbon dioxide refrigeration cycle with the addition of parallel compression economization. *6th IIR Gustav Lorentzen conference on natural working fluids, Glasgow, UK*, paper 2/A/4.30.

Bhattacharyya, S., Mukhopadhyay, S., Kumar, A., & Sarkar, J. (2005). Optimization of CO₂-C₃H₈ cascade system for refrigeration and heating. *International Journal of Refrigeration*, 28(8), 1284-1292.

Boccardi, G., Calabrese, N., Celata, G. P., Mastrullo, R., Mauro, A. W., Perrone, P., & Trinchieri, R. (2013). Experimental performance evaluation for a carbon dioxide light commercial cooling application under trans-critical and subcritical conditions. *Applied Thermal Engineering*, 54(2), 528-535.

Boewe, D.E., Bullard, C.W., Yin, J.M., & Hrnjak P.S. (2001). Contribution of internal heat exchanger to trans-critical R-744 cycle performance. *HVAC Research*, 7(2), 155-168.

Brown, J. S., Yana-motta, S. F., & Domanski, P. A. (2002). Comparitive analysis of an automotive air conditioning systems operating with CO₂ and R134a. *International Journal of Refrigeration* 25, 19-32.

Bullard, C., & Rajan, J. (2004). Residential Space Conditioning and Water Heating with Trans-critical CO₂ Refrigeration Cycle. *International Refrigeration and Air Conditioning Conference. Paper 693*.

<http://docs.lib.purdue.edu/cgi/viewcontent.cgi?article=1692&context=iracc>

Cabello, R., Sánchez, D., Llopis, R., & Torrella, E. (2008). Experimental evaluation of the energy efficiency of a CO₂ refrigerating plant working in trans-critical conditions. *Applied Thermal Engineering*, 28(13), 1596-1604.

Cabello, Ramón, Sánchez, D., Patiño, J., Llopis, R., & Torrella, E. (2012). Experimental analysis of energy performance of modified single-stage CO₂ trans-critical vapour compression cycles based on vapour injection in the suction line. *Applied Thermal Engineering*, 47, 86-94.

Calm, J. M., & Didion D. A. (1997). Trade-offs in refrigerant selections: past, present, and future. *Proceeding of the SHRAE/NIST Refrigerants Conference, Gaithersburg, MD. USA*.

[http://jamesmcalm.com/pubs/Calm%20JM,%20Didion%20DA,%201997.%20Trade-Offs%20in%20Refrigerant%20Selections.%20ASHRAE-NIST%20Refrigerants%20Conference%20\(Gaithersburg,%20MD,%20USA,%201997.10.06-07\),%20ASHRAE.pdf](http://jamesmcalm.com/pubs/Calm%20JM,%20Didion%20DA,%201997.%20Trade-Offs%20in%20Refrigerant%20Selections.%20ASHRAE-NIST%20Refrigerants%20Conference%20(Gaithersburg,%20MD,%20USA,%201997.10.06-07),%20ASHRAE.pdf)

Casini D. CO₂ compressors and equipment, use and availability, *EURO cooling and heating, Centro Studi Galileo*,

http://www.eurocooling.com/public_html/article.htm

zilio C

Casson, V., Cecchinato, L., Corradi, M., Fornasieri, E., Giroto, S., Minetto, S., Zamboni, L., et al. (2003). Optimization of the throttling system in a CO₂ refrigerating machine. *International Journal of Refrigeration* 26, 926-935.
26(8)

delete

Cavallini, A., Cecchinato, L., Corradi, M., Fornasieri, E., & Zilio, C. (2005). Two stage trans-critical carbon dioxide cycle optimization: A theoretical and experimental analysis. *Int J Refrigeration* 28(8), 1274-1283.

International Journal of Refrigeration

Cecchinato, L., Chiarello, M., Corradi, M., Fornasieri, E., Minetto, S., Stringari, P., Zilio, C., et al. (2009). Thermodynamic analysis of different two-stage trans-critical carbon dioxide cycles. *International Journal of Refrigeration*, 32(5), 1058-1067.

delete

Cecchinato, L., & Corradi, M. (2011). Trans-critical carbon dioxide small commercial cooling applications analysis. *International Journal of Refrigeration*, 34(1), 50-62.

Cecchinato, L., Corradi, M., Fornasieri, E., & Zamboni, L. (2005). Carbon dioxide as refrigerant for tap water heat pumps: A comparison with the traditional solution. *International Journal of Refrigeration*, 28(8), 1250-1258.

Cecchinato, L., Corradi, M., & Minetto, S. (2010). A critical approach to the determination of optimal heat rejection pressure in trans-critical systems. *Applied Thermal Engineering*, 30(13), 1812-1823.

delete

Cen, J., Liu, P., & Jiang, F. (2012). A novel trans-critical CO₂ refrigeration cycle with two ejectors. *International Journal of Refrigeration*, 35(8), 2233-2239.

Chang, Y.-S., & Kim, M. S. (2007). Modeling and Performance Simulation of a Gas Cooler for a CO₂ Heat Pump System. *HVAC&R Research*, 13(3), 445-456.

Chen, J., & Wu, C. (1996). Optimization of a two-stage combined refrigeration system. *Energy Conversion and Management*, 37(3), 353-358.

Chen, W., Liu, M., Chong, D., Yan, J., Little, A. B., & Bartosiewicz, Y. (2013). A 1D model to predict ejector performance at critical and sub-critical operational regimes. *International Journal of Refrigeration*, 36(6), 1750-1761.

Chen, Y., Pridasawas, W., & Lundqvist, P. (2010). Dynamic simulation of a solar-driven carbon dioxide trans-critical power system for small scale combined heat and power production. *Solar Energy*, 84(7), 1103-1110.

delete

Chen, Ying, & Gu, J. (2005). The optimum high pressure for CO₂ trans-critical refrigeration systems with internal heat exchangers. *International Journal of Refrigeration* 28, 1238-1249.

delete

Cheng, L., Ribatski, G., & Thome, J. R. (2008). Analysis of supercritical CO₂ cooling in macro- and micro-channels. *International Journal of Refrigeration*, 31(8), 1301-1316.

28(8)

Cheng, L., & Thome, J. R. (2009). Cooling of microprocessors using flow boiling of CO₂ in a micro-evaporator: Preliminary analysis and performance comparison. *Applied Thermal Engineering*, 29(11-12), 2426-2432.

g.c.p

Silva DLD, Hermes CSL, Melo C,
Goncalves JM, Weber AC



Note: See page 173 comments, This paper
is linked to there

Chesi, A., Ferrara, G., Ferrari, L., & Tarani, F. (2012). Setup and characterisation of a multi-purpose test rig for R744 refrigerating cycles and equipment. *International Journal of Refrigeration*, 35(7), 1848–1859.

Cho, H., Baek, C., Park, C., & Kim, Y. (2009). Performance evaluation of a two-stage CO₂ cycle with gas injection in the cooling mode operation ~~Evaluation~~. *International Journal of Refrigeration*, 32(1), 40–46.

Cho, H., Ryu, C., & Kim, Y. (2007). Cooling performance of a variable speed CO₂ cycle with an electronic expansion valve and internal heat exchanger. *International Journal of Refrigeration* 30, 664-671.

Cho, H., Ryu, C., Kim, Y., & Kim, H. Y. (2005). Effects of refrigerant charge amount on the performance of a transcritical CO₂ heat pump. *International Journal of Refrigeration*, 28(8), 1266–1273.

Cho, J. M., & Kim, M. S. (2007). Experimental studies on the evaporative heat transfer and pressure drop of CO₂ in smooth and micro-fin tubes of the diameters of 5 and 9.52mm. *International Journal of Refrigeration*, 30(6), 986–994.

Churchill, S.W. (1977). Friction-factor equation spans all fluid-flow regimes. *Chemical Engineering* 84(7), 91-92.

Corradi, M., Cecchinato, L., Schiochet, G., & Zilio, C. (2006). Modeling fin-and-tube gas-cooler for trans-critical carbon dioxide cycles. *International Refrigeration and Air Conditioning Conference. Paper 761*.

<http://docs.lib.purdue.edu/cgi/viewcontent.cgi?article=1760&context=iracc>

Damseh, R. (2006). Influence of variable fluid properties during in-tube cooling on performance of CO₂ refrigeration cycle. *Forschung im Ingenieurwesen*, 70(4), 231–235.

Dang, C., & Hihara, E. (2004). In-tube cooling heat transfer of supercritical carbon dioxide. Part 1. Experimental measurement. *International Journal of Refrigeration*, 27(7), 736–747.

Deng, J., Jiang, P., Lu, T., & Lu, W. (2007). Particular characteristics of trans-critical CO₂ refrigeration cycle with an ejector. *Applied Thermal Engineering*, 27, 381–388.

Dubey, S.K., Rajput, SPS, & Dubey, M. (2007). Computer Aided Performance Analysis of Trans Critical CO₂ Refrigeration Cycle with Ejector Expansion. *Proceedings of International Conference on Modeling & Simulation-CITICOMS 2007; CIT Coimbatore (TN)*, 247-252.

Dubey, M., Rajput, SPS, & Dubey, S. K. (2008). Pros and Cons of Adopting CO₂ as a Viable, Alternative, Natural Refrigerant. *Journal of Environmental Research and Development*, 2008, 2(4), 737-753.

Diogo, L., Hermes, C. L. L., Gonc, J. M., & Weber, G. C. (2009). A study of trans-critical carbon dioxide flow through adiabatic capillary tubes. *International Journal of Refrigeration*, 32, 978–987.

Eisenhower, B. a., & Runolfsson, T. (2008). System level modeling of a trans-critical vapor compression system for bistability analysis. *Nonlinear Dynamics*, 55, 13–30.

Elbel, S. (2007). Experimental and analytical investigation of a two phase ejector used for expansion work recovery in a trans-critical R744 air-conditioning system. *University of Illinois at Urbana-Champaign, Ph.D. Dissertation, Urbana, IL, USA.*

Elbel, S. (2011). Historical and present developments of ejector refrigeration systems with emphasis on trans-critical carbon dioxide air-conditioning applications. *International Journal of Refrigeration*, 34(7), 1545–1561.

Elbel, S., & Hrnjak, P. (2004). Flash gas bypass for improving the performance of trans-critical R744 systems that use microchannel evaporators. *International Journal of Refrigeration*, 27(7), 724–735.

Elbel, S., & Hrnjak, P., (2006a). Experimental validation and design study of a trans-critical CO₂ prototype ejector system. *Proceedings of the 7th IIR-Gustav Lorentzen Conference on Natural Working Fluids, Trondheim, Norway.*

<http://docs.lib.purdue.edu/cgi/viewcontent.cgi?article=1883&context=iracc>

Elbel, S., & Hrnjak, P., (2006b). A thermodynamic property chart as a visual aid to illustrate the interference between expansion work recovery and internal heat exchange. *11th International Refrigeration and Air Conditioning Conference at Purdue, West Lafayette, USA, Paper R165.*

Elbel, S., & Hrnjak, P. (2007). Experimental investigation of trans-critical CO₂ ejector system performance. *22nd IIR International Congress of Refrigeration, Beijing, China, Paper ICR07-E1-72.*

Elbel, S., & Hrnjak, P. (2008). Experimental validation of a prototype ejector designed to reduce throttling losses encountered in trans-critical R744 system operation. *International Journal of Refrigeration*, 31(3), 411–422.

Fang, X.D. (1999). Modeling and Analysis of Gas Coolers. *ACRC CR-16, Department of Mechanical and Industrial Engineering, University of Illinois at Urbana-Champaign, USA.*

[http://www.researchgate.net/publication/251668010_Modified_heat_transfer_equation_for_in-tube_supercritical_CO_2_cooling.](http://www.researchgate.net/publication/251668010_Modified_heat_transfer_equation_for_in-tube_supercritical_CO_2_cooling)

Fang, X., & Xu, Y. (2011). Modified heat transfer equation for in-tube supercritical CO₂ cooling. *Applied Thermal Engineering*, 31, 3036–3042.

Fang, X., Zhou, Z., & Li, D. (2013). Review of correlations of flow boiling heat transfer coefficients for carbon dioxide. *International Journal of Refrigeration*, (article in press) 36(8), 2017–2029.

Fangtian, S., & Yitai, M. (2011). Thermodynamic analysis of trans-critical CO₂ refrigeration cycle with an ejector. *Applied Thermal Engineering*, 31, 1184–1189.

Fartaj, A., David, S. K. T., & Yang, W. W. (2004). Second law analysis of the trans-critical CO₂ refrigeration cycle. *Energy Conversion and Management*, 45, 2259–2281.

Fernandez, N., Hwang, Y., & Radermacher, R. (2010). Comparison of CO₂ heat pump water heater performance with baseline cycle and two high COP cycles. *International Journal of Refrigeration*, 33(3), 635–644.

Note

Always Part I will come before
Part II
of any paper)

change its
position suitably ←



make it (2011a)
Fronk, B. M., & Garimella, S. (2011a). Water-coupled carbon dioxide microchannel gas cooler for heat pump water heaters: Part II – Model development and validation. *International Journal of Refrigeration*, 34(1), 17–28.

make it (2011a)
Fronk, B. M., & Garimella, S. (2011b). Water-coupled carbon dioxide microchannel gas cooler for heat pump water heaters: Part I - Experiments. *International Journal of Refrigeration*, 34(1), 7–16.

Fukuta, M., Radermacher, R., Lindsay, D., & Yanagisawa, T. (2000). Performance of vane compressor for CO₂ cycle. 4th IIR-Gustav Lorentzen Conference on natural working Fluids, West Lafayette. 339-346.
<http://docs.lib.purdue.edu/cgi/viewcontent.cgi?article=2767&context=icec>

Fukuta, M., Yanagisawa, T., Kosuda, O., & Ogi, Y. (2006). Performance of scroll expander for CO₂ refrigeration cycle. *International Compressor Engineering Conference*, Paper 1768.
<http://docs.lib.purdue.edu/cgi/viewcontent.cgi?article=2767&context=icec>

Garimella S. (2002). Microchannel gas coolers for carbon dioxide air conditioning system. *ASHRAE Transaction*, 108(1), 492-499. ✓

Ge, Y. T., & Cropper, R. T. (2009). Simulation and performance evaluation of finned-tube CO₂ gas coolers for refrigeration systems. *Applied Thermal Engineering*, 29, 957–965.

A
29(5-6)
Ge, Y. T., & Tassou, S. A. (2011a). Performance evaluation and optimal design of supermarket refrigeration systems with supermarket model “SuperSim”, Part I: Model description and validation. *International Journal of Refrigeration*, 34(2), 527–539. ✓

A
Ge, Y. T., & Tassou, S. A. (2011b). Performance evaluation and optimal design of supermarket refrigeration systems with supermarket model “SuperSim”. Part II: Model applications. *International Journal of Refrigeration*, 34(2), 540–549. ✓

Ghajar, A. T., & Asadi, A. (1986). Improved forced convective heat transfer correlation for liquids in the near critical region. *AIAA Journal*, 24 (12), 2030-2037. ✓

Gnielinski, V. (1976). New equations for heat and mass transfer in turbulent pipe and channel flow. *International Journal of Chemical Engineering*, 16, 359-368.

Giroto, S., Minetto, S., & Neksa, P. (2004). Commercial refrigeration system using CO₂ as the refrigerant. *International Journal of Refrigeration*, 27(7), 717–723. ✓

Kim SG, Kim YJ, Lee G, Kim MS
Goo, S., Je, Y., Lee, G., & Seo, M. (2005). The performance of a transcritical CO₂ cycle with an internal heat exchanger for hot water heating. *International Journal of Refrigeration*, 28, 1064–1072. ✓
delete

28(7),
Goodman, C., Fronk, B. M., & Garimella, S. (2011a). Trans-critical carbon dioxide microchannel heat pump water heaters: Part I – System simulation and optimization. *International Journal of Refrigeration*, 34(4), 870–880. ✓
II

delete
Goodman, C., Fronk, B. M., & Garimella, S. (2011b). Trans-critical carbon dioxide microchannel heat pump water heaters: Part II – validated component simulation modules. *International Journal of Refrigeration*, 34(4), 859–869. ✓
make it 2011b
make it 2011a

also see comment on page 170

Plz check

There are 2 research articles similar to each other

Silva DLD, Hermes CJL, Melo C, Gonçalves JM
& Weber GC (2000) A Study of transcritical carbon dioxide flow through adiabatic capillary tubes, International Journal of Refrigeration 22(5) 978-987

Silva DLD, Ronzoni AL, Melo C & Hermes JL (2011) A study of transcritical carbon dioxide flow through diabatic capillary tubes, International Journal of Refrigeration 34(11) 836-843

Which of the above 2 will come here

— According place it at its proper place as per alphabetic arrangement

Plz check this reference properly
In many research article it is written as
Per connection suggested.

92 JSME seems to be unacceptable

Refer Applied Thermal Engineering
20(2000) 831-841
Liao, Zhao, Jakobsen

Guangming, C., Xiaoxiao, X., Shuang, L., Lixia, L., & Liming, T. (2010). An experimental and theoretical study of a CO₂ ejector. *International Journal of Refrigeration*, 33(5), 915-921. ✓

Haiqing, G., Yitai, M., & Minxia, L. (2006). Some design features of CO₂ swing piston expander. *Applied Thermal Engineering* 26, 237-243. 26(2-3) ↗ gap

Heo, J., Kang, H., & Kim, Y. (2011). Optimum cycle control of a two-stage injection heat pump with a double expansion sub-cooler. *International Journal of Refrigeration*, 35(1), 58-67. ↗

~~Hermes, C. J. L., Diogo, L., & Ronzoni, A. F. (2011). A study of transcritical carbon dioxide flow through adiabatic capillary tubes. *International Journal of Refrigeration*, 34, (2011) 834-843. ↗ delete LC~~

Heyl, P., & Quack, H. (1999). Free piston expander-compressor for CO₂ - design, applications and results. *20th International Congress of Refrigeration, IIR/IIF, Sydney*, Paper 516.

Hua, T., Yitai, M., Minxia, L., Haiqing, G., & Zhongyan, L. (2011). Influence of a non-condensable gas on the performance of a piston expander for use in carbon dioxide trans-critical heat pumps. *Applied Thermal Engineering*, 31, 1943-1949. 31(11-12)

Huai, X. L., Koyama, S., & Zhao, T.S. (2005). An experimental study of flow and heat transfer of supercritical carbon dioxide in multi-port mini channels under cooling conditions. *Chemical Engineering Science*, 40, 3337-3345. 60(12), 3337-3345.

Huang, D., Quack H., & Ding G., (2007). Experimental study of throttling of carbon dioxide refrigerant to atmospheric pressure. *Applied Thermal Engineering*, 27, 1911-1922. 27(11-12)

Huff, H-J., & Radermacher, R. (2003). CO₂ compressor-expander analysis, *ARTI final report ARTI-21CR/611-10060-01*.

Hwang, Y., Radermacher, R., Jin, D., & Hutchins, J. W. (2005). Performance Measurement of CO₂ Heat Exchangers. *ASHRAE Transaction*, 306-316. Jin, D.H.

Hwang, Y., & Radermacher, R. (1999). Experimental investigation of the CO₂ refrigeration cycle. *ASHRAE Transaction*, 105(1), 1219-1227.

Inokuty, H. (1923). Approximate graphical method of finding compression pressure of CO₂ refrigerant machine for maximum coefficient of performance. *92th Japan Society of Mechanical Engineers - The Fifth International Congress of Refrigeration*.

Jia, X., Zhang, B., Pu, L., Guo, B., & Peng, X. (2010). Improved rotary vane expander for trans-critical CO₂ cycle by introducing high-pressure gas into the vane slots. *International Journal of Refrigeration*, 34(3), 732-741. ↗ some

Jin, J., Chen, J., & Chen, Z. (2011). Development and validation of a microchannel evaporator model for a CO₂ air-conditioning system. *Applied Thermal Engineering*, 31, 137-146. 31(2-3)

Jung, J.-Y., & Yun, R. (2013). Prediction of gas cooling heat transfer coefficients for CO₂-oil mixtures. *International Journal of Refrigeration*, 36(1), 129-135. ✓

Kauf, F. (1999). Determination of the optimum high pressure for trans-critical CO₂ refrigeration cycles. *International Journal of Thermal Science*, 38, 325-330. ↗ delete

Kim HJ, Ahn JM, Cho SO, Cho KR



- Khan, J., & Zubair, S.M. (1998). Design and rating of a two-stage vapour compression refrigeration system, *Energy*, 23(10), 867-878.
- Kim, M. H., Lee, S., Mehendale, S., & Webb, R. (2003). Microchannel heat exchanger design for evaporator and condenser applications. *Adv Heat Transfer* (37), 297-429.
- Kim, H.J., An, K.J., & Ahn, J. M. (2004a). Performance comparison of various types of CO₂ compressors for heat pump water heater application. *6th IIR Gustav Lorentzen conference on natural working fluids*, Glasgow, UK, paper 6/A/12.00.
- Kim, M. H., Pettersen J., & Bullard C. W. (2004b). Fundamental process and system design issues in CO₂ vapor compression systems. *Progress in Energy and Combustion Science*, 30 (2), 119-174.
- ~~Kim, H. J., Min, J., Oug, S., & Cho, K. R. (2008). Numerical simulation on scroll expander - compressor unit for CO₂ trans-critical cycles. *Applied Thermal Engineering*, 28, 1654-1661.~~ 28(13)
- Kim, M., & Bullard, C. W. (2001). Development of a microchannel evaporator model for a CO₂ air-conditioning system, *Energy*, 26, 931-948.
- Kim, S. C., Won, J. P., & Kim, M. S. (2009). Effects of operating parameters on the performance of a CO₂ air conditioning system for vehicles. *Applied Thermal Engineering*, 29(11-12), 2408-2416.
- Kim, Y. J., Cho, J. M., & Kim, M. S. (2008). Experimental study on the evaporative heat transfer and pressure drop of CO₂ flowing upward in vertical smooth and micro-fin tubes with the diameter of 5mm. *International Journal of Refrigeration*, 31(5), 771-779.
- ~~Klockner~~ Klockner
Klo, K., Schmidt, E. L., & Steimle, F. (2001). Carbon dioxide as a working fluid in drying heat pumps *International Journal of Refrigeration*, 24, 100-107. 24(1)
- Kohsokabe, H., Funakoshi, S., Tojo, K., Nakayama, S., Kohno, K., & Kurashige, K. (2006). Basic operating characteristics of CO₂ refrigeration cycles with expander-compressor unit. *International Refrigeration and Air Conditioning Conference*, Paper 789.
- <http://www.scribd.com/doc/152084744/Basic-Operating-Characteristics-of-CO2-Refrigeration-Cycles>
- Kondou, C., & Hrnjak, P. (2011). Heat rejection from R744 flow under uniform temperature cooling in a horizontal smooth tube around the critical point. *International Journal of Refrigeration*, 34(3), 719-731.
- Krasnoshchekov, E.A., Kuraeva, I.V., & Protopopov, V.S. (1969). Local heat transfer of carbon dioxide under supercritical pressure under cooling conditions. *Teplofizika Vysokikh Temperatur* 7 (5) (1969) 922-930.
- Kuang, G., Ohadi, M., & Dessiatoun, S. (2008). Semi-empirical correlation of gas cooling heat transfer of supercritical carbon dioxide in microchannels. *HVAC & R Research* 14(6), 861-871.
- Lawrence, N., & Elbel, S. (2013). Theoretical and practical comparison of two-phase ejector refrigeration cycles including first and second Law analysis. *International Journal of Refrigeration*, 36(4), 1220-1232.

Refer Int J Heat Mass Transfer
45(2002) 5025-5031
1970

174

Lee, J. S., Kim, M. S., & Kim, M. S. (2011). Experimental study on the improvement of CO₂ air conditioning system performance using an ejector. *International Journal of Refrigeration*, 34(7), 1614–1625. ✓

Li, D. Q., & Groll, E. A. (2004). Trans-critical CO₂ refrigeration cycle with ejector-expansion device. *International Refrigeration and Air Conditioning Conference*, Paper 707.

Li, D., & Groll, E. A. (2005). Trans^{critical} CO₂ refrigeration cycle with ejector-expansion device. *International Journal of Refrigeration*, ~~28~~²⁸⁽⁵⁾, 766–773.

Liao, S.^M, Zhao, T.^S, & Jakobsen, A.^A. (2000). A correlation of optimal heat rejection pressures in trans^{critical} carbon dioxide cycles. *Applied Thermal Engineering*, 20(9), 831–841. ^{delete}

Liao, S.M., & Zhao, T.S. (2002a). An experimental investigation of convection heat transfer to supercritical carbon dioxide in miniature tubes. *International Journal of Heat and Mass Transfer*, 45, 5025-5034. ✓

Liao, S.M., & Zhao, T.S. (2002b). Measurements of heat transfer coefficients from supercritical carbon dioxide flowing in horizontal mini/micro channels. *Journal of Heat Transfer*, ~~124~~¹²⁴⁽³⁾, 413-420.

Liu, F., & Groll, E. A. (2008). Analysis of a two phase flow ejector for trans^{critical} CO₂ cycle (2008). *International Refrigeration and Air Conditioning Conference*, Paper 924. ^{delete} ^{July 14-17, 2008}
<http://docs.lib.purdue.edu/cgi/viewcontent.cgi?article=1923&context=iracc>

Liu, F., Li, Y., & Groll, E. A. (2012). Performance enhancement of CO₂ air conditioner with a controllable ejector. *International Journal of Refrigeration*, 35(6), 1604–1616.

Liu, H., Chen, J., & Chen, Z. (2005). Experimental investigation of a CO₂ automotive air conditioner. *International Journal of Refrigeration*, 28(8), 1293–1301. ✓

Lorentzen, G., & Pettersen, J. (1993). A new, efficient and environmentally benign system for car air-conditioning. *International Journal of Refrigeration*, 16(1), 4-12.

Lorentzen, G. (1994). Revival of carbon dioxide as a refrigerant. *International Journal of Refrigeration*, 17(5), 292-300. ✓

Lorentzen, G. (1995). The use of natural refrigerants: a complete solution to the CFC/HCFC predicament. *International Journal of Refrigeration*, 18(3), 190-197. ✓

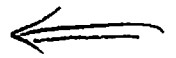
Lucas, C., & Koehler, J. (2012). Experimental investigation of the COP improvement of a refrigeration cycle by use of an ejector. *International Journal of Refrigeration*, 35(6), 1595–1603. ✓

Lucas, C., Koehler, J., Schroeder, A., & Tischendorf, C. (2013). Experimentally validated CO₂ ejector operation characteristic used in a numerical investigation of ejector cycle. *International Journal of Refrigeration*, 36(3), 881–891. ✓

Ma, Y., He, Z., Peng, X., & Xing, Z. (2012). Experimental investigation of the discharge valve dynamics in a reciprocating compressor for trans-critical CO₂ refrigeration cycle. *Applied Thermal Engineering*, 32, 13–21. ✓

- Madsen, K. B., Poulsen, C. S., & Wiesenfarth, M. (2005). Study of capillary tubes in a trans-critical CO₂ refrigeration system. *International Journal of Refrigeration*, 28, 1212–1218. ↑ 2
- Mancini, F., Minetto, S., & Fornasieri, E. (2011). Thermodynamic analysis and experimental investigation of a CO₂ household heat pump dryer. *International Journal of Refrigeration*, 34(4), 851–858. ✓
- ~~Manjili, F. E., & Yavari, M. A.~~ (2012). Performance of a new two-stage multi-intercooling trans-critical CO₂ ejector refrigeration cycle. *Applied Thermal Engineering*, 40, 202–209. A ← connect ✓
- Martínez-Ballester, S., Corberán, J.-M., & González-Maciá, J. (2013). Numerical model for microchannel condensers and gas coolers: Part II – Simulation studies and model comparison. *International Journal of Refrigeration*, 36(1), 191–202. ✓
- Martínez-Ballester, S., Corberán, J.-M., González-Maciá, J., & Domanski, P. A. (2011). Impact of classical assumptions in modelling a microchannel gas cooler. *International Journal of Refrigeration*, 34(8), 1898–1910. A
- Minetto, S. (2011). Theoretical and experimental analysis of a CO₂ heat pump for domestic hot water. *International Journal of Refrigeration*, 34(3), 742–751.
- Nagata, H., Kakuda, M., Sekiya, S., Shimoji, M., & Koda, T. (2010). Development of a scroll expander for the CO₂. *International Symposium on Next-generation Air Conditioning and Refrigeration Technology*, Tokyo, Japan.
- <http://www.nedo.go.jp/content/100080146.pdf>
- Nakagawa, M., Marasigan, A. R., & Matsukawa, T. (2011). Experimental analysis on the effect of internal heat exchanger in trans-critical CO₂ refrigeration cycle with two-phase ejector. *International Journal of Refrigeration*, 34(7), 1577–1586. delete
- Neksa, P., Dorin, F., Rekestad, M., & Bredesen, A. (1999). Development of two-stage semi-hermetic CO₂-compressor. *20th International Congress of Refrigeration IIR/IIF, Sidney*, paper 424.
- Neksa, P. (2002). CO₂ heat pump systems. *International Journal of Refrigeration*, 25, 421–427. ↑ 25(4)
- Nekså, P., Hoggen, R. L., Aflekt, K., Jakobsen, A., & Skaugen, G. (2004). Fan-less exchanger concept for CO₂ heat pump system. *6th IIR Gustav Lorentzen conference on natural working fluids, Glasgow, UK*, Paper 6/A/11.40.
- Nekså, P., Hoggen, R. L., Aflekt, K., Jakobsen, A., & Skaugen, G. (2005). Fan-less heat exchanger concept for CO₂ heat pump systems. *International Journal of Refrigeration*, 28(8), 1205–1211.
- Neksa, P., Rekestad, H., Zakeri, G. R., & Schiefloe, P.A. (1998). CO₂-heat pump water heater: characteristics, system design and experimental results. *International Journal of Refrigeration*, 21(3); 172-179.
- Neksa, P., Rekestad, H., Zakeri, G. R., & Schiefloe, P.A. (1999). Commercial heat pumps for water heating and heat recovery. *CO₂ technology in refrigeration, heat pump and air conditioning systems, Mainz, Germany*.

Rigola J, Ablanque N, Perez-segama C D,
Oliva A



Note: Now the position of this network will
change

1233

This reference is repeated, so delete it.

Neksfit, P., Rekstad, H., Zakeri, G. R., & Schiefloe, P. A. (1998). CO₂-heat pump water heater: characteristics, system design and experimental results. *International Journal of Refrigeration*, 21(3), 172-179.

Nickl, J., Will, G., Quack, H., & Kraus, W. E. (2005). Integration of a three-stage expander into a CO₂ refrigeration system. *International Journal of Refrigeration*, 28, 1219-1224.

Nieter, J. J. (2006). Experiences with Application of a CO₂ Reciprocating Piston Compressor for a Heat Pump Water Heater. *International Compressor Engineering Conference*, Paper 1722.

<http://docs.lib.purdue.edu/cgi/viewcontent.cgi?article=2721&context=icec&sei-redir=1&referer=http%3A%2F%2Fscholar.google.co.in>

Oh, H.K., & Son, C.H. (2010). New correlation to predict the heat transfer coefficient in-tube cooling of supercritical CO₂ in horizontal macro-tubes. *Experimental Thermal and Fluid Science* 34 (8), 1230-1241.

Onaka, Y., Miyara, A., & Tsubaki, K. (2010). Experimental study on evaporation heat transfer of CO₂/DME mixture refrigerant in a horizontal smooth tube. *International Journal of Refrigeration*, 33(7), 1277-1291. ✓

Park, C. Y., & Hrnjak, P. (2007). Effect of heat conduction through the fins of a microchannel serpentine gas cooler of trans-critical CO₂ system. *International Journal of Refrigeration*, 30(3), 389-397. ✓

~~Pe, C. D., Oliva, A., & Rigola, J. (2010). Numerical simulation and experimental validation of internal heat exchanger influence on CO₂ trans-critical cycle performance. *International Journal of Refrigeration*, 33, 664-674.~~

Petrov, N.E., & Popov, V.N. (1985). Heat transfer and resistance of carbon dioxide being cooled in the supercritical region. *Thermal Engineering*, 32 (3), 131-134.

Pefferen

~~Pettersen, J., Hafner, A., & Skaugen, G. (1998). Development of compact heat exchangers for CO₂ air-conditioning systems. *International Journal of Refrigeration*, 21(3), 180-193.~~

Pettersen, J., & Skaugen, G. (1994). Operation of trans-critical CO₂ vapour compression systems in vehicle air conditioning. *IIR International Conference in New Applications of Natural Working Fluids in Refrigeration and Air Conditioning*, Germany, 495-505.

Pettersen, J. (1997). Experimental results of carbon dioxide in compression systems. *ASHRAE/NIST Conference Refrigeration for the 21st Century*, Gaithersburg, MD, 27-37. ✓

Pettersen, J., Rieberer, R., & Munkejord, S.T. (2000). Heat transfer and pressure drop for flow of supercritical and subcritical CO₂ in microchannel tubes. *Final Report for US Army*, Contract No. N-68171-99-M-5674. ✓

Petukhov, B.S., & Kirillov, V.V. (1958). On heat exchange at turbulent flow of liquid in pipes, *Teploenergetika*, 4, 63-68. ✓

check the gap
↓

Petukhov, B.S., & Popov, V. V. (1963). Theoretical calculation of heat exchange and frictional resistance in turbulent flow in tubes of an incompressible fluid with thermophysical properties. *High Temperature* 1 (1), 69-83.

Petukhov, B.S., Kurganov, V.A., & Gladuntsov, A.I. (1973) Heat transfer in turbulent pipe flow of gases with variable properties, *Heat Transfer & Soviet Research* 5(4), 109-116.

Pitla, S.S., Robinson, D.M., Groll, E.A., & Ramadhyani, S. (1998). Heat transfer from supercritical carbon dioxide in tube flow: a critical review. *HVAC&R Research*, 4(3), 281-301.

Pitla, S.^{S.}, Groll, E.^{P.}, & Ramadhyani, S. (2001). Convective heat transfer from in-tube cooling of turbulent supercritical carbon dioxide: part 2 – experimental data and numerical predictions. *HVAC&R Research*, 7(4), 367-382.

Pitla, S.^{S.}, Groll, E.^{A.}, & Ramadhyani, S. (2002). New correlation to predict the heat transfer coefficient during in-tube cooling of turbulent supercritical CO₂. *International Journal of Refrigeration*, 25(7) 887-895.

Qi, P.-C., He, Y.-L., Wang, X.-L., & Meng, X.-Z. (2013). Experimental investigation of the optimal heat rejection pressure for a trans-critical CO₂ heat pump water heater. *Applied Thermal Engineering*, 56(1-2) 120-125.

Richter, M. R., Song, S. M., Yin, J. M., Kim, J. M., Bullard, C. W., & Hrnjak, P. S. (2003). Experimental results of trans-critical CO₂ heat pump for residential application. *Energy*, 28(10), 1005-1019.

Rigola, J., Raush, G., Pérez-Segarra, C. D., & Oliva, A. (2005). Numerical simulation and experimental validation of vapour compression refrigeration systems. Special emphasis on CO₂ trans-critical cycles. *International Journal of Refrigeration*, 28(8), 1225-1237.

Riffat, S. B., Afonso, C.F., Oliveira A.C., & Reay, D. A. (1997) Natural refrigerants for refrigeration and air-conditioning systems. *Applied Thermal Engineering*, 17(1), 33-42. ✓

Robinson, D. M., Groll, E. A., ~~Laboratories, R. W. H., & Lafayette, W.~~ (1998). Efficiencies of trans-critical CO₂ cycles with and without an expansion turbine. *International Journal of Refrigeration*, 21(7), 577-589.

Rozhentsev, A., & Wang, C.-C. (2001). Some design features of a CO₂ air conditioner. *Applied Thermal Engineering*, 21(8), 871-880.

Schmidt, E. L., Klöcker, K., Flacke, N., & Steimle, F. (1998). Applying the trans-critical CO₂ process to a drying heat pump. *International Journal of Refrigeration*, 21(3), 202-211.

Sánchez, D., Torrella, E., Cabello, R., & Llopis, R. (2010). Influence of the superheat associated to a semihermetic compressor of a trans-critical CO₂ refrigeration plant. *Applied Thermal Engineering*, 30(4), 302-309.

Sarkar, J., & Bhattacharyya, S. (2010). Performance of a Trans-critical CO₂ Heat Pump for Simultaneous Water Cooling and Heating, *ASHRAE Transaction*, 116(1), 534-541.

Sarkar, J., Bhattacharyya, S., & Gopal, M. R. (2004). Optimization of a trans-critical CO₂ heat pump cycle for simultaneous cooling and heating applications. *International Journal of Refrigeration*, 27(8), 830-838.

✓ Sarkar, J., Bhattacharyya, S., & Gopal, M. R. (2006). Simulation of a trans-critical CO₂ heat pump cycle for simultaneous cooling and heating applications. *International Journal of Refrigeration*, 29(5), 735-743.

Sarkar, J., Bhattacharyya, S., & Gopal M. R. (2007). Natural refrigerant based subcritical and transcritical cycles for high temperature heating. *International Journal of Refrigeration*, 30, 3-10.

Sarkar, J., Bhattacharyya, S., & Gopal, M. R. (2005). Trans-critical CO₂ heat pump systems: exergy analysis including heat transfer and fluid flow effects. *Energy Conversion and Management*, 46(12-14), 2053-2067.

Sarkar, J. (2010). Review on Cycle Modifications of Trans-critical CO₂ Refrigeration and Heat Pump Systems. *Journal of Advanced Research in Mechanical Engineering* 1(1), 22-29.

Sarkar, J. (2011). Performance of nanofluid-cooled shell and tube gas cooler in trans-critical CO₂ refrigeration systems. *Applied Thermal Engineering*, 31(14-15), 2541-2548.

Sarkar, J., Bhattacharyya, S., & Ramgopal, M. (2010). Experimental investigation of trans-critical CO₂ heat pump for simultaneous water cooling and heating. *Thermal Science*, 14(1), 57-64.

Sawalha, S. (2013). Investigation of heat recovery in CO₂ trans-critical solution for supermarket refrigeration. *International Journal of Refrigeration*, 36(1), 145-156.

→ Son, C.H. & Park, S.J. (2006). An experimental study on heat transfer and pressure drop characteristics of carbon dioxide during gas cooling process in a horizontal tube. *International Journal of Refrigeration* 30, 539-546.

↳ Süß J., & Kruse, H. (1998). Efficiency of the indicated process of CO₂-compressors. *International Journal of Refrigeration*, 21(3), 194-201.

Srinivasan, K., Sheahan, P., & Sarathy, C. S. P. (2010). Optimum thermodynamic conditions for upper pressure limits of trans-critical carbon dioxide refrigeration cycle. *International Journal of Refrigeration*, 33(7), 1395-1401.

Subiantoro, A., & Ooi, K. T. (2010). Design analysis of the novel Revolving Vane expander in a trans-critical carbon dioxide refrigeration system. *International Journal of Refrigeration*, 33(4), 675-685.

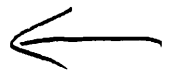
Subiantoro, A., & Tiew, K. (2013). Economic analysis of the application of expanders in medium scale air-conditioners with conventional refrigerants. *International Journal of Refrigeration*, 36(5), 1432-1432.

Tanaka, H., Nishiwaki, N., & Hirata, M. (1967). Turbulent Heat Transfer to Supercritical Carbon dioxide. *Semi-International Symposium, Japan Society of Mechanical Engineers, Tokyo, Japan*, pp. 127-136.

Thevenot, R. (1979). A history of refrigeration throughout the world, *International Institution of Refrigeration, Paris, France*.

Li, X., Li, M., Ma, Y., Yan, Q.,

(change its position suitably)

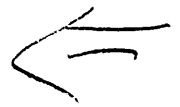


Both references indicate Yang et al (2010)
To distinguish write (2010a) and (2010b)
and accordingly do necessary correction
in text.



Write as 2010a
and
2010b

This will be used
in Page A11



Waltrich, M., Hermes, C. J. L., Goncalves, J. M., & Melo, C. (2010). A first-principles simulation model for the thermo-hydraulic performance of fan supplied tube-fin heat exchangers. *Applied Thermal Engineering*, 30(14-15), 2011–2018. ✓

Wang, Jianfeng, & Hihara, E. (2002). Study on carbon dioxide gas cooler heat transfer process under supercritical pressures. *International Journal of Energy Research*, 26(14), 1237–1251. ✓

Wang, Jing, Cao, F., Wang, Z., Zhao, Y., & Li, L. (2012). Numerical simulation of coiled adiabatic capillary tubes in CO₂ trans^{delete}critical systems with separated flow model including metastable flow. *International Journal of Refrigeration*, 35(8), 2188–2198.

Wang, S., Tuo, H., Cao, F., & Xing, Z. (2013). Experimental investigation on air-source trans^{delete}critical CO₂ heat pump water heater system at a fixed water inlet temperature. *International Journal of Refrigeration*, 36(3), 701–716.

Westphalen, D. & Dieckmann, J. (2004). Scroll expander for carbon dioxide air conditioning cycles. *International Refrigeration and Air Conditioning Conference*, Paper 690. ✓

<http://docs.lib.purdue.edu/cgi/viewcontent.cgi?article=1689&context=iracc>

White, S. D., Yarrall, M. G., Cleland, D. J., & Hedley, R. A. (2002). Modelling the performance of a trans^{delete}critical CO₂ heat pump for high temperature heating. *International Journal of Refrigeration*, 25, 479–486. 25(4)

William S, & Bodinus P. E. (1999). The rise and fall of carbon dioxide systems, *ASHRAE Journal*, 41(4), 37-42. ✓

~~Xiaofeng, L., Minxia, L., Yitai, M., & Qihui, Y. (2013). The influence of Nitrogen on an Expander in a Carbon Dioxide Trans-critical Heat Pump. *Applied Thermal Engineering*, (Article in press), 59(1-2), 182-188.~~

Yang, B., Peng, X., He, Z., Guo, B., & Xing, Z. (2009). Experimental investigation on the internal working process of a CO₂ rotary vane expander. *Applied Thermal Engineering*, 29(11-12), 2289–2296. ✓

Yang, J. L., Ma, Y. T., Li, M. X., & Guan, H. Q. (2005). Exergy analysis of trans^{delete}critical carbon dioxide refrigeration cycle with an expander, *Energy*, 30, 1162–1175.

Yang, J. L., Ma, Y. T., Li, M. X., & Hua, J. (2010). Modeling and simulating the trans-critical CO₂ heat pump system. *Energy*, 35(12), 4812–4818.

Yang, J., Ma, Y., Li, M., & Tian, H. (2010). Simulation of the optimal heat rejection pressure for trans-critical CO₂ expander cycle. *Front. Energy Power Eng. China* 2010, 4(4): 522–526. ✓

Yin, J M, Bullard, C. W., Hrnjak, P. S., & Phoenix, H. (2001). Elements for the design of new generation of heat exchangers for trans-critical CO₂ heat pumps. *ACRC CR-37*.

Yin, J. M., Min, Bullard, C. W., & Hrnjak, P. S. (2001). R-744 gas cooler model development and validation. *International Journal of Refrigeration*, 24, 692–701. 24(7)

Yin, M., Bullard, C. W., Hrnjak, P. S., & Conditioning, A. (2000). R744 Gas Cooler Model Development and Validation. *ACRC CR-29*.

<https://www.ideals.illinois.edu/bitstream/handle/2142/13353/CR029.pdf?sequence=2>

Yoon, S. H., Kim, J. H., Hwang, Y. W., Kim, M. S., Min, K., & Kim, Y. (2003). Heat transfer and pressure drop characteristics during the in-tube cooling process of carbon dioxide in the supercritical region. *International Journal of Refrigeration*, 26, 857–864.

Yoshida H., Sakuda, A., Futagami, Y., Morimoto, T., & Ishii, N., Clearance control of scroll compressor for CO₂ refrigerant. *International Compressor Engineering Conference*, Paper 1848.

Yu, P. Y., Lin, K. H., Lin, W. K., & Wang, C. C. (2012). Performance of a tube-in-tube CO₂ gas cooler. *International Journal of Refrigeration*, 35(7), 2033–2038.

Zha, S., Hafner, A., & Neksa, P. (2008). Investigation of R-744 Voorhees transcritical heat pump system. *International Journal of Refrigeration*, 31(1), 16–22.

Zhang, F. Z., Jiang, P. X., Lin, Y. S., & Zhang, Y. W. (2011). Efficiencies of subcritical and transcritical CO₂ inverse cycles with and without an internal heat exchanger. *Applied Thermal Engineering*, 31(4), 432–438.

Zhang, W. J., & Zhang, C. L. (2011). A correlation-free on-line optimal control method of heat rejection pressures in CO₂ trans-critical systems. *International Journal of Refrigeration*, 34(4), 844–850.

Zhang, Z., Ma, Y., Wang, H., & Li, M. (2013). Theoretical evaluation on effect of internal heat exchanger in ejector expansion trans-critical CO₂ refrigeration cycle. *Applied Thermal Engineering*, 50(1), 932–938.

APPENDIX A

Appendix A.1: Optimum design and operating conditions (Temperature zone I)

<i>Two Pass Gas Cooler</i>											
P_d	u_a	Tube	Pass	T_{evp}	E_{isen}	COP	RE in TR	AT	P_{drop}	GC capacity	W_c
9000	2	48	2	268.15	0.6	1.958002	1.926041	2.215972	4.009552	10.10712	3.346721
9000	2	48	2	273.15	0.6	2.280944	1.903588	2.038728	3.886002	9.504939	2.823346
8500	2	48	2	278.15	0.6	2.715799	1.749442	2.895006	4.069294	8.29559	2.15505
9000	2	48	2	268.15	0.7	2.27999	1.932205	2.100838	3.917979	9.650659	2.868618
9000	2	48	2	273.15	0.7	2.652762	1.909056	1.93542	3.805787	9.120797	2.420011
8500	2	48	2	278.15	0.7	3.158435	1.757541	2.777813	3.998773	8.016153	1.847186
9000	2	48	2	268.15	0.8	2.600599	1.938224	1.987633	3.846225	9.313208	2.510041
8500	2	48	2	273.15	0.8	3.024308	1.793807	2.885472	4.063463	8.272155	1.975893
8500	2	48	2	278.15	0.8	3.59839	1.765632	2.659021	3.942946	7.813655	1.616288
<i>Three Pass Gas Cooler</i>											
8000	2	54	3	268.15	0.6	2.138675	1.856227	1.568946	4.671271	9.456121	2.940763
8000	2	54	3	273.15	0.6	2.525291	1.829581	1.498899	4.553324	8.859166	2.437336
8000	2	54	3	278.15	0.6	3.03235	1.791967	1.417089	4.426616	8.258383	1.968579
8500	1.5	54	3	268.15	0.7	2.491848	1.952474	1.097592	4.322486	9.551619	2.698436
8000	2	54	3	273.15	0.7	2.931635	1.833154	1.451018	4.482883	8.523517	2.089145
8000	1.5	54	3	278.15	0.7	3.517271	1.742777	2.047816	4.531361	7.804502	1.687354
8500	1.5	54	3	268.15	0.8	2.842812	1.954276	1.065612	4.259219	9.220642	2.361132
8000	2	54	3	273.15	0.8	3.331909	1.835547	1.418734	4.429277	8.270773	1.828002
8000	1.5	54	3	278.15	0.8	4.009684	1.745815	2.011045	4.483677	7.604244	1.476435
<i>Four Pass Gas Cooler</i>											
8000	1.5	48	4	268.15	0.6	2.187516	1.865165	1.301581	4.009274	9.487491	2.940763
8000	1.5	48	4	273.15	0.6	2.589944	1.836819	1.253187	3.911768	8.884571	2.437336
8000	1.5	48	4	278.15	0.6	3.121788	1.79709	1.199042	3.809426	8.276365	1.968579
8000	1.5	48	4	268.15	0.7	2.54802	1.867571	1.269114	3.943037	9.075828	2.520654
8000	1.5	48	4	273.15	0.7	3.014662	1.838977	1.223841	3.854728	8.543953	2.089145
8000	1.5	48	4	278.15	0.7	3.617559	1.792649	1.25952	3.76932	7.979553	1.687354
8000	1.5	48	4	268.15	0.8	2.906608	1.869478	1.243259	3.892409	8.767439	2.205572
8000	1.5	48	4	273.15	0.8	3.436665	1.840712	1.200135	3.811663	8.288901	1.828002
8000	1.5	48	4	278.15	0.8	4.120307	1.794185	1.238659	3.733446	7.774024	1.476435

Appendix A.2: Optimum design and operating conditions (Temperature zone II)

<i>Two Pass Gas Cooler</i>											
P_d	u_a	Tube	Pass	T_{evp}	E_{isen}	COP	RE in TR	AT	P_{drop}	GC capacity	W_c
11000	2	48	2	268.15	0.6	1.352616	1.61008	1.288143	3.735642	9.719952	4.068572
11000	2	48	2	273.15	0.6	1.533668	1.581738	1.22335	3.646108	9.062377	3.510478
11000	1.5	48	2	278.15	0.6	1.754174	1.518363	1.576822	3.642255	8.313931	2.984477
11000	2	48	2	268.15	0.7	1.57421	1.613177	1.232191	3.658104	9.149597	3.487347
11000	1.5	48	2	273.15	0.7	1.788575	1.560626	1.602405	3.668291	8.486779	3.008981
11000	1.5	48	2	278.15	0.7	2.045306	1.521917	1.513484	3.579331	7.900051	2.558123
11000	1.5	48	2	268.15	0.8	1.798827	1.591326	1.624217	3.690791	8.636982	3.051429
11000	1.5	48	2	273.15	0.8	2.042997	1.563699	1.547728	3.613087	8.12144	2.632858
11000	1.5	48	2	278.15	0.8	2.334881	1.524677	1.464144	3.531723	7.589975	2.238358
<i>Three Pass Gas Cooler</i>											
10500	1.5	54	3	268.15	0.6	1.415104	1.592962	0.477353	4.10798	9.488909	3.897612
10500	1.5	54	3	273.15	0.6	1.612125	1.562144	0.459367	4.021496	8.830767	3.347641
10500	1.5	54	3	278.15	0.6	1.849549	1.519512	0.441991	3.931635	8.163626	2.830137
11000	1	54	3	268.15	0.7	1.64864	1.647211	0.606378	3.98613	9.269057	3.487347
10500	1.5	54	3	273.15	0.7	1.876804	1.562902	0.447066	3.957728	8.355193	2.869407
10500	1	54	3	278.15	0.7	2.15268	1.499786	0.761462	4.013907	7.690081	2.425832
11000	1	54	3	268.15	0.8	1.884423	1.648754	0.577681	3.927632	8.838556	3.051429
10500	1.5	54	3	273.15	0.8	2.139984	1.563385	0.439233	3.909345	7.998211	2.510731
10500	1	54	3	278.15	0.8	2.459407	1.501015	0.741777	3.967712	7.391166	2.122603
<i>Four Pass Gas Cooler</i>											
11000	1	48	4	268.15	0.6	1.416894	1.650321	0.548251	3.462055	9.861198	4.068572
10500	1	48	4	273.15	0.6	1.615474	1.549809	0.660255	3.546568	8.78747	3.347641
10500	1	48	4	278.15	0.6	1.856816	1.507574	0.636689	3.468727	8.121723	2.830137
11000	1	48	4	268.15	0.7	1.652477	1.651078	0.534141	3.401149	9.282631	3.487347
10500	1	48	4	273.15	0.7	1.884135	1.550835	0.643771	3.491298	8.312839	2.869407
10500	1	48	4	278.15	0.7	2.165202	1.508553	0.620945	3.420816	7.720852	2.425832
11000	1	48	4	268.15	0.8	1.887734	1.65169	0.52272	3.354632	8.848861	3.051429
10500	1	48	4	273.15	0.8	2.152362	1.551669	0.630372	3.449141	7.957088	2.510731
10500	1	48	4	278.15	0.8	2.472962	1.509336	0.608315	3.384429	7.420374	2.122603

Appendix A.3: Optimum design and operating conditions (Temperature zone (iii))

III capital 1eHe2

<i>Two Pass Gas Cooler</i>											
P_d	u_a	Tube	Pass	T_{evp}	E_{isen}	COP	RE in TR	AT	P_{drop}	GC capacity	W_c
12500	2	48	2	268.15	0.6	1.146612	1.5229	0.994666	3.531168	9.89598	4.550601
12500	1.5	48	2	273.15	0.6	1.287795	1.476566	1.291605	3.531398	9.152726	3.969979
12500	1.5	48	2	278.15	0.6	1.451019	1.436538	1.216204	3.449952	8.462686	3.420438
12500	1.5	48	2	268.15	0.7	1.338555	1.508277	1.296048	3.536304	9.194568	3.900515
12500	1.5	48	2	273.15	0.7	1.502038	1.479516	1.231074	3.46575	8.595939	3.402839
12500	1.5	48	2	278.15	0.7	1.691567	1.439196	1.16153	3.392936	7.983382	2.931804
12500	1.5	48	2	268.15	0.8	1.529323	1.510798	1.244329	3.47994	8.715851	3.412951
12500	1.5	48	2	273.15	0.8	1.715407	1.481805	1.184022	3.41619	8.178618	2.977484
12500	1.5	48	2	278.15	0.8	1.930934	1.441243	1.119371	3.350087	7.624092	2.565329

<i>Three Pass Gas Cooler</i>											
12000	1.5	54	3	268.15	0.6	1.196151	1.516145	0.125496	3.864508	9.716319	4.394649
12000	1.5	54	3	273.15	0.6	1.345205	1.485318	0.104292	3.792727	9.034716	3.821252
12000	1	54	3	278.15	0.6	1.520774	1.429422	0.340088	3.823503	8.296527	3.279257
12000	1	54	3	268.15	0.7	1.393969	1.503876	0.362661	3.910706	9.045448	3.766842
12000	1.5	54	3	273.15	0.7	1.566881	1.486391	0.083579	3.734761	8.49259	3.275358
12000	1	54	3	278.15	0.7	1.774603	1.431152	0.306903	3.767984	7.834136	2.810791
12500	1	54	3	268.15	0.8	1.593198	1.558179	0.257721	3.72537	8.882158	3.412951
12000	1	54	3	273.15	0.8	1.793444	1.474526	0.313226	3.792466	8.041523	2.865939
12000	1	54	3	278.15	0.8	2.026903	1.43173	0.295772	3.726605	7.484816	2.459443

<i>Four Pass Gas Cooler</i>											
12000	1	48	4	268.15	0.6	1.19143	1.498498	0.465645	3.417692	9.654377	4.394649
12000	1	48	4	273.15	0.6	1.340711	1.467232	0.453032	3.354788	8.971235	3.821252
12000	1	48	4	278.15	0.6	1.515211	1.424227	0.439729	3.289944	8.278292	3.279257
12000	1	48	4	268.15	0.7	1.389515	1.499103	0.45411	3.360121	9.028693	3.766842
12000	1	48	4	273.15	0.7	1.563389	1.467776	0.442637	3.303958	8.427253	3.275358
12000	1	48	4	278.15	0.7	1.768054	1.42591	0.40754	3.244933	7.815735	2.810791
12000	1	48	4	268.15	0.8	1.587317	1.49957	0.445195	3.316366	8.559477	3.295987
12000	1	48	4	273.15	0.8	1.78714	1.469382	0.41194	3.264611	8.023468	2.865939
12000	1	48	4	278.15	0.8	2.019163	1.426307	0.399932	3.211699	7.46578	2.459443

APPENDIX B

Appendix B.1: Performance Results and Optimum Conditions for Zone I
(Evap. Temperature = 268K)

Parameters	Compressor Efficiency	Without Expander	Expander Efficiency				
			0.6	0.65	0.7	0.75	0.8
Refrigeration Capacity (kW)	0.6	6.5153576	6.843676	6.871194	6.718621	6.747354	6.776086
	0.7	6.8531828	6.675736	6.704334	6.732931	6.761529	6.790126
	0.8	6.8595105	6.687256	6.715764	6.744271	6.772779	6.801286
Compressor Work (kW)	0.6	2.9407633	2.716236	2.688718	2.590346	2.561613	2.532881
	0.7	2.6984362	2.229318	2.20072	2.172123	2.143525	2.114928
	0.8	2.3611317	1.915313	1.886805	1.858298	1.82979	1.801283
COP	0.6	2.1386749	2.519544	2.555565	2.593716	2.634025	2.675249
	0.7	2.4918479	2.99452	3.046427	3.099701	3.154397	3.210571
	0.8	2.8428118	3.49147	3.559331	3.629274	3.701396	3.775802
COP Improvement (%)	0.6	0	17.80865	19.49289	22.83765	24.74668	26.69902
	0.7	0	21.60578	23.7137	25.87713	28.09828	30.3795
	0.8	0	24.17204	26.58547	29.07296	31.63795	34.28413
Optimum Conditions							
Pressure	} unit		8000	8000	8000	8000	8000
Velocity		0.6	2	2	2	1.5	1.5
Tubes			54	54	54	54	54
Pressure	} unit		8500	8000	8000	8000	8000
Velocity		0.7	1.5	1.5	1.5	1.5	1.5
Tubes			54	54	54	54	54
Pressure	} unit		8500	8000	8000	8000	8000
Velocity		0.8	1.5	1.5	1.5	1.5	1.5
Tubes			54	54	54	54	54

Appendix B.2: Performance Results and Optimum Conditions for Zone
(Evaporator Temperature = 273K)

Parameters	Compressor Efficiency	Without Expander	Expander Efficiency				
			0.6	0.65	0.7	0.75	0.8
Refrigeration Capacity (kW)	0.6	6.4218299	6.51516	6.539078	6.562995	6.586913	6.61083
	0.7	6.4343718	6.52839	6.552173	6.575955	6.599738	6.62352
	0.8	6.4427706	6.53964	6.563423	6.587205	6.610988	6.63477
Compressor Work (kW)	0.6	2.4373364	2.202158	2.17824	2.154323	2.130405	2.106488
	0.7	2.0891455	1.855583	1.831801	1.808018	1.784236	1.760453
	0.8	1.8280023	1.594437	1.570654	1.546872	1.523089	1.499307
COP	0.6	2.5252907	2.958535	3.002	3.046431	3.091859	3.138319
	0.7	2.9316353	3.518242	3.576903	3.637107	3.698916	3.762395
	0.8	3.3319086	4.101536	4.178782	4.258404	4.340512	4.425225
COP Improvement (%)	0.6	0	18.19929	19.93582	21.71091	23.52586	25.38202
	0.7	0	20.6164	22.62748	24.69147	26.81048	28.98674
	0.8	0	23.23274	25.55364	27.94592	30.4129	32.95814
Optimum Conditions							
Pressure	0.6	8000	8000	8000	8000	8000	8000
Velocity		2	2	2	1.5	1.5	1.5
Tubes		54	54	54	54	54	54
Pressure	0.7	8000	8000	8000	8000	8000	8000
Velocity		2	1.5	1.5	1.5	1.5	1.5
Tubes		54	54	54	54	54	54
Pressure	0.8	8000	8000	8000	8000	8000	8000
Velocity		2	1.5	1.5	1.5	1.5	1.5
Tubes		54	54	54	54	54	54

Appendix B.3: Performance Results and Optimum Conditions for Zone I
(Evaporator Temperature = 278K)

Parameters	Compressor Efficiency	Without Expander	Expander Efficiency				
			0.6	0.65	0.7	0.75	0.8
Refrigeration Capacity (kW)	0.6	6.2898041	6.334767	6.354185	6.373602	6.39302	6.412437
	0.7	6.2995659	6.347727	6.3671	6.386472	6.405845	6.425217
	0.8	6.1278096	6.357807	6.377157	6.396507	6.415857	6.435207
Compressor Work (kW)	0.6	1.9685794	1.787394	1.767976	1.748559	1.729141	1.709724
	0.7	1.6873538	1.506705	1.487332	1.46796	1.448587	1.429215
	0.8	1.4764346	1.296053	1.276703	1.257353	1.238003	1.218653
COP	0.6	3.0323495	3.544136	3.594044	3.64506	3.697222	3.750569
	0.7	3.5134175	4.212987	4.280886	4.350577	4.422132	4.495628
	0.8	4.0096836	4.905516	4.995021	5.087282	5.182426	5.280592
COP Improvement (%)	0.6	0	17.31371	18.9657	20.65438	22.38098	24.1468
	0.7	0	19.78	21.71045	23.69185	25.72625	27.81579
	0.8	0	22.34172	24.57395	26.87489	29.24775	31.69597
Optimum Conditions							
Pressure	} <i>unit</i>	8000	8000	8000	8000	8000	8000
Velocity		0.6	2	1.5	1.5	1.5	1.5
Tubes			54	54	54	54	54
Pressure	} <i>unit</i>	8000	8000	8000	8000	8000	8000
Velocity		0.7	2	1.5	1.5	1.5	1.5
Tubes			54	54	54	54	54
Pressure	} <i>unit</i>	8000	8000	8000	8000	8000	8000
Velocity		0.8	1.5	1.5	1.5	1.5	1.5
Tubes			54	54	54	54	54

I do this calculation at remaining pages also

Appendix B.4: Performance Results and Optimum Conditions for Zone II
(Evaporator Temperature = 268K)

Parameters	Compressor Efficiency	Without Expander	Expander Efficiency				
			0.6	0.65	0.7	0.75	0.8
Refrigeration Capacity (kW)	0.6	5.5912972	6.082096	6.123024	6.163951	6.204879	6.245806
	0.7	5.5946106	6.007666	6.049179	5.826091	5.868054	5.910016
	0.8	5.7871273	6.014056	6.055501	5.827576	5.869516	5.911456
Compressor Work (kW)	0.6	3.8976117	3.460026	3.419098	3.378171	3.337243	3.296316
	0.7	3.34081	2.862276	2.820763	2.655262	2.613299	2.571337
	0.8	3.0514291	2.445482	2.404037	2.256928	2.214988	2.173048
COP	0.6	1.4151042	1.79083	1.757818	1.824642	1.859283	1.894784
	0.7	1.648213	2.098912	2.144518	2.194168	2.245458	2.298422
	0.8	1.8844227	2.459252	2.518889	2.582083	2.649909	2.720352
COP Improvement (%)	0.6	0	24.21828	26.5511	28.94044	31.38839	33.89713
	0.7	0	27.99427	30.77538	35.79787	38.97221	42.25015
	0.8	0	31.16021	34.34083	40.11104	43.79144	47.6139
Optimum Conditions							
Pressure		10500	10500	10500	10500	10500	10500
Velocity	0.6	1.5	1.5	1.5	1.5	1.5	1.5
Tubes		54	54	54	54	54	54
Pressure		10500	10500	10500	10000	10000	10000
Velocity	0.7	1.5	1	1	1.5	1.5	1.5
Tubes		54	54	54	54	54	54
Pressure		11000	10500	10500	10000	10000	10000
Velocity	0.8	1	1	1	1.5	1.5	1.5
Tubes		54	54	54	54	54	54

Appendix B.5: Performance Results and Optimum Conditions for Zone II
(Evaporator Temperature = 273K)

Parameters	Compressor Efficiency	Without Expander	Expander Efficiency				
			0.6	0.65	0.7	0.75	0.8
Refrigeration Capacity (kW)	0.6	5.4831258	5.56593	5.60247	5.63901	5.67555	5.71209
	0.7	5.4857862	5.84214	5.87841	5.64063	5.677125	5.71362
	0.8	5.6811561	5.84628	5.495123	5.532405	5.569688	5.60697
Compressor Work (kW)	0.6	3.3476411	2.794289	2.757749	2.721209	2.684669	2.648129
	0.7	2.8694067	2.453779	2.417509	2.267664	2.231169	2.194674
	0.8	2.6328582	2.09591	1.919357	1.882075	1.844792	1.80751
COP	0.6	1.6121248	1.991895	2.031537	2.072244	2.114059	2.157028
	0.7	1.8768037	2.380875	2.431599	2.487419	2.544462	2.603402
	0.8	2.1418441	2.789375	2.863001	2.939525	3.019141	3.102041
COP Improvement (%)	0.6	0	25.56289	28.06183	30.62787	33.26377	35.97241
	0.7	0	27.19238	29.90216	34.71281	37.80214	40.99422
	0.8	0	30.39605	37.33541	41.00615	44.82526	48.80192
Optimum Conditions							
Pressure		10500	10500	10500	10500	10500	10500
Velocity	0.6	1.5	1.5	1.5	1.5	1.5	1.5
Tubes		54	54	54	54	54	54
Pressure		10500	10500	10500	10000	10000	10000
Velocity	0.7	1.5	1	1	1.5	1.5	1.5
Tubes		54	54	54	54	54	54
Pressure		11000	10500	10000	10000	10000	10000
Velocity	0.8	1	1	1	1	1	1
Tubes		54	54	54	54	54	54

Appendix B.6: Performance Results and Optimum Conditions for Zone II

(Evaporator Temperature = 278K)

Parameters	Compressor Efficiency	Without Expander	Expander Efficiency				
			0.6	0.65	0.7	0.75	0.8
Refrigeration Capacity (kW)	0.6	5.3334883	5.354487	5.385852	5.417217	5.448582	5.479947
	0.7	5.3348369	5.248017	5.280035	5.312052	5.34407	5.376087
	0.8	5.2685625	5.255397	5.287392	5.319387	5.351382	5.383377
Compressor Work (kW)	0.6	2.8301374	2.34775	2.316385	2.28502	2.253655	2.22229
	0.7	2.4258321	1.924474	1.892457	1.860439	1.828422	1.796404
	0.8	2.1226031	1.638608	1.606613	1.574618	1.542623	1.510628
COP	0.6	1.8495489	2.280689	2.325111	2.370753	2.417665	2.465901
	0.7	2.1516974	2.726988	2.790043	2.855268	2.922778	2.992694
	0.8	2.459407	3.207232	3.291018	3.378208	3.469015	3.563668
COP Improvement (%)	0.6	0	24.78657	27.2171	29.71436	32.28113	34.92035
	0.7	0	29.41395	32.40634	35.50172	38.7055	42.02349
	0.8	0	33.1273	36.6051	40.22423	43.99348	47.9224
Optimum Conditions							
Pressure		10500	10000	10000	10000	10000	10000
Velocity	0.6	1.5	1.5	1.5	1.5	1.5	1.5
Tubes		54	54	54	54	54	54
Pressure		10500	10000	10000	10000	10000	10000
Velocity	0.7	1.5	1	1	1	1	1
Tubes		54	54	54	54	54	54
Pressure		10500	10000	10000	10000	10000	10000
Velocity	0.8	1	1	1	1	1	1
Tubes		54	54	54	54	54	54

Appendix B.7: Performance Results and Optimum Conditions for Zone III

(Evaporator Temperature = 268K)

Parameters	Compressor Efficiency	Without Expander	Expander Efficiency				
			0.6	0.65	0.7	0.75	0.8
Refrigeration Capacity (kW)	0.6	5.3216693	5.664946	5.650951	5.699146	5.747341	5.795536
	0.7	5.4674238	5.610766	5.658916	5.707066	5.755216	5.803366
	0.8	5.469207	5.613556	5.661639	5.395441	5.444604	5.493766
Compressor Work (kW)	0.6	4.3946493	3.716327	3.627479	3.579284	3.531089	3.482894
	0.7	3.9005151	3.071338	3.023188	2.975038	2.926888	2.878738
	0.8	3.4129507	2.618492	2.57041	2.383061	2.333899	2.284736
COP	0.6	1.1961507	1.52434	1.557818	1.592259	1.62764	1.664
	0.7	1.3946036	1.826815	1.871837	1.918317	1.966326	2.015941
	0.8	1.5931984	2.143812	2.202621	2.26408	2.332836	2.404552
COP Improvement (%)	0.6	0	28.34728	31.87907	34.79472	37.78995	40.86808
	0.7	0	32.44128	35.70533	39.07504	42.55562	46.15263
	0.8	0	36.00426	39.7351	47.70017	52.18558	56.86402
Optimum Conditions							
Pressure		12000	11500	11500	11500	11500	11500
Velocity	0.6	1.5	1.5	1	1	1	1
Tubes		54	54	54	54	54	54
Pressure		12500	11500	11500	11500	11500	11500
Velocity	0.7	1	1	1	1	1	1
Tubes		54	54	54	54	54	54
Pressure		12500	11000	11000	11500	11500	11500
Velocity	0.8	1	1	1	1	1	1
Tubes		54	54	54	54	54	54

Appendix B.8: Performance Results and Optimum Conditions for Zone III
(Evaporator Temperature = 273K)

Parameters	Compressor Efficiency	Without Expander	Expander Efficiency				
			0.6	0.65	0.7	0.75	0.8
Refrigeration Capacity (kW)	0.6	5.3903762	5.43246	5.475053	5.517645	5.560238	5.60283
	0.7	5.1698033	5.43651	5.479103	5.521695	5.564288	5.60688
	0.8	5.1755847	5.4429	5.485425	5.20746	5.25075	5.29404
Compressor Work (kW)	0.6	3.9699785	3.177005	3.134412	3.09182	3.049227	3.006635
	0.7	3.2753585	2.652972	2.610379	2.567787	2.525194	2.482602
	0.8	2.8659387	2.260757	2.218232	2.046702	2.003412	1.960122
COP	0.6	1.3394527	1.709932	1.746756	1.784595	1.823491	1.863489
	0.7	1.5688613	2.049215	2.098968	2.150371	2.203509	2.258469
	0.8	1.7934442	2.407557	2.472882	2.544317	2.620903	2.700872
COP Improvement (%)	0.6	0	28.13008	30.88944	33.72482	36.63941	39.63658
	0.7	0	31.62262	34.81828	38.11995	41.533	45.06317
	0.8	0	35.23624	38.90565	46.65431	51.06872	55.67813
Optimum Conditions							
Pressure		12500	11500	11500	11500	11500	11500
Velocity	0.6	1.5	1	1	1	1	1
Tubes		54	54	54	54	54	54
Pressure		12000	11500	11500	11500	11500	11500
Velocity	0.7	1	1	1	1	1	1
Tubes		54	54	54	54	54	54
Pressure		12000	11500	11500	11000	11000	11000
Velocity	0.8	1	1	1	1	1	1
Tubes		54	54	54	54	54	54

Appendix B.9: Performance Results and Optimum Conditions for Zone III
(Evaporator Temperature = 278K)

Parameters	Compressor Efficiency	Without Expander	Expander Efficiency				
			0.6	0.65	0.7	0.75	0.8
Refrigeration Capacity (kW)	0.6	5.0172708	5.226147	5.263542	5.300937	5.338332	5.375727
	0.7	5.0233443	5.228937	4.94735	4.985172	5.022995	5.060817
	0.8	5.0253733	4.912767	4.950522	4.988277	5.026032	5.063787
Compressor Work (kW)	0.6	3.2792567	2.705214	2.667819	2.630424	2.593029	2.555634
	0.7	2.8107914	2.2583	2.086333	2.04851	2.010688	1.972865
	0.8	2.4594425	1.805198	1.767443	1.729688	1.691933	1.654178
COP	0.6	1.5207742	1.931879	1.972976	2.01524	2.058724	2.103481
	0.7	1.7746026	2.315431	2.371314	2.43356	2.498147	2.565212
	0.8	2.0269029	2.721456	2.800952	2.883917	2.970586	3.061211
COP Improvement (%)	0.6	0	24.78657	27.2171	29.71436	32.28113	34.92035
	0.7	0	29.41395	32.40634	35.50172	38.7055	42.02349
	0.8	0	33.1273	36.6051	40.22423	43.99348	47.9224
Optimum Conditions							
Pressure		12000	11500	11500	11500	11500	11500
Velocity	0.6	1	1	1	1	1	1
Tubes		54	54	54	54	54	54
Pressure		12000	11500	11000	11000	11000	11000
Velocity	0.7	1	1	1	1	1	1
Tubes		54	54	54	54	54	54
Pressure		12000	11000	11000	11000	11000	11000
Velocity	0.8	1	1	1	1	1	1
Tubes		54	54	54	54	54	54

LIST OF PUBLICATIONS

International Journals

Dileep Kumar Gupta and M. S. Dasgupta, *Simulation and performance Optimization of finned-tube gas cooler for trans-critical CO₂ refrigeration system in Indian context*; International Journal of Refrigeration 38 (2014), 153-167.doi: 10.1016/j.ijrefrig.2013.09.041.

Dileep Kumar Gupta and M. S. Dasgupta, *Simulation and Performance Evaluation of Finned Tube Gas Cooler for Trans-Critical CO₂ Refrigeration Systems*; Applied Mechanics and Materials and Energy Vol. 281 (2013) pp 324-328, Trans Tech Publications, Switzerland.

Dileep Kumar Gupta, Deepak Kumar Singh, and M. S. Dasgupta, *Environmental Effect on Gas Cooler Design for Trans-critical Carbon Dioxide Refrigeration System in Indian Context*; Journal of Advanced Research in Mechanical Engineering (Vol.1-2010/Iss.3) pp 147-152.

International Conferences

Dileep Kumar Gupta and M. S. Dasgupta, *simulation and performance evaluation of air-cooled finned-tube gas cooler for trans-critical carbon dioxide refrigeration system in Indian context*; 2nd IIR International Conference on Sustainability and the Cold Chain, PARIS, Paper ID S3/3, April 2-4, 2013.

Dileep Kumar Gupta and M. S. Dasgupta, *Simulation and Performance Evaluation of Finned Tube Gas Cooler for Trans-Critical CO₂ Refrigeration Systems*; ^Pproc. of ICMEME 2012, Dalian, China.

Dileep Kumar Gupta, and M. S. Dasgupta, *Gas cooler Design Issues for Trans-critical Carbon Dioxide Based Refrigeration System in Indian Context*; ^Pproc. of ^Int. ^Conference in Advances of ^Mechanical ^Engineering, ICAME-2010, pp. 229-233, SVNIT, Surat, India.

↑ ↑
gap dot

Brief Biography of the Candidate

Mr. Dileep Kumar Gupta did his B.E. (Mechanical Engineering) from Govt. Engineering College, Jagdalpur, Chhattisgarh, in 2004 and M.Tech. (Heat Power Engineering) from VNIT, Nagpur in 2006. He is presently working as a Lecturer with Department of Mechanical Engineering, BITS-Pilani, Pilani campus. He has over 7 years of teaching experience at both under graduate and graduate levels. His areas of research interest are energy efficient and eco-friendly system, alternative refrigerant, trans-critical CO₂ refrigeration system, computational heat transfer, and bio fuels.

Brief Biography of the Supervisor

Dr. M. S. Dasgupta is presently Professor in the Department of Mechanical Engineering of BITS-Pilani, Pilani Campus, India. He is unit chief of Placement unit BITS Pilani since several years. He was Head of the Department (HOD) of Mechanical Engineering and Engineering & Technology department from 2011 and 2013. He has over 20 years of teaching & research experience and 12 years of administrative experience in various capacities at BITS Pilani. His research interest includes Mechanical Engineering Design and Environment friendly Technologies. His research publications are in the areas of application of Fuzzy Logic & Neural Network, Two-phase flow, E-waste management, CO₂ Trans-critical applications etc. Dr. Dasgupta has primary teaching interests in Mechanical Design and System Design, Kinematics and Dynamics, Engineering Graphics, Thermodynamics and Transport Phenomena. He has completed four sponsored projects from DST and UGC and currently has one DST Major Project and a Consultancy Project with industry. He has reviewed 8 Ph.D. thesis reports and acted as Doctoral advisory committee member for more than 10 Ph.D. candidates. Dr. Dasgupta is also NAAC Associate faculty and is member of UGC Nominated advisory committee for sponsored project at JMI Central University, New Delhi. Dr. Dasgupta has visited Germany, Thailand, UAE and China in connection with his research and consultancy work.